UNIVERSITY OF CALIFORNIA,
IRVINE

HEALTH, CLIMATE AND ELECTRICITY GRID IMPACTS OF HIGH PENETRATIONS OF VARIABLE RENEWABLE ENERGY

DISSERTATION

submitted in partial satisfaction of the requirements
for the degree of

DOCTOR OF PHILOSOPHY

in Engineering

by

Daniel Bost Howard

Dissertation Committee:
Professor Jean-Daniel Saphores, Chair
Associate Professor Diego Rosso
Associate Professor Jun Wu

2018

DEDICATION

To

Bruce and Karen, for giving me a strong sense of self-worth, self-efficacy and self-love

Aaron, for teaching how to deeply care about another human

My grandparents, for their love and support

Michelle, for teaching me how to be a compassionate partner

And my friends, for sharing their lives and making me feel loved and accepted

TABLE OF CONTENTS

LIST OF FIGURES

LIST OF TABLES

ACKNOWLEDGMENTS

It is with deep gratitude that I write these words.

First and foremost, I would like to thank my advisor, Professor Jean-Daniel Saphores. The standard that he held me to greatly improved this work, as well as my self-confidence and research capabilities. I also want to thank him for his high level of integrity, and his ability to provide wise suggestions for the project while still giving me space to explore and learn on my own. Thank you Professor Saphores, for all your time and energy.

Second, I would like to thank the National Science Foundation (NSF) for awarding me a Graduate Research Fellowship. Without NSF funding, this research would not have happened. "This material is based upon work supported by the National Science Foundation Graduate Research Fellowship Program under Grant No. DGE-1321846. Any opinions, findings, and conclusions or recommendations expressed in this material are those of the author(s) and do not necessarily reflect the views of the National Science Foundation."

I was fortunate to have a handful of mentors that supported me throughout the project, especially in the beginning. Dr. Brian Tarroja was the first, who provided key insight and support at the times I needed it most. Thank you Brian, without you, I might not have continued on this journey. I am also very grateful for Professor Rufus Edwards, who received my project with excitement and provided excellent advice. My committee members, Professor Jun Wu and Professor Diego Rosso, also contributed excellent ideas and suggestions. Thank you all.

Collaboration was a key part to executing this big picture and detailed interdisciplinary study. I am grateful for the additional funding provided by the NSF Graduate Research Opportunities Worldwide program and the United States Agency for International Development to perform research in Brazil. To my colleagues at the Federal University of Rio de Janeiro, who warmly received me for two summers, thank you so much. A special thanks to Professor Roberto Schaeffer for his kindness and sagacious research insight, as well as to Mauro Chávez-Rodríguez and Jonas Rocha for welcoming me into their homes. I am also very grateful to Professor Rafael Soria, who provided fundamental data for the Brazilian electricity system.

Neal Fann hosted me at the U.S. Environmental Protection Agency (EPA) during the summer of 2016 and provided essential modeling advice and data. Thank you so much, Neal. This collaboration was funded by the NSF Graduate Research Internship Program, for which I am very thankful.

I want to sincerely thank Professor Jesse Thé, who provided detailed meteorological data for Brazil. This was an essential part of the project that we did not have funding for. Thank you, Jesse.

The SoCAL Association of Energy Engineers (AEE) chapters and the American Council of Engineering Companies also provided scholarships, for which I am very appreciative. Special thanks to Gene Beck for supporting the AEE Student Chapter at UCI.

I am extremely thankful for the Civil and Environmental Engineering Department at the University of California, Irvine, for the resources, TA positions and financial support once my project was out of funding. I am also very thankful for the administrative staff for keeping the department running smoothly.

I am also so thankful for the teachers at YogaWorks, specifically Erika Burkhalter and Simon Ballard, for the mental clarify and physical/emotional well being their classes offer. I am also very grateful for Alta Coffee Shop and everyone who works there for letting me write for long hours during so many nights, and for the hundreds of tea refills.

It took more than just research skills to complete this project. I am exceptionally grateful for Zat Baraka and the work he does with men on emotional mastery, conscious relating, leadership, integrity and healing. I am also extremely grateful for Michael Romine and all the other men supporting our deep inner work.

To all my friends, thank you, I love you. You fill my life with love and joy, and you have helped me cultivate self-esteem and compassion. Your friendship has taught me the beauty of humanity, and inspires me to do this work. Special thanks to Jason Panzarino, who went through grad school with me and made life way more fun.

To my parents, Bruce and Karen, thank you for doing your best. Thank you for giving me what you did and didn't receive. Thank you for raising me with a strong sense of self-worth, self-efficacy and self-love, thank you for encouraging me to take my own path, thank you for patience, love and support. Most importantly, thank you for teaching me what love is.

To my brother Aaron, thank you for being an incredible brother through the thick and thin. Caring about you has taught me how to truly love another human without needing anything in return. I'm looking forward to surfing through life with you.

And to Michelle, thank you for teaching me how to be a loving, supportive and compassionate partner. Thank you for being there for me during the toughest part of my Ph.D. Thank you for sharing your life and your love. Te amo.

CURRICULUM VITAE

Daniel Bost Howard

2004-08	B.A. in Mathematics-Economics, University of California, Santa Barbara
2006-08	Technology Entrepreneurship Certification, University of California, Santa Barbara
2008-12	Account Executive, RightScale Inc.
2012-14	M.S. in Environmental Engineering, with a concentration in Energy and Air Quality, University of California, Irvine
2014-15	Research and Innovation Fellow, United States Agency for International Development
2016	Fellow, United States Environmental Protection Agency
2013-18	Graduate Research Fellow, National Science Foundation
2014-18	Ph.D. in Engineering, with a concentration in Environmental Engineering, University of California, Irvine

FIELD OF STUDY

Health, climate and energy nexus

PUBLICATIONS

"Health Benefits and Control Costs of Particulate Matter Emissions Standards: The case of Coal Power Plants in Northeast Brazil." Unpublished manuscript, Civil and Environmental Engineering Department, University of California, Irvine, USA.

ABSTRACT OF THE DISSERTATION

Health, Climate and Electricity Grid Impacts of High Penetrations of Variable Renewable Energy

By

Daniel Bost Howard

Doctor of Philosophy in Engineering

University of California, Irvine, 2018

Professor Jean-Daniel Saphores, Chair

This dissertation proposes a methodology applicable worldwide to assess key health, climate and electricity system impacts of high penetrations of variable renewable energy (VRE), such as wind and solar energy, in the production of electricity. Three primary questions are addressed: (1) what are the health benefits and control costs of tightening emission standards for particulate matter (PM); (2) what are the health, climate and electricity grid impacts of high penetrations of VRE; and (3) is a 100% Renewable Portfolio Standard (RPS) electricity grid technically feasible in Northeast (NE) Brazil, and what are the associated health and climate benefits? The methodology I developed to answer these questions combines highly resolved spatial and temporal electricity grid simulation (via Plexos), atmospheric dispersion of power plant emissions (via CALPUFF), and human health impacts estimation (via BenMAP). The methodology is validated extensively over detailed case studies in NE Brazil, a region that has exceptionally high VRE and hydroelectric potential. Results for Question (1) indicate that when tightening emission standards, the health benefits outweigh the control costs by at least 50 times, even

in a relatively clean region. Results for Question (2) show that health and climate benefits exceed US$267 million/yr and US$1.2 billion/yr respectively if NE Brazil transitions to a 45% VRE instead of a 30% VRE penetration in 2030. For Question (3), I find that a 100% RPS is not feasible using only wind, solar PV and hydroelectric resources in NE Brazil unless ~13% of demand can be flexibly imported and ~23% of generation can be flexibly exported; otherwise additional types of generation, storage and load balancing technology would need to be deployed. For this case, the health and climate benefits are at least US$433 million/yr and US$2.4 billion/yr respectively if NE Brazil transitions to a 100% RPS instead of a 30% VRE penetration in 2030.

1 Introduction

Energy planning is typically based on technical and economic cost minimization that does not consider health and environmental impacts. The main health and environmental impacts related to electricity production are a product of local and regional pollutant emissions, such as particulate matter (PM) and ozone (0_3), and global pollutant emissions such as carbon dioxide (CO_2) and methane (CH_4). Local and regional pollutants have a number of adverse health impacts such as respiratory and cardiovascular illness, as well as premature mortality, while global pollutants cause global climate change.

The purpose of this dissertation is to propose a spatially and temporally resolved methodology that can be used to assess health and climate benefits as well as other key implications of current and future electricity infrastructure scenarios. I use this methodology to answer three questions: (1) What are the health benefits of tightening PM standards for coal power plants and how do they compare to control costs?; (2) What are the health, climate and electricity grid impacts of high penetrations of variable renewable energy (VRE)?; and (3) Is it technically feasible given current technology to achieve 100% renewable energy electricity grids, and what are the associated health and climate benefits? My work illustrates the importance of accounting for health and climate benefits in energy planning.

The subject of this dissertation is directly relevant to some of the most pressing global initiatives: air quality, climate change and renewable energy based electricity systems. It is projected that world energy consumption will increase by 60% from 2010 to 2040, with 85% of the energy demand increase occurring in non-

OECD countries (Leahy *et al.*, 2013). Increasing fossil energy production to meet this demand is likely to have catastrophic impacts via global climate change. In addition to increasing energy demand, in the December 2015 Paris Agreement, nearly 200 countries committed to reducing greenhouse gas (GHG) emissions in order to collectively keep global average temperature increases below 2 degrees Celsius (United Nations, 2015). However, it is not clear how to achieve this goal. In particular, questions remain about how to increase the share of VRE (i.e. wind and solar) in the production of electricity, while reliably meeting demand.

At the same time, local/regional air pollution from the combustion of fossil fuels is increasingly of concern in developed and developing countries because of the adverse health impact of pollutants such as PM (Brauer *et al.,* 2015). Over the last 20 years, epidemiological and health economics studies have established clear connections between air pollutant concentrations and adverse health effects (Babin *et al.,* 2007; Krewski *et al.,* 2009*;* Laden *et al.,* 2006*;* Lepeule *et al.,* 2012; Moolgavkar, 2000; Ostro *et al*., 2007; Pope *et al*., 2009; Wu *et al*., 2009; Zanobetti *et al.,* 2009). In particular, ambient $PM_{2.5}$ (airborne particulate matter whose diameter is less than 2.5 micrometers) was ranked the fifth largest contributor to global disease in 2015 (Institute of Health Metrics and Evaluation, 2015).

Over the last four decades, the impacts of PM pollution have been worsening. From 1990 to 2015 the number of deaths attributable to ambient $PM_{2.5}$ exposure increased from 3.5 million to 4.2 million (Cohen *et al.*, 2017). Approximately 87% of the world's population resides in areas exceeding the World Health Organization (WHO) air quality guideline of 10 $\mu g/m^3$ $PM_{2.5}$ (annual average) (Brauer *et al.*,

2015). From 1990 to 2013 the population-weighted annual average $PM_{2.5}$ increased by 20.4% globally, and although it decreased 34.5% in the U.S., it increased 70.4% in Brazil (Brauer *et al.*, 2015). The global exposure to PM and its substantial contribution to global disease is the reason why this dissertation focuses on PM.

A number of studies have shown that reducing emissions yields monetary savings from avoiding adverse health effects that are an order of magnitude greater than the cost of the emission control equipment (e.g., see Krupnick and Portney 1991; Palmer *et al.,* 1995; Pervin *et al.,* 2008). However, these studies do not model the dispatch of power plants in an electric grid, which is necessary to obtain a more realistic representation of the link between electricity generation and ambient air concentrations and their health impacts.

In reviewing the literature, I did not find any study at the electric grid level that directly compares the health benefits of tightening emissions standards with the corresponding emission control costs. Furthermore, there are few papers concerned with the health impacts from power plants in Latin America. I found only two studies in Brazil (Alves *et al.,* 2010; Avelino *et al.*, 2015) and one in Mexico (Lopez *et al.,* 2005).

Increasing concerns about the health and climate change impacts of energy generation are pressuring energy regulators worldwide to shift to renewable energy to reduce air pollution and GHG emissions. At the same time, electricity grid loads are forecasted to increase significantly as sectors such as transportation, industrial and cooling/heating switch to electricity to meet GHG and air quality goals (Wei *et al.*, 2013; Yang *et al.*, 2014).

To meet electricity demand as well as climate change and air quality goals, new legislation is being implemented in the U.S. and internationally. In California, Senate Bills 350 (2015) mandates electricity service providers to increase eligible renewable energy resources to 50% of California's total electricity sales by 2030 (de Leon & Leno, 2015). In Brazil, Law number 10,438, which was enacted in 2002, created the Program of Incentive to Alternative Source of Energy (PROINFA) to increase the share of wind, biomass and small hydroelectric power plants (Francisco, 2012).

I selected Brazil as the country of analysis for this dissertation because it has rapidly increasing energy demand and electricity infrastructure capacity, large hydroelectric and VRE potential, varying PM_{10} emission standards, and thermal power plants near densely populated cities. Within Brazil, I focused on NE Brazil's electricity grid because it is a semi-arid region with exceptionally high capacity factors for wind and solar electricity production (Krauter, 2005), and because the electricity generation installed capacity is increasing by more than five percent per year (Ministério de Minas e Energia, 2014). Moreover, legislative initiatives are working to reduce dependency on hydroelectric sources and increase renewable generation (Law number 10,438). Additionally, 45.5% of the NE Brazil electric grid installed capacity is hydroelectric, which provides large quantities of flexible dispatch energy along with pumped hydroelectric energy storage. Flexible dispatch and energy storage resources are needed to balance load and generation during the spikes and drops of VRE generation.

Temporal and spatial resolutions are important for accurately simulating the electric system, emissions dispersion and human exposure. First, hourly electricity supply must meet hourly demand under the constraints of the electric system. Models without hourly temporal resolution overestimate the contribution of baseload generation and underestimate the contribution of intermittent renewables as well as the importance of supply-demand management. Second, meteorological conditions (such as wind) vary based on time and space, and affect how emissions disperse. Third, geographic conditions vary spatially and affect dispersion dynamics. Last, gridded air quality concentrations must be overlaid with gridded demographic data to determine how changes in air quality affect human exposure.

In this context, my dissertation makes several contributions. First, I developed a new integrated modeling methodology to assess key health, climate and electricity grid impacts of increasing the share of renewables. This methodology consists of three models integrated sequentially and is applicable in any country. For the first modeling stage, I built a spatially and temporally (hourly) resolved electricity dispatch model for the electric grid of NE Brazil, in order to better capture the link between electricity generation and ambient pollution concentrations. To obtain realistic PM concentrations, I input hourly PM emissions for an entire year into CALPUFF View (Lakes Environmental, 2017), an atmospheric dispersion model with high spatial and temporal resolutions. To assess the primary health benefits of tightening PM emission standards, I developed a health benefits mapping tool (BenMAP) database for NE Brazil using the latest integrated exposure-

response model, which maps changes in air quality to changes in health outcomes (BenMAP; U.S. EPA, 2017).

A second contribution my dissertation makes is a direct comparison of the monetary value of the health benefits from tighter PM emission standards with the corresponding emission control costs. To calculate these costs, I relied on the integrated environmental control model from Carnegie Mellon University (2017).

A third contribution is an assessment of health, climate, and electric grid storage and stability implications of high penetrations of VRE, including an assessment of the implications of a 100% renewable energy electricity grid in NE Brazil.

This dissertation is organized as follows. Chapter 2 presents background information and explains why my proposed work is novel and important. Chapter 3 reviews selected studies dealing with energy, air quality and health in Latin America and globally. In Chapters 4-6, I explain my integrated modeling methodology: I motivate why each model was selected, how the different models were used and integrated, and how the sources of uncertainty were examined. In Chapter 7, I present results for each of the three questions analyzed. In Chapter 8, I summarize key conclusions, discuss some policy implications and propose ideas for future work.

2 Background

Climate change and air quality goals are motivating developed and developing countries to reduce greenhouse gas and air pollutant emissions. In this background section I discuss how climate change and air pollution are products of power systems, along with the global burden of disease attributable to air pollution and particulate matter (PM, the sum of suspended solid and liquid particles that are hazardous). Next, I present background information on Brazil, their electrical system, and the Northeast Brazil study area. I then review the air quality and power plant emission standards in Brazil, and briefly discuss their enforcement.

2.1 Climate change and air pollution

Many energy infrastructures rely heavily on the combustion of solid, liquid and gaseous fossil fuels. Two of the main issues with fossil fuel combustion are the products of complete combustion as well as the products of incomplete combustion. Carbon dioxide (CO_2) is a primary product of complete combustion and is the highest contributing anthropogenic gas to Earth's global energy imbalance (Hansen *et al.*, 2005). For example, coal releases on average between 214 and 229lbs CO_2/MMBtu, gasoline and diesel release between 157 and 161lbs CO_2/MMBtu, and natural gas releases 117 lbs CO_2/MMBtu (U.S. Energy Information Administration, 2017b).

Electricity and heat production emissions account for 25% of global anthropogenic greenhouse gas emissions, as well as a substantial part of air quality pollutants. Agriculture and land use account for approximately 24% of global GHG

emissions, followed by industry (21%), transportation (14%), buildings (6.4%) and other energy (9.6%) (IPCC WGII AR5, 2014).

CO_2 is the main greenhouse gas (GHG) contributing to climate change and is produced when carbon molecules in fossil fuels are oxidized to CO_2 during a combustion process. Carbon dioxide absorbs short ray radiation that is reflected off the earth, which is why it is known as a greenhouse gas. The second methane (CH_4) and third nitrous oxide (N_2O) highest contributing greenhouse gases are also released during the lifecycle of energy production (Edenhofer *et al.*, 2014).

Anthropogenic greenhouse gases are changing the Earth's atmospheric composition, the Earth is currently absorbing 0.85 $\pm$0.15 W/m, and thus causing a planetary energy imbalance. Temperature increase, ice sheet disintegration, sea level rise, more extreme weather events and biodiversity extinction are a few of the already observed and expected consequences of the Earth's energy imbalance (Hansen *et al.*, 2005).

Products of incomplete combustion include regional air pollutants, such as particulate matter (PM), nitrogen oxides (NO_x), sulfur oxides (SO_x) and carbon monoxide (CO) (Smith *et al.*, 2013). These pollutants are among the primary contributors to air pollution related premature mortality and morbidity. In particular, ambient $PM_{2.5}$ (airborne particulate matter whose diameter is less than 2.5 micrometers) is now the fifth largest contributor to global disease (Institute of Health Metrics and Evaluation, 2015).

The products of incomplete combustion include particulate matter, mono-nitrogen oxides, nitrous oxides, sulfur oxides, volatile organic compounds and

others, and are transported and transformed and contribute to air pollution. Epidemiological and health economics studies over the last 20 years have established a clear connection between air pollutant concentrations and adverse health effects (Bell *et al.,* 2008; Burnett *et al.,* 2014; Cromar *et al.,* 2016; Jerrett *et al.,* 2005; Moolgavkar 2000; Ostro *et al.,* 2007; Pope *et al.,* 2009; Pope *et al.,* 2002).

Meeting GHG and air pollution goals requires decarbonizing electricity systems as well as electrifying sectors such as transportation and industry, which will substantially increase load on the electric grid (Wei *et al*., 2013). This underscores the importance of understanding the internal and external costs of electricity production. Strategic long-term energy planning can reduce the total cost of meeting energy demand, including the large and often hidden environmental and health costs.

2.2 Global burden of disease relating to air quality

According to the 2015 Global Burden of Disease study, ambient $PM_{2.5}$ now ranks as the fifth largest contributor to global disease, following high blood pressure, smoking, diabetes and high cholesterol (Institute of Health Metrics and Evaluation, 2015). The deaths attributable to ambient $PM_{2.5}$ exposure increased from 3.5 million in 1990 to 4.2 million in 2015. The second largest air pollutant contributing to global disease is ozone, which caused an additional 254,000 deaths in 2015, and was ranked the 34th largest risk factor for global deaths (Aaron J. Cohen *et al*., 2017).

The main ambient pollutants caused by power plants that affect human health are nitrous oxides (NO_x), sulfur dioxide (SO_2), carbon monoxide (CO), ozone (O_3)

and particulate matter (PM) (Smith *et al.,* 2013). This study focuses on particulate matter because it is the main contributor to air pollution related global mortality and morbidity rates (Institute of Health Metrics and Evaluation, 2015).

In their 2015 study, Brauer *et al.* (2015) found that 87% of the world's population lives in areas exceeding the World Health Organization (WHO) Air Quality Guideline of 10 μg/m^3 $PM_{2.5}$ (annual average). From 1990 to 2013 the population-weighted annual average $PM_{2.5}$ increased by 20.4% globally, and increased by 70.4% in Brazil (Brauer *et al.,* 2015).

Table 1 displays the top five causes of mortality worldwide, taken from the World Health Organization 2013 Global Burden of Disease publication. Air quality, or lack thereof, is a strong influence on development of many of the top diseases.

Table 2.1. Top five causes of mortality worldwide in 2012

Rank	Cause	Deaths (000s)	% Deaths	Deaths per 100,000 population
	All Causes	**55859**	**100**	**789.5**
1	Ischemic heart disease	7356	13.2	104
2	Stroke	6671	11.9	94.3
3	Chronic obstructive pulmonary disease	3104	5.6	43.9
4	Lower respiratory infections	3052	5.5	43.1
5	Trachea, bronchus, lung cancers	1600	2.9	22.6

Source: World Health Organization (2015).

In the United States, cardiovascular diseases accounted for approximately 30.7% of deaths in 2012, or 815,700 people. Respiratory diseases accounted for approximately 8.0% of deaths (World Health Organization, 2015). Similarly in Brazil cardiovascular related diseases caused 31% of total deaths, respiratory diseases accounted for 5.5%, and respiratory infections accounted for an additional 6.1% of deaths.

Table 2 displays the cardiovascular and respiratory related deaths in Brazil.

Table 2.2. Cardiovascular and respiratory related deaths in Brazil (2012)

Mortality cause	Number of people ('000)	Percent of total mortality
Population	*198,656*	
All causes of mortality	1318.4	
Cardiovascular disease	408.2	31.0%
1 Rheumatic heart disease	2.9	0.2%
2 Hypertensive heart disease	62.0	4.7%
3 Ischemic heart disease	139.0	10.5%
4 Stroke	123.1	9.3%
5 Cardiomyopathy, myocarditis,…	18.4	1.4%
6 Other circulatory diseases	62.8	4.8%
Respiratory disease	72.7	5.5%
1 Chronic obstructive pulmonary disease	44.8	3.4%
2 Asthma	3.0	0.2%
3 Other respiratory diseases	24.9	1.9%
Respiratory infection	80.7	6.1%
1 Lower respiratory infections	80.3	6.1%
2 Upper respiratory infections	0.3	0.0%
3 Otitis media	0.1	0.0%

Source: (World Health Organization, 2015)

2.3 Brazil

Brazil is the world's fifth largest country by area and spans over 8.5 million km^2 (Instituto Brasileiro de Geografia e Estatistica, 2016). Brazil is both a large producer of oil, the ninth producer of crude oil and other liquids in the world in 2016 for, and is a large producer of renewable energy (U.S. EIA, 2017). In particular, Brazil relies on renewable energy (mainly hydroelectricity) for over 85% of its electricity production.

Electricity demand has been increasing by an average of 4.55% per year in Brazil for the last 20 years (World Bank, 2015). Torrini *et al.* (2016) have forecasted that the average annual electricity demand would increase by 4.72% across Brazil from 2015 to 2030. By comparison, the U.S. Energy Information Administration forecasted a 60% increase in world energy consumption from 2010 to 2040, with 85% of the world energy consumption increase happening in non-OECD (Organization for Economic Co-operation and Development member countries, which includes Brazil (Leahy *et al.,* 2013).

Brazil has been steadily investing in additional electricity infrastructure capacity (REN21, 2017). However, severe droughts (most recently in 2015) have caused the Brazilian government to reconsider the country's dependency on hydroelectricity. Although Brazil has a decadal electricity expansion plan promoting the expansion of renewable generation (e.g., Law number 10,438; Ministério de Minas e Energia, 2014), there is now a debate about how much of the increasing energy demand should be met with hydroelectricity versus thermal versus

intermittent renewable generation (Silva *et al.,* 2016; Ministério de Minas e Energia, 2014).

Thermal generation offers a number of advantages, including low costs as well as predictable and flexible generation to balance load and generation, but it has a number of substantial health and climate impacts (IPCC, 2013; Lelieveld *et al.,* 2015).

Increasing the shares of wind and solar electricity in Brazil's electricity system can, however, create substantial problems at the local (near power plant) and system levels (de Jong *et al.,* 2016). Local issues include voltage control, fault currents (abnormal electrical currents) and harmonic distortion and flicker (when current and voltage waveforms are non-sinusoidal). System issues include a potential imbalance between load and generation, reactive power generation and reduced frequency control (Anaya-Lara *et al*. 2009; Borba *et al*., 2012).

Apart from its size, I initially selected Brazil because of Brazil's rapidly increasing electricity demand, a planned electric system capacity increase of 57% from 2013-2023, large hydroelectric capacity and dependency, and the tremendous intermittent renewable generation potential in Northeast (NE) Brazil (*Ministério de Minas e Energia, 2014*). Additionally, detailed electricity grid data for Brazil was available through a collaboration with the Center for Energy and Environmental Economics (CENERGIA) at the Federal University of Rio de Janeiro. These data have been used in previous studies of NE Brazil's electric grid, such as Miranda *et al*. (2017), Pupo *et al*. (2016), Soares *et al*. (2012a) and Soria *et al*. (2016).

2.4 Organization of Brazil's electricity sector

Since 1990, the Brazilian electricity sector has transitioned from full state-owned to a market where public and private companies compete.

A wholesale electricity market was created in 1998 along with the National Grid Operator (ONS) for coordinating generation and transmission. Electricity is sold in a Free Trade Environment (ACL) controlled by the Brazilian Electric Energy Regulatory Agency (ANEEL), which is the only place electricity distributors are allowed to purchase electricity. Brazilian energy policy, research and regulation groups include (Francisco, 2012):

1. Brazilian Committee of Energetic Policies (CNPE): proposes policies to the Ministry of Mines and Energy.
2. Ministry of Mines and Energy (MME): plans and develops policies for the electric energy sector.
3. Brazilian Electric Sector Monitoring Committee (CMSE): evaluates the stability and security of the electric energy supply.
4. Company of Energetic Research (EPE): is responsible for energy research supporting long-term energy planning in Brazil.
5. Brazilian Electric Energy Regulatory Agency (ANEEL): regulates the electricity sector.
6. Chamber of Electric Energy Trade (CCEE): regulates the wholesale electricity market.
7. National Grid Operator (ONS): coordinates the generation and transmission of electricity.

An electricity crisis from 2001-2002 caused by a few years with less precipitation than average prompted Law 10,848 in 2004, which establishes clear rules to ensure reliable energy supply and energy infrastructure expansion (Francisco, 2012).

2.5 Brazil's electricity system

Brazil has two main electricity subsystems: the S1 subsystem includes the South, Southeast and Midwest regions, and the S2 subsystem includes the North and Northeast regions. As isolated subsystem R provides power in the Amazon.

Figure 2.1. Subsystems of Brazil's electric system

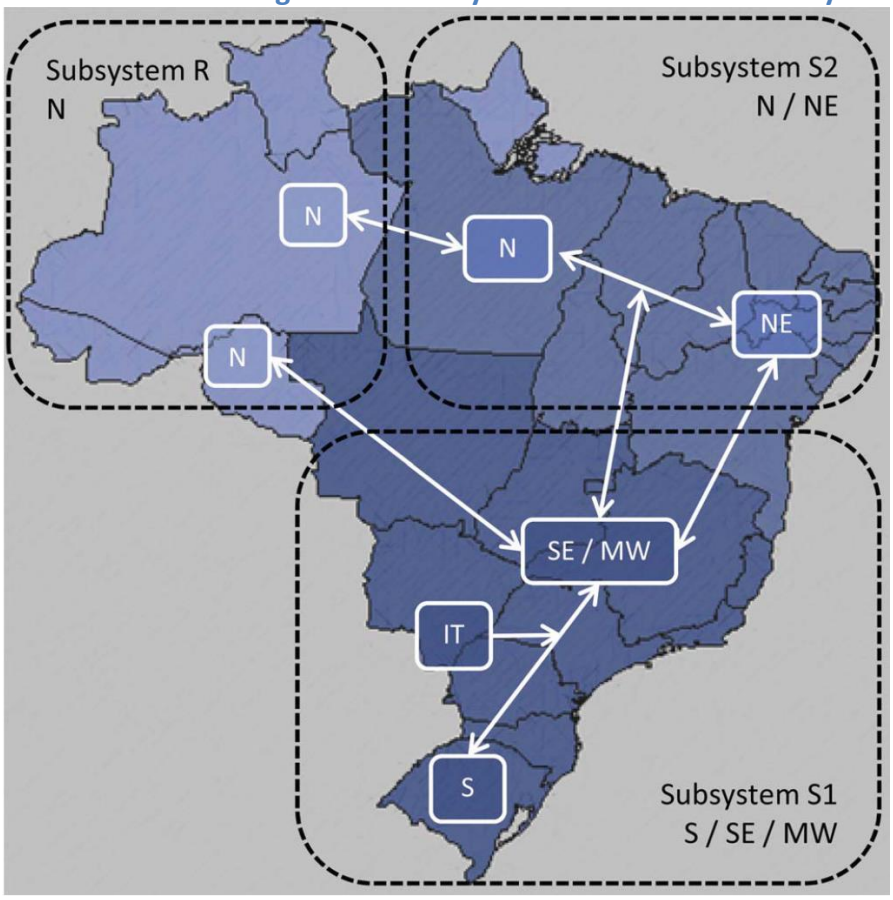

Source: (Soares *et al.* 2012)

Brazil's Interconnected System (SIN), the transmission system that connect Subsystem S1 and Subsystem S2, is displayed on Figure 2. The numbers represent the numbers of circuits and each color represents the transmission line voltage capacity, with solid lines representing current transmission infrastructure and dotted lines representing planned transmission infrastructure (ANEEL, 2017).

Figure 2.2. Transmission system in Brazil

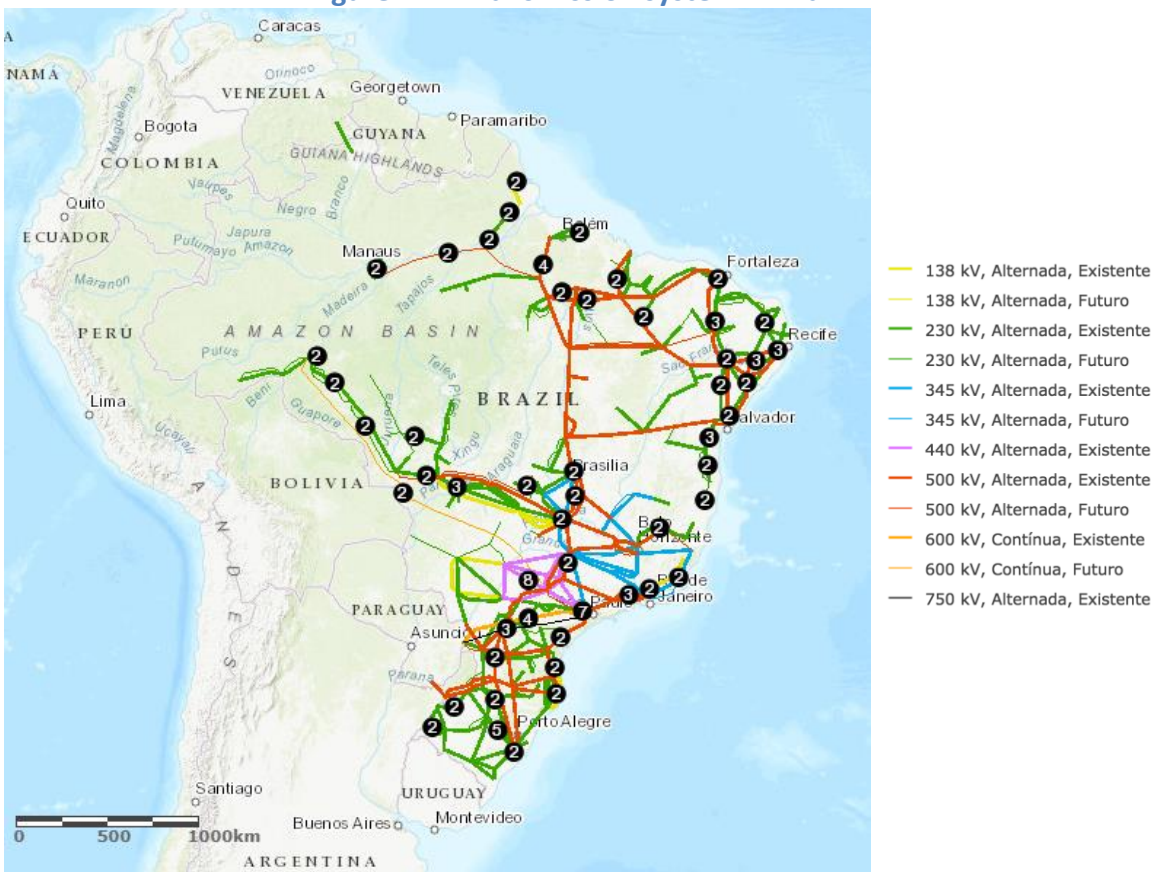

Source: (http://sigel.aneel.gov.br/portal/home/)

As of 2014, Brazil's electricity production was 66.6% hydroelectric, 8.6% natural gas, 8.1% biomass, 4.5% imported, 4.2% wind, 3.7% oil, 2.4% coal, 1.4% nuclear, 0.5% process gas (gas produced by industrial processes) and

approximately 0% solar. Only 3.4 % of the generation occurs in the Amazon, which is known as the isolated (R) system (Ministério de Minas e Energia, 2014).

Many factors are driving Brazil's current energy infrastructure expansion planning (Avelino, Hewings, & Guilhoto, 2015):

- Meet electricity increasing energy demand
- Reduce contributions to climate change;
- Improve energy security;
- Reduce dependency on hydroelectric power;
- Reduce dependence on fossil fuels;
- Increase wind and solar generation; and
- Address electric grid issues with large renewable penetrations, including voltage control, fault current, harmonic distortion and flicker, load and generation balancing, reactive power generation and frequency control.

With these priorities in mind, in 2014 the Ministry of Mines and Energy in collaboration with the Company of Energetic Research approved an energy expansion plan from 2013 to 2023, which shown in Table 2.3.

Table 2.3. Brazilian energy expansion plan through 2023

	Evolution of installed capacity per generation source (GW)											Increase (%)
	2013	2014	2015	2016	2017	2018	2019	2020	2021	2022	2023	2013-2023
Type												
Renewable	103.2	110.3	118.6	125.4	133.2	142.8	146	149.7	154.5	158.8	164.1	59%
Hydroelectric	79.9	82.6	87.2	92.2	96.1	100.9	101.9	103.3	106.2	108.9	112.2	40%
Imported	6.1	6	5.9	5.8	5.7	5.6	5.4	5.3	5.1	4.9	4.7	-23%
Other	17.4	21.7	25.5	27.4	31.4	36.3	38.7	41.1	43.2	45.1	47.2	171%
Small Hydro	5.3	5.5	5.7	5.7	5.9	6.3	6.4	6.6	6.8	6.9	7.3	38%
Wind	2.2	5.5	9	10.8	14.1	17.4	18.4	19.4	20.4	21.4	22.4	918%
Biomass	9.7	10.7	10.8	10.9	10.9	11.6	12.4	13.1	13.5	13.7	14	44%
Solar	0	0	0	0	0.5	1	1.5	2	2.5	3	3.5	N/A
Non-renewable	21.3	22.1	22.8	22.8	22.7	24.2	24.7	26.2	27.7	29.2	31.7	49%
Nuclear	1.9	1.9	1.9	1.9	1.9	3.4	3.4	3.4	3.4	3.4	3.4	79%
Natural Gas	10.7	11.4	12.2	12.2	12.5	12.5	13	14.5	16	17.5	20	87%
Coal	3.2	3.2	3.2	3.2	3.2	3.2	3.2	3.2	3.2	3.2	3.2	0%
Fuel Oil	3.4	3.5	3.5	3.5	3.5	3.5	3.5	3.5	3.5	3.5	3.5	3%
Diesel Oil	1.4	1.4	1.3	1.3	0.9	0.9	0.9	0.9	0.9	0.9	0.9	-36%
Process Gas	0.7	0.7	0.7	0.7	0.7	0.7	0.7	0.7	0.7	0.7	0.7	0%
Renewable	82.8%	83.3%	83.9%	84.6%	85.4%	85.5%	85.5%	85.1%	84.8%	84.5%	83.8%	1%
Non-renewable	17.1%	16.6%	16.1%	15.4%	14.6%	14.5%	14.5%	14.9%	15.2%	15.5%	16.2%	-5%
Total Capacity	124.5	132.4	141.4	148.2	155.9	167	170.7	175.9	182.2	188	195.8	57%

Source: Ministério de Minas e Energia *(2014)*.

Total installed capacity is expected to increase by 57% from 2013 to 2023, with renewable capacity (including hydropower) increasing by 59% and non-renewable capacity increasing by 49% (Ministério de Minas e Energia, *2014*). This expansion plan supports Law number 10,438, which was approved in 2002 to create the Program of Incentive to Alternative Source of Energy (PROINFA) to increase the share of wind, biomass and small hydroelectric power plants (Francisco, 2012).

The installed capacity of most energy sources is planned to increase substantially: hydroelectric 40%, wind 918%, natural gas 87%, nuclear 79%, biomass 44%, and solar from 0 to 3.5%. The installed capacity of diesel power plants is planned to decrease 36%, along with a 23% reduction in imported electricity. The installed capacity of coal power plants is not planned to change (Ministério de Minas e Energia, *2014*).

2.6 Northeast Brazil study area

The northeast region of Brazil (NE Brazil) includes nine states with a combined population of 54 million people over 1,500,000 km^2. The main cities of NE Brazil are Recife, Fortaleza and Salvador with populations of 3.69 million, 3.61 million and 3.57 million respectively (Instituto Brasileiro de Geografia e Estatistica, 2016).

Electricity system demand is forecasted to increase an average of 4.77% per year across the nine states in NE Brazil (Torrini *et al.,* 2016). While integrating large quantities of VRE in the NE Brazil grid will create electricity grid stability issues

(Miranda *et al.,* 2017; Borba *et al.,* 2012), fossil fuel combustion causes substantial health and climate problems (IPCC WGII AR5, 2014; Lelieveld *et al*., 2015).

The installed capacity (total capacity of all power plants) in NE Brazil exceeds 29,000 megawatts (MW), with an annual electricity demand of over 85,000 GWh (Operador Nacional do Sistema Eletrico 2016). The installed capacity of electric generators regulated by the central dispatch authority Operador Nacional do Sistema Elétrico ONS in NE Brazil is shown in Table 4.1 in the Plexos Methodology chapter.

One of the reasons I selected the NE Brazil electricity grid for this study is because NE Brazil is a semi-arid region with exceptionally high capacity factors for wind and solar electricity production, along with large hydroelectric potential (Silva *et al.,* 2016; Krauter 2005). Another reason is that NE Brazil has two large coal power plants: Porto do Pecem I (720 MW) and Porto do Pecem II (360 MW). Both are located within 30 km of the Fortaleza metropolitan area (see Figure 1). Additionally, a number of diesel and gas power plants are located within 5 km of the metropolitan areas of Fortaleza, Recife and Salvador.

2.7 Ambient air quality standards in Brazil and worldwide

Ambient air quality standards are set to limit human exposure to unsafe air pollutants in order to protect sensitive populations such as children, asthmatics and the elderly, as well as public health in general (U.S. Environmental Protection Agency, 2017b). Air quality standards are based on the average concentration of pollutants in an area over a specific time interval, such as an hour, a day or a year.

In their review of 170 countries, Joss *et al.* (2017) found that $PM_{2.5}$ air quality standards vary from 10 µg/m^3 to close 100 µg/m^3 (annual average). Figure 4 shows PM_{10} ambient air quality standards by country, including 57 countries that still did not have official air quality standards as of 2016. Note that most countries set ambient air quality standards based on PM_{10}, while a few others (including the U.S.) set ambient air quality standards in terms of $PM_{2.5}$.

Figure 2.3. PM_{10} standards worldwide

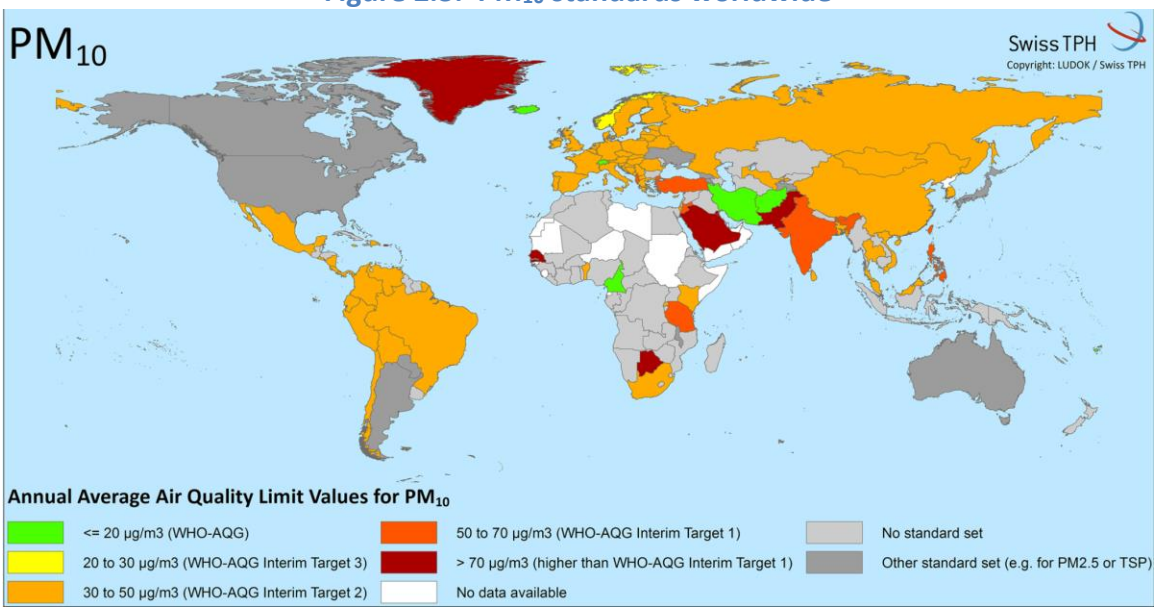

Source: Joss *et al.* (2017)

Of the 53 countries in the European Union, 50 countries have at least one ambient air quality standard, and almost all of those countries have a PM_{10} standard within the WHO interim target 2, between 30 and 50 µg/m^3 (annual average). China also has a PM_{10} air standard in the WHO interim target 2, along with most countries in Latin America. India's PM_{10} air quality standard is in the WHO interim target 1,

between 50 and 70 μg/m^3. Most countries in Africa do not have standards or no data was available (Joss *et al.*, 2017).

The United States and some other countries, like Canada and Australia, have $PM_{2.5}$ air quality standards. The National Ambient Air Quality Standard for the U.S. is an annual average of 12.0 μg/m^3 for primary $PM_{2.5}$ and 15.0 μg/m^3 for secondary $PM_{2.5}$ (U.S. Environmental Protection Agency, 2017b). Secondary $PM_{2.5}$ forms when primary emissions react with other gases to form new particles.

Table 2.4. Air quality standards in Brazil

Pollutant	Time of Sampling	Primary Pattern μg/m^3	Secondary Pattern μg/m^3	Method of Measurement
CO	1h	40,000	40,000	Infra-red or non-dispersive
	8h	10,000	10,000	
Smoke	24h	150	100	Reflectance or similar
	Yearly average	60	40	
Inhalable particles	24h	150	150	Inertial separation, filtration or similar
	Yearly average	50	50	
NO2	1h	320	190	Chemiluminesence or similar
	Yearly average	100	100	
O3	1h	160	160	Chemiluminesence or similar
Total Suspended Particles	24h	240	150	Large volume sampling or other
	Yearly average	80	60	
SO2	24h	365	100	Pararosaniline or other
	Yearly average	80	40	

Source: (Vormittag, 2014)

While Brazil does not have air quality standards for $PM_{2.5}$, it has ambient air quality standards for several the pollutants outlined in Table 2.4. There are 252 monitoring stations in 10 of Brazil's largest cities (Vormittag, 2014).

Mean $PM_{2.5}$ concentrations have been measured in Brazilian cities. In the six cities of São Paulo, Rio de Janeiro, Belo Horizonte, Curitiba, Porto Alegre and Recife, the average $PM_{2.5}$ concentrations over the winter of 2007 and 2008 were 28, 17.2, 14.7, 14.4, 13.4, and 7.3 µg/m3, respectively (Andrade *et al.,* 2012).

The Conselho Nacional do Meio Ambiente (CONAMA, Brazilian National Environmental Council) is expected to implement a $PM_{2.5}$ standard in Brazil, but it has not yet happened (Vormittag, 2014).

2.8 PM emission standards in Brazil and worldwide

Emission standards regulate the amount of pollutants that a source can release into the air, typically per unit of energy output or input, or per unit volume of air. Power plant emission standards can be defined in different units, however they are often technology specific and defined per unit of electricity generated (gram per kilowatt-hour g/kWh) or per volume of exhaust gas flow (milligram per cubic meter mg/m^3).

Emissions from power plants are a product of the quantity of electricity generated and the emission rate per unit of electricity generation of each pollutant. The quantity of emissions produced is directly proportional to the emission rate.

In an analysis of emissions from coal power plants in India, Guttikunda & Jawahar (2014) reviewed emissions standards for coal power plants in India, China, Australia, the EU and U.S., which they presented in mg/Nm^3 (milligrams per normal

cubic meter, which is a cubic meter at 0° Celsius). Table 2.5 summarizes the PM emission standards by country. Guttikunda and Jawahar reported that India had the loosest standards of the countries they reviewed, ranging from 150 to 350 mg/Nm^3, and that the U.S. had the strictest standards – ranging from 6 mg/Nm^3 for new plants to 37 mg/Nm^3 for older plants.

Table 2.5. PM emission standards by country

Country	Applicability	PM Emission Standard (mg/Nm3)
India	<210 MW	350
	>210 MW	150
China	All regions	30
	Key regions	20
Australia	1997-2005	100
	After 2005	50
European Union	Pre-2003, <500 MW	100
	Pre-2003, >500MW	50
	Post-2003, <100 MW	50
	Post-2003, >100 MW	30
USA	Old	37
	New	6

While reviewing documents published by Brazil's national agencies, I found numerous emission standards for thermal power plants, including a very large range for PM emissions from coal power plants using imported and domestic coal. The Brazilian PM emission standards for coal power plants were higher compared to the U.S., EU, Australia and China.

The Ministry of Mines and Energy's (MME) reports a very high PM_{10} emission standard of 28.15 g/kWh for power plants using imported coal, and an even higher PM_{10} emission standard of 254.5 g/kWh was reported for power plants using

Brazilian coal (Ministério de Minas e Energia, 2007). It is important to note that the predominant environmental concern with using Brazilian coal as opposed to imported coal is that the British thermal unit BTU value of Brazilian coal is about half of the U.S. average coal BTU value, requiring twice as much coal to generate the same amount of electricity. Moreover, burning one ton of Southern Brazilian coal compared to burning one ton of U.S. coal releases about twice as many environmentally concerning elements, and about four times as much mercury (Silva *et al.,* 2009).

Ferreira *et al.* (2014) published a study on the air quality standards and emission limits in Brazil and reported a PM_{10} emission standard by Brazil's national environmental council (CONAMA) for coal power plants over 70 MW of 800 g/10^6 kcal, which is approximately 390 mg/Nm^3 or 0.69 g/kWh (Ferreira *et al.,* 2014).

A report by the Government of Ceara states that the Porto do Pecem coal power plants, which are the only coal power plants in NE Brazil, must meet a lower than normal PM_{10} standard of 204 mg/Nm^3, or 0.36 g/kWh. This is because the Brazilian Development Bank provided funding for new power plants under the condition that they meet this standard (Governo do Estado do Ceará, n.d.).

Previous studies have also found multiple PM_{10} emission standards for coal power plants in Brazil. Alves and Uturbey (2010) used three PM_{10} emission rates for coal power plants published by the MME to estimate health costs under different standards: 254.5 g/kWh for domestic coal, 28.15 g/kWh for imported coal, and 1.53 g/kWh based on a CONAMA standard.

In summary, I found at least three different PM_{10} standards for coal power plants in Brazil when reviewing standards from Brazil's Ministry of Energy, National Counsel of the Environment and Brazilian Development Bank:

1) 28.15 g/kWh, in a 2030 National Energy Plan (Ministério de Minas e Energia, 2007);
2) 390 mg/Nm^3, published by the National Counsel of the Environment (CONAMA) (Ferreira *et al.,* 2015); and
3) 204 mg/Nm^3, which is the Brazilian Development Bank (BNDES) standard for power plants receiving BNDES funding (Governo do Estado do Ceará, n.d.).

Emission standards are reported in different units. I converted the units to g/kWh because the national emissions standards for all types of power plants in Brazil are presented in g/kWh (Ministério de Minas e Energia, 2007). The coal power plant standards were converted using data for the Porto do Pecem coal power plants, which are the only coal power plants in NE Brazil. A flue gas flow rate, which is the volumetric flow rate of combustion exhaust gas exiting the power plant, of 636,000 Nm^3/h was assumed based on data from the Porto do Pecem power plants, however, data required for an extensive thermodynamic analysis was not available, even when checking a detailed atmospheric dispersion study of the Porto do Pecem Industrial Complex (Governo do Estado do Ceará, n.d.). This flue gas flow rate is very similar to the flue gas flow rate of 621,000 m^3/h that was measured for a similar size power coal power plant (290 MW) in the U.S. (Klein *et al*., 1975).

To convert emissions standards from g/kWh to mg/Nm^3, the capacity (360 MW) of one of the Porto do Pecem power plant units was converted to power output

in terms of kwh/h. The power output of one of Porto do Pecem coal power plant units, which is approximately 360,000 kWh/h, was then multiplied by the emission standard (g/kWh) to obtain the emissions per hour (g/h). The emissions per hour were then divided by the flue gas flow rate per hour (636,000 Nm^3/h), to determine the quantity of emissions per flue gas flow rate (g/Nm^3). The emissions per flue gas flow rate (g/Nm^3) were then converted from g/Nm^3 to mg/Nm^3.

Equation (1) displays the equation for converting an emission standard in g/kWh to g/Nm^3, which can be multiplied by 1000 (mg/g) to obtain the standard in mg/Nm^3. The same calculations can be performed in reverse to convert emissions standards from mg/Nm^3 to g/kWh.

$$\frac{emission\ standard\ \left(\frac{g}{kWh}\right) * power\ output\ \left(\frac{kWh}{h}\right)}{flue\ gas\ flow\ rate\ (\frac{Nm3}{h})} = emission\ standard\left(\frac{g}{Nm3}\right) \quad (1)$$

In reviewing the U.S. EPA PM emission standards, which has some of the strictest standards worldwide, a PM_{10} emission standard of 0.09 lb/MWh was set for all electric utility steam generating units constructed after May 3, 2011 (US Environmental Protection Agency, 2015). This standard, which is fuel independent, is equivalent to approximately 0.04 g/kWh[1].

Table 2.6 displays the emission standard conversion for the three PM_{10} standards for coal power plants in Brazil and the U.S. EPA PM_{10} standard for electric utility steam generating units (which includes coal power plants).

[1] 1 lb/MWh = 0.4536 kg/MWh = 0.4536 g/kWh

Table 2.6. Emission standard conversion

Emission standard (g/kWh)	Power output (kWh/h)	Emissions per hour (g/h)	Flue gas flow rate (Nm3/h)	Emission per m3 (g/Nm3)	Emission standard (mg/Nm3)
28.15	360000	10134000	636000	15.934	15934
0.69	360000	248400	636000	0.391	390
0.36	360000	129600	636000	0.204	204
0.04	360000	14400	636000	0.023	23

I selected the three Brazilian PM_{10} emission standards and the most recent U.S. PM_{10} emission standards to set the stage for analyzing the health benefits and control costs of tightening emissions standards. I developed three scenarios for assessing the health benefits and control costs of tightening PM emission standards: Scenario 1 moves from a very high PM_{10} emission standard of 28.15 g/kWh to a moderate standard of 0.69 g/kWh; Scenario 2 tightens the PM_{10} standard further, from 0.69 g/kWh to 0.36 g/kWh; and Scenario 3 tightens PM_{10} standard from 0.36 g/kWh to a very low standard of 0.04 g/kWh.

In the simulations designed to assess the health, storage and grid stability implications of high penetrations of renewables, the two coal power plants of NE Brazil (Porto do Pecem I and II) are assumed to emit 0.36 g/kWh PM_{10} based on the emission standard specific to the Porto do Pecem power plants published in the report by the Government of Ceara (Governo do Estado do Ceará, n.d.).

2.9 Environmental policy enforcement

As Brazil is a developing country, it is important to consider the level of enforcement of emissions standards. Most countries in Latin America have separate state and federal regulations, with federal regulations setting minimum

environmental standards and individual states having the power to impose and enforce tighter standards. The greater the penalty for failure to comply with environmental policy, the more attention firms are likely to pay to regulatory legislation (Da Motta *et al*. 1999).

While command and control (a specific standard set and enforced by law) and market based incentive approaches for environmental policy have been successful, they also can increase the technical and financial burdens on fragile institutional structures, making effective monitoring and enforcement difficult (Da Motta *et al.,* 1999).

Power generation companies have faced regulatory and social pressure to reduce pollution in Brazil for some time. While power generation companies benefit from advertising environmental improvements, Barton *et al.* (2000) found that the documentation and claims from power generation companies and the realities of emission levels are of concern. Estimating actual levels of emissions reductions then places a burden on regulatory agencies (Barton *et al.,* 2000).

Brazilian government agencies regulating environmental policy have varying resources, monitoring styles, and enforcement strategies depending on the state. For example, the Sao Paulo regulatory agency Environmental Company of the State of Sao Paulo (CETESB) closely monitors agreements to reduce emissions, while the Rio de Janeiro regulatory agency State Foundation of Environmental Engineering (FEEMA) struggles with low resources. Further differences arise with the allocation of levied penalties. While FEEMA in Rio de Janeiro requires non-compliant firms to invest the penalties in environmental improvements, the penalties levied in Sao

Paulo go to the state treasury and the regulatory agency CETESB does not receive any of the funds (Barton *et al.,* 2000).

Although the Brazilian regulatory system varies in terms of delivering and enforcing environmental policy deterrents and incentives, it seems that firms are responsive to regulatory pressures, despite different starting points, paces of change and relationships with regulators (Barton *et al.,* 2000).

How firms' respond to emissions enforcement has also be studied in the U.S. Keohane *et al.* (2009) used a discrete choice model to estimate that in 1999, when the U.S. EPA sued the owners of 46 plants for emissions violations, emissions fell approximately 10% at the plants with one standard deviation greater probability of being sued (Keohane *et al.,* 2009). In their review of empirical evidence from the U.S. EPA and other sources in the U.S. on the impacts of environmental monitoring and enforcement Gray and Shimshack (2011) found that monitoring and enforcement reduces violations at the targeted firms and at facilities other than the targeted ones, resulting in reductions in violations and emissions.

Although this dissertation does not assess the costs of enforcing tighter emissions standards, it does provide a monetary valuation of health benefits, where it becomes very clear that additional enforcement costs would be far outweighed by the magnitude of health benefits.

3 Literature Review

To inform my modeling choices and contextualize my contributions, I reviewed selected studies relating to energy, air quality and health impacts in Brazil and around the world.

I first review key studies relating to power plant emissions and health impacts in Brazil and Latin America. Next, I consider studies related to energy sector emissions and air pollution in Brazil and Latin America, followed by the U.S., Europe, and elsewhere. I also review selected epidemiological studies to understand how connections between air pollution exposure and health impacts have been derived, with an emphasis on Brazil and Latin America, as well as the U.S. and other parts of the world. To understand how previous studies have monetized health impacts related to air pollution, I also cover some monetary valuation studies. In the last section, I discuss how high penetrations of renewables can impact the electric grid operation and utilities.

3.1 Key electricity grid emissions and health impact studies

I found two key studies for Brazil (Avelino *et al.*, 2015; Alves and Uturbey, 2010), and one in Mexico (Lopez *et al.,* 2005), which are reviewed in detail below.

Avelino *et al.* (2015) developed an energy planning model that quantifies economic, environmental and social impacts of electricity generation. Their study quantifies the electricity generation, employment opportunities, emissions and expected disease incidence of constructing a 150 MW wind turbine in 3 different states of Brazil. The Energy Module estimates electric grid dispatch using outputs

from the proprietary NEWAVE model, which is the dispatch model that has been used by ONS since 1979. The dispatch process is based on marginal price and flexibility constraints as follows: weather selection -> precipitation profile and hydro generation constraints -> power plant dispatch based on price and flexibility.

The environmental module takes emissions data from ONS (2010) and ANEEL (2010), which provide information like fuel type, nominal power, geographic coordinates and municipality. GIS data were used for meteorological conditions and applied in a Gaussian Plume Model (GPM) for each region to determine air quality concentrations of nitrous oxides (NO_x) and carbon monoxide (CO). Only primary emissions were considered. As there were no available gridded emissions by industry databases for Brazil, each municipality within a state was allocated a share of emissions proportional to its industrial GDP. Additionally, they assumed that the terrain is flat, and that all emissions stack heights are 50 m. GIS information on wind speed, bearing and latitude/longitude at the municipal level was gathered from CEPEL SWERA with a 10km x 10km resolution.

The health module adds pollutant concentrations from emissions to existing pollution. The authors did not specify from which studies they selected dose-response functions. They monetized health outcomes using local treatment costs obtained from the national Brazil healthcare system DATASUS.

Results confirm the importance of temporal and spatial dimensions. A dry season results in ~5% increase in morbidity treatment costs, with very little variation between study areas of Rio Grande do Sul, Ceara and Rio Grande do Norte (Avelino *et al.,* 2015).

In a second key study for Brazil, Alves and Uturbey (2010) applied monetary health and environmental damage costs to the Brazilian electricity matrix from 2007 to 2016. The authors' purpose is to highlight the importance of external costs in long-term energy planning in Brazil.

Local pollution due to particulate matter and global warming costs were analyzed. Local pollution costs were estimated in a four-step process: source emissions -> pollutant concentrations -> exposure to impact -> economic valuation of impact. The impact on human health was estimated by deriving an estimate of the number of diseases/kWh and deaths/kWh. Diseases/kWh were based on simplified dispersion assumptions, where meteorological conditions are not taken into account and wind speeds are uniformly assumed at 3 m/s. An individual risk index was calculated by multiplying the PM concentration associated to source 'n' by a dose response coefficient. A morbidity risk index, representing the collective risk, was calculated by multiplying the individual risk by one of three population density indexes: high density (> 1000 inhabitants/km^2), medium density (> 100 inhabitants/km^2) and low (>20 inhabitants/km^2 density) .

A mortality risk index was calculated by taking health data from the Brazilian Health Ministry (http://www.datasus.gov.br/DATASUS/index.php) to relate the number of respiratory hospitalizations to respiratory deaths. The relationship was 0.02623 respiratory deaths/respiratory hospitalization (Alves and Uturbey, 2010). While only public records are available, 90% of Brazilians use public healthcare (Avelino *et al.,* 2015).

The value of a statistical life (VSL) was used to monetize mortality. Contingent valuation, based on willingness to pay for reducing risks of premature disease, was used by previous work to adapt European values to Brazil. Alves and Uturbey (2010) used per capita income, life expectancy, health expenses and income-elasticity data in a benefits transfer technique to derive a VSL in Brazil of US$800,258. Morbidity was monetized using the disease cost method to monetize the cost of hospitalizations, medical care, medicines and lost work days at an average of US$1,985.03 per disease. This does not take into consideration prevention costs, pain or lost leisure time. A correction factor of 1.85 was used to determine a more complete willingness to pay for reducing respiratory disease risks at US$3672.20 per disease. The total economic value to human health impacts of PM emissions was calculated by multiplying the morbidity value by the morbidity risk index, and the mortality value by the mortality risk index (Alves and Uturbey, 2010).

To monetarily value environmental degradation, the electricity generation by thermal plants each year from 2007 – 2016 was calculated to determine annual CO2e emissions for each source, and then a value of 19 EUROS/tCO2e was applied. Interestingly, results indicate that on a basis of 19 EUROS/tCO2e, society could incur greater costs from local pollution caused by a small number of plants than from global warming (Alves and Uturbey, 2010).

There are many sources of uncertainty in Alves and Uturbey study, which come from the assumptions they made, available data, and model constraints. First, spatial and temporal resolutions are not included. They assumed that the whole

population receives the same pollutant doses and the number of respiratory diseases associated to electricity generation pollution is equal to respiratory-related hospitalizations. However, not all persons with respiratory disease are hospitalized. Similarly, linear C-R coefficients were used, which implies a linear relationship, while most C-R curves are non-linear. Relative risk also varies by age, which was not accounted for (Alves and Uturbey, 2010). While there are many ways that the study of external costs in Brazil relating to electricity production could be improved to reduce uncertainties, this study highlights the magnitude of external costs in energy production, even in electricity grids with high penetrations of renewables.

The third key study was contributed by Lopez *et al.* (2005), who focus on Mexico. The authors used CALPUFF to assess $PM_{2.5}$ health impacts from one of Mexico's largest power plants located on the eastern coast. Concentrations of primary $PM_{2.5}$, SO_2 and NO_x were estimated, along with the secondary particulate matter species ($(NH_4)_2SO_4$, HNO_3 and NH_4NO_3 across a 120 km x 120 km modeling domain. They analyzed impacts due to long term mortality, ignoring morbidity because hospital records were not available and because mortality effects due to long term mortality are far greater than hospital admissions and mortality affects due to short term exposure. Concentration-response (C-R) functions based on U.S. studies were used because of a dearth of long-term mortality studies in Mexico. Using a 0.4 income elasticity with willingness to pay to avoid negative health impacts, a VSL of $530,000 in 2001 US dollars was derived. They found an annual average $PM_{2.5}$ of 0.12 $\mu g/m^3$ (0.00 – 1.43 $\mu g/m^3$), resulting in approximately 30 deaths annually valued at US$8 million. Secondary particulate matter formation

contributed to over 80% of mortality impacts, most of which due to sulfate formation caused by the high sulfur content fuel oil used by the power plant (López *et al.,* 2005). The authors noted that future studies should include a larger study domain and simulate an entire year of air quality concentrations.

3.2 Air pollution studies in Brazil and Latin America

Air quality health impact studies analyze how changes in air quality can affect human health. The changes in air quality can be a product of introducing a new program, such as tighter emissions standards in the electricity or transportation sector, the adoption of new technology, such as electric vehicles, or reducing observed air quality pollutant concentrations by implementing a lower emission standard.

Bell *et al.* (2006) assessed how health effects vary between a business as usual scenario and an emissions control policy in Sao Paulo (Brazil), Mexico City (Mexico) and Santiago (Chile). Annual PM_{10} and ozone pollution levels were estimated in Sao Paulo, Mexico City and Santiago under both scenarios.

To estimate health impacts, Bell *et al.* (2006) selected a set of C-R functions from existing studies, using a weighted average between available Latin America data and other countries. For the health endpoints where Latin American C-R functions were not available, results were pooled from multiple locations using a random effects model. To monetize health impacts, the authors used both a willingness-to-pay and a cost-of-illness valuation method. Bell and colleagues gathered data from valuation studies in Sao Paulo, Mexico City, Santiago, and

Buenos Aires, and when Latin American valuation data were not available, they used United States values from BenMAP with income adjustment factors.

Results show that from 2000-2020, the reductions in air pollution prompted by the control scenario could save approximately $21 billion (COI) to $165 billion (WTP) in avoided health outcomes across the three cities. Assumptions include population growth, air pollutant concentrations in future years, concentration–response functions, and the economic value of avoided health outcomes (Bell *et al.,* 2006).

Shindell *et al.* (2011) examined how tighter emissions standards, relative to current trends, would affect premature deaths, ozone-related agricultural yield losses and radiative forcing in North America, Europe, Africa, Middle East and Latin America. Two sets of C-R functions were used to capture uncertainty. Premature mortality was characterized using the value of a statistical life (VSL) approach, with one trial using the USEPA preferred VSL of $9,500,000 for all regions, and a second trial adding in the USEPA elasticity of 0.40 between income and WTP to estimate country-specific VSLs on the basis of the relationship between country-specific income per capita and that of the U.S., using World Bank data (Shindell *et al.*, 2011).

Alves and Uturbey (2010) calculated a mortality risk index by taking health data from the Brazilian Health Ministry to relate the number of respiratory hospitalizations to respiratory deaths (they assumed that the total population receives the same pollutant doses). Additionally, Lopez *et al.* (2005) used CALPUFF to estimate that a large fuel oil power plant in Mexico contributes an annual average

of 0.12 μg/m^3 (0.00 – 1.43 μg/m^3) $PM_{2.5}$, resulting in approximately 30 additional deaths annually, valued at 8 million USD/yr.

Miraglia *et al.* (2005) applied the Disability-Adjusted Life Years (DALY) method to assess the health burden and cost estimate due to air quality in Sao Paulo, Brazil. The DALY method, developed in 1996 and advanced by the World Bank and World Health Organization, standardizes health cost estimates worldwide by using a single measure of health outcome to express costs and avoid monetary variations and limit uncertainty. Miraglia estimated that 28,212 DALYs were caused by air pollution in Sao Paulo in 2003. They concluded that Sao Paulo contributed 0.4% to the global burden of disease caused by air pollution with a population that is only 0.17% of the world's population, which suggests that in 2003 Sao Paulo contributed 2.4 times the global per capita average towards the global burden of disease caused by air pollution (Miraglia *et al.*, 2005).

Andre *et al.* (2012) analyzed the health impacts of delaying clean diesel technology standards in Brazil. Using Brazil specific C-R functions (Braga *et al.,* 2001; Gouveia *et al.,* 2004) for children's (0 to 4 years) respiratory related hospital admissions and the WHO guideline of a 1.006 relative risk increase in adult mortality per μg/m^3 increase of $PM_{2.5}$, they estimated that up to 13,984 excess deaths would result from delaying the clean diesel standard (Andre *et al.,* 2012).

3.3 Electric grid emissions impact studies in the U.S., Europe, China and India

While the impact of electric grid emissions on air quality and human health has been studied in many developed and developing countries, the majority of these studies

deal with the U.S. The design of these studies varies in complexity, from simple estimations of power plant emissions and atmospheric dispersion, to more complex electricity dispatch and three-dimensional atmospheric dispersion with chemical transformation models. Most studies estimated power plant emissions instead of simulating electric grid operation in time and space, which is important because the impacts of air pollutants depends on when and where pollution is emitted.

Among the studies that used sophisticated three-dimensional computer models to capture dispersion and chemical transformation of regional electric grid emissions, Carreras-Sospedra *et al.* (2010) used a three-dimensional dispersion model to assess the air quality impacts of central power generation versus distributed generation in the South Coast Air Basin of California. Similarly, Vutukuru *et al.* (2011) assessed future impacts of distributed power generation on ambient ozone and PM concentrations in the San Joaquin Valley Air Basin using state-of-the-art three-dimensional computer models.

Several studies have used the Lagrangian non-steady state plume model CALPUFF to assess air quality impacts from electric grid emissions. Levy *et al.* (2002) relied on CALPUFF to simulate $PM_{2.5}$ emissions dispersion from nine power plants in Illinois. They found that 320 premature deaths are expected due to emissions from nine power plants in their modeling region, which includes 33 million people (Levy *et al.,* 2002).

In China, Hao *et al.* (2007) relied on CALPUFF to estimate air quality impacts and human exposure from six of China's largest power plants. They found that control measures such as fuel substitution, flue gas desulfurization and denitration

will greatly reduce SO_2 and PM_{10} pollution, with further controls needed for reducing NO_x pollution.

In 2003, Zhou *et al.* used CALPUFF to show how human exposure to power plant emissions can be measured by calculating the fraction of a pollutant emitted that is eventually inhaled or ingested by a population (intake fraction) in Beijing, China. They found the intake fraction for fine particulates is on the order of 10^{-5} and the intake fraction for sulfates and nitrates is on the order of 10^{6} (Zhou *et al.,* 2003).

In India, Guttikunda and Jawahar (2014) estimated individual power plant emissions and used the CAMx chemical transport model to deduce that these emissions resulted in 80,000 to 115,000 premature deaths and 20.0 million asthma cases from $PM_{2.5}$ exposure. They estimated that the resulting adverse health impacts cost the public between US$3.2 and US$4.6 billion annually.

Other studies have utilized lower resolution modeling to assess impacts on a statewide and national level. Using BenMAP, Machol *et al.* (2013) estimated that the total economic value of health impacts from fossil fuel electricity in the United States is between $361.7 and $886.5 billion annually, which is 2.5 to 6.0% of the US GDP. Additionally, Machol *et al.* estimated the health impact $/kWh of coal, oil and natural gas. The health impact costs for coal were 2.4 times higher than the average $0.135/kWh cost in California, while the health impact costs for natural gas were 15% of the average CA electricity cost (Machol & Rizk, 2013).

Figure 3.1. Health costs per kWh in the U.S.

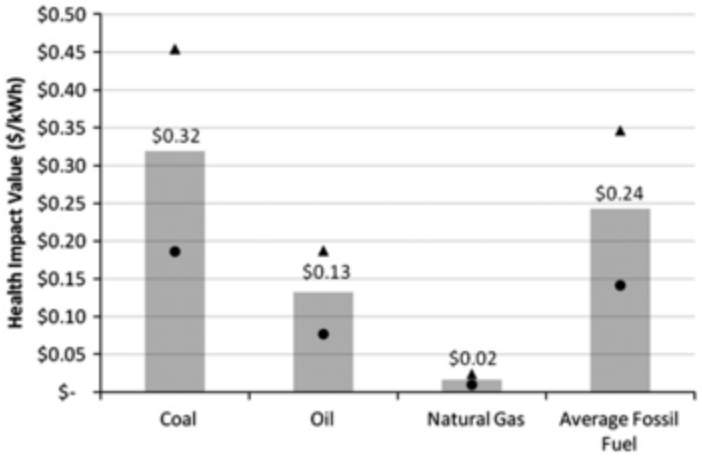

Source: Machol and Rizk (2013).

In Europe, Markandya and Wilkinson (2007) estimated the deaths/TWh of electricity generation by source. They found that oil combustion caused approximately 7 times more deaths than gas combustion, and coal combustion caused approximately 9 times more deaths than gas combustion.

3.4 Global and U.S. air pollution impact studies

Local air pollution from the combustion of fossil fuels is increasingly of concern in developed and developing countries alike because of the adverse health impacts of pollutants such as particulate matter (Brauer *et al.,* 2015). In particular, ambient $PM_{2.5}$ is now the fifth largest contributor to global disease (Institute of Health Metrics and Evaluation, 2015). However, emissions standards for PM vary widely. In their review of 170 countries, Joss *et al.* (2017) found that $PM_{2.5}$ air quality

standards vary from 10 µg/m^3 to close 100 µg/m^3 (annual average), and 57 countries still have no official air quality standards.

Between 1990 and 2015, the number of deaths attributable to ambient $PM_{2.5}$ exposure increased from 3.5 million in to 4.2 million (Cohen *et al.*, 2017). Approximately 87% of the world's population now lives in areas exceeding the World Health Organization (WHO) air quality guideline of 10 µg/m^3 $PM_{2.5}$ (annual average), according to Brauer *et al.* (2015) who used satellite and ground measurements from 79 countries to assess global $PM_{2.5}$ exposure in 2013 and $PM_{2.5}$ trends from 1990 to 2013.

Figure 3.2. Annual average $PM_{2.5}$ ambient concentrations in 2013

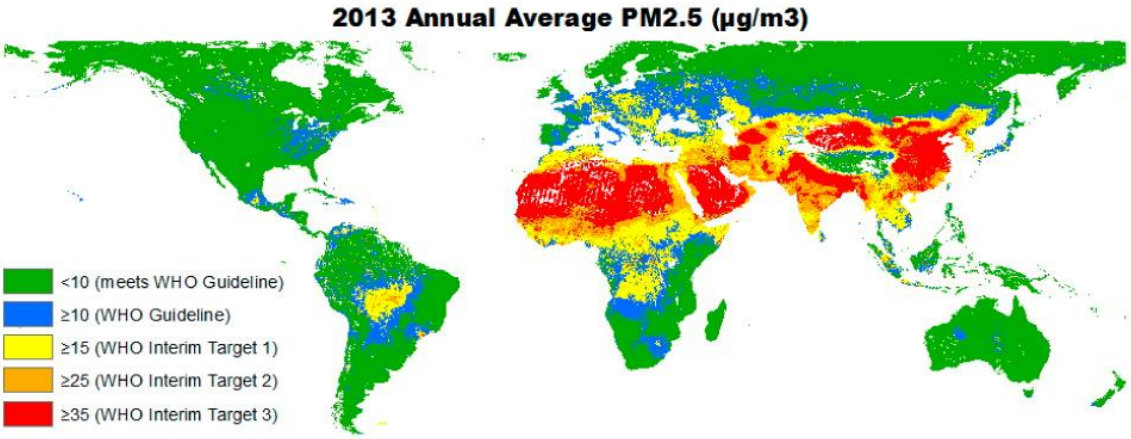

Source: Brauer *et al.* (2015).

Apte *et al.* (2015) applied the integrated exposure response (IER) model to global $PM_{2.5}$ exposure. They reported that 3.2 million deaths could be avoided globally by enforcing strict $PM_{2.5}$ standards. In a separate study, Lelieveld *et al.* (2015) used the IER developed to assess the contribution of outdoor air pollution sources to premature mortality on a global scale. They found that premature

mortality due to outdoor air pollution could double by 2050 with business-as-usual emission scenarios (Lelieveld *et al.,* 2015).

Fann *et al.* (2012) used BenMAP to estimate deaths related to $PM_{2.5}$ and O_3 in the United States due to 2005 air quality levels. They estimated that 130,000 $PM_{2.5}$-related deaths and 4,700 ozone-related deaths resulted from 2005 air quality levels. Fann *et al.* used all-cause mortality because it is the most comprehensive estimate of PM-related morality.

Cromar *et al.* (2016) relied on the Standard EPA Health Functions in BenMAP for $PM_{2.5}$ and O_3 to estimate that 9,320 deaths and 21,400 morbidities happen each year in the U.S. due to concentrations of these pollutants over the American Thoracic Society recommended standard of 11 μg/m^3 $PM_{2.5}$ and 0.060 ppm O_3.

In 2006, the Urban Air Pollution Working Group (part of the Health Effects Institute) estimated that 3% of mortality from cardiopulmonary disease, 5% of mortality from trachea, bronchus and lung cancer and approximately 1% of mortality due to acute respiratory infections in children under 5 were due to ambient air pollution worldwide (A J Cohen *et al*., 2005).

Davidson *et al.* (2007) demonstrated BenMAP's ability to analyze $PM_{2.5}$ pollution control policy scenarios by quantifying benefits of a national-level air quality control program and of attaining two annual $PM_{2.5}$ standards in California.

3.5 Epidemiology concentration-response studies in Latin America

Estimating mortality due to long-term exposure to fine particulate matter ($PM_{2.5}$) requires understanding the shape and magnitude of relative risk functions. Studies in the U.S., Europe and Latin America were reviewed to inform the selection of exposure-response functions for this study.

I found four health studies for PM-related mortality or morbidity for Brazil (Braga *et al.,* 2001; Conceição *et al.,* 2001; Martins *et al.,* 2004; Saldiva *et al.,* 1995), along with four others for Latin America (Bell *et al.,* 2006; Cifuentes *et al.,* 2000; Loomis *et al.,* 1999; Ostro, 1998). All of these studies are based on PM_{10} exposure, except Loomis *et al*. (1999), who derive a relationship between $PM_{2.5}$ exposure and infant mortality in Mexico City, and Cifuentes *et al.* (2000).

Saldiva *et al.* (1995) used time series regression from 1990 to 1991 to estimate a 13% increase in elderly (65+ years) mortality per 100 $\mu g/m^3$ increase in PM_{10} and reported an almost linear relationship. The more recent studies above generally found a higher relative risk increase per increase in PM_{10} concentration.

Another study used regression analysis on respiratory related deaths from 1997 to 1999 in Sao Paulo, Brazil and found that respiratory mortality varied on average 5.4% for a 10 $\mu g/m^3$ increase in PM_{10} (Martins *et al.,* 2004).

Conceição *et al.* (2001) estimated mortality in children from 0-5. They reported a 7% relative risk increase for mortality in children 0-5 given the average PM_{10} concentration from 1994 to 1997 in Sao Paulo, Brazil(Conceição *et al*., 2001).

Braga *et al.* (2001) defined a concentration-response relationship for PM_{10}-related respiratory hospital admissions for children and adolescents developed in Sao Paulo, Brazil.

In Mexico City, Loomis *et al.* (1999) found that infant deaths increased 6.9% due to acute exposure of an increase of 10 $\mu g/m^3$ of PM_{10}.

Cifuentes *et al.* (2000) regressed daily counts of non-accidental mortality from 1988 to 1996 against six pollutants in Santiago, Chile. They found that mortality associated with mean levels of air pollution varied from 4 to 11%.

Mehta *et al.* (2011) used a Bayesian estimate a C-R function for increased risk in acute lower respiratory infections per 10 $\mu g/m^3$ increase in annual average $PM_{2.5}$ concentration based on studies in the U.S., Latin America and South Korea.

Although there have been PM related studies in Sao Paulo, Mexico City, and Santiago, most were time series studies limited in scope by pollutant, age range and health endpoints. Additionally, the Latin American studies focus on PM_{10}, where as the main focus of recent studies is $PM_{2.5}$.

Before selecting a set of exposure-response studies for this dissertation, I also reviewed selected epidemiology studies in the U.S., Europe and globally.

3.6 U.S. and international epidemiology concentration-response studies

There are many factors to take into account when selecting appropriate epidemiological and concentration-response functions, including whether the study was peer reviewed, study design and location, characteristics of the target population, and how recently the study was performed (Fann *et al.,* 2012). When

available, epidemiology studies and concentration-response functions specific to Brazil and Latin America were utilized in this study. However, for many health endpoints, Latin American studies are not available (Bell *et al.,* 2006).

The shape of the exposure-response relationship between health impacts and fine particulates has been estimated by numerous studies. To unify results obtained over a number of studies, a group of distinguished epidemiologists and health economists developed an integrated exposure-response (IER) model for mortality across the global range of $PM_{2.5}$ exposure for adults aged 25 to 99 (Burnett *et al.,* 2014).

The IER model consists of piecewise relative risk (or C-R) functions over the entire global exposure ranges for mortality in adults, including the main air pollution causes of mortality: ischemic heart disease, cerebrovascular disease, chronic obstructive pulmonary disease, lower respiratory infection and lung cancer. The C-R functions come from a range of studies, including ambient air pollution, second hand tobacco smoke, household solid cooking fuel, and active smoking Burnett *et al.* (2014).

Lepeule *et al*. (2012) performed an extended follow up on the Harvard Six Cities study to analyze 11 additional years with lower concentration levels. They reported high mortality relative risk ratios of 14% to 37% per 10 $\mu g/m^3$ of $PM_{2.5}$ at low concentration levels.

BenMAP includes a number of EPA Standard Health Impact Functions for $PM_{2.5}$ related mortality, including Lepeule *et al.* (2012), Pope *et al*. (2002), Laden *et al*. (2006) and Krewski *et al*. (2009).

The EPA Standard Health Impact Function set also includes C-R functions for $PM_{2.5}$ related hospital admissions. Zanobetti *et al*. (2009) study, which found a 1.89% increase in cardiac related hospital admissions and a 2.05 increase in respiratory related hospital admissions per 10 $\mu g/m^3$ increase in $PM_{2.5}$ (Zanobetti *et al*., 2009). Moolgavkar (2000) found a 1.4% increase in cardiovascular related hospital admissions for persons 20-64 per each $PM_{2.5}$ increase of 10 $\mu g/m^3$.

Many other studies have quantified the link between PM exposure and mortality. Pope *et al.* (2009) defined the shape of the exposure-response relationship between cardiovascular mortality and fine particulates from cigarette smoke and ambient air pollution (Pope *et al.,* 2009). In a separate 2009 study, Pope *et al.* analyzed the impact of PM on life expectancy from 1979 to 2000 for 51 metropolitan areas and 200 counties (Pope *et al.,* 2009).

In a previous study, Pope *et al.* (2002) reported that each 10$\mu g/m^3$ increase in $PM_{2.5}$ correlates with an increase in risk of 4% for all-mortality causes, 6% for cardiopulmonary mortality and 8% for lung cancer mortality.

Based on a European expert panel elicitation, Hoek *et al.* (2009) derived probability distributions between ultrafine particles and all-cause mortality and cardiovascular and respiratory hospital admissions.

Samoli *et al.* (2005) defined exposure-response curves relating PM_{10} and black smoke concentration to the percentage increase in deaths in 22 European cities and found a high correlation.

Currie *et al.* (2009) examined the connection between air pollution on infant death in California. Their study suggests that reducing carbon monoxide from 2.4-

1.4 ppm and PM_{10} from 48.8 to 32.8 μg/m^3 from 1989-2000 prevented 1000 infant deaths.

After reviewing 14 mortality studies, Song *et al.* (2014) concluded that the increase in relative risk of COPD related mortality due to an increased chronic exposure of 10 μg/m^3 is 1.04 in the European Union, 1.03 in the United States, 1.01 in China and 1.04 for two studies in areas outside of the E.U., U.S. and China.

Ostro *et al.* (2007) linked $PM_{2.5}$ and several constituents to multiple mortality categories. Cardiovascular deaths increased by 1.6% for $PM_{2.5}$, 2.1% for elemental carbon, 1.6% for organic carbon and 1.5% for nitrates in the higher quartile ranges.

Finally, in assessing 202 U.S. counties from 1999-2005, Bell *et al.* (2008) reported a 1.05% increase in respiratory disease hospital admissions per increase of 10μg/m^3 of $PM_{2.5}$.

3.7 Monetary valuation of health impacts in Brazil

For understanding tradeoffs, monetary valuation techniques have been applied to changes in health outcomes. This allows for a more straightforward cost-benefit analysis, where the cost emission control technology required to achieve reductions in air pollutant concentrations can be directly compared with the monetary valuation of expected health benefits.

In the Alves and Uturbey (2010) study, per capita income, life expectancy, health expenses and income-elasticity data were used in a benefits transfer to calculate a VSL for Brazil of US$800,258. They valued the cost of hospitalizations, medical care, medicines and lost work days at an average of US$1985.03 per

disease. A correction factor of 1.85 was used to obtain a more complete willingness to pay for reducing respiratory disease risks of USD 3672.20 USD per disease (Alves and Uturbey, 2010).

The Bell *et al.* (2006) study estimated the avoidable health costs using a cost-of-illness valuation method and a willingness-to-pay (WTP) valuation method over a 20 year period Sao Paulo, Mexico City, and Santiago.

Shindell *et al.* (2011) used the EPA preferred VSL of $9,500,000. As a first approach, they applied the VSL uniformly across all countries. As a second approach, they derived country specific VSLs using the USEPA's elasticity of 0.40 between income and WTP to avoid adverse health impacts.

In Miraglia *et al.* (2005), a life expectancy of 67.53 years in Brazil was used and monetized air pollution results were compared using two different VSLs. With a VSL of $7,714 US$, the total DALYs attributable to air pollution was US$3,222,676. With a VSL of $500,000, they totaled US$208,884,940 (Miraglia *et al.,* 2005).

My review of monetary valuation in Latin American studies reveals that there is large variance between derived VSL dollar amounts for developing countries, depending on the method employed and the currency year. The monetary valuation of disease incidence does not vary much when the cost of illness technique is employed and can vary some with the willingness to pay technique, although not nearly as much as the values of statistical lives.

3.8 Renewable integration impacts the electric grid operation and utilities

As this dissertation analyzes the health benefits, storage requirements and grid stability implications of high penetrations of renewables, it is important to note that integrating large penetrations of renewables will also impact electricity grid operation and electric utility companies. Although this dissertation does not focus on utility side impacts, it is worth mentioning them.

NE Brazil has exceptionally high capacity factors for wind and solar energy, yet there are technical, economic and political issues involved with connecting renewable energy resources into Brazil's electric grid.

On the political front, there can be issues connecting new and remotely located energy sources, such as wind, solar, biomass and small hydroelectric generation to transmission lines in Brazil. To address this, a Central Generation (ICG) model was created by ANEEL to hold auctions that have been successful in providing access for remote renewable electricity generation to the transmission system (Agencia Nacional de Energia Eletrica, 2016). Another political issue is that electricity producers need to sell their energy into the market ahead of time in a Public Call, which can create issues for intermittent renewables (i.e. wind and solar). Transmission line construction delays can also prevent newly constructed power plant from connecting to the grid, or restrict the amount of electricity from existing power plants due to capacity limits (Francisco 2012).

There are also technical issues with incorporating high penetrations of renewables into Brazil's grid, arising locally and at the system level. Local issues caused by integrating intermittent renewable generation (i.e. wind and solar),

include voltage control, fault current, harmonic distortion and flicker (Soares *et al.,* 2012). Fault currents are any abnormal electrical currents that can cause circuit failures (Anaya-Lara *et al.,* 2009). Harmonic distortion and flicker occur when current and voltage waveforms are non-sinusoidal and contain distortions. This places additional waveforms onto the fundamental current waveform, which creates multiple frequencies within the frequency range that the electric supply system is supposed to operate in (Emerson, 2010).

Systemwide impacts caused by increasing intermittent renewable generation include balancing generation and load, reactive power generation and reduced frequency control (Soares *et al.,* 2012). For example, when load exceeds generation, generation can be increased from load following power plants or by power plants that have additional capacity contracted to be on reserve to dispatch when needed (known as reserve resources), or by dispatching stored energy in the form of batteries or hydro storage. Alternatively, load can be reduced through demand response programs when decreasing generation is not readily available. When generation exceeds load, generation can be reduced by ramping down load following generators or by storing excess energy with pumped hydro. Reactive power generation, which maintains the transmission line voltage level to allow electricity to flow freely, is affected when generation from intermittent renewables is suddenly dropped because it causes a reduction in the system's frequency control (Emerson, 2010).

Due to local and systemic issues caused by increasing intermittent generation in electric grids, Krauter (2005) found that depending on the power system,

integrating wind power beyond 30% penetration into large interconnected systems could require redesigning the existing power system and its operation.

Along with operational impacts, there are also business model impacts associated with renewable integration. Richter (2012) discussed how there are two general business models when considering the integration of high penetrations renewables: a utility-side business model that consists of a small number of large-scale projects, and a consumer-side business model that consists of a large number of small-scale projects. Richter contrasted the two and discussed the utility business model implications of choosing a residential scale versus a utility scale renewable integration approach. He found that there are a number of advantages of utility-side business models compared to consumer-side.

Additionally, Schleicher-Tappeser (2012) analyzed how managing the interface between power consumption and weather-dependent power production is a key issue for utilities that challenges traditional top-down control logic. Increasing flexibility and autonomy of consumers drives a more decentralized and multi-layer systems (Schleicher-Tappeser, 2012).

Milligan *et al.* (2011) studied how coordination among WECC balancing authorities could affect renewable integration costs. Multiple scenarios were modeled with existing commitment strategies and coordination possibilities. Increasing cooperation between WECC balancing authorities can significantly reduce operating costs. While there are significant benefits of coordination within WECC with real-time dispatch, only 20% to 40% of the total operating cost savings potential is possible if existing commitment strategies are upheld. Maximum

savings occur when commitment and dispatch strategies are coordinated. Potential coordination savings increase as renewable generation increases.

Renewable integration also has public and private costs and benefits. Borenstein (2011) analyzed how renewable generation is more expensive than conventional generation, yet it reduces pollution externalities. This tradeoff is hard to monetize, because renewables like wind and solar are intermittent and the value of electricity is dependent on the time and the location of its production. Similarly, pollution benefits from renewables depend on the type of generation that renewables displace, as well as the time and place where the pollution is reduced. Without incorporating these factors, cost-benefit analyses of renewable generation will likely be misleading (Borenstein 2011).

Borenstein's (2011) study makes argues that spatial and temporal resolution is needed to quantify externalities of fossil fuel vs. renewable generation, and more importantly, that cost benefit analysis of fossil fuel vs. renewable generation is misleading without considering the time and space dependent costs of pollution (Borenstein, 2012). This dissertation improves on past methodologies by using a highly resolved spatial and temporal methodology to produce insightful results that help policy makers understand tradeoffs of more stringent emissions standards and integrating high penetrations of renewables.

3.9 100% RPS studies in Brazil and abroad

Two previous studies have analyzed 100% renewable energy scenarios in Brazil. Gils *et al.* (2017) assessed the least cost option for a 100% renewable energy supply

for Brazil in 2050, and Barbosa *et al*. (2016) simulated a 100% renewable electric grid for Brazil using hourly resolution. Additionally, a number of studies have analyzed 100% renewable energy systems in countries and regions globally, which are summarized below.

Gils *et al*. (2017) used the REMix model with hourly resolution to analyze the least-cost composition and operation of a fully renewable energy supply across all sectors in Brazil in 2050. Their study focuses on the role of sector coupling and regional development, including both the challenges arising from an additional power demand for electric mobility and hydrogen production, and the opportunities offered by the flexibility of these loads.

They found that with its abundance of dispatchable renewable energy (hydropower and bioenergy) and VRE (wind and solar) potential, Brazil is a good prospect for a carbon neutral energy system. Interestingly, they reported that the expansion of wind and solar power is more cost-efficient than the construction of additional hydroelectric plants. This is primarily because the Brazilian power system has plenty of reservoir hydro stations to balance VRE generation, including 65 GW and 43 GW of run-of-river stations based on future investment opportunities. They also assumed that pumps could be installed in all reservoir hydro stations as an additional source of flexibility and storage, which unfortunately is not realistic. Biomass CHP plants, fuel cells and wave energy power plants were also considered.

Results from the Gils *et al.* (2017) study indicate that hydro power would need to be more fully utilized to balance load and generation by importing and exporting energy between areas with high VRE potential (ex. Northeast Brazil) and

high hydropower (ex. Northern Brazil). Furthermore, enhanced coupling of power, heat and transport sectors through flexible electric heating, electric mobility and hydrogen electrolysis would also need to significantly contribute to the balancing of intermittent power generation. However, the authors acknowledge that the role of regional power exchange, sector coupling, and industrial demand response (DR) in a completely RE system is not yet fully understood for Brazil.

Due to the load and generation balancing capabilities offered by pumped storage and sector coupling, Gils *et al*. (2017) concluded that the transformation strategy in Brazil can be primarily based on other criteria such as regional development, public acceptance, environmental impact or industrial policy without major impacts on system costs.

Barbosa *et al*. (2016) simulated a 100% renewable energy electricity system for Brazil in 2030 using hourly resolution. They used a linear system optimization model that considered solar PV, solar CSP (concentrated solar power), onshore wind, hydropower, biomass, waste-to-energy and geothermal power plants for electricity production.

To buffer VRE generation, four categories of flexibility were considered: generation management (hydro dams and biomass plants), demand side management (power to gas, synthetic natural gas seawater desalination), energy storage (batteries, compressed air storage and thermal storage), and transmission grids (high voltage direct current technology) for importing and exporting electricity. Electricity distribution was not considered.

Their results for a least-cost 100% renewable power sector include 165 GW of solar PV, 85 GW of reservoir hydro stations, 12 GW of hydro run-of-river, 8 GW of biogas, 12 of GW biomass and 8 of GW wind power. They found that 243 GWh of battery capacity is needed to balance wind and solar generation, as well as 1 GWh of pumped hydro storage, 23 GWh of compressed air storage and 1 GWh of heat storage. The total system levelized cost of electricity decreased from 61 Euros/MWh to 53 Euros/MWh.

The feasibility of 100% renewable energy power system in South and Central America based on hydro, wind and solar was also studied by Barbosa *et al*., (2017). They used an hourly resolved energy model and considered three scenarios with different levels of high voltage direct current development (region, country, and area-wide) interconnecting all countries in Central and South America. Additionally, they modeled an integrated scenario that considers water desalination and industrial gas demand supplied by synthetic natural gas produced by power-to-gas. The same technologies were considered as in Barbosa *et al*. (2016).

Barbosa *et al*. (2017) found that renewable energy could cover the 1813 TWh of forecasted electricity demand as well as the electricity required to desalinate 3.9 billion m^3 of water and supply 640 TWh_{LHV} of synthetic natural gas. Importing and exporting electricity is critical for balancing load and generation, as well as pumped hydro storage. The levelized cost of energy ranged from 62 Euros/MWh for a decentralized grid scenario to 56 Euros/MWh for a centralized grid scenario. Integrating desalination and power-to-gas reduced electricity costs by 5% and total system costs by 8%.

The feasibility of 100% renewable energy systems in specific countries in Europe and by interconnecting the EU has also been studied. Ćosić *et al*. (2012) used the EnergyPLAN model to assess the feasibility of a 100% renewable energy electric system in Macedonia, They found that a 50% renewable energy system in 2030 is much more likely than a 100% renewable energy system in 2030. Lund and Mathiesen (2009) also assessed the feasibility of a 2030 50% RPS and a 2050 100% RPS. They reported that in Denmark a 100% RPS in 2050 is physically possible and that a 50% RPS in 2030 is a feasible first step. However, a large share of either biomass resources is required to balance load and generation, which has implications for farming areas, or hydrogen energy storage, which leads to system inefficiencies.

Another study using the EnergyPLAN model with hourly resolution assessed the feasibility of a 100% renewable energy system for electricity, heat and transportation in Ireland. The modeling efforts focused on three renewable resources (biomass, hydrogen and electricity). The authors concluded that while that a 100% RPS system is possible, a number of assumptions need to be validated and explored before creating a renewable energy transition plan for Ireland.

A few studies have also investigated the feasibility as well as the technical and economic impacts of a 100% RPS in the European Union (EU). Bussar *et al*. (2014) reported that a cost effective 100% renewable energy system could be achieved in the EU with a heavy reliance on an interconnected transmission system as well as a high capacity of energy storage options. Using the Genetic Optimization of a European Energy System (GENESYS), the authors found that 2,500 GW of

renewable energy, 240,000 GWh of storage (corresponding to 6% of energy demand), and a high voltage direct current transmission system of 375,000 GWkm would be required to balance supply and demand at an estimated cost of 6.87 ct/kWh.

In a separate study, Connolly *et al.* (2016) developed a Smart Energy System approach to transitioning Europe to a 100% renewable energy system. They found it is possible, without consuming an unsustainable amount of bioenergy, to have a 100% renewable energy system in Europe by coupling the electricity, heating, cooling and transport sectors, which would enable an 80% VRE penetration. The Smart Energy Europe is projected to create 10 million jobs and increase energy costs by 10-15%.

With respect to 100% renewable energy systems in the US, Jacobson *et al* developed a road map for 100% of California's energy supply to be provided by wind, water and solar resources Jacobson *et al*. (2014). This effort was then extended to all 50 states (Jacobson *et al*., 2015). Their roadmaps include demand projections for electrifying all residential, commercial, industrial and transportation sectors, generator and land requirements, resource availability, costs of infrastructure, air pollution and greenhouse gas warming costs, job creation and loss, as well as a timeline for implementation and recommendations. They found that a 100% wind, water and solar energy supply is technically and economically feasible with little downside.

Interestingly, the WWS roadmaps by Jacobson *et al*. are based on aggregate energy transfers and do not include temporal resolution, which limits their

usefulness because the degree of uncertainty is unknown. Their assumption of leaving out temporal resolution is based on a 2011 paper, where Hart and Jacobson simulated California's hourly electricity system dispatch for 2005 and 2006 and found that supply and demand can be balanced with 99.8% of electricity being produced carbon-free. This was demonstrated using a Monte Carlo approach to generator portfolio planning. The exact amount of necessary storage was not listed, but all wind, solar PV and CSP resources were assumed to have 3-hours of storage.

Bogdanov and Breyer have analyzed 100% renewable energy scenarios in large interconnected areas, including Central and South America, Eurasia, North-East Asia, Sub-Saharan Africa and India. They used an hourly resolved energy system model based on linear optimization to determine least cost 100% renewable energy electricity systems with high voltage direct current transmission lines connecting sub-regions within each study region. A summary of their findings from is provided below (they were also involved in the Barbosa *et al.* studies).

The costs and feasibility of 100% renewable energy systems outside Central and South America have also been studied. Bogdanov and Breyer (2016) modeled the implications of building a Super Grid connecting Eurasian regions from east Russia to Belarus with high voltage direct current power lines using an hourly resolved linear optimization energy system model. They defined a distributed and a centralized optimal cost mix of energy technologies and storage options for each region, considering a broad range of generation technology (PV, CSP, wind, hydro, biomass, biogas, waste-to-energy and geothermal) as well as storage technology (battery storage, pumped hydro storage, compressed air energy storage, thermal

energy storage and power-to-gas. Optimal infrastructure capacities and hourly generation were simulated for each sub-region. Results indicated that a 100% renewable energy super grid is lower in cost than nuclear and fossil fuel with carbon capture and storage alternatives.

Bogdanov and Breyer (2016) also assessed a 100% renewable energy scenario for connecting North-East Asia power systems. They concluded that renewable energy can supply projected electricity and gas demand predicted for 2030 and deliver 2000 TWh_{th} of heat. The total area system cost could be as low as 69.4 Euros/MWh, if infrastructure were available to allow 20% of energy to be exchanged between the 12 regions and 27% of generation to be stored. Results indicate that a 100% renewable energy system is feasible and less than nuclear and fossil fuel with carbon capture and storage alternatives. A similar study was done for interconnecting Southeast Asia with similar results (Gulagi *et al.* 2017).

Least cost electricity solutions based on 100% renewable energy have also been studied in Sub-Saharan Africa using the same hourly resolved linear optimization model as the studies above (Barasa *et al.*, 2016). By connecting 16 sub-regions with high voltage direct current HVDC transmission lines, the authors reported that renewable electricity could supply the projected 866.4 TWh of electricity demand, 319 million m^3 of desalinated water and 268 TWh_{LHV} of synthetic natural gas demand. The levelized cost of energy ranges between 57.8 Euros/MWh for a decentralized grid to 54.7 Euros/MWh for a centralized grid. Results indicate a large reliance on gas storage (25,754 GWh_{th}), electricity imports and exports between regions, and coupling electricity demand with gas and

desalination demands. Gulagi *et al.* (2016) performed a similar study in India and found similar results, with a higher levelized cost of energy due to greater battery storage requirements.

On a global basis, a 2014 study investigated the global energy storage demand for a global VRE supply based on hourly demand profiles for 163 countries. It reported that high-temperature thermal energy storage in combination with CSP, steam turbines and heating rods is the preferred over batteries and power-to-gas. A world average levelized cost of energy of 142 EUR/MWh was estimated. The authors concluded that hydropower, grid interconnections and coupling electricity with other energy sections such as heat, transportation and desalination were necessary to further reduce costs (Pleßmann *et al.,* 2014).

There are a few key commonalities that make it possible for 100% renewable energy based electricity system solutions discussed above to meet electricity demand at (or even lower than) current levelized costs of energy. These technologies and operational approaches are: high voltage direct current transmission lines for flexibly importing and exporting electricity, a portfolio of variable and dispatchable generation technologies, a portfolio of storage technologies, and coupling electricity with other energy sectors such as industrial gas demand, transportation and desalination.

3.10 Literature review table

A literature review table summarizing the key questions, methodology and results of each paper in this literature review is below.

Table 3.1. Literature review table

Authors	Key Questions	Methodology	Results
Barbosa *et al.* (2017)	What is the cost optimal mix of energy sources for a 100% RPS electric system interconnecting all countries in Central and South America?	Linear optimization model with hourly resolution. HVDC lines connecting all regions, portfolios of generation and storage considered. Electricity sector coupled with projected industrial heat and desalination demand.	100% RPS electric system can supply projected demand. LCOE is 62 Euros/MWh for decentralized grid and 56 Euros/MWh for centralized grid.
Gils *et al.* (2017)	What is the least cost option for a 100% renewable energy supply across all sectors in Brazil in 2050?	Remix model was used with hourly resolution, coupling sectors such as transportation and hydrogen production. A portfolio of generation and storage technologies were considered, as well as retrofitting existing hydro plants with pumped storage	Due to the load and generation balancing capabilities offered by pumped storage and sector coupling, Brazil can transition to 100% renewable energy without large impacts to energy costs. Other criteria such as regional development, public acceptance and environmental impact should be considered.
Gulagi *et al.* (2017)	Is a 100% renewable super grid interconnecting India feasible and cost-effective?	Linear optimization model with hourly resolution. HVDC lines connecting 16 sub-regions, portfolios of generation and storage considered. Electricity sector coupled with projected industrial heat and desalination demand.	Yes, but there are large battery storage requirements that raise the LCOE.

Barasa *et al*. (2016)	Is a 100% renewable super grid interconnecting Sub-Saharan Africa feasible and cost-effective?	Linear optimization model with hourly resolution. HVDC lines connecting 16 sub-regions, portfolios of generation and storage considered. Electricity sector coupled with projected industrial heat and desalination demand.	The levelized cost of energy range from €57.8/MWh for a decentralized grid to €54.7/MWh for a centralized grid. A large reliance on gas storage (25,754 GWh_{th}), electricity imports and exports between regions, and coupling electricity demand with gas and desalination.
Barbosa *et al.* (2016)	What is the cost optimal mix of energy sources for a 100% renewable electricity system in Brazil in 2030?	Linear optimization model with hourly resolution. HVDC, Portfolios of generation and storage technologies considered, including power to gas.	Least cost portfolio includes portfolio of renewable generation, 243 GWh of battery capacity as well as other storage required. Levelized cost of electricity decreases by more than 10% in 100% RPS scenario.
Bogdanov and Breyer (2016)	Is a 100% renewable super grid interconnecting Eurasia feasible and cost-effective?	Linear optimization model with hourly resolution. HVDC lines connecting all regions, portfolios of generation and storage considered. Electricity sector coupled with projected industrial heat and desalination demand.	100% renewable energy Eurasian super grid is lower in cost than nuclear and fossil fuel with carbon capture and storage alternatives
Bogdanov and Breyer (2016)	Is a 100% renewable super grid interconnecting North-East Asia feasible and cost-effective?	Linear optimization model with hourly resolution. HVDC lines connecting all regions, portfolios of generation and storage considered. Electricity sector coupled with projected industrial heat and desalination demand.	100% renewable energy Eurasian super grid is lower in cost than nuclear and fossil fuel with carbon capture and storage alternatives
Connolly *et al.* (2016)	What is the best approach for transitioning Europe to a 100% renewable energy system?	A Smart Energy Europe approach was developed and modeled, focusing on VRE and constraining bioenergy use to a sustainable amount.	The Smart Energy Europe approach enables an 80% VRE penetration when electricity, transportation and heating and cooling are coupled. 10 million jobs are created and

			energy costs decrease 10-15%.
Cromar *et al.* (2016)	What health effects are associated to concentrations over the American Thoracic Society (ATS) standards?	Health Functions in BenMAP for $PM_{2.5}$ and O3 were used with the ATS standards of 11 μg/m^3 $PM_{2.5}$ and 0.060 ppm O_3 as the control scenario.	9,320 deaths and 21,400 morbidities happen due to $PM_{2.5}$ and O_3 concentrations in excess of ATS standards.
Apte *et al.* (2015)	What is the global mortality due to $PM_{2.5}$ exposure?	The integrated exposure response (IER) model was applied to global $PM_{2.5}$ exposure from the GBD.	3.2 million deaths could be avoided globally by enforcing strict $PM_{2.5}$ standard.
Brauer *et al.* (2015)	What is the global exposure to ambient $PM_{2.5}$?	Satellite and ground measurements were used from 79 countries to assess global $PM_{2.5}$ exposure in 2013 and $PM_{2.5}$ trends from 1990 to 2013.	87% of the world lives in areas that exceed WHO $PM_{2.5}$ standards.
Jacobson *et al*. (2015)	What are the ideal 100% wind, water and solar energy mixes for each state in the U.S.?	A spatially but not temporally resolved model simulates the optimal mix and location of wind, water and solar resources. All sectors coupled.	A 100% wind, water and solar energy supply is technically and economically feasible with little downside.
Burnett *et al.* (2014)	What is the connection between $PM_{2.5}$ and acute lower respiratory infections?	Piecewise C-R functions are integrated over the entire global exposure ranges for mortality in adults from a range of studies.	The IER model was a superior predictor of relative risk changes due to $PM_{2.5}$ exposure compared with seven other prediction methods.
Bussar *et al*. (2014)	What are the technical and economic impacts of a 100% RPS interconnected EU electric system?	A model, Genetic Optimization of a European Energy System (GENESYS), was developed to determine the cost optimal mix of energy generation and storage technologies to meet electricity demand in the EU via a system interconnected with HVDC lines.	A cost effective 100% renewable energy system can be achieved in the EU with a heavy reliance on an interconnected transmission system as well as a high capacity of energy storage options.

Jacobson *et al*. (2014)	What are the ideal 100% wind, water and solar energy mixes for CA?	A spatially but not temporally resolved model simulates the optimal mix and location of wind, water and solar resources. All sectors coupled.	A 100% wind, water and solar energy supply is technically and economically feasible with little downside.
Pleßmann *et al*. (2014)	What is the global energy storage demand for a global VRE supply?	Hourly demand profiles for 163 countries were estimated. A portfolio of storage options were assessed.	high-temperature thermal energy storage in combination with CSP, steam turbines and heating rods is the preferred over batteries and power-to-gas. A world average levelized cost of energy of 142 EUR/MWh was estimated.
Machol and Rizk (2013)	What are the economic value of health impacts associated with $PM_{2.5}$ and $PM_{2.5}$ precursors on a per kilowatt hour basis?	Calculations include (Tons of $PM_{2.5}$)*(Benefit/Ton)/(Annual gross load), same for NOx and SOx. Calculates $/kWh for each technology and in each state. BenMAP used.	The economic value of improved human health associated with avoiding emissions from fossil fuel electricity in the United States ranges from a low of $0.005–$0.013/kWh in California to a high of $0.41–$1.01/kWh in Maryland.
Avelino *et al.* (2012)	What are the economic, environmental and health impacts of building a wind farm in Brazil?	Emissions by power plant type are from ONS and ANEEL. Air quality modeling with a Gaussian Plume Model.	Importance of temporal and spatial dimensions: dry season results in ~5% increase in morbidity treatment costs, with little variation between study areas.
Borenstein *et al.* (2012)	What are the public and private costs of renewable energy integration?	Costs of un-priced pollution externalities, improved energy security, price sustainability, and job creation are compared.	Pollution benefits from renewables depend on the type of generation that renewables displace, as well as the time and place where the pollution is reduced.
Ćosić *et al*. (2012)	Is a 100% RPS electricity grid feasible in Macedonia?	EnergyPLAN model utilized for a 50% RPS in 2030 and a 100% RPS for 2050 based on VRE and storage.	A 50% renewable energy system in 2030 is much more likely than a 100% renewable energy system in 2050.
Fann *et al.* (2012)	What is the mortality associated with	The U.S. population exposure to 2005 $PM_{2.5}$ and O_3 levels was	130,000 $PM_{2.5}$-related deaths and 4,700 ozone-related deaths resulted

	exposure to $PM_{2.5}$ and O_3 in the United States?	calculated and input into U.S. C-R and monetary valuation functions.	from 2005 air quality levels.
Richter *et al.* (2012)	What are the pros and cons of utility-side and consumer-side business models?	Characteristics of utility-side and consumer-side business models are compared.	There are a number of advantages to utility-side business models compared to consumer-side business models.
Soares *et al.* (2012)	How can hybrid plug in vehicles be used as storage to increase the renewable mix?	An optimization tool was applied to the electric system in NE Brazil, analyzing dispatch of wind farms.	500,000 PHEVs could be charged overnight Jan. – June in 2015 with potential to increase to 1.5M PHEVs by 2030.
Schleicher-Tappeser *et al.* (2012)	What are the conflicts and opportunities utilities face when integrating renewables?	Management of production, spatial compensation, consumption and storage were considered.	The interface between power consumption and weather-dependent power production challenges traditional top-down control logic.
Hart and Jacobson (2011)	What is the least cost dispatch for CA with large penetrations of variable renewables?	California's hourly electricity system dispatch was simulated combining a deterministic renewable portfolio planning module with Monte Carlo simulation of system operation.	Supply and demand can be balanced with 99.8% of electricity being produced carbon-free.
Mehta *et al.* (2011)	What is the connection between $PM_{2.5}$ and acute lower respiratory infections?	A C-R function for increased risk in ALRI due to $PM_{2.5}$ was estimated from existing $PM_{2.5}$ studies in the U.S., Latin America and South Korea using a Bayesian approach.	There is a 12% increased risk in ALRI occurrence per 10 $\mu g/m^3$.
Milligan *et al.* (2011)	How will coordination among WECC balancing authorities affect renewable integration costs?	Multiple levels of renewable penetration were modeled with existing commitment strategies and coordination possibilities.	Coordination with real-time dispatch will reduce costs. Only 20% to 40% of the total cost savings potential is possible if existing commitment strategies are upheld.
Vutukuru *et al.* (2011)	What are the impacts of distributed power	A 3D dispersion and transformation model was used to simulate distributed generation	The air quality impacts of distributed generation were small due to stringent air emission

	generation on ambient ozone and PM?	emissions based on best available control technology.	standards applied to all distributed generation units.
Shindell *et al.* (2011)	How will tighter emissions standards affect radiative forcing and premature deaths?	C-R functions for PM mortalities related to cardiopulmonary illness and lung cancer were used to estimate health impacts.	For China, India and Latin America, the current path reduces radiative forcing but increases deaths and ozone-related agricultural losses.
Alves and Uturbey (2010)	What are the external costs related to PM and GHG emissions by the Brazilian electrical matrix?	Monetary valuation applied to PM and CO2e external costs, expressed in per kWh of generated energy.	Based on 19 EUROS/tCO2e, society could incur greater costs from local pollution caused by a small number of plants than global warming.
Carreras-Sospedra *et al.* (2010)	What are the air quality impacts of central power generation versus the impacts of distributed generation?	Impacts in the South Coast Air Basin were assessed using a 3D atmospheric dispersion and chemical transformation model.	Air quality impacts were greater from central generation than distributed generation, even though central generation emissions were lower. Spatial and temporal dimensions must be considered.
Emerson (2010)	What are the international standards for harmonic distortion and flicker?	The background and consequences of harmonics and flicker are investigated.	Consequences include heating lower transmitted power, fuses melting, zero-crossings, impacts to conductors, transformers, and breakers.
Anaya-Lara *et al.* (2009)	How can wind energy generation be modeled and controlled?	An in depth book detailing many aspects of modeling wind energy generation.	Many local and system level issues can arise, such as abnormal electrical currents that can cause circuit failures.
Currie *et al.* (2009)	What is the connection between air pollution on infant death?	Four criteria pollutant concentrations were tracked and mapped to infant death from 1989-2000.	Reducing CO from 2.4-1.4 ppm and PM from 48.8 to 32.8 µg/m^3 from 1989-2000 would have saved 1000 infant deaths.
Hoek *et al.* (2009)	Ultra fine particulate (UFP) C-R functions related to mortality and morbidity are reviewed.	A panel elicitation of eleven European experts with different backgrounds was performed.	Substantial differences in the estimated UFP health effect and its uncertainty were found between experts. The lack of studies on long- term exposure to UFP was rated

			as the most important source of uncertainty.
Lund and Mathiesen (2009)	Is a 100% RPS electricity grid feasible in Denmark?	A 50% RPS electricity grid in 2030 and a 100% RPS grid in 2050 were modeled with a focus on biomass resources or hydrogen generation for balancing load and generation.	A 100% RPS in 2050 is physically possible and that a 50% RPS in 2030 is a feasible first step.
Pope *et al.* (2009)	What is the connection between PM2.5 and mortality?	The C-R relationship between cardiovascular mortality and fine particulates is derived from cigarette smoke and ambient air pollution exposure.	The C-R relationship is relatively steep at low levels and flattens out at higher exposures.
Pope *et al.* (2009)	How does PM exposure impact life expectancy?	A total of 51 metropolitan areas and 200 counties were analyzed from 1979 to 2000.	A decrease of 10 μg/m^3 of fine particulate matter was associated with an increase in life expectancy of 0.61±0.20 years.
Davidson *et al.* (2007)	What are the benefits of: a national-level air quality control program, and benefits of attaining two annual $PM_{2.5}$ standards in California.	The U.S. EPA Environmental Benefits Mapping and Analysis Program (BenMAP) was used to assess health impacts of air quality deltas between cases.	The control of $PM_{2.5}$ emissions results in $100 billion of benefits annually. Attaining the more stringent standard (12 μg/m^3) would result in approximately 2000 fewer premature deaths each year than the 15 μg/m^3 achieves.
Markandya *et al.* (2007)	What are the health effects of coal, oil, biomass, gas and nuclear electricity generation?	The deaths per TWh of electricity generation are estimated by generation source.	Oil combustion causes approximately 7 times more deaths than gas combustion, and coal combustion causes approximately 9 times more deaths than gas combustion.
Ostro *et al.* (2007)	What is the connection between 19 $PM_{2.5}$ components and daily mortality?	Daily data from 2000 to 2003 on mortality and $PM_{2.5}$ mass and components was obtained along with $PM_{2.5}$ speciation data for the 4-year period 2000 through 2003 from the CARB (CARB 2004).	For a 3-day lag, $PM_{2.5}$, EC, OC, and nitrates increased by 1.6, 2.1, 1.6, and 1.5% based on interquartile ranges of 14.6, 0.8, 4.6, and 5.5 μg/m^3, respectively.

Ostro *et al.* (2007)	What are the links between $PM_{2.5}$ and several constituents to mortality causes?	Associations between 19 unique $PM_{2.5}$ constituents and daily mortality in six California counties are examined.	Cardiovascular deaths increased by 1.6% for $PM_{2.5}$, 2.1% for elemental carbon, 1.6% for organic carbon and 1.5% for nitrates in the higher quartile ranges.
Bell *et al.* (2006)	What is the cost of health impacts that are avoidable by implementing readily available technology in Santiago, São Paulo, and Mexico City?	PM_{10} and O_3 levels were estimated in Sao Paulo, Mexico City and Santiago under scenarios. C-R functions were derived using a weighted average.	Results show that from 2000-2020, the reductions in air pollution prompted by the control scenario could save approximately $21 billion (COI) to $165 billion (WTP) in avoided health outcomes across the three cities.
Cohen *et al.* (2005)	How does ambient air pollution contribute to mortality and morbidity in children under 5?	Air pollution worldwide is mapped to mortality and morbidity causes.	It is estimated that 3% of mortality from cardiopulmonary disease, 5% of mortality from trachea, bronchus and lung cancer and about 1% of mortality due to acute respiratory infections in children under 5 is due to ambient air pollution worldwide.
Krauter *et al.* (2005)	What are the impacts of wind power on power systems?	Large-scale wind penetrations were analyzed at the local and system wide levels.	Integrating wind beyond 30% into large interconnected systems could require redesign of the system and operation.
Lopez *et al.* (2005)	What are the health impacts from one of Mexico's largest power plants?	Excess deaths related to PM, NO_x, SO_2 are estimated using CALPUFF and C-R functions.	Annual average $PM_{2.5}$ was 0.12 µg/m^3 (0.00 – 1.43 µg/m^3), resulting in approximately 30 deaths annually valued at 8 million USD.
Miraglia *et al.* (2005)	What is the health burden cost estimate due to air quality in Sao Paulo?	The relative risk of (1) 20% of the less polluted days and (2) 20% of the most polluted days were analyzed.	With a life expectancy of 67.53 years and a VSL of USD 7,714, the total cost of air pollution is USD 3M. Considering a US VSL of $500,000, the costs are USD 208M.
Samoli *et al.* (2005)	What are the exposure-response curves	The exposure-response relationship between	Concentrations of PM^{10} and black smoke have a high correlation to death

	relating PM^{10} and black smoke to mortality?	ambient particles and mortality was analyzed.	rates in 22 European cities.
Ying Zhou *et al.* (2003)	How can human exposure to power plant emissions be calculated?	The intake fraction for fine particulates, sulfates and nitrates is calculated using CALPUFF in Beijing, China.	They find the intake fraction for fine particulates is on the order of 10^{-5} and the intake fraction for sulfates and nitrates is on the order of 10^{-6}.
Levy *et al.* (2002)	What are the expected health impacts caused by nine power plants in Illinois?	CALPUFF is used to simulate primary $PM_{2.5}$ emissions with chemical transformation from nine power plants in Illinois.	There were 320 premature deaths/yr due to primary PM emissions and secondary sulfates and nitrates.
Conceição *et al.* (2001)	What is the relative risk increase in child mortality from PM_{10} exposure in Sao Paulo, Brazil?	A time-series analysis was performed from 1994 to 1997.	A 7% relative risk increase in mortality in children from 0-5 years of age was found.
Cifuentes *et al.* (2000)	How did mortality correlate to six pollutant concentrations in Santiago, Chile?	Daily counts of non-accidental mortality from 1988 to 1996 were regressed against six pollutants in Santiago, Chile.	The authors find that mortality associated with mean levels of air pollution varied from 4 to 11%.
Loomis *et al.* (1999)	How does infant mortality vary in respect to acute exposure to PM_{10}?	A time-series study from 1993 to 1995 on infant mortality in the southwestern part of Mexico City was performed using mortality data from death registrations and air pollution measurements from a monitoring station.	A 10 $\mu g/m^3$ increase in PM10 from mean concentration was associated with a 6.9% increase in infant mortality.
Saldiva *et al.* (1995)	What is the relative risk increase of mortality in elderly people relative to PM_{10} exposure in Sao Paulo?	A time series study from 1990 to 1991 on elderly (65+ years) mortality in Sao Paulo.	A relative risk increase of 13% for PM10-related mortality per 100 $\mu g/m^3$.

4 Methodology: electricity grid simulations (Plexos)

This integrated modeling methodology combines three models to sequentially integrate three simulations: electricity grid simulations (Plexos), air quality modeling (CALPUFF) and human health benefits mapping (BenMAP). I separated my methodology into three distinct chapters to describe each modeling stage in details, especially for the development of the electricity grid dispatch model for Brazil.

4.1 Purpose

This chapter describes the simulation of electricity grid operation and emissions under current and future scenarios in NE Brazil. Figure 1 displays the NE Brazil transmission system, with green lines representing a 230 kV transmission capacity and red lines representing a 500 kV transmission capacity.

The main purpose of developing a NE Brazil Plexos model is to simulate hourly electric grid dispatch of all power plants and their spatially and temporal emissions. The modeling software, study area, scenarios, simulation data and constraints are first described. Then the system validation, model refinements, scenario results and sensitivity tests are discussed.

I also discuss important electricity grid dynamics, such as whether the NE Brazil electric grid can handle large penetrations of renewables and still meet load, voltage and frequency requirements. However, to comprehensively answer the question of the electric grid's ability to handle large penetrations of renewables, more in-depth modeling at the transmission and distribution level of electric grid

interaction would be required. These technical constraints include transmission and distribution voltage and frequency limits, stochastic analysis of varying electric load and intermittent renewable generation patterns, and adapting grid operation procedures, such as flexible AC transmission (FACT), phase shifting transformers, high voltage DC lines, dynamic line ratings and topological corrections. This modeling is being done at the Federal University of Bahia (de Jong *et al.*, 2016) and Federal University of Rio de Janeiro (Miranda *et al.,* 2017).

Figure 4.1. NE Brazil transmission system

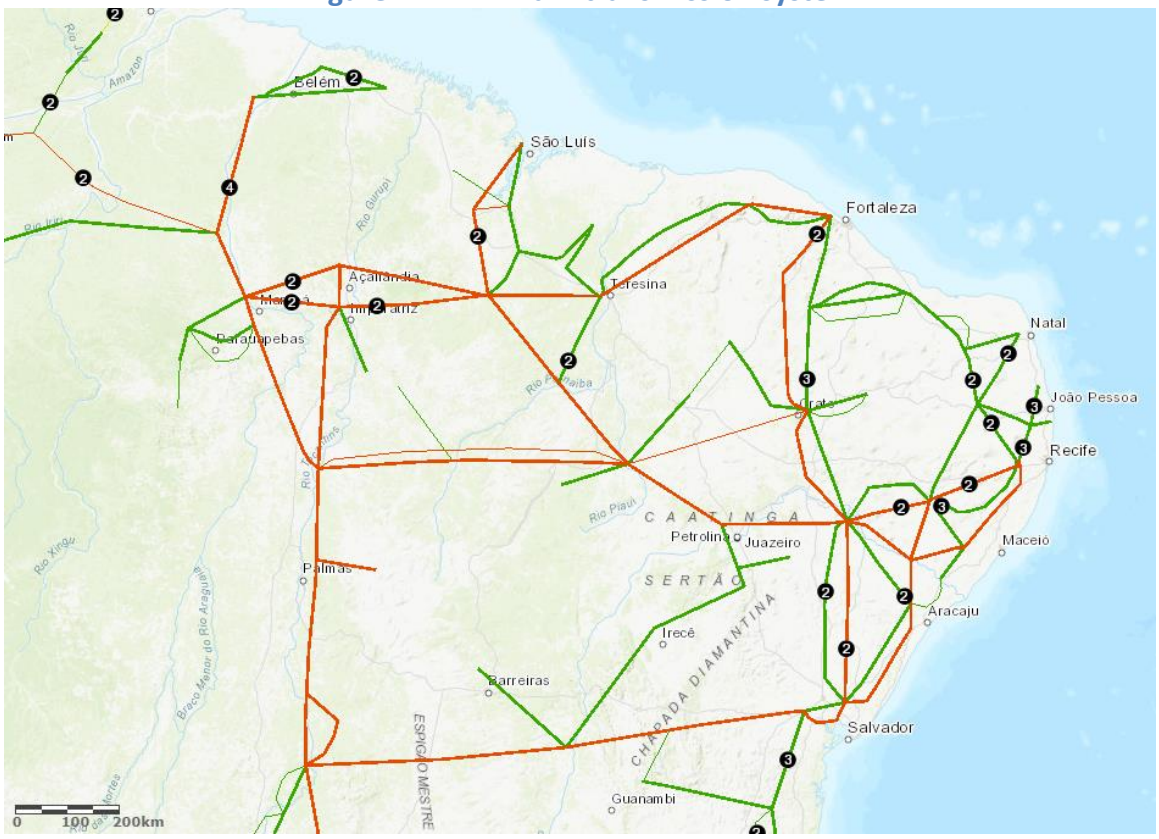

Source: (http://sigel.aneel.gov.br/portal/home/)

4.2 Overview

An overview of my methodology with a high level view of each model and how its output becomes an input for the following model is displayed in the integrated modeling methodology diagram below.

Figure 4.2. Integrated modeling methodology

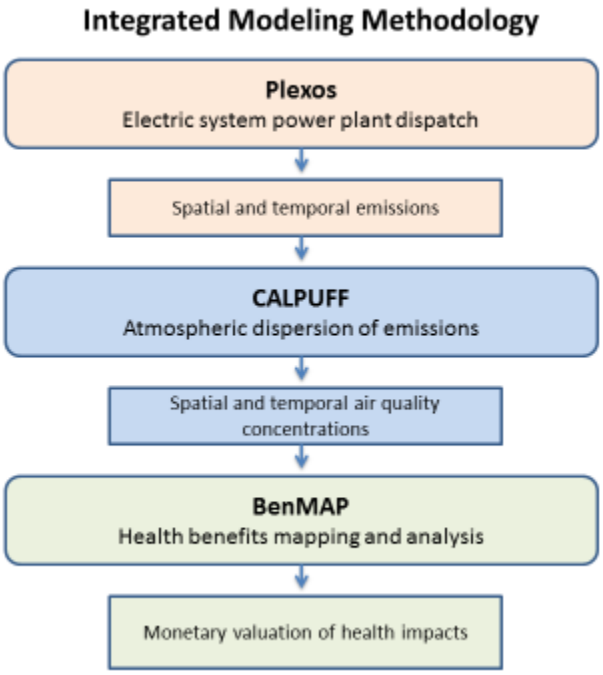

Each model requires a set of components to perform simulations. Figure 4.3 provides an overview of the simulation components.

Figure 4.3. Simulation component overview

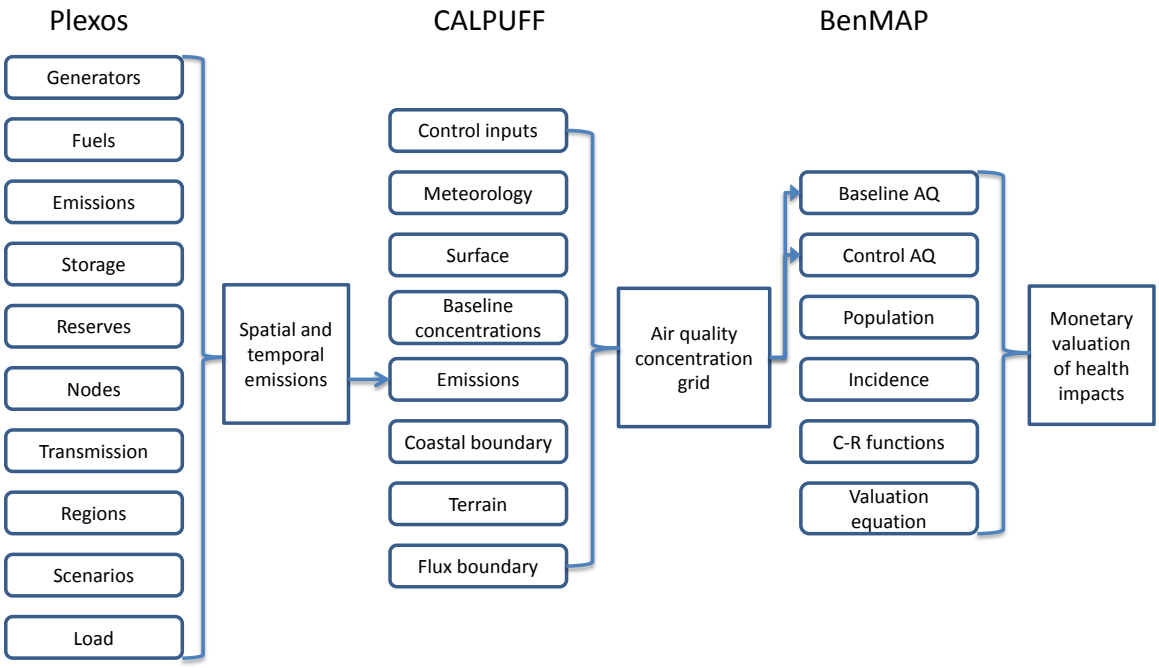

4.3 Modeling Software

An electricity dispatch model for NE Brazil was developed using the Plexos software published by Energy Exemplar LLC. Plexos is an electricity infrastructure dispatch and expansion planning simulation tool. Dispatch refers to the optimal output of electricity generation facilities, to match system load and generation at the lowest cost, under transmission and operational constraints.

Plexos works with commercial and academic solvers, such as CPLEX, Gurobi, MOSEK and XPRESS-MP to solve linear, quadratic and mixed integer programming problems that occur while simulating dispatch in the same way as is done to clear energy markets worldwide. Unit commitment and economic dispatch are designed to be mathematically consistent, and co-optimized with decisions relating to energy availability and demand, ancillary services (services such as frequency control and

spinning reserve resources needed to support reliable transmission of electricity) and gas production.

The NE Brazil Plexos model simulates hourly individual power plant dispatch to balance load (demand) and generation (supply) based on the marginal cost of generation. Emissions profiles for each power plant generated in Plexos are then dispersed in CALPUFF (Energy Exemplar, 2014).

4.4 Study Area

As discussed previously, I selected Brazil because of its rapidly increasing energy demand, high wind and solar generation potential, large hydroelectric capacity and dependency, and data availability. Within Brazil, I selected the NE Brazil electricity grid area because it has some of the highest wind and solar generation capacity factors in the world and because of the location of thermal generators to densely populated cities. My study areas for the main questions this dissertation addresses are described below.

4.4.1 Study area for tightening PM standards

To assess the health benefits of tightening PM standards, I simulated the entire NE Brazilian electricity system on an hourly basis for 2015. Of particular importance for assessing the impacts of tightening PM standards are the only two large coal power plants in NE Brazil, Porto do Pecem I (720 MW) and Porto do Pecem II (360 MW), which are located 30km from the Fortaleza metropolitan region.

Figure 4.4 displays the Fortaleza region relative to NE Brazil and South America. The generators surrounding Fortaleza are superimposed on a population density map of the Fortaleza, where the black dots represent coal power plants, brown dots represent oil power plants and the grey dot represents a natural gas power plant. I limited the air quality modeling and human health benefits mapping to Fortaleza because the only coal power plants in NE Brazil are located near Fortaleza, in addition to some smaller oil and gas power plants.

Figure 4.4. Power plants near Fortaleza

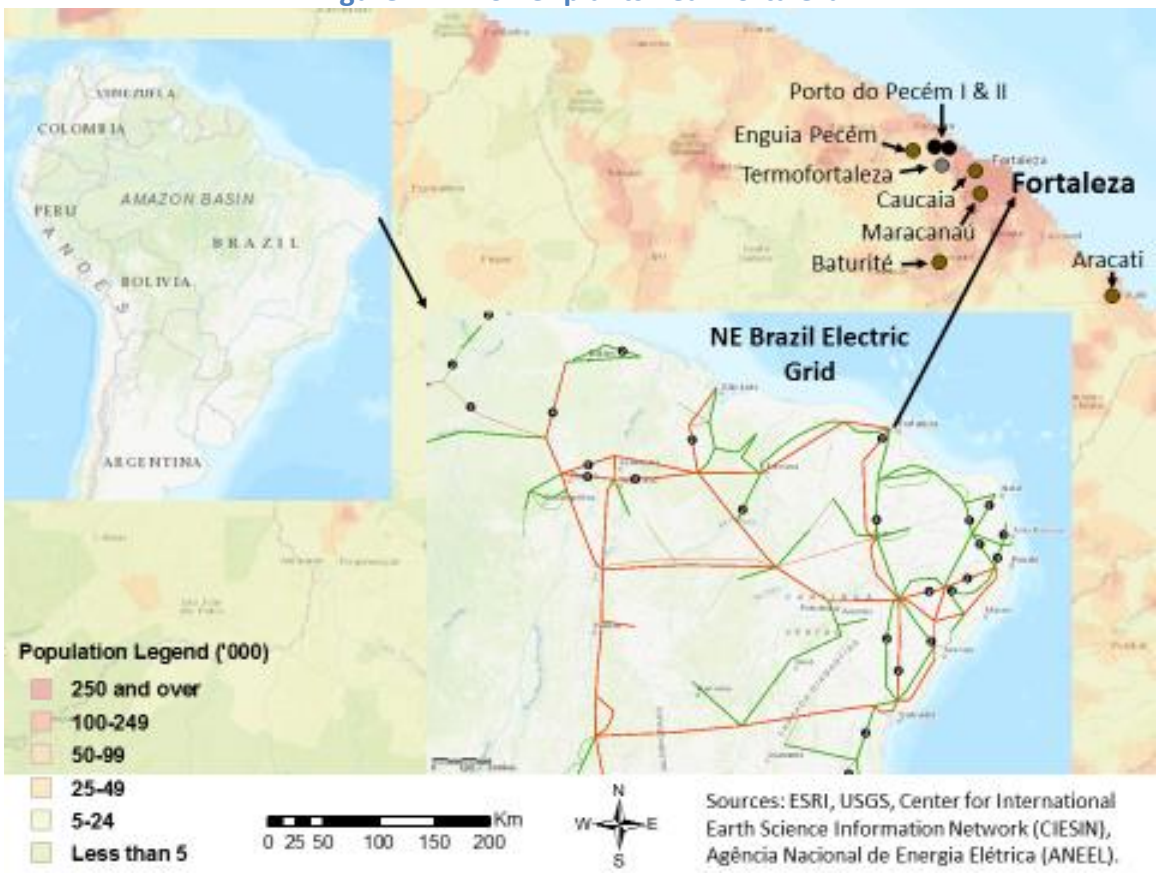

4.4.2 Study area for assessing health, storage and grid implications

In addition to the Porto do Pecem coal power plants, there are approximately 25 diesel and gas power plants located within 5-10 km of NE Brazil's most populated cities, including Recife, Salvador and Fortaleza (Operador Nacional do Sistema Eletrico, 2016b). These plants create the potential for adverse air quality and health impacts for residents of these cities mostly because of PM emissions. I selected NE Brazil's three most densely populated areas for air quality modeling and human health benefits: Fortaleza region (320km x 320km), Recife region (320km x 320km), and Salvador region (320km x 320km) for emission dispersion and health impact analysis. I selected these three regions because a majority of NE Brazil's centrally dispatched thermal generators are located there near densely populated areas.

4.5 Scenario Development

Scenarios were developed to for each of the three primary topics of this dissertation: (1) the health benefits and control costs of tightening PM standards; (2) the health, climate, and grid storage and stability requirements of high penetrations of VRE; and (3) key implications of a 100% renewable energy electricity system.

4.5.1 Scenarios for tightening PM standards

I found several published PM emission factors for coal power plants while reviewing regulatory documents from Brazil's national agencies. I selected three Brazilian standards and one US standard to analyze the health impacts of moving from a high

to a moderate PM standard, from a moderate to a low PM standard, and from a low PM standard to a very low PM standard.

The highest emissions standard is the 28.15 g/kWh standard set by the Brazilian Ministry of Mines and Energy (MME) in a 2030 National Energy Plan (Ministério de Minas e Energia, 2007), the 0.69 g/kWh standard represents a lower emission standard set by the national Counsel of the Environment in Brazil (CONAMA) (Ferreira *et al.,* 2015), 0.36 g/kWh is the lowest standard in Brazil set by the Brazilian Development Bank (BNDES) (Governo do Estado do Ceará, n.d.), and 0.04 g/kWh is cleanest standard that was set by the US Environmental Protection Agency (EPA) for all fossil fuel combusting electric utility steam generating units greater than 73 MW in capacity constructed after May 3, 2011 (US Environmental Protection Agency, 2015). More details on each standard are presented in the emission standards section of the Background chapter.

Electricity grid dispatch and emissions were simulated for each emission standard. Each standard is implemented under the same infrastructure and operation in the NE Brazil electricity grid for 2015, therefore, the only variable that changes in the above scenarios is the emission standards for coal power plants.

I selected 2015 as the base year to simulate NE Brazil electric grid dispatch because it was the most recent year for which data were available. In 2015, NE Brazil's installed electric capacity exceeded 29,000 MW and had an annual electricity demand of over 85,000 GWh (Operador Nacional do Sistema Eletrico 2016). The installed capacity of electric generators regulated by the central dispatch authority ONS in NE Brazil is shown in Table 4.1.

Table 4.1. NE Brazil installed system capacity in 2015

Type	Generator (#)	Capacity (MW)	System Capacity (%)
Wind	291	7,650	25.9%
Solar	52	1,325	4.5%
Hydro	11	14,721	49.8%
Biomass	1	17	0.1%
Natural gas	7	2,094	7.1%
Coal	2	1,080	3.7%
Oil	29	2,684	9.1%
Total	**393**	**29,570**	**100.0%**

4.5.2 Scenarios for assessing health, climate, and grid storage and stability

This next set of simulations for 2015 and 2030 were developed to assess the health, climate, and grid storage and stability implications of different levels of high renewable penetrations. There are three primary scenarios and three expanded scenarios designed to analyze system sensitivity:

1. **2015 BC** - 2015 Base case.
2. **2030 HR** - 2030 Hydro-renewable with 45% VRE, 79% total renewables.
3. **2030 HT** – 2030 Hydro-thermal with 30% VRE, 72% total renewables.
4. **2015 DY** – 2015 Dry Year. Same as 2015 BC, with dry year conditions limiting hydroelectric production instead of 2015 precipitation.
5. **2030 HR DY** – 2030 Hydro-renewable Dry Year. Same as 2030 HR with dry year conditions.
6. **2030 HT DY 5.5%** – 2030 Hydro-thermal High Demand Dry Year. Same as 2030 HT, with a 5.5% instead of a 4.77% average annual electricity demand increase and dry year conditions.

The 2030 HR scenario represents a realistic best-case scenario and the 2030 HT HD DY scenario represents a worst case for emissions. All scenarios assume the 4.77% average annual electricity demand projection for NE Brazil by Torrini *et al*. (2016), except the 2030 HT DY 5.5% scenario.

I developed three initial scenarios for NE Brazil, a 2015 Base case and two 2030 scenarios that represent different yet realistic electricity infrastructure expansion paths that NE Brazil could take to meet future demand. The scenarios are defined in terms of installed capacity as a percentage of total electric system installed capacity to be in the same format as Brazil's 2013-2023 decadal electricity expansion plan, which regulates electricity infrastructure expansion based on installed capacity (Ministério de Minas e Energia Secretaria de Planejamento e Desenvolvimento Energético, 2014).

The purpose of these scenarios is to simulate the PM and CO_2 emissions in NE Brazil according to the 2015 electric grid interaction, and how PM and CO_2 emissions change in 2030 if a Hydro-renewable expansion with a system capacity of 45% intermittent renewables (79% total renewables) is adopted over a Hydro-thermal expansion with a system capacity of 30% intermittent renewables (72% total renewables). Table 4.2 and Table 4.3 present the scenarios by system capacity as a percentage of total capacity and by number of generators and MW per power plant type.

Table 4.2. Scenarios by installed capacity (% of total)

Type	2015 Base case Capacity (%)	2030 Hydro-renewable Capacity (%)	2030 Hydro-thermal Capacity (%)
Wind (%)	25.9%	39.0%	25.2%
Solar (%)	4.5%	6.8%	4.4%
Hydro (%)	49.8%	33.1%	42.0%
Biomass (%)	0.1%	0.1%	0.1%
Natural gas (%)	7.1%	16.3%	15.9%
Coal (%)	3.7%	1.4%	3.6%
Oil (%)	9.1%	3.4%	8.8%
System Cap (MW)	29,570	78,478	60,783

The scenarios are defined below in terms of the numbers of generators and MW of installed capacity to quantify how installed capacity changes between scenarios.

Table 4.3. Scenarios by installed capacity (number of generators and MW)

	2015 Base case		2030 Hydro-renewable		2030 Hydro-thermal	
Type	Generator (number)	Capacity (MW)	Generator (number)	Capacity (MW)	Generator (number)	Capacity (MW)
Wind	291	7,650	1,164	30,601	582	15,300
Solar	52	1325	208	5300	104	2650
Hydro	11	14,721	25	25,987	25	25,544
Biomass	1	17	2	67	2	67
Natural gas	7	2,094	20	12,760	18	9,693
Coal	2	1,080	2	1,080	4	2,160
Oil	29	2,684	29	2,684	58	5,368
Total	393	29,570	1,450	78,478	793	60,783

Each of the initial scenarios is described below. The expanded scenarios, which were formed for sensitivity analysis, are described in the following subsection.

1) **2015 Base case**. This scenario includes all generators that were available for producing power as of January, 2015. A 2015 load profile was forecasted based on the actual 2013 hourly load profile from Brazil's national electricity system operator, ONS.
2) **2030 Hydro-renewable with 45% intermittent renewables**. System capacity was extrapolated based on trends in Brazil's 2013-2023 electricity expansion plan. Wind and solar installed capacities were quadrupled, hydroelectric increased by 73%, natural gas increased by 509%, and biomass was increased by one generator that has already been approved for 2020. This scenario is 45% intermittent renewable (wind and solar) energy by installed capacity, and 79% renewable including hydroelectric resources.
3) **2030 Hydro-thermal with 30% intermittent renewables**. System capacity was forecasted based on Brazil's 2013-2023 decadal electricity expansion plan published by Brazil's Ministry for Mines and Energy. Wind, solar, coal and oil installed capacities were doubled from the 2015 baseline, natural gas increased by 363%, hydroelectric was increased 73%, and biomass was increased by one generator that had been approved for 2020.

To increase the installed capacity of generation technology, identical generators were added, holding the generation capacity and technical, economic and spatial characteristics constant. To decrease installed capacity of thermal generators in the 2030 hydro-renewable scenario, coal, oil and natural gas generators were decommissioned in an equal fashion from each sub-region of Northeast Brazil.

I ensured that the installed capacity for each category of generation in the 2030 scenarios was lower than the technical potential of each generation category in Brazil. The potential for wind power generation in NE Brazil is 71,000 MW and the potential for solar power generation is greater than 1,000,000 MW (Gils *et al.*, 2017), which are at least 2.3 times and 200 times greater than the installed wind and solar capacity in the 2030 scenarios, respectively.

I based the potential of hydropower in NE Brazil on the Atlas of Electric Energy of Brasil published by Brazil's national energy regulator ANEEL (Agencia Nacional De Energia Electrica, 2000). The two main hydrographic basins in Northeast Brazil are the Bacia do Altântico Nordeste-Norte and the Bacia do Rio São Francisco, and a small portion of Bacia Atlântico Leste is also in NE Brazil.

The Bacia do Altantico has a hydroelectric potential of 3,402 MW. The Bacia do Rio São Francisco has a hydroelectric potential of 26,319. However, the southern portion of the basin is not in NE Brazil. To calculate the hydroelectric potential of the portion of Bacia do Rio São Francisco that is in NE Brazil, the hydroelectric sub-basins of the Bacia do Rio São Francisco that are in NE Brazil were summed. Similarly, the hydroelectric potential of the sub-basins of the Bacia Atlântico Leste that are in NE Brazil were also considered.

The hydroelectric potential of the hydrographic sub-basins that are in NE Brazil are reported in Table 4.4. A total hydroelectric potential of 26,330 MW was calculated for Brazil.

Table 4.4. Hydroelectric potential in NE Brazil by basin and sub-basin

Basin	Sub-basin	Hydroelectric potential (MW)
Bacia do Altântico Norte/Nordeste		3,402
Bacia do Rio São Francisco		
	Rios São Francisco, Verde Grande	493
	Rios São Francisco, Carinhanha	354
	Rios São Francisco, Grande	816
	Rios São Francisco, Jacaré	1,050
	Rios São Francisco, Pajeú	1,533
	Rios São Francisco, Moxotó	17,578
Bacia do Altântico Leste		
	Rios Vaza-Barris, Itapicuru	11
	Rios Paraguaçu, Jequiriçá	805
	Rios de Contas	153
	Rios de Cachoeira	135
Hydroelectric potential in NE Brazil (MW)		**26,330**

Following the trends from the 2030 decadal electricity expansion plan for Brazil, the 2030 scenarios install hydroelectric power plants close to, but not greater than, the total hydroelectric potential in NE Brazil.

4.5.3 Scenarios for 100% RPS implications

A 2030 100% RPS scenario was formed to explore the tradeoffs between health, climate, and grid storage and stability when moving from a high penetration of renewables to a 100% renewable portfolio standard. The 2030 100% RPS scenario is based on the 2030 HR scenario, however all thermal generators are

decommissioned, and in place more wind, solar and hydroelectric power plants were added.

In the 100% RPS base scenario, installed wind energy capacity was increased to 53,446 MW and solar energy was increased to 9,214 MW. The wind and solar capacities were increased by the same proportion of installed wind energy to installed solar energy capacity as were installed in NE Brazil in 2015. This is approximately 75% of the 71,000 MW potential for wind energy in NE Brazil, and 0.9% of the 1,000,000+ MW solar energy potential in NE Brazil.

The installed hydroelectric capacity was increased to 26,250 MW by adding the hydroelectric investment opportunities reported by Fichter *et al.* (2017). These plants were not identified as having pumped storage potential because the surrounding geography is not sufficiently steep. The installed hydroelectric capacity is maximized in the 100% RPS scenario based on the hydroelectric potential in NE Brazil, with 26,250 MW installed of the approximate 26,300 MW potential capacity. This provides the highest amount of potential hydroelectric flexibility to balance load and generation under high penetrations of fluctuating VRE generation.

The resulting unserved load and dump energy in the 2030 100% RPS scenario will be an indication of the amount of electricity imports and exports needed to balance a 100% RPS electric grid in NE Brazil. North Brazil has an abundance of hydro resources, which could be used to export electricity to NE Brazil when needed to minimize unserved load, as well as import electricity from NE Brazil when generation is greater than load to minimize dump energy.

A graphic representation of Brazil's hydroelectric potential (MW) by hydrographic sub-basin is presented in Figure 4.5. A substantial amount of Brazil's hydroelectric resources are in North Brazil, which had 31,899 MW of installed hydroelectric capacity in the year 2000 and a total potential of 105,410 MW (Agencia Nacional De Energia Electrica, 2000). It is estimated that Brazil has a total hydroelectric potential capacity of 520,190 MW (Agencia Nacional De Energia Electrica, 2000), capable of generating 1,488 TWh/year (Pereira *et al.*, 2012).

Figure 4.5. Brazil's hydroelectric potential (MW) per hydrographic sub-basin

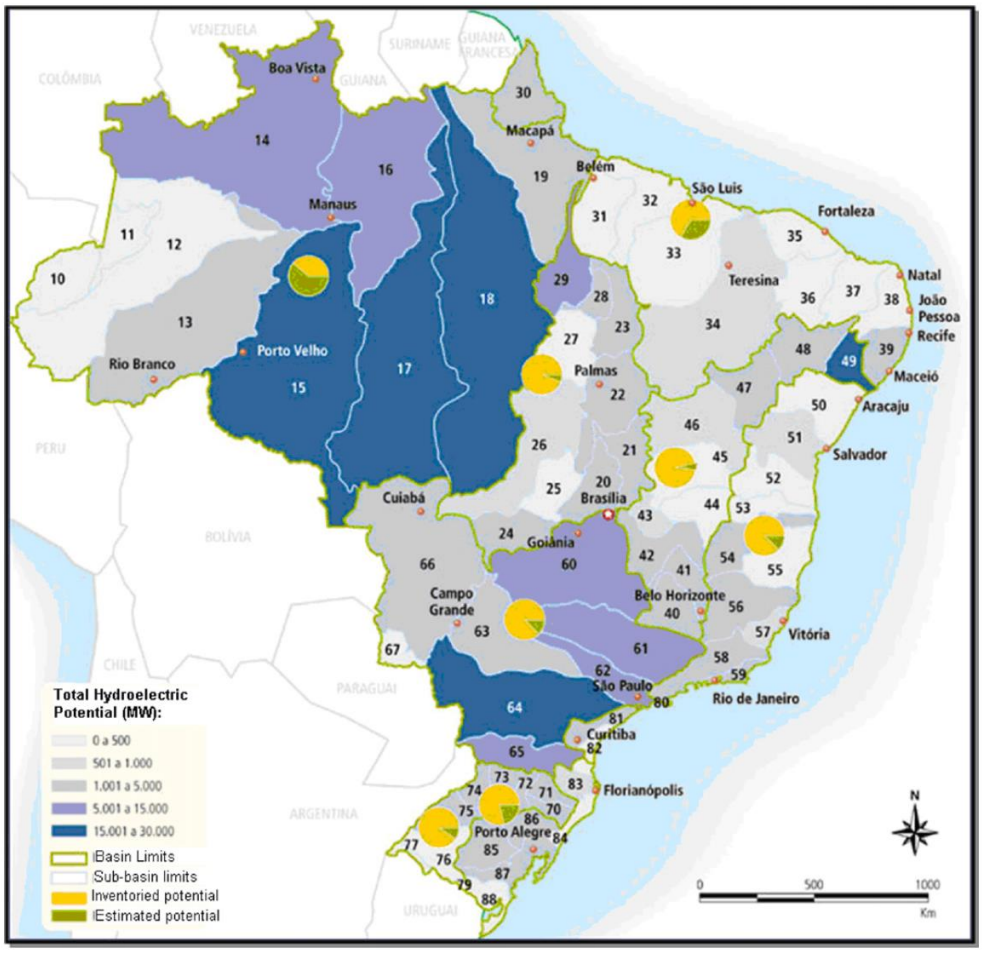

Source: Pereira *et al.* (2012).

4.6 Expanded Scenarios

I formed expanded scenarios to assess how electricity system dispatch, pumped storage, emissions and grid stability are affected by dry conditions and a higher than forecasted electricity growth rate. Below are descriptions of each of the expanded scenarios.

4.6.1 Dry year scenarios

From 2013 to 2015, Brazil experienced the worst drought since 1930, with the main impact happening in SE Brazil. This drought made it difficult for Brazil to meet water demand in SE Brazil, as well as energy demand around the country (Nazareno & Laurance, 2015). During years with significantly less than average precipitation (dry years), there is less water stored in the reservoirs, leading to less hydropower availability, which causes many thermal generators to be dispatched throughout the year (Avelino *et al.,* 2015).

Annual precipitation data were acquired for the NE Brazil water basin from 1983 to 2015. The NE Brazil water basin was selected because it is the water basin that the hydroelectric power plants in NE Brazil are connected to. Annual precipitation variability from 1983 to 2015 was much larger in the NE Brazil water basin than in Brazil has a whole (Center for Hydrometeorology and Remote Sensing, 2016), likely because it is a country larger than the continental U.S. and inter-regional variations balance each other.

To simulate a dry year, water reservoir initial and final fill levels and hydro generator max energy per month were decreased by 30.5%, which is the percentage

difference between the average annual precipitation levels and the precipitation levels in 2012, which was the driest year since 2000 (Center for Hydrometeorology and Remote Sensing, 2016). Reducing hydropower availability increases dependence on thermal generators, specifically the oil and gas generators in Recife and Salvador, to be dispatched as load following generators to match electric demand and generation, as well as frequency and voltage control.

The internal combustion (IC) generators in the 2015 scenario are rarely dispatched because there is sufficient hydroelectric and natural gas capacity to balance load and generation. Therefore, simulating a dry year causes IC generators to be dispatched more frequently, which could substantially impact emissions in Recife and Salvador, where the majority of the IC generators are located.

4.6.2 Projected and higher than projected electricity demand increase rates

Torrini *et al.* (2016) projected electricity demand in Brazil from 2014 to 2030 using a fuzzy logic approach. Their approach projects demand region-by-region and sector-by-sector, and their results forecast a 4.77% electricity demand increase in NE Brazil from 2014 to 2030. I used this projected 4.77% average annual electricity demand increase in NE Brazil to forecast energy demand. Using the Plexos load forecasting algorithm and the 2013 actual hourly load profile (obtained from Operador Nacional do Sistema Eletrico, 2016a), a maximum hourly electricity demand (MW) and a targeted annual electricity demand (MWh) were derived and used in creating hourly load profiles for 2015 and 2030.

As it is possible that the actual average annual electricity demand increase in NE Brazil may be even higher than the projected 4.77%, a scenario with a 5.5% average annual electricity demand increase from 2015 to 2030 was created, using the same forecasting algorithm. I selected 5.5% because there were five non-consecutive years between 1996 to 2016 where annual electricity demand grew 5.5% or more (World Bank, 2015).

4.6.3 Varying intermittent generation and electric load patterns

A typical sensitivity test that can be performed when assessing the electricity system impacts of higher penetrations of renewables is to vary intermittent wind and solar generation patterns relative to electricity demand patterns. NE Brazil is a semi-arid region with very high and consistent wind speeds and solar radiation exposure (Krauter, 2005).

Varying wind and solar generation patterns, without changing total annual generation, could potentially increase or decrease thermal generation and emissions. For example, VRE generation needs to be curtailed at any hour where baseload generation plus renewable generation is greater than demand (Chang *et al*., 2013; Eichman *et al*., 2013). If the VRE generation patterns match electric demand profiles more closely, there is less curtailment, which means less thermal generation if annual demand is constant. Similarly, if VRE generation patterns are less similar to electric load patterns, this would cause greater ramping up and ramping down of load following power plants, which would decrease efficiency and

increase emissions, assuming that annual electricity demand is constant (Makarov *et al.*, 2009).

While changing intermittent generation and electric load patterns affects the electric system, it is not likely that emissions will change substantially because total load and generation are held constant. However, simulating an annual electricity demand increase from 2015 to 2030 of 5.5%, as opposed to 4.77%, increases total electricity demand in 2030 from 194,562 GWh to 218,881 GWh. This additional increase of 11.1% of total electricity demand in the high energy demand scenario would put substantial pressure on thermal generators and even surpass total system capacity occasionally, leading to unserved load.

Similarly, dry year conditions are likely to cause the oil and gas generators in Recife and Salvador to be dispatched much more frequently than during a normal or wet year. In that case, the load following thermal generators could be needed on a more regular basis to balance load and generation during dry year conditions when hydroelectric availability is decreased. This is especially true for oil generators, which are dispatched after available natural gas resources due to higher marginal fuel costs for oil generators.

4.7 Simulation Data

Building an electricity dispatch model requires a comprehensive dataset, including all generators, fuel sources, emissions, storage units, reserves, transmission lines and their corresponding technical and economic properties and constraints. Hourly electricity demand, which is technically called system load, is also required. This

section outlines the data requirements, selections and assumptions involved with developing an electric dispatch model for NE Brazil. Figure 4.6 provides a high level view of the data types and properties selected for this study.

The Plexos software provides a vast array of energy infrastructure properties, technical and economic, to consider when simulating electricity grid operation. The flowchart shown on Figure 4.6 depicts the objects, memberships and properties selected for generators, fuels, emissions, storage, reserves, transmission system and simulation dynamics.

The data I used for the Plexos simulations were collected in collaboration with the Center for Energy and Environmental Economics at the Federal University of Rio de Janeiro. These data are the same as those used in the MESSAGE Brazil model, which is currently the only integrated energy system assessment tool for Brazil and has been used in a variety of applications (Herreras *et al.,* 2015; Lima *et al*., 2015; Lucena *et al*., 2016; Pupo *et al*., 2016; Soares *et al.,* 2012; Soria, Lucena *et al*., 2016; Soria *et al*., 2016).

Figure 4.6. Plexos data for electric grid simulations

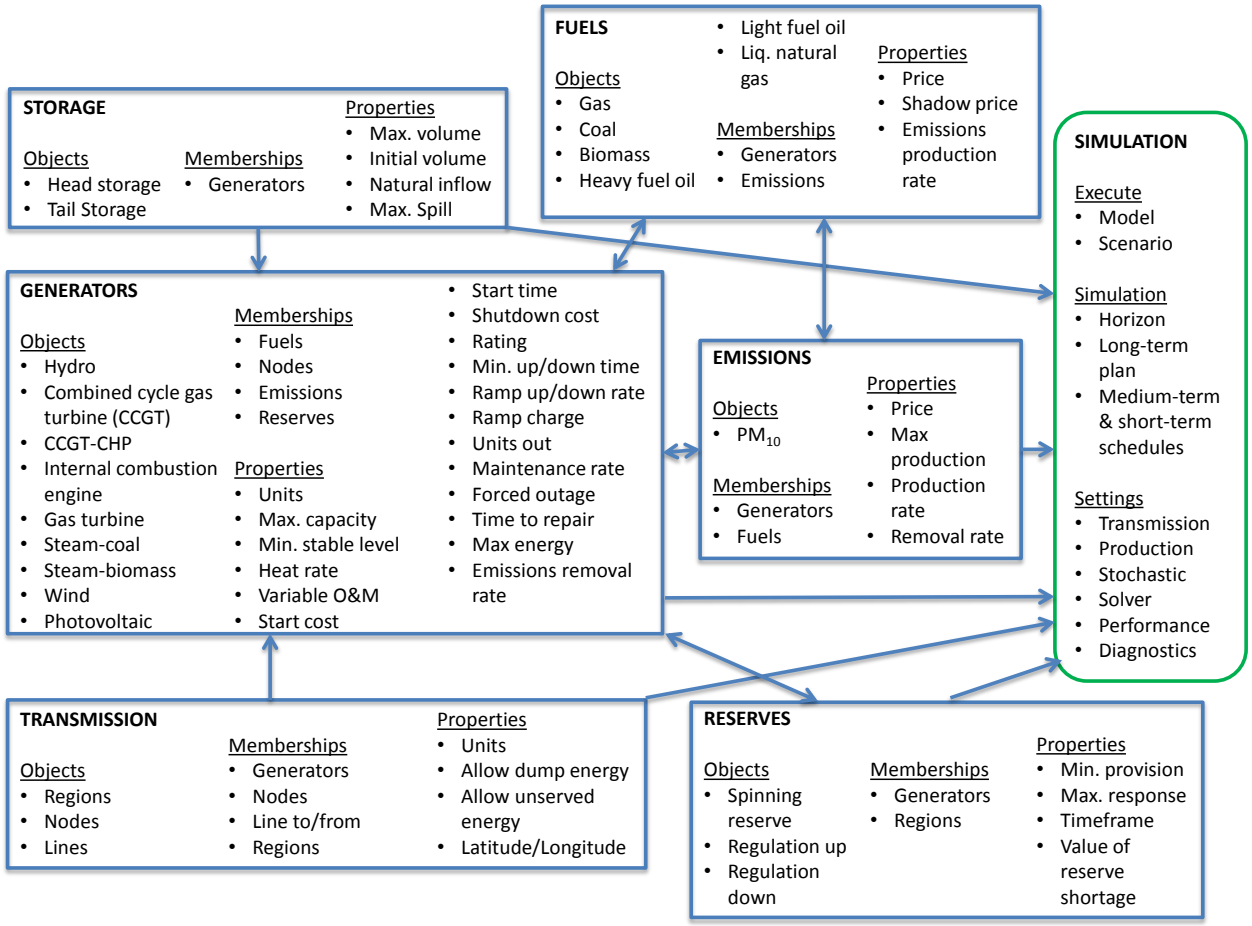

The data were sourced primarily from Brazil's national electricity operation authority (ONS) and the national energy regulator (ANEEL) (Agencia Nacional de Energia Eletrica, 2016; Operador Nacional do Sistema Eletrico, 2016a).

The following subsections provide details on the generators, fuels, emissions, storages, reserves, nodes, transmission system and constraints that were used when developing the NE Brazil model.

4.7.1 Generators

As of 2015, the installed capacity (total capacity of all power plants) of the NE Brazil electric grid exceeds 29,000 MW, with an annual electricity demand over 85,000 GWh (Operador Nacional do Sistema Eletrico 2016). NE Brazil's electric grid has 393 generators with an aggregate capacity of over 29,000 MW.

Table 4.5. NE Brazil electric grid installed capacity by generator type[2]

Type	Number of Generators	Capacity (MW)	System Capacity (%)
Wind	291	7,650	25.9%
Solar	52	1,325	4.5%
Hydro	11	14,721	49.8%
Biomass	1	17	0.1%
Natural gas	7	2,094	7.1%
Coal	2	1,080	3.7%
Oil	29	2,684	9.1%
Total	**393**	**29,570**	**100.0%**

Source: ANEEL and ONS

[2] CCGT – combined cycle gas turbine
CCGT-CHP – combined cycle gas turbine with combined heat and power
GT – gas turbine
HFO – high fuel oil
LFO – low fuel oil

Although the average hourly load in 2015 was 10,600 MW, a much larger system capacity is needed because most of the capacity of the electric grid is provided by hydroelectric and wind generators, which have low capacity factors relative to thermal generators. Table 4.5 displays NE Brazil's electric system installed capacity by generator type.

4.7.2 Fuels

The type of fuel consumed by a generator influences the cost of electricity production, emissions, and the potential to produce electricity under fuel availability constraints.

Some types of electricity generation facilities do not require fuel, such as wind and solar, but their production is constrained by the intermittent and fluctuating availability of wind and solar resources. Other types of electricity generation facilities, such as hydroelectric or geothermal, are constrained by the availability of water (in the case of hydroelectric) or high temperature geothermal resources located near the Earth's surface.

Coal power plants in Brazil use domestic as well as imported coal that vary in chemical makeup, biomass plants use solid biomass as a fuel (as opposed to biogas plants that use biogas), oil generators can use heavy fuel oil (diesel), light fuel oil (petroleum), or biofuels (such as sugar cane-based ethanol), and gas turbines can use natural gas, renewable natural gas made from anaerobic digestion of biomass, or even liquefied natural gas.

The two coal power plants in NE Brazil use imported coal, which releases approximately 50% less greenhouse gas and air pollutant emissions per MWh than Brazilian coal. This is because Brazilian coal has about half the energy density (BTU content) as imported coal, requiring approximately twice as much Brazilian coal to be burned per MWh compared to imported coal (Silva *et al.*, 2009).

All combined cycle gas turbines and gas turbines use natural gas, except for one that uses imported liquefied natural gas. The biomass steam turbines (there is one in the 2015 scenarios and two in the 2030 scenarios) uses bagasse (a fibrous material that remains after the production of products like ethanol from sugarcane, and the internal combustion engines either use heavy fuel oil (diesel) or light fuel oil (petroleum).

Some generators use a different start fuel than operational fuel. In the NE Brazil electric grid, the start fuel is the same as the operational fuel for all thermal generators, except that a portion of the heavy fuel oil generators use light fuel oil as start fuel.

4.7.3 Emissions

One of the main foci of this dissertation study is to analyze how changes in electric grid emissions change air quality concentrations of pollutants and human health impacts. Therefore, simulating spatial and temporal emissions profiles as accurately as possible given the publicly available data is critical.

Emissions in the NE Plexos model are defined at the generator level and at the fuel level. Defining emissions at the generator level accounts for emissions

control technology unique to each generator. However, data on installed emissions controlled technology at each power plant in Brazil is not available.

The PM emission factors used in this study are based on the emission rate standards in Brazil's National Energy Plan for 2030 report, published by Brazil's Ministry of Mines and Energy (Ministerio das Minas e Energia) and Brazil's national energy research organization (Empresa de Pasquisa Energeticam (Ministerio das Minas e Energia and Empresa de Pasquisa Energetica 2007). These standards were selected for several reasons. First, they are defined for each combustion fuel and technology used in Brazil, and they provide a uniform set of standards from a single authoritative source. The standards also make sense when comparing emission factors across fuel sources, and they have been used in previous studies (Alves & Uturbey, 2010).

Northeast Brazil has only two coal power plants, both of which are located in Porto do Pecem, near the Fortaleza metropolitan area. The Brazilian Development Bank (BNDES) provided funding for both coal power plants, and requires them to meet an emission standard of 0.36 g/kWh, which is lower than the emission standard published by the National Counsel of the Environment (CONAMA) and Ministry of Mines and Energy (MME). The BNDES emission standard specific to the Porto do Pecem power plants is used in all scenarios, except for the scenarios that were developed to assess the health benefits and control costs of tightening PM standards.

Table 4.6. PM_{10} emission rate standards

Fuel	Technology	PM_{10} Standard	Source
Porto do Pecem (imported coal)	Steam boiler	0.36 g/kwh	Governo do Estado do Ceará; Instituto Centro de Ensino Technologico
Natural gas	Combined cycle gas turbine	0.0418 g/kwh	Ministerio das Minas e Energia, Empresa de Pasquisa Energetica 2007
Diesel	Combustion engine	0.3685 g/kwh	Ministerio das Minas e Energia, Empresa de Pasquisa Energetica 2007
Biomass	Steam boiler (60 bar)	0.49 g/kwh	Ministerio das Minas e Energia, Empresa de Pasquisa Energetica 2007, Alves *et al.* 2010

I assume that thermal power plants will install sufficient emissions controls to meet these emissions standards, including at the Porto do Pecem coal power plants, which is consistent with Alves and Uturbey (2010). However, in the scenarios used to assess the impact of tightening PM standards, the PM_{10} emission standard for the Porto do Pecem coal power plants was varied from very high to low. In these scenarios, I also assume that power plants reduce emissions to the standard set by the scenario.

To assess GHG emissions, CO_2 emissions were defined at the fuel level for each fuel type. The amount of CO_2 released when a fuel is burned is based on the carbon content of the fuel. During complete combustion, a fuel reacts with oxygen and produces CO_2 and water (as opposed to incomplete combustion, when there is not is not enough oxygen to allow the fuel to react completely to produce CO_2 and

water). The amount of CO_2 released by different fuels has been extensively studied and documented.

Different types of coal emit different amounts of CO_2 per energy input. The two coal power plants in NE Brazil use coal imported from Colombia. Approximately 90% of the coal that Brazil imports from Colombia is bituminous coal (Vasconcelos, 2014). Bituminous coal produces approximately 4.5% less CO_2 per energy output than lignite or subbituminous coal, and approximately 10% less CO_2 per energy output as anthracite coal (U.S. Energy Information Administration, 2017a).

The following CO_2 emission rates were selected based on a U.S. Energy Information Administration study on CO_2 emission coefficients: 88.42 kg CO_2 per GJ of bituminous coal (205.7 lb/MMBtu), 69.34 kg CO_2 per GJ of diesel fuel (161.3 lb/MMBtu), and 50.30 kg CO_2 per GJ of natural gas (117 lb/MMBtu) (U.S. Energy Information Administration, 2017a).

I did not consider the quantity of CO_2 released from biomass power plants because CO_2 released from bioenergy production is typically considered carbon neutral, and can even be carbon negative depending on the process (Lehmann, 2007). GHG emissions beyond CO_2 were not considered.

4.7.4 Storages

Energy storage becomes critical for balancing load and generation as intermittent renewable penetration levels increase (Callaway, 2009; Liu *et al.*, 2011). In Northeast Brazil, energy storage is provided by pumped hydro storage plants.

Pumped hydro storage plants store energy by pumping water from a lower elevation tail storage to a higher elevation head storage during off-peak when electricity costs are lower. This consumes more energy than is generated when the water is released from the head storage to the water turbine, but overall the system benefits because of the price differences between when water is pumped and dispatched (Crampes & Moreaux, 2010).

The 2015 BC uses the existing pumped hydro storage reservoir capacities, which consists of four hydroelectric power plants with an aggregate generation capacity of 5,949 MW. The 2030 scenarios include the pumped hydro storage reservoirs that have been approved but not yet constructed, as well as new pumped hydro reservoirs that are projected to be constructed (Ministério de Minas e Energia Secretaria de Planejamento e Desenvolvimento Energético, 2014).

Hydro pump efficiency, generator head storage, generator tail storage, storage maximum volume, storage minimum volume, storage initial volume and storage final volume are defined for each pumped storage generator. A round-trip percentage efficiency of 80% implies that 1/0.80 = 1.25 units of energy are required to pump water that will produce one unit of energy from the tail to head storage, which further implies that the price received when generating electricity must be at least 25% greater than electricity prices when pumping water (Energy Exemplar, 2014). Applicable memberships, which are associations such as to a hydroelectric power plant and transmission node, as well as technical and economic properties are assigned to each hydro storage reservoir.

4.7.5 Reserves

Reserve resources, also known as ancillary services, play an important role in balancing electric grid load and generation.

Spinning reserve resources are generators that have contracts to run at less than full capacity and the ability to quickly ramp up or down production as needed to balance load and generation. Regulation up and down resources are generators under contracts that are available for very quick ramping up and down to ensure that frequency and voltage constraints of the transmission system are not exceeded as exceeding these constraints would create an outage (Energy Exemplar, 2014).

When deciding whether a resource is dispatched to regulate load balancing or frequency and voltage constraints, the marginal dispatch cost is compared with the alternative cost of unserved load in the case when load would exceed generation. If generation is greater than load, the cost of ramping down generation is compared with the cost to dump the excess load (dump energy cost). Unless unserved load or dump energy costs are unusually low, it costs less to utilize the resource than to incur the unserved load or dump energy penalty.

4.7.6 Nodes and Transmission lines

The transmission system data were obtained from colleagues at the Federal University of Rio de Janeiro. The transmission system was modeled nodally, where each generator is connected to a node via a transmission line, and each node is connected to at least one other node via a transmission line. This network of transmission lines creates the electric grid, which allows for the rapid transportation

of electricity within a grid and between interconnected grids (Energy Exemplar, 2014). Figure 4.1 displays the NE Brazil transmission system, which includes 230 kV and 500 kV lines.

4.7.7 Constraints

There are constraints at each level of electricity system, ranging from generators to fuels to emissions to transmission lines. These constraints are defined in Plexos as properties of each object class. There are hard constraints that cannot be exceeded, such as maximum capacity, and soft constraints that can be broken at a cost, such as generation being greater than or less than load.

Generator constraints include maximum capacity, minimum stable level, start time, minimum uptime, minimum down time, run up rate, run down rate, ramp up rate, rap down rate and maintenance rates. Maximum capacity is the maximum potential production of the generator (MW) and minimum stable level is the lowest stable level of electricity production in (MW), which is usually set at 30% of the maximum capacity. Minimum uptime is the minimum amount of time that a generator can be operating for after being started, and minimum down time is the minimum amount of time that a generator must stay turned off after being shut down. Start time is the amount of time that it takes to ramp up a generator to minimum stable level. The run up rate is the rate (MW/min) that a generator increases electricity production from being started at 0 MW to the minimum stable level, and the ramp up rate is the rate (MW/min) at which a generator increases production between the minimum stable level and the maximum capacity. The run

down rate is the rate (MW/min) that a generator decreases electricity production from the minimum stable level to 0 MW, and the ramp down rate is the rate (MW/min) at which a generator decreases production between maximum capacity and the minimum stable level.

Fuel constraints are based on availability, such as water for hydroelectric generation, bagasse for biomass steam turbines and fossil fuel for fossil fuel based engines and turbines. Emissions production is constrained to production rate and removal rate, as well as total maximum emissions production constraints.

Energy storage in NE Brazil is in the form of hydroelectric pumped storage, constrained by maximum volume, natural inflows and maximum spill amounts. Reserves are constrained by minimum provision and maximum response, along with the generator specific constraints defined for each reserve generator.

Transmission constraints include voltage capacity and the ability to allow unserved load (when electricity demand is not met at a particular hour) or dump energy (when generation is greater than load and needs to be dissipated to heat). Unserved load and dump energy is allowed in the NE Brazil model, because when there is high penetrations of intermittent renewables, unserved load and dump energy is more common. Indeed, intermittent renewables like wind and solar can have large, fast and unpredictable changes in generation, which makes predicting intermittent renewable generation more difficult, with an uncertainty comparable to forecasting load, which makes balancing load and generation more difficult (Brouwer *et al.*, 2014). The electricity supply and demand section discusses the dynamics between intermittent renewable generation and dump energy and

unserved load, and system validation section discusses the modeling refinements pertaining to unserved load and dump energy.

4.7.8 Simulation classes and solvers

The four simulation classes in Plexos are long-term expansion plan, projected assessment of system adequacy, medium-term plan and short-term plan. This dissertation uses all the simulation classes except for long-term expansion planning, because the objective is comparing health, storage and grid stability metrics between scenarios on an annual basis. The 2030 scenarios are based on extrapolating current trends from Brazil's 2013-2023 electricity expansion plan.

The medium term schedule optimizes decisions that occur over timescales longer than a day or a week, such as hydro storages, fuel supply and emission constraints. This is a difficult optimization problem involving non-continuous variables, where the simulator must optimize decisions spanning weeks and months, and simultaneously optimize decisions spanning hours and days.

The short-term schedule optimizes decisions hourly, or finer, to emulate the dispatch and pricing of real market-clearing engines. It uses a mixed-integer programing optimization technique.

The functions of projected assessment of system adequacy (PASA) are to create maintenance events for the medium and short-term schedules as well as compute reliability statistics. Attributes include transmission limits, reliability (Energy Exemplar, 2014).

4.8 Electricity Supply and Demand Dynamics

Electric system operators regulate the electric system such that hourly or sub-hourly electricity supply meets but does not exceed hourly demand. When supply is greater than demand, the additional electricity must be stored, or electricity generation must be curtailed. When demand is greater than supply, spinning reserve resources are dispatched. When the electric grid frequency (60 Hz in the Americas, including Brazil) in the United States is too high or too low, frequency regulation resources are dispatched.

Electric system frequency is the nominal frequency of the oscillations of alternating current transmitted from a power station to a consumer. At any moment, the exact frequency of the grid is varying around the nominal frequency because changes in generation and load change the frequency of the system. For example, when the rotor speed of a synchronous generator increases (or decreases), the system frequency also increases (or decreases). Similarly, if there is an increase in load, the electric frequency will decrease (Ackermann, 2005).

The market for matching load (demand) and generation (supply) is unique and difficult to manage in that some generation, such as baseload electricity production by coal, nuclear or hydroelectric plants, can be known ahead of time, but other intermittent generation energy sources can only be imperfectly predicted. Similarly, load can also be only imperfectly predicted.

Generator dispatch is based on marginal cost as well as technical, economic, and environmental constraints. Typically, baseload generators are large generators that cannot easy ramp up or down (here large coal plants). After baseload

generators, wind and solar and other intermittent renewables are dispatched because their fuel cost is zero and thus they have a very low marginal generation cost. After baseload and intermittent renewable generation, load following generators are dispatched to make up the difference between load and generation, and to meet voltage control and frequency regulation constraints. Load following generators typically include hydroelectric, natural gas, and oil/diesel generators. When hydroelectric installed capacity is a significant portion of total installed capacity, hydroelectric plants can be run for baseload generators as well as load following generators that can be flexibly dispatched (Chang *et al.*, 2013).

Wind and solar generation varies based on local solar radiation and wind speeds, and the amount of electricity generated each moment must be either absorbed into the grid, dumped at a high price or future generation must be curtailed. To simulate intermittent wind and solar generation potential, eleven wind hotspots and three solar hotspots were developed while I was with the Center for Energy and Environmental Economics at the Federal University of Rio de Janeiro. Based on local hourly wind speed or solar irradiation at each hotspot, the potential hourly generation per installed MW [actual generation (MW)/capacity (MW)], also known as nominalized generation, was quantified and formatted into hourly nominalized generation profiles for each hotspot.

Hydroelectric generation potential varies based on water availability and environmental constraints. A portion of hydroelectric generation in NE Brazil is run continuously as baseload generation, and the remaining capacity is utilized as load following generation to balance the difference between supply and demand.

To simulate hydroelectric generation, natural inflows, precipitation, initial and end period reservoir fill levels, maximum and minimum reservoir fill levels, as well as past generations patterns were used to develop constraints on maximum hydroelectric energy dispatch per month based on approximate availability of water for a given month. This modeling approach allows for electricity generation to vary hourly based on the need to match demand and generation, while respecting water availability constraints as well as start of the year and end of the year reservoir fill level constraints.

The hourly demand of electricity varies daily, seasonally and annually. To project hourly electricity demand for future scenarios, the actual hourly demand load profile from 2013 were used in conjunction with a load forecasting algorithm and published annual electricity demand projections for NE Brazil (Energy Exemplar, 2014; Torrini *et al.*, 2016).

4.8.1 Wind and solar hotspots

Wind and solar electricity production is intermittent and depends on the temporal variation of wind speed and solar radiation exposure at the power plant location. Based on previous work by the Energy Planning Program at the Federal University of Rio de Janeiro, three solar and eight wind hotspots were identified with high wind or solar radiation exposure and close to or within the transmission system network (Soria *et al.*, 2016).

Nominalized wind generation profiles for each hotspot (hourly electricity generation/power plant capacity) were developed by inputting hourly wind speeds into an excel program developed at CENERGIA that outputs hourly generation. Nominalized solar generation profiles for each hotspot were generated by CENERGIA using the United States National Renewable Energy Laboratory System Advisory Model (Blair *et al.*, 2014). These nominalized wind and solar generation profiles were then entered into Plexos and used to calculate hourly generation of each wind and solar generator at each hot spot.

4.8.2 Hydroelectric dispatch

Hydroelectric power plant dispatch aims to minimize the expected value of thermal generation over the simulation period subject to constraints. This is the typical hydro-thermal coordination problem solved in electricity dispatch simulations and real-time markets.

Hydro systems have technical, environmental and regulatory constraints. Technical constraints include capacity, storage and the generator ramp rates (rate of increasing or decreasing generation in units of MW/min). Environmental constraints include water availability, and regulatory constraints include maximum and minimum stream flows as well as upstream and downstream water use allocations. Regulatory constraints, such as minimum and maximum stream flows, can be optimized to maximize hydroelectric dispatch revenue while limiting ecosystem damage (Premalatha *et al*., 2014; Ray and Sarma, 2011).

Hydro-thermal coordination can be solved several ways. A myopic solution would be to dispatch as much hydropower as needed and available in each hour until hydroelectric generation availability is depleted. However, it is more efficient to take the entire simulation horizon (one year here) into account to make the correct tradeoffs between using hydropower now versus in future periods.

Plexos takes a two-stage approach that combines the Medium Term (MT) Schedule algorithm with the Short Term (ST) Schedule algorithm to optimize hydroelectric dispatch over all periods in a simulation. The MT Schedule simulates a year-long step and finds the optimal hydro dispatch over that step, and then the ST Schedule finds the optimal hourly release guided by the MT Schedule solution (Energy Exemplar, 2014).

The modeling of hydropower availability takes into account natural inflows, the value of the storage in the initial and final periods and the minimum and maximum reservoir fill volumes.

I designed the hydropower dispatch optimization so that the initial fill level of each reservoir equals the percentage of NE hydro storage capacity that each reservoir contributes, multiplied by the stored energy in January 2015. In 2014, the NE Brazil watershed had 16% less annual precipitation than the average calculated from 1983 to 2015 (Center for Hydrometeorology and Remote Sensing, 2016). The final fill level of each reservoir is set to equal the percentage of NE hydro storage capacity that each reservoir contributes, multiplied by the stored energy in December 2015. In 2015, the NE Brazil watershed had 27% less annual

precipitation than average (Center for Hydrometeorology and Remote Sensing, 2016).

To simulate hydroelectric dispatch similarly to previous years, I set the maximum energy per month based on prior year hydroelectric dispatch records to account for seasonality in precipitation patterns and electricity demand. To account for dry year conditions in the 2015 dry year scenario sensitivity test, I reduced initial fill level, max energy per month and final fill levels proportionally according to the difference in precipitation levels between 2015 and 2012.

In the 2030 Hydro-thermal and Hydro-renewable scenarios, hydro storage capacity, initial fill level, final fill level, maximum and minimum fill level and maximum energy per month are assumed to be the same for each of the 2015 generators. New 2030 hydro-electric generators were created assuming the same profiles as those of the 2015 generators.

For the 2030 dry year sensitivity tests, initial fill level, max energy per month and final fill levels were reduced proportionally according to the difference in precipitation levels between 2015 and the driest year projection between 2015 and 2030 based on data from RainSphere, a tool from the Center for Hydrometeorology and Remote Sensing at the University of California, Irvine (Center for Hydrometeorology and Remote Sensing, 2016). RainSphere is an integrated system for global satellite precipitation data and information. It produces three annual precipitation scenarios based on three IPCC representative concentration pathways (RCP): RCP2.6 (low emissions), RCP4.5 (stabilization emissions) and RCP8.5 (high emissions).

4.8.3 Load forecasting

Hourly load profiles are not publicly available for Brazil's electric grids. I produced hourly load profiles for the 2015 and 2030 scenarios using the 2013 load profile from Brazil's national electric system operator, ONS, in conjunction with the Plexos load forecasting algorithm. This algorithm requires three inputs: an hourly load profile for the base year, a maximum hourly energy demand (MW) for the future year, and the targeted energy consumption (GWh) for the future year. I used a 4.77% average increase in annual electricity demand for NE Brazil, a maximum hourly energy demand and a targeted energy consumption for 2030.

The maximum hourly energy demand was forecasted for 2015 and 2030 by taking the maximum hourly energy demand in 2013 (12,980 MW) and applying the projected 4.77% annual energy demand growth. This gave a maximum hourly energy demand of 14,248 MW for 2015 and 28,680 MW for 2030. With the same approach, the 2013 annual energy use of 88,059 GWh was projected to 96,385 GWh for 2015 and 194,562 GWh for 2030.

4.9 Plexos sensitivity tests

I characterized uncertainty in the electricity grid dispatch and emissions simulations for NE Brazil by running sensitivity tests. While numerous sensitivity tests could be run, I selected a few tests based on their potential to impact results.

After reviewing the documentation on PM emissions factors in Brazil from many sources, I found little variation for oil, gas and biomass emission factors; however, there was large variation with emission factors for coal power plants,

ranging from 0.36 g/kWh to 28.15 g/kWh for imported coal (Alves & Uturbey, 2010; EPE, 2007; Ferreira *et al.*, 2015; Governo do Estado do Ceará, n.d.; Ministerio das Minas e Energia & Empresa de Pesquisa Energetica, n.d.; Ministério de Minas e Energia, 2007). As indicated above, I also considered a 0.04 g/kWh PM_{10} emission standard in the health benefits versus emissions control costs analysis.

Another sensitivity test with the potential to significantly impact results is simulating dry year conditions. Most oil generators, and some natural gas, are only dispatched occasionally due to the region's large hydroelectric potential; however, in years of drought, the hydroelectric potential substantially decreases, which causes the oil and gas generators to be dispatched more frequently and emit more emissions.

I simulated dry year sensitivity tests for the 2015 and 2030 scenarios in Plexos to quantify impacts on generation and emissions. As most oil and gas generators in NE Brazil are close to the densely populated cities of Salvador and Recife, increasing oil and gas generator emissions has the potential to substantially increase emissions in those two regions. It is also worth noting that dry years are expected to become more common with changing precipitation patterns due to climate change (Center for Hydrometeorology and Remote Sensing, 2016).

To assess the impact of higher than expected energy demand, I also simulated a high electricity demand scenario with a 5.5% annual average electricity growth rate. While a 5.5% annual average electricity growth rate is not likely, there were five non-consecutive years between 1996 to 2016 where annual electricity demand grew by 5.5% or more.

Other sensitivity tests, which could be investigated in future work, include assessing the impacts of primary versus secondary PM formation, assessing other pollutants such as NO_x and SO_x, varying electricity demand patterns, varying intermittent wind and solar generation patterns.

4.10 System validation

All simulations for 2015 and 2030 were extensively tested with respect to their technical, economic and environmental characteristics. The model refinements were primarily with hydroelectric dispatch, wind and solar dispatch, and the Fortaleza coal power plant emissions factors.

4.10.1 Technical validation

The aggregate yearly electricity generation for each technology type as a percentage of total generation over the year was compared between 2013 actual generation and the 2015 simulation. Total generation in the simulation was 0.6% greater than the 2015 predicted actual load that is based on the 2013 actual load profile from the Brazilian National System Operator (Operador Nacional do Sistema Eletrico, 2016a). Hydroelectric generation in the 2015 simulation was within 3.2% of the actual hydroelectric generation in 2013.

As thermal generation varies significantly with load, selected daily and weekly thermal generation were compared between the simulation and actual daily and weekly dispatch. They showed close alignment in total generation, even though the daily and weekly generation patterns can differ from the simulation as they are

subject to unpredictable electric load variations, as well as other technical and economic factors (Operador Nacional do Sistema Eletrico, 2016b).

Hourly generation dispatch profiles were analyzed to make sure generation was within constraints, such as capacity, ramp rates, start and stop time, and fuel availability. Additionally, hourly profiles were spot checked to make sure the dispatch patterns made sense, for example that coal power plants are run continuously as baseload, and that wind and solar power plants are dispatched each hour at their full potential. This is because wind and solar power plants are not typically curtailed, which means that they generate their maximum potential each hour given wind and solar conditions, and everything generated must be absorbed into the grid unless there is onsite energy storage.

In addition, hourly and annual profiles were examined for each scenario to validate that the simulation was within constraints and that the results make sense. I considered the following categories:

1. Generators: generation (GWh) and curtailment (%)
2. Fuels: price ($/GWh), cost ($), and generation (GWh)
3. Emissions: PM_{10} and CO_2 production (metric ton)
4. Storages: initial volume (GWh), end volume (GWh), inflow (GWh), and Release (GWh)
5. Reserves: Provision (GWh), and shortage (GWh)
6. Region: Load (GWh), generation (GWh), pump load (GWh), unserved energy (GWh), and dump energy (GWh)

7. Nodes: load (GWh), generation (GWh), pump load (GWh), unserved energy (GWh), and dump energy (GWh)
8. Lines: flow (GWh), export limit (MW), and import limit (MW)

In addition, I checked that emissions at any point as well as their annual total equal generation multiplied by the corresponding emission factor.

4.10.2 Hydroelectric dispatch corrections

In initial simulations, hydroelectric generation in the 2015 simulation was 30-35% greater than in 2013 actual generation. The reason was that reservoir final fill levels were not constrained, resulting in drawdown until the minimum fill level at the end of the simulation horizon.

This is not reasonable because it is more profitable, and also it increases energy security, to save a portion of the capacity of a hydro reservoir for the beginning months of the next year to have potential to dispatch water during high cost peak periods (Eichman *et al*., 2013).

Hydroelectric dispatch was corrected by setting a final fill volumes for each reservoir. This final fill volume was selected for each reservoir based on its storage capacity as a percentage of total reservoir storage in NE Brazil and total pumped hydro energy storage (GWh) in December 2015, similar to how the initial fill volume is based on each reservoir's storage capacity as a percentage of total reservoir storage in January 2015. After this adjustment, the simulated hydroelectric production in 2015 was within 3.2% of actual hydroelectric production in 2015.

4.10.3 Intermittent generation corrections

In addition to comparing annual aggregate generation per technology, daily, weekly and monthly generation profiles for each technology type in the 2015 simulation were compared to the actual generation per technology type in 2013.

Hourly generation for each generator was assessed by exporting results to excel and checking that hour-to-hour generation was within the defined constraints, such as hydroelectric energy potential, thermal generator ramp rates and nominalized wind speed and solar irradiation profiles for intermittent generation. Upon validating hourly generation profiles per generator, there were issues with the 2015 BC and 2030 scenarios.

The first correction I made was creating eight 2030 wind hot spots and three 2030 solar hot spots based on identical 2015 hotspots, assuming that the average wind speed and solar radiation in 2015 would be the same in 2030. While wind and solar conditions vary from year to year, Northeast Brazil has very consistent wind speed and direction, as well as solar radiation exposure, which yields wind and solar farm capacity factors that are among the highest in the world (Krauter, 2005).

To assess the potential impact of global climate change on wind and solar resources, I looked for relevant published studies. A 2015 study of all countries in Southern Africa (Fant *et al.*, 2015) found a median change close to zero by 2050 in the long-term mean of both wind speed and Global Horizontal Irradiance (GHI), which is used to measure solar irradiation exposure and solar generation performance. Extreme possibilities yield a 15% increase or decrease, but these changes have very low probabilities.

Another issue with wind and solar dispatch arose when only a percentage of the maximum generation potential, according to a wind speed or solar radiation profile, of a particular wind or solar generator was dispatched. This situation could be advantageous if it is sunny and windy during the middle of the day, electric demand is low, and no storage is available. However, it is usually not feasible to turn on and off parts of or all of an entire wind and solar node on an hourly basis according to demand.

This issue was corrected with a technique used in the California Energy Commission WECC model (Western Electricity Coordinating Council, 2016). Each solar and wind generator was divided into units of 1 MW, with the total number of units equal to the maximum capacity of each wind and solar generator. Then, the feature 'commit' and 'minimum stable level' were used to ensure that all wind or solar units would be dispatched, and that they would be brought to their minimum stable level, which was set equal to the nominalized wind speed or solar radiation profile. This technique forces all wind and solar generators to be dispatched at their full potential every hour based on local hourly wind and solar irradiation patterns.

4.10.4 Unserved load and dump energy

Unserved load is electricity demand that is not met. For the 2030 load profile based on the projected 4.77% average annual electricity demand, there was substantial unserved load in the 2030 HR scenarios. This implies that greater installed capacities are required for future energy infrastructure scenarios with larger

penetrations of renewables. This is significant in Brazil because its decadal electricity expansion plans are based on installed capacity.

There are multiple causes for unserved load. First, wind and solar energy have an average capacity factor of 20% to 35% in NE Brazil. While these are some of the highest capacity factors in the world, they are much smaller than the average capacity factor for continuously running thermal generators, which typically range from 85% to 90%. Therefore, additional electric system capacity is needed in scenarios with higher penetrations of renewables. Additionally, wind and solar generation is intermittent and does not follow demand patterns, which requires storage to shift generation to match load. When there is not enough storage, excess renewable energy must be disposed of, which is called dump energy.

NE Brazil has substantial hydroelectric pumped storage potential, which is utilized in the 2030 scenarios. If generation exceeds load at any hour, it can be stored if storage is available, and dumped otherwise. To find a maximum penetration of renewable energy in NE Brazil given hydroelectric pumped storage projections, I increased wind and solar resources until dump energy exceeded 3-5% of total generation. It is not economical to dump energy because the levelized cost of energy (total cost/generation) produced by wind and solar farms increases when part of the generation cannot be sold and must be dumped. Additionally, dumping energy is expensive because most methods require expensive controls to convert the excess electricity to heat (Doolla & Bhatti, 2006).

After a maximum renewable energy penetration was reached, natural gas generators were added to the 2030 Hydro-renewable scenarios to decrease

unserved load. When adding another natural gas generator would result in that generator having a capacity factor less than 2%, I assumed that it was not economical to add another generator. This resulted in unserved load of 0.01% for the 2030 HR scenario, 0.77% for the HR DY scenario, and 0.02% for the 2030 HT scenario.

Unserved load was 5.54% of total load in the 2030 HT HD 5.5% scenario. I did not add natural gas generators in this scenario to highlight how higher than forecasted electricity demand combined with dry year conditions could produce significant energy shortages, even after a significant thermal expansion. Additionally, allowing for unserved load in the 2030 HT HD 5.5% scenario forces all diesel generators to be dispatched at times when the demand is greater than baseload plus renewable plus natural gas load following generation. This leads to a high emissions scenario because the PM_{10} emission standard for diesel generators is 8.6 times higher than for natural gas generators.

4.10.5 Transmission constraints and node participation

A transmission system comprised of 230 kV and 500 kV lines connects nodes and transports electricity between nodes to balance load and generation. If a particular node is generating more electricity than demanded at that node, the electricity is transported to another node that is generating less electricity than demanded.

The 230 kV and 500 kV transmission line limits are enforced in Plexos, although there is an option to ignore these limits. Similarly, Plexos can model load

and generation zonally (node by node) or regionally. I modeled the NE Brazilian system zonally and enforced transmission line limits.

A small portion of unserved load was due to transmission constraints in the 2030 scenarios. I validated this by increasing natural gas infrastructure and observing that the unserved load did not change. Although Brazil's electric grid has additional transmission capacity that has been approved but not yet built, specifically in interconnecting the subsystems, upgrade plans at the detailed node level were not found. The unserved load occurred at two nodes on the western edge of the NE Brazil grid, which are on the opposite side of where most of the population and most of the generators are located. To address the unserved load and transmission constraints in the 2030 scenarios, three natural gas power plants were moved from the nodes with the most generation to the nodes that had unserved load. This reduced the unserved load from 0.2% of total load (391 GW) to 0.01% of total load (30 GW) in the 2030 HR scenario.

4.10.6 Economic validation

Basic economic validation for each scenario was performed. The levelized cost of energy (LCOE) for each generator was compared to typical Brazilian LCOE ranges, based on data collected by the Center for Energy and Environmental Economics at the Federal University of Rio de Janeiro, to make sure that the LCOE between generator types was consistent with industry costs so that generators would be dispatched in a proper order, since generators are dispatched based on marginal

costs and subject to an array of constraints. Total fuel costs per generation technology were validated by multiplying fuel consumption by fuel costs.

The cost of dump energy was set at $500/MWh and the cost of unserved load was set at $10,000/MWh to minimize dump energy and unserved load in the NE Brazil electric system dispatch simulations. The total dump energy and unserved load costs ($/yr) were compared to the amount of dump energy (GWh) and unserved energy (GWh) multiplied by the cost per MWh to ensure they matched.

The acceptable level of lost load (unserved load) is typically set by a regulator external to the market (Sioshansi & Pfaffenberger, 2006). In checking the regulations set by ANEEL, the regulator of Brazil's electricity market, I could not find a defined acceptable level of unserved load nor historical reports of lost load levels (Agencia Nacional de Energia Eletrica, 2016).

4.10.7 Environmental validation

Annual, monthly and daily emissions per technology type were divided by their corresponding emission factors to see if the total emissions per technology type per pollutant divided by emissions factors were equivalent to generation profiles.

Gross emissions production are equal to net emissions production in the NE Brazil Plexos model because I assumed that the necessary emissions controls have been installed to reduce emissions to the emission standards selected for each technology type. Public reporting of power plant emissions and monitoring programs are not readily available, which I confirmed by speaking with the Energy Planning Department at the Federal University of Rio de Janeiro (March 2017).

As discussed in the previous chapter, Barton *et al.,* (2000) found that Brazilian firms are responsive to regulatory pressures, despite different starting points, paces of change and relationships with regulators. In their 2010 study of the Brazilian electric system, Alves *et al.* also assume that power plant operators install sufficient technology to reduce emissions to the required standards.

For fine resolution validation, generation profiles for several generators in each technology were multiplied by the technology and pollutant specific emissions factors to check and see if they are equivalent to the emission profiles. Generator emissions were spot-checked by dividing emissions from a particular generator by the emission factor to check if aggregate and hourly emissions profiles matched generation profiles. The generation production of emissions was exactly equal to the generation profile multiplied by the emission factor.

Annual water withdrawal for each hydroelectric reservoir was subtracted from the initial volume to make sure that initial volume plus inflow minus annual water withdrawal was greater than or equal to the end volume constraint. None of the reservoir volume constraints were violated.

4.11 Emission control costs

To compare the expected health benefits from tightening the PM_{10} emission standard with the corresponding control costs in Question 1, I estimated the emission control costs of achieving tighter standards in each case.

I selected the Integrated Environmental Control Model (IECM) by Carnegie Mellon University (2017) to estimate control costs because it is a comprehensive

and flexible model that supports calculating costs based on specific power plant characteristics, such as plant design, fuel, performance, emission control costs, location and many other variables.

There are two PM control technologies available in the IECM model, electrostatic precipitators and fabric filers, both of which I considered. ESPs and fabric filers are the two most common PM control technologies, which have PM collection efficiencies of up to 98% and 99.7%, respectively (Zhang, 2016). I developed a control cost model specific to the Porto do Pecem coal power plants in NE Brazil. The model includes capital costs, fixed costs and variable costs.

The capital costs include the particle collector, ductwork, fly ash handling, fan, general facilities costs, engineering fees, pre-production costs, process contingency costs and interest costs. A total capital cost of US$47,170 per net MW was calculated for an ESP, and US$56,780 per net MW for a fabric filter.

The fixed costs include operating and maintenance labor, maintenance material and administrative labor. The total fixed costs were calculated at US$0.3293 per MWh for an ESP, and US$0.4166 per MWh for a fabric filter. The variable costs include electricity and solid waste disposal, for a total of US$0.4790 per MWh for an ESP and US$0.4986 for a fabric filer.

I used the specific characteristics of the two coal power plants in NE Brazil based on the available data, such as the capacity of 360 MW per unit, the plant life of 30 years and the type of imported coal (bituminous). The equipment and material costs were assumed to be 38.4% greater for Brazil than for the U.S., based on an estimate of the additional costs, including freight and insurance costs, import fees,

customs expenses and Brazilian taxes of bringing equipment to Brazil. Brazilian labor costs were assumed to be 21% of U.S. labor costs, based on the Brazil to U.S. gross national income per capita ratio.

I found that the annualized cost of removing one metric ton of PM_{10} is $87.98 with an electrostatic precipitator and $119.90 with a fabric filter for a 360 MW power plant. To estimate the control costs of tightening the PM_{10} emission standard in Scenarios 1 and 2, I multiplied the number of metric tons of PM_{10} to remove by the unit cost per metric ton for an electrostatic precipitator because it is the cheapest control method and has a sufficient PM collection efficiency.

Tightening emission standard to the most stringent standard (Scenario 3) requires approximately 99.8% of PM emissions to be removed. To ensure sufficient PM removal, I calculated the PM removal costs by multiplying the number of metric tons of PM_{10} to remove by the unit cost per metric ton for an ESP plus a fabric filter, for a total cost of $207.88 per metric ton of PM_{10} removed.

The emission control costs of tightening PM standards play an important role because they can be compared with the health benefits to develop a health benefit to control cost ratio. The following two chapters on the atmospheric dispersion of air pollutants and human health benefits mapping describe how human health benefits can be calculated based on changes in electricity grid emissions.

5 Methodology: air quality modeling (CALPUFF)

Atmospheric dispersion modeling is a key step to estimate how emissions from the NE Brazil electric grid impact air quality. This chapter discusses how changes in air quality concentrations of PM are simulated using the CALPUFF Dispersion Modeling System. After some background information, I present how the Plexos emissions are integrated into CALPUFF, followed by meteorological and geophysical terrain inputs and air dispersion data requirements, before describing sensitivity tests and results validations.

5.1 Air quality modeling background

Air pollutant dispersion in CALPUFF is a mathematical simulation of how air pollutants are transported and transformed, along with their fate. The required data include:

1) Meteorological conditions such as wind speed and direction, turbulence levels, air temperature, inversion layer heights, cloud cover and solar radiation;
2) Quantity of emissions released, location, height, release source, exit velocity, exit temperature, mass flow rate; and
3) Terrain elevations and type, receptors locations, obstruction locations and dimensions.

Two types of approaches are commonly used to disperse pollutants: plume models and puff models. Plume models simulate straight-line trajectories. They

have several limitations, including short dispersion ranges, steady-state meteorological conditions, no support for low wind speeds and they only work with single wind fields.

Puff models simulate pollutant releases as a series of puffs. These models work with non-steady state meteorological conditions, they support low wind speeds and 3-D wind fields. Puff models have several advantages, including longer-range transport, geophysical and meteorological changes, coastal effect and slope flow simulation. In this work, I relied on puff models.

5.2 CALPUFF Dispersion Modeling System

I selected CALPUFF to disperse PM emissions from NE Brazil power plants because it is widely used and well suited for this study. The CALPUFF transport and dispersion model was originally developed by Sigma Research Corporation with funding by the California Air Resources Board. CALPUFF is a non-steady-state Lagrangian Gaussian puff model that includes modules for complex terrain effects, overwater transport, coastal interaction effects, building downwash, wet and dry removal and simple chemical transformations. CALPUFF simulates the dispersion of puffs of material emitted from selected sources. While there are more sophisticated models, such as the Community Multiscale Air Quality Modeling System, the scope of this study was limited to simulating the transport of power plant emissions and not their chemical transformation.

CALPUFF has been widely used for primary emissions dispersion of power plants (Hao *et al.*, 2007; Holmes & Morawska, 2006; Levy *et al.*, 2002; López *et al.*,

2005; Zhou *et al*. 2003). CALPUFF view, the commercial version of CALPUFF I used, includes a user interface and built in modules for meteorological conditions, geophysical terrain, puff dispersion modeling and post-processing of results. Additionally, CALPUFF View provides an intuitive user interface and excellent support documentation, making the process of running CALPUFF much quicker.

CALPUFF can model domains from ten to hundreds of kilometers from a source, it can handle time-varying sources as well as inert pollutants or pollutants subject to inert removal and chemical conversion, and it can deal with rough or complex terrains.

CALPUFF can be used on its own or in conjunction with other sub-models, such as CALMET. CALMET is a meteorological model that develops wind and temperature fields with parameterized treatments of slope flows, kinematic terrain effects, terrain blocking effects, a divergence minimization procedure and a micro-meteorological model for overland and overwater boundary layers. CALPUFF may use fields generated by CALMET or non-gridded meteorological data, like many other existing plume models. The effects of temporal and spatial variations in the meteorological fields are simulated throughout the emission dispersion period.

The primary CALPUFF outputs are concentrations and deposition fluxes at selected receptors. CALPOST is a post-processing program used to process output files by the CALPUFF and CALGRID models. CALPOST produces tabulations that summarize simulation results, such as the highest and average 1-hour, 24-hr and 8760-hour concentrations of the receptor grid. Visibility impacts can also be computed based on the EPA Interagency Workgroup on Air Quality Modeling

(IWAQM) and the Federal Land Managers' Air Quality Related Values Workgroup (FLAG) recommendations.

5.3 Plexos and CALPUFF integration

The CALPUFF air dispersion model was run sequentially after the electricity grid dispatch and emissions simulation in Plexos because the spatial and temporal emissions from the NE Brazil electric grid must be formatted into point source emissions inputs for the CALPUFF model.

Specific scenarios were formed to simulate electric grid dispatch and emissions to address the health benefits of tightening PM standards as well as the health, storage and grid stability implications of high penetrations of renewables. For the latter, I formed a handful of scenarios and compared the results in Plexos, then selected the most interesting scenarios to run in CALPUFF for air quality modeling. The purpose of selecting a subset of scenarios is to keep this study manageable and focus the air quality modeling on the scenarios that represented realistic extremes with health benefits, storage requirements and grid stability.

5.3.1 Scenario selection for PM standard analysis

All of the scenarios simulated in Plexos to assess the health benefits of moving to lower PM emissions standards were run in CALPUFF. As a refresher, four PM_{10} emission standards were applied to the same 2015 NE Brazil electric grid simulation. All properties were held constant in the three scenarios except for the

PM_{10} emission standard for coal power plants. These four standards are: 28.15 g/kWh, 0.69 g/kWh, 0.36 g/kWh and 0.04 g/kWh.

I developed an air quality gird spanning 320 km x 320 km with 5.4 km x 5.4 km resolution surrounding the Fortaleza region. This area was selected because the only two coal power plants in NE Brazil are near the densely populated Fortaleza region, along with several gas and diesel power plants. There was a total of 39 thermal power plants in NE Brazil in 2015, and 8 of them are in the proximity of Fortaleza.

I ran a total of four air quality simulations in the Fortaleza region, one for each of the PM standards considered. To address the health, storage and grid implications of high penetrations of renewables, more scenarios and regions were required.

5.3.2 Scenario selection for health, storage and grid stability analysis

To assess the health benefits, storage and grid implications of very high penetrations of renewables, five of the eight scenarios simulated in Plexos were selected to run in CALPUFF (see Table 2 for installed capacity details):

1. **2015 BC** - 2015 Base case.
2. **2030 HR** - 2030 Hydro-renewable with intermittent renewables making up 45% of installed capacity.
3. **2030 HT** – 2030 Hydro-thermal with 30% intermittent renewables making up 30% of installed capacity.

4. **2030 HR DY** – 2030 Hydro-renewable Dry Year. Same as 2030 HR with dry year conditions.

The first three scenarios establish a baseline for changes in health benefits, storage requirements and grid implications. The fourth scenario was designed to assess changes emissions, storage and grid stability with a very high penetration of renewables (45% intermittent renewables, 79% total renewables) during extreme drought conditions.

Air quality changes were simulated in the three most densely populated regions of NE Brazil (Fortaleza, Recife and Salvador), for each of the first four scenarios, for a total of 12 air quality simulations. These three regions were selected because health impacts depend on the quantity of emissions as well as their dispersion pathways and the number of people exposed along those pathways. This is discussed in greater detail in the next section.

For the air quality impacts of a 100% RPS electricity grid, I assumed that all thermal power plants were decommissioned so that there were no PM emissions from the electricity sector. Therefore, the PM air quality concentrations were calculated by subtracting air quality concentrations from the 2015 electric grid simulation (under the BNDES standard) from the 2015 ambient PM concentrations in NE Brazil, which includes all sectors.

5.3.3 Domain and emissions integration

There are many considerations when deciding on how to model air pollutant concentrations, including domain size, meteorological conditions, geophysical

terrain, primary and secondary pollutant formation, puff or plume modeling, building downwash and other factors.

Northeast Brazil is approximately 1200 km wide by 1500 km long. While the EPA has recommended CALPUFF for long-range transport simulation, there are large uncertainties with long-range puff transport modeling (Levy *et al*., 2002). To capture air quality impacts of a broad region while preserving accuracy, three regions of 320 km x 320 km were defined around the three densely populated major cities in NE Brazil for air quality modeling: Fortaleza, Recife and Salvador.

The air quality domain surrounding Fortaleza includes 8 of the 39 thermal generators in NE Brazil in 2015. It is important to note that some emissions of these 8 power plants will disperse beyond the 320km x 320km domain, and that power plants outside this domain could also affect air quality concentrations in this domain. However, most of the PM air pollution due to electricity generation in the Fortaleza study area is likely due to these 8 power plants.

To assess the health, storage and grid stability implications of varying levels of high penetrations of renewables in NE Brazil, all three of the air quality modeling domains were considered because 28 of the 39 thermal generators that were operational in NE Brazil in 2015 are located near or in these three cities. However, each of these regions has different types and numbers of thermal generators, some of which are upwind and some of which are downwind of the populated areas.

The health impacts from emissions depend not only on the quantity of emissions, but also on the pathways of emissions and the number of people exposed along the pathways. Before simulating air quality changes and mapping those to

human health impacts, it is difficult to know how the three regions will fare for a given scenario. For this reason, I simulated air quality changes in the three most densely populated regions of NE Brazil for each of the four scenarios considered.

Furthermore, the large majority of emissions happen within the air quality modeling domains, for a couple reasons. First, the two coal power plants in NE Brazil are in Fortaleza, which contributed 49% of PM emissions in the 2015 BC. Second, all but three of the large natural gas combined cycle generators are located within the air quality modeling domains. While 11 of the 19 internal combustion diesel generators are outside, these are the less frequently dispatched because of high fuel costs.

Another reason I focused the air quality modeling on NE Brazil's three most densely populated cities is that that small increases in air pollutant concentrations in densely populated areas have greater effects than large increases in less populated areas (Fann *et al.,* 2012). Indeed, changes in disease incidence are calculated by multiplying the relative risk change of incurring a disease by the entire population, and the densely populated areas in Brazil have orders of magnitude more people than the rural areas (Instituto Brasileiro de Geografia e Estatistica, 2016). Additionally, $PM_{2.5}$ dose-response curves increase quickly and then start to level off as exposure concentrations increase.

5.4 Meteorological conditions and geophysical preprocessing

CALMET is a 3-D meteorological model that converts 3-D meteorological inputs, such as wind speed and direction, temperature and precipitation, to a three-

dimensional meteorological grid that is used to disperse emissions in CALPUFF. I acquired 3-D meteorological Weather and Research Forecasting (WRF) inputs through a collaboration with colleagues at the University of Waterloo. WRF files include surface meteorological data, such as wind speed and direction, temperature, surface pressure, precipitation and cloud cover, as well as vertical profiles of wind speed and direction, temperature and pressure.

The Weather Research and Forecasting (WRF) model is one of the most recent mesoscale numerical weather prediction systems. Three WRF datasets with 4 km x 4 km resolution were initially developed based on 2015 conditions, one for Fortaleza, one for Recife and one for Salvador. Each region spans an area of 320 km x 320 km. Additionally, three WRF datasets were developed based on 2012 meteorological data to simulate dry year conditions (one for each region mentioned above). I selected 2012 meteorological conditions to represent a dry year because 2012 was the driest year for the NE Brazil watershed in the available data that range from 1983 to 2015 (Center for Hydrometeorology and Remote Sensing, 2016). In total, six WRF datasets were developed.

I decided to use 4 km x 4km resolution for the WRF files, as opposed to 12 km x 12 km resolution, to have a higher resolution of air quality concentrations. This is important when overlaying air quality concentrations with population density for human health impacts mapping, especially around areas where population density changes significantly.

5.4.1 CALMET input files

CALMET requires meteorological data, geophysical data and control information. The meteorological data includes hourly precipitation and vertical columns of meteorological conditions, like wind speed and direction, temperature and pressure. These data are included in the WRF files.

The geophysical data requirements include terrain elevations and land use characteristics, which were acquired using the geophysical processor in CALPUFF. I developed the geophysical terrain using three publically available map files (SRTM1, SRTM3 and GTOPO30) to account for land and ocean effects because Fortaleza and the Porto do Pecem power plants are close to the Atlantic coast. The control information includes horizontal and vertical grid data, start and end dates and time, as well as optional model settings (Sigma Research Corporation, 2011).

5.5 Air quality simulations

Information about emissions sources, receptors, meteorological data, geophysical data and model control parameters are required to perform simulations in CALPUFF. The parameters selected and the assumptions I made are discussed below, including details on the custom time-varying emissions input files that were developed to capture the hourly power plant emissions simulated in Plexos.

5.5.1 Input files

Information is passed to CALPUFF through a series of input files, which are described below. The first input files I used are WRF files, which I subsequently

processed in CALMET to form meteorological grids that can be paired with geophysical terrain maps. As mentioned above, I used three geophysical terrain map files to account for ocean and land effects.

Figure 5.1. CALPUFF inputs and options

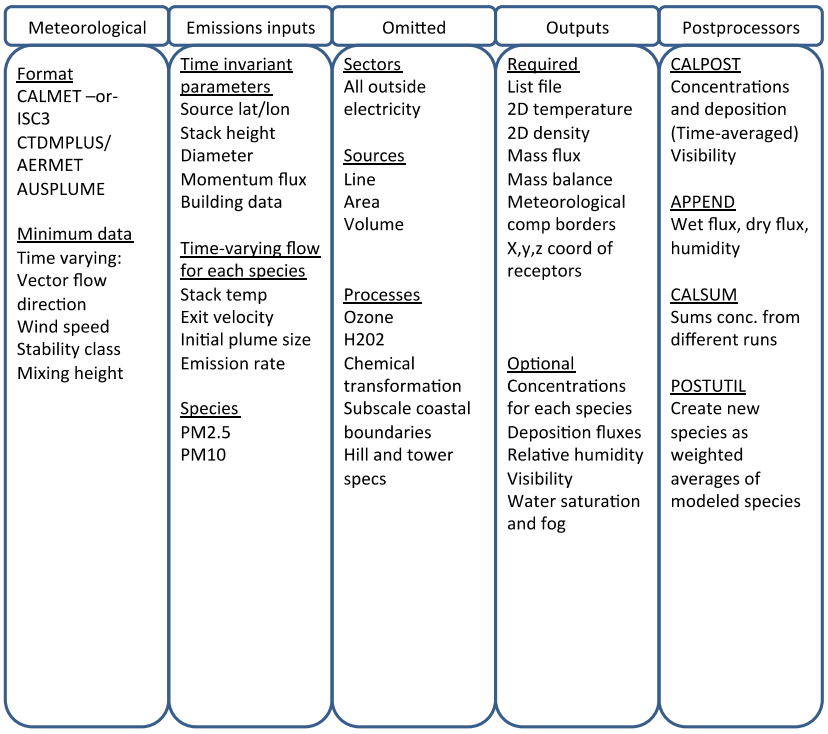

Integrated Modeling Methodology

Next, custom point source time varying emissions files were developed for each power plant. These emission files include time variant and time invariant characteristics, which are described in detail in the variable emission file section. Last, modeling parameters appropriate for the terrain and the meteorology in NE Brazil were set, including puff modeling for the plume elements, temperature

gradients for inversion strength, and partial plume path adjustment. Figure 5.1 displays most of the required and optional input files.

5.5.2 $PM_{2.5}$ and PM_{10} dispersion simulation

While PM_{10} emissions were simulated in Plexos because the emission standards for power plants in Brazil are set for PM_{10}, I used $PM_{2.5}$ C-R functions in BenMAP because studies show that finer particles have a greater health impact than coarser particles (Kampa & Castanas, 2008). This is discussed in detail in the BenMAP methods section.

$PM_{2.5}$ air quality concentrations are required to use $PM_{2.5}$ C-R functions. These can be obtained by converting PM_{10} emissions to $PM_{2.5}$ emissions using the ambient ratio method and then dispersing the $PM_{2.5}$ emissions. Alternatively, PM_{10} emissions could be dispersed and the resulting PM_{10} air quality concentrations could be converted to $PM_{2.5}$ using the ambient ratio method. I considered both ways as a robustness test.

To first simulate $PM_{2.5}$ dispersion, I converted PM_{10} emissions from Plexos to $PM_{2.5}$ emissions using the ambient ratio method before atmospheric dispersion in CALPUFF (Boldo *et al.*, 2006). I calculated a ratio by mass of primary $PM_{2.5}/PM_{10}$ of 0.775 by taking the average of all reported $PM_{2.5}$ to PM_{10} emissions (by mass) for coal, oil and natural gas generation in the U.S. (U.S. Environmental Protection Agency, 2017c). U.S. data were used because emissions data from Brazil's electric grid were not available. As the ratio of $PM_{2.5}/PM_{10}$ varies based on fuel source and technology, the ratio of $PM_{2.5}/PM_{10}$ for each fuel source was weighted based on the

percentage of emissions per fuel source divided by the total emissions of the NE Brazil electric grid.

Time-varying hourly emissions input files for each generator in each scenario were formed for the Fortaleza air quality modeling domain to assess the health benefits of tightening PM standards. Similarly, customized hourly emissions input files for each generator in each scenario were created for the Fortaleza, Recife and Salvador air quality modeling domains for assessing health, storage and grid implications.

5.5.3 Variable emissions files

CALPUFF considers four types of emissions sources: point, line, area and volume sources. Power plants are point sources. While CALPUFF has the ability to define hourly, daily and weekly emissions rates for each point source on a repeating basis for the simulated time horizon, power plant emissions vary based on hourly dispatch so they do not necessarily repeat patterns. This is partially because electricity demand varies hourly, daily and seasonally, as does the quantity of electricity from intermittent sources like wind and solar. Even baseload power plants are ramped down at times because of scheduled maintenance or unforeseen outages.

Some published studies assumed continuous power plant emissions and others estimated power plant emissions by multiplying a power plant's expected capacity factor (actual generation/plant capacity) by its capacity (MW) to estimate expected annual or seasonal generation, and then the expected output is multiplied

by an emission standard to get expected emissions (Hao *et al*., 2007; Levy *et al*., 2002; López *et al*., 2005; Zhou *et al*., 2003). While these methods provide a rough estimate for power plants that are run continuously for baseload generation, it does not capture electricity grid interactions and the dispatch and emissions of load following natural gas and diesel power plants. Capturing the emissions of load following power plants is necessary to quantify grid-level emissions, which includes baseload and load following thermal generators.

The NE Brazil Plexos model I built simulates electricity grid interaction and hourly dispatch of power plants. This provides insights into how power plants are ramped up and down, as well as turned on and off, on an hourly basis to balance load and generation. In simulating hourly dispatch, the temporal fluctuation in emissions per power plant can be captured. The value of pollution reduction varies based on the time, place and quantity of emissions released (Borenstein, 2012), which can only be captured through simulating power plant dispatch and emissions in spatially and temporally resolved simulations.

To model the atmospheric dispersion of varying emissions, point source emissions files with time-varying emissions (PTEMARB.DAT) were developed for each scenario. PTEMARB.DAT files require general data, time-invariant data and time varying data.

The general data include the map projection (Universal Transverse Mercator), time zone, start and stop times of simulation, number of sources, number of species and their molecular weight. The sources in each scenario are the power plants. I modeled both $PM_{2.5}$ and PM_{10} species in separate runs. I derived a

molecular weight of 36.7 g/mol for $PM_{2.5}$ by taking a weighted average of the molecular weight of each of the major constituents of $PM_{2.5}$: elemental carbon (0.12), nitrate (0.19), ammonium (0.1), sulfate (0.1), crustal (0.08) and organics (0.41). As the mass contribution of each constituent varies seasonally, a seasonal average of the mass contribution of each constituent was taken (South Coast Air Quality Management District, 2016). A molecular weight for PM_{10} of 45.5 g/mol was derived using the same process.

Time invariant data include source coordinates, stack height, and stack diameter. I assumed a stack height of 60 m for oil and gas plants and a stack height of 110 m for the Porto do Pecem power plants, along with a stack diameter of 10 m and a stack base elevation height of 30 m based on a report by the government of Ceara that discusses power plant stack height in NE Brazil (Governo do Estado do Ceará, n.d.). I did not model building downwash, which happens when buildings are near the emission source. They can then affect the emission plume rise and create turbulent wake zones that put a downward pressure on pollutants (Sigma Research Corporation, 2011).

Time varying data include the time, exit temperature, exit velocity and emission rate of the species modeled. I assumed an exit temperature of 350 K and an exit velocity of 10 m/s (Governo do Estado do Ceará, n.d.). The emission profiles in Plexos were converted from kg/h to g/s, as required by the CALPUFF input files.

Three PTEMARB files were created for Fortaleza to assess the impacts of tightening emissions standards. To assess health, storage and grid stability implications, one PTEMARB file was developed for each of the three regions

(Fortaleza, Recife and Salvador) in each of the four scenarios, for a total of 12 files. Each PTEMARB file contains similar general and time-invariant data, along with 8760 time varying entries for each power plant (one per hour for a whole year).

5.5.4 Emissions dispersion

After preparing the CALPUFF input files, I selected parameters specific to atmospheric dispersion. In all scenarios the same set of standard puff modeling parameters were assumed, including puff modeling for the plume elements, temperature gradients for inversion strength, and partial plume path adjustment according to terrain.

As mentioned above, I simulated the dispersion of primary PM emissions from power plants and did not consider the chemical transformation of PM into secondary pollutants. To also estimate the health impacts related to secondary PM, all related pollutant background concentrations involved in the chemical transformation reactions, as well as the primary emissions and the chemical transformation of these related pollutants, would need to be modeled. Therefore, the CALPUFF simulations did not consider chemical transformation, and the air quality and health impacts of species such as secondary particulate matter, ozone and hydrogen peroxide are left to future work.

5.6 CALPUFF sensitivity tests

A number of sensitivity tests could be run in CALPUFF. For example, the computational grid resolution could be increased from 5.4 km grids to 2 km grids;

however, this is not likely to significantly affect results because the WRF meteorological dataset has a 4 km resolution. Other possible sensitivity tests include changing the molecular weight of $PM_{2.5}$ used in the CALPUFF dispersion, and converting PM_{10} to $PM_{2.5}$ before as well as after dispersion.

Although PM constituents vary, even if the seasonal variations in the portion of constituents by mass are considered, the average molecular weight would change by less than 10% - 20% (South Coast Air Quality Management District, 2016).

The primary sensitivity test I ran in CALPUFF compared the results of converting PM_{10} to $PM_{2.5}$ before and after dispersion. In the first runs, I scaled PM_{10} emissions to $PM_{2.5}$ emissions and then simulated the dispersion of $PM_{2.5}$ in CALPUFF. In the following runs, I simulated the dispersion of PM_{10} emissions in CALPUFF and then scaled the resulting PM_{10} concentrations to $PM_{2.5}$ concentrations using the ambient ratio method. The molecular weight used for PM_{10} was 45.5 g/mol and the molecular weight used for $PM_{2.5}$ was a weighted average of 36.7 g/mol (discussed in Section 2.5.3). In both scenarios, $PM_{2.5}$ concentrations per grid cell varied by less than 1% on average.

5.7 Air quality simulation validation

CALPUFF results were validated in multiple ways. To check for congruency between power plant emission input files and emission plumes, spikes in the time-varying power plant emissions input files were checked with the corresponding air quality concentration increases. Additionally, the 1-hr, 24-hr and annual $PM_{2.5}$ concentration averages and maxima were compared within grid cells in each

simulation, as well as between simulations. For example, I compared annual average concentrations in selected grid cells between the CONAMA 0.69 g/kWh emission standard scenario and the BNDES 0.36 g/kWh emission standard scenario, to validate the concentrations are proportionally lower in the lower emission standard scenario.

CALPUFF results were also checked by comparing the plume animations with the wind roses. A wind rose is a graphic tool that indicates the distribution of wind speed and direction. Figures 5.2 to 5.5 display the 2015 wind roses for Fortaleza, Recife, and Salvador. They show very little variability in direction and speed in all three regions, which is consistent with wind data from the Brazilian Electrical Energy Research Center. I searched for past meteorological station data to compare with the wind roses for further validation, but could not find data.

The wind rose for Fortaleza in 2012 are displayed in Figure 5.3, which is the year I selected to simulate dry year meteorological conditions because it was the driest year in NE Brazil in the available dataset from 1983 to 2015 (Center for Hydrometeorology and Remote Sensing, 2016). The wind rose for Fortaleza in 2012 has a slightly stronger southeasterly contingent than the 2015 wind rose, as shown by the larger bar in the SE corner of the 2012 wind rose. This could have an effect on the emission plume pathway in the dry year scenarios, transporting the emissions slightly more northwest than in the non-dry year scenarios.

By observing the wind roses, it becomes clear that Fortaleza has the highest consistent wind speed and is the most easterly. The Recife wind rose is the most southerly, and it has the lowest average speeds, as seen by having more red and less

blue color than the Fortaleza and Salvador wind roses. The average speed of the Salvador wind rose is greater than Recife and less than Fortaleza, and the direction is more southeasterly than Fortaleza but less southeasterly than Recife.

Figure 5.2. Wind rose for Fortaleza in 2015

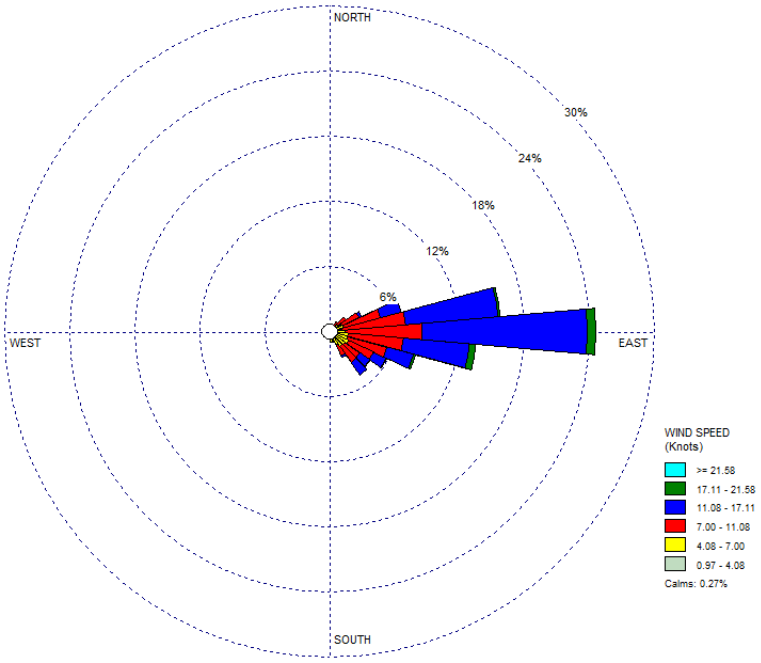

Figure 5.3. Wind rose for Fortaleza in 2012 (dry year conditions)

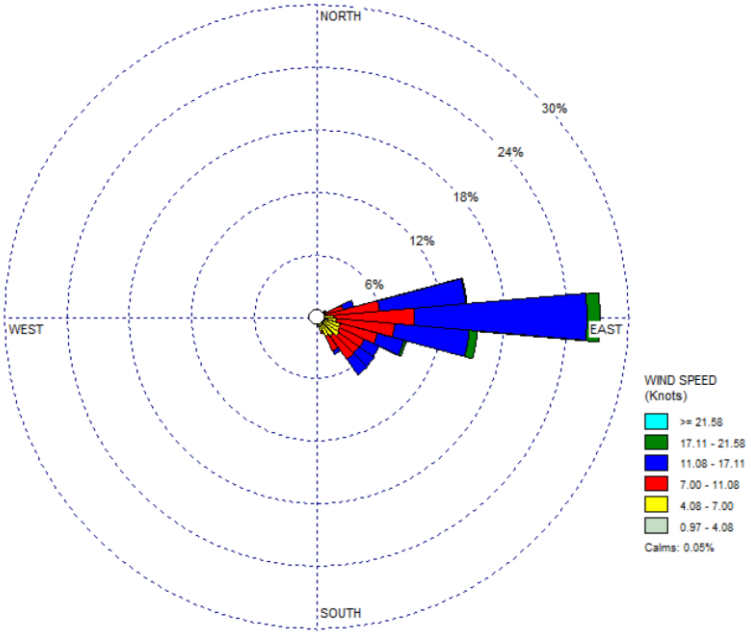

Figure 5.4. Wind rose for Recife

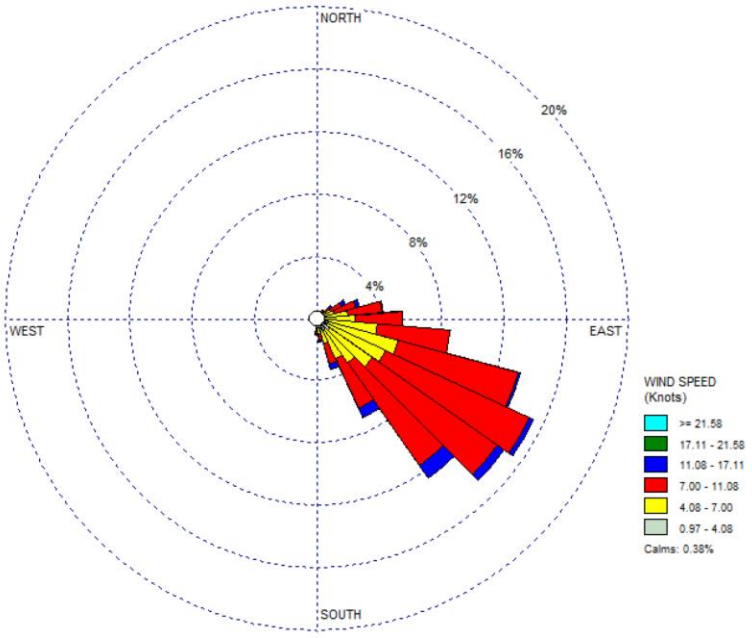

Figure 5.5. Wind rose for Salvador

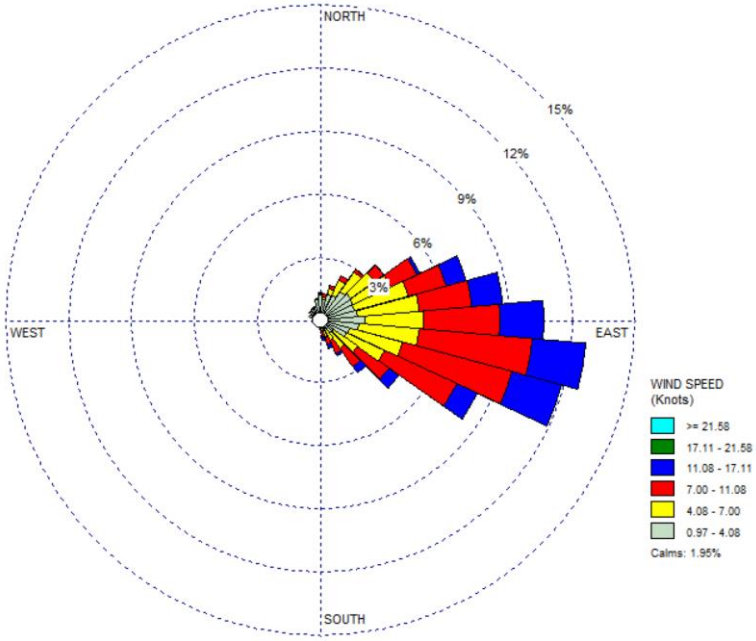

6 Methodology: human health and climate benefits valuation

The Environmental Protection Agency's (EPA) Environmental Benefits Mapping and Analysis Program (BenMAP) is the final model in my integrated modeling methodology. I used BenMAP to assess how changes in long-term human exposure to $PM_{2.5}$ concentrations impact selected health outcomes and health costs.

There are 12 multinational air pollution health impact assessment tools that were analyzed and compared by Anenberg *et al.* (2016). These tools varied based on their spatial resolution and on the pollutants and health effects they can evaluate. I selected BenMAP because it has the broadest range of functionality along with the ability to handle datasets with varying levels of spatial and temporal resolution. In addition, BenMAP is open source, and it was used in numerous studies to estimate health impacts due to changes in air quality concentrations in different industries across many countries. BenMAP also provides advanced functionality to design health impact (C-R) functions and monetary valuation, and it provides versatile results aggregation and post-processing options (U.S. Environmental Protection Agency, 2016a).

The next sections give an overview of BenMAP and it describes, the database of inputs BenMAP require along with selected health impact functions, the valuation techniques and the sensitivity tests performed for this study.

6.1 Health benefits mapping process

BenMAP performs a series of spatial and temporal calculations to assess how changes in air quality concentrations between two states impact selected disease

incidences and related health costs in a population.

In the first step, changes in air quality concentrations of $PM_{2.5}$ are calculated from transitioning from a baseline to a control option (e.g., a lower air pollutant concentration here). Air quality grids consisting of air pollutant concentrations, with the same domain and resolution as the air dispersion grid used in CALPUFF, are created and then overlaid to calculate changes in pollutant concentrations. Next, spatially resolved population data and baseline disease incidence data for each selected health endpoint are mapped to changes in pollutant concentrations. Concentration-response (C-R) functions are then used to estimate how changes in pollutant exposure change the relative risk of premature mortality and hospital admissions for various diseases. Last, monetary valuation techniques using the Value of a Statistical Life (VSL) and cost of illness (COI) data are applied to changes in mortality and hospital admissions to place an economic value on expected health outcomes. Figure 6.1 outlines the main components of BenMAP and Figure 6.2 displays an overview of BenMAP's inputs and outputs.

6.2 Pollutant selection

The main ambient pollutants affecting human health from electricity generation are nitrous oxides (NO_x), sulfur dioxide (SO_2), carbon monoxide (CO), ozone (O_3) and particulate matter (PM) (Smith *et al.*, 2013). I focused on particulate matter because it is the largest contributor to air pollution related global mortality and morbidity. In fact, exposure to ambient particulate matter was ranked the fifth largest

contributor to global disease in 2015, behind high blood pressure, smoking, high fasting plasma glucose (diabetes), and high cholesterol (Cohen *et al*., 2017).

Figure 6.1. BenMAP process flow

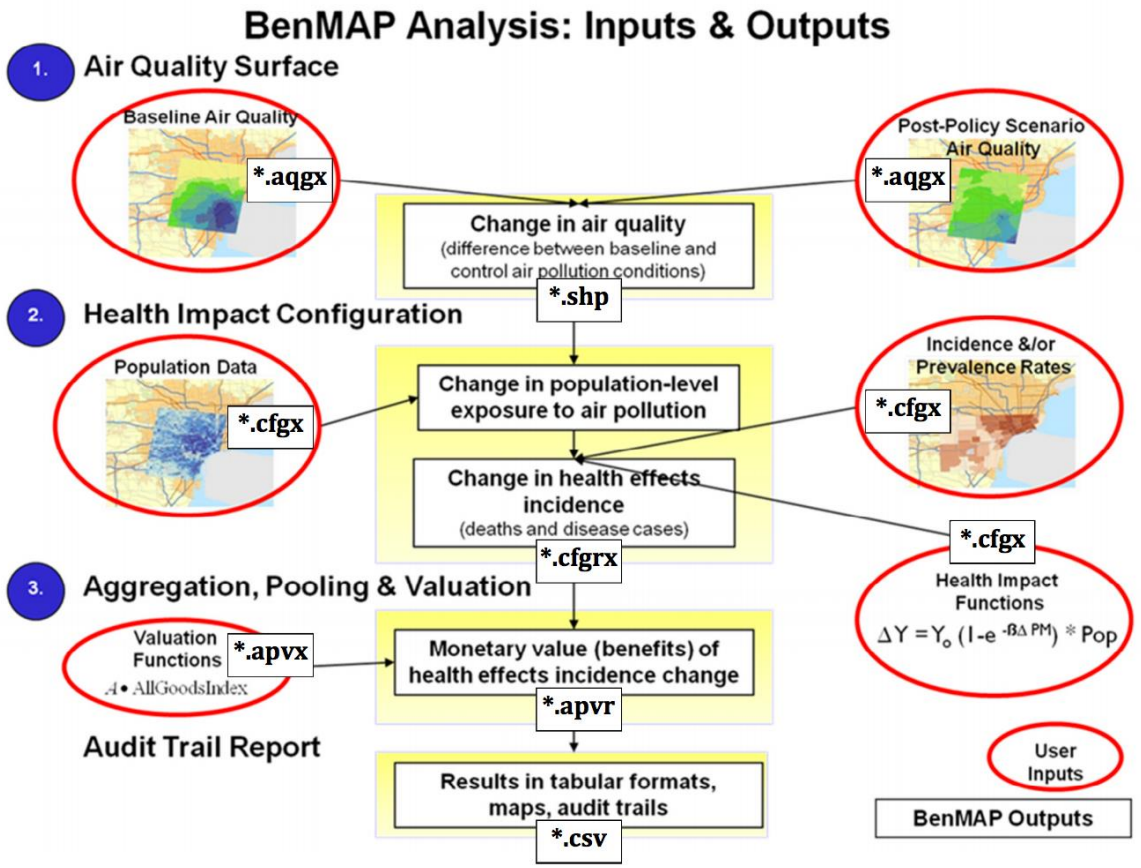

Source: EPA (2015)

Brazil has emission standards for PM_{10} but not yet for $PM_{2.5}$. However, most recently developed C-R functions relating long-term particulate matter exposure and mortality are based on $PM_{2.5}$ instead of PM_{10} exposure (Atkinson *et al.*, 2014). This is because finer particles are more damaging to health, as they can travel further into the lungs, enter the blood stream and reach other vital organs (Kampa &

Castanas, 2008).

Figure 6.2. BenMAP inputs and outputs

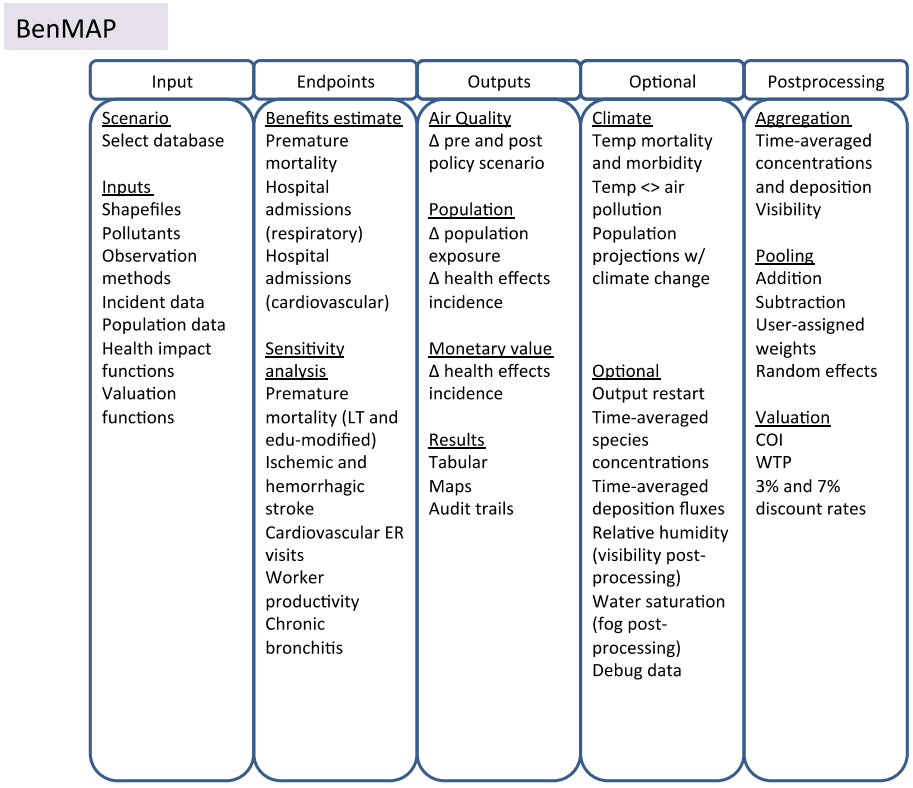

Integrated Modeling Methodology

For these reasons, this study assesses the health impacts of changes in $PM_{2.5}$ exposure. Although I found a couple C-R functions specific to Sao Paulo, Brazil, that associate PM_{10} exposure to premature death in infants (Concieção *et al.*, 2001) and the elderly (Saldiva *et al.,* 1995), and one in Santiago, Chile, for premature mortality related to $PM_{2.5}$ exposure (Cifuentes *et al.*, 2000) I decided to use a recently published integrated exposure-response (IER) model to associate $PM_{2.5}$ exposure to premature mortality. The IER model by Burnett *et al*. (2014) and updated by Cohen

et al. (2017) was developed based on a global set of studies that span the entire range of human exposure to $PM_{2.5}$. The IER was found to perform better than seven other models it was tested against (Burnett *et al*., 2014). Detailed information on the health impact functions I selected can be found in Section 6.3.6.

Selecting the IER model for $PM_{2.5}$ related mortality over PM_{10} related mortality narrowed the focus of this dissertation to the air pollutant with the most severe health impacts, and in turn made this dissertation more manageable by reducing the number of required air quality and human health mapping simulations.

6.3 BenMAP inputs

BenMAP requires a comprehensive database of inputs, including shapefiles, air quality grids, population, disease incidence, health impact functions and valuation functions. For applications in the United States and China, BenMAP includes default inputs such as basic shapefiles, population, monitoring data, health impact functions, valuation functions and inflation datasets. Even with these default inputs, custom shapefiles must be created for each specific study location, and health impact and valuation functions need to be selected to fit the purpose of a study.

To use BenMAP in regions outside of the U.S. or China, shapefiles, air quality grids, disease incidence and population datasets, as well as health impact and valuation functions need to be developed and formatted for the region of study. While a number of studies have been published in the United States and China (Chen *et al*. 2017; Cromar *et al*. 2016; Davidson *et al*. 2007; Fann *et al*. 2012; Neal Fann, Baker, and Fulcher 2012; He *et al*. 2010; Sangkapichai *et al*. 2010; Voorhees *et al*.

2014; Wesson *et al*. 2010), I found only a few peer reviewed BenMAP studies elsewhere, such as in South Korea and Malaysia (Chae & Park, 2011; Ha & Moon, 2013; Nordin *et al.*, 2016). Additionally, I found a few non-peer reviewed articles that use BenMAP in Spain and South Africa (Boldo *et al.,* 2010; Roy 2016).

The following sections discuss the development of a BenMAP database for NE Brazil, including shapefiles, ambient $PM_{2.5}$ concentrations, air quality grids, population data, disease incidence, health impact functions and valuation functions.

6.3.1 Shapefiles

Shapefiles store non-topological geometry and attributes, such as points, lines and area features that are used in geographic information system (GIS) software (Environmental Systems Research Institute, 1998). BenMAP requires shapefiles for multiple layers of data: air quality concentrations, population, disease incidence and for the desired level of aggregation of health impacts and costs (e.g., at the grid cell, city, or regional levels). One advantage of BenMAP is its ability to overlay datasets and shapefiles of different sizes and resolutions when performing calculations, allowing each shapefile to have a unique domain and grid resolution to match the best available data and resolution for each dataset.

Unique shapefiles for the Fortaleza, Recife and Salvador regions were developed to create air quality grids based on the CALPUFF dispersion results for each scenario. Air pollutant differences, also called air quality deltas, were calculated by overlaying the air quality grids of two different scenarios. The

Fortaleza, Recife and Salvador shapefiles were gridded with a 5.4 km x 5.4km resolution to match exactly the air quality modeling grids that I created in CALPUFF.

The shapefiles for population data, disease incidence and results aggregation were downloaded from the BenMAP regional datasets webpage (U.S. Environmental Protection Agency, 2017a). The BenMAP regional datasets provide recent population, disease incidence and background concentration datasets with corresponding shapefiles for many countries. These datasets are discussed below.

6.3.2 Background air quality concentrations

This study considers background air quality concentrations because the C-R functions I selected are non-linear. If the C-R functions used in this study were linear, then including background concentrations would not be necessary because a given change to concentration exposure would produce the same change in the relative risk of incurring an adverse health outcome regardless of the magnitude of exposure.

For most of the C-R functions selected for this study, the relative risk of incurring a health impact increases exponentially at low concentrations and then flattens out to a more linear curve at high concentrations (known as supralinear curves). Accordingly, changes to exposure at low concentrations of total exposure cause a greater change to the relative risk of incurring a health impact than the same magnitude of change to exposure at high concentrations. Therefore, the change in relative risk of incurring adverse health outcomes is dependent on the change in exposure as well as the magnitude of exposure. For this reason, it is important to

consider total exposure to a pollutant when assessing changes relative to a specific source or sector.

In NE Brazil, the background $PM_{2.5}$ concentrations are relatively low, generally between 5 and 10 $\mu g/m^3$. When background concentrations are low, small changes and large changes to $PM_{2.5}$ can cause substantial changes to disease incidence due to the shape of many C-R functions. This study looks at small and large changes to $PM_{2.5}$ concentrations, spanning a range from less than 1 $\mu g/m^3$ to 100 $\mu g/m^3$.

A 10 km x 10 km grid of baseline $PM_{2.5}$ pollutant concentrations for Brazil was downloaded from the BenMAP regional datasets website. This dataset was sourced from the 2013 Global Burden of Disease study (Institute of Health Metrics and Evaluation, 2015). It was convenient because there was a gridded 10 km x 10 km shapefile for Brazil to match the background concentrations.

To match the background $PM_{2.5}$ concentrations with a 10 km x 10 km resolution with the 5.4 km x 5.4 km resolution air quality modeling grids produced in CALPUFF, I spatially interpolated the background $PM_{2.5}$ concentrations from a 10 km x 10 km to a 5.4 km x 5.4 km grid in ArcGIS. For robustness, I used kriging as well as the inverse distance weighting (IDW) method and compared the results.

The IDW method assumes that the degree of influence of nearby sample points is greater than the effect of more distant points (Deligiorgi & Philippopoulos, 2011). IDW predicts the value at a prediction point by using a weighted average of known values within its neighborhood, where the weights of the known values are inversely related to the distances between the sampled points and the prediction

point. The inverse distance weights are modified by a constant power parameter, usually between 0.5 and 3, to diminish the strength of relationship as the distance between the prediction point and sampled points increases (Lu & Wong, 2008). The default power parameter in the ArcGIS IDW algorithm is 2, which is what I used because it is common in air quality modeling (Deligiorgi & Philippopoulos, 2011).

Kriging works slightly differently. It fits a mathematical function to a specified number of points to calculate a prediction value for an unmeasured location, where the surrounding measured values are weighted. Like IDW, kriging weights the surrounding values based on distance, yet it also takes the spatial arrangement of measured points into consideration. This complex process includes data analysis, variogram modeling and surface creation. Kriging is most often used in soil science and geology (Environmental Systems Research Institute Inc., 2016).

For both interpolation methods, the 10 km x 10 km shapefile for Brazil (which includes over 70,000 points) was used as the base layer. The spatial coordinates of each row and column numbered cell in the base layer shapefile were used to convert the spatial coordinates of the background concentrations dataset, which were initially in row and column format, to decimal degrees in order to overlay background concentrations over the center point of each grid cell in the base layer shapefile of Brazil.

For each air quality modeling region (Fortaleza, Recife and Salvador), a polygon was created in the background $PM_{2.5}$ concentration shapefile for Brazil. Each polygon had at least 12 surrounding cells for the spatial interpolation calculations, which is the default value for both kriging and IDW in ArcGIS. As a

sensitivity test, I also calculated the attribute value of prediction points using 20 cells instead of 12 cells. The average difference was 0.24% per cell, with a maximum difference of 1.85% for the Fortaleza region. I decided to use 12 surrounding cells for my calculation because it is the common number of sample points in air quality modeling (Deligiorgi & Philippopoulos, 2011).

Results were obtained using IDW and Kriging by spatially interpolating 5.4 km x 5.4 km $PM_{2.5}$ concentrations from the 10 km x 10 km background $PM_{2.5}$ concentrations. The background $PM_{2.5}$ concentrations were gridded for a 10 km x 10 km shapefile that only includes $PM_{2.5}$ concentrations over land. The kriging and IDW interpolation grids, along with the air quality modeling grids, cover both land and ocean.

The mean difference in the predicted $PM_{2.5}$ values between kriging and IDW was 0.016 $\mu g/m^3$ (0.77%). I decided to proceed with the IDW results because recent studies (Akkala *et al.*, 2010; Lu & Wong 2008) suggest that IDW is preferable to Kriging or Thiessen polygons for environmental data.

Figure 6.3 displays the spatial interpolation results, as a surface and as points, using the IDW method for the Fortaleza region with 12 sample points and a power parameter of 2. As seen in the legend, the background $PM_{2.5}$ concentrations vary between 6.31 and 8.35 $\mu g/m^3$. The same process was used to develop 5.4 km x 5.4 km $PM_{2.5}$ background concentration grids for Recife and Salvador.

Figure 6.3. Spatial interpolation results for Fortaleza

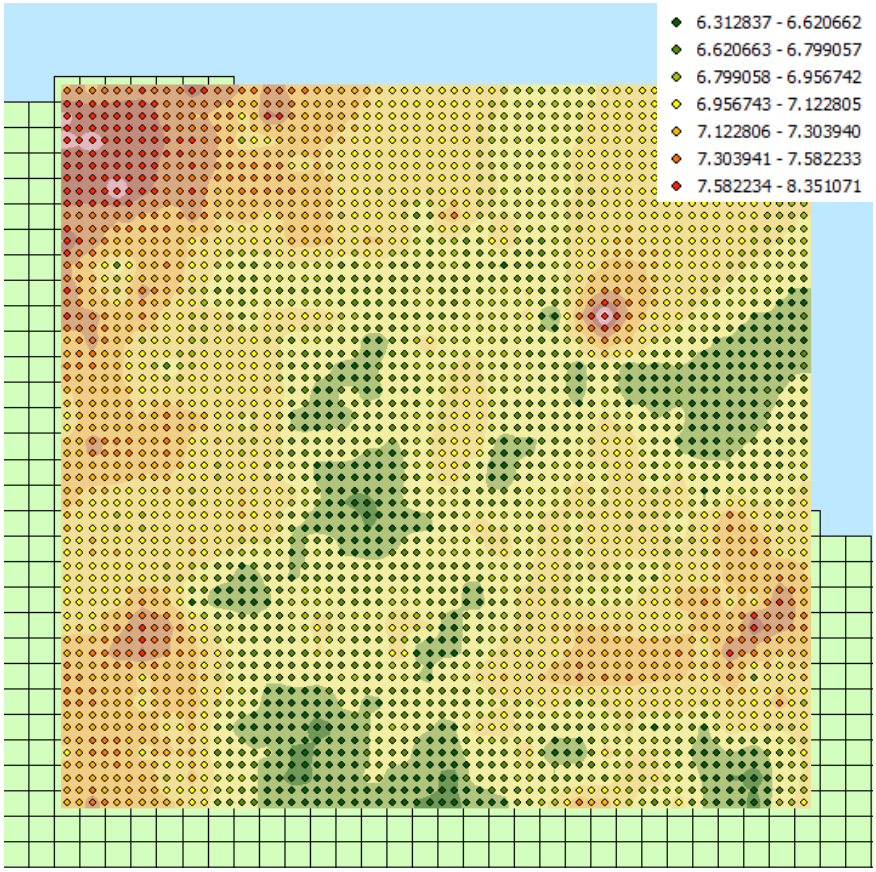

6.3.3 Air quality grids

To calculate changes in air pollutant concentrations under a scenarios, BenMAP overlays two air quality grids of the same domain and resolution. A baseline and a control air quality grid are required for each pollutant considered.

Air quality grids can be defined using daily or annual mean concentrations. This study focuses on long-term $PM_{2.5}$ health impacts because electricity generation in NE Brazil does not create acute short-term health risks. Long-term exposure to $PM_{2.5}$ increases the risk of developing the main causes for PM-related mortality in adults, including ischemic heart disease, cerebrovascular disease, chronic obstructive pulmonary disease, lung cancer and lower respiratory infections

(Burnett *et al.*, 2014).

Concentration-response (C-R, also known as exposure-response, dose-response, relative risk, and health impact functions) functions are used to estimate how changes in air quality affect the relative risk of morbidity and mortality from a variety of diseases.

To develop $PM_{2.5}$ air quality grids for each region in each scenario, I first gridded annual mean $PM_{2.5}$ concentrations from electricity production that were generated by CALPUFF. A unique grid for each region was developed with 3600 5.4 km x 5.4 km grid cells spanning each 320 km x 320 km domain.

The next subsections describe how the gridded $PM_{2.5}$ air quality concentrations from electricity production were combined with the background $PM_{2.5}$ concentrations to form baseline and control scenarios.

6.3.3.1 Air quality grids for tightening PM standards

Baseline and control air quality grids were developed to assess the air pollutant concentration changes under each of the three scenarios developed to assess the health benefits of tightening PM standards.

The baseline air quality grid for Scenario 1 was developed by adding the gridded emissions from the NE Brazil electric grid simulation under the 28.15 g/kWh standard to the gridded 2015 ambient $PM_{2.5}$ concentrations and then subtracting the gridded emissions from the electric grid simulation under the 0.36 g/kWh standard. The ambient $PM_{2.5}$ concentrations include electricity sector emissions, therefore the 2015 electricity grid emissions, which are represented by

the simulation under 0.36 g/kWh emission standard, must be subtracted in order to avoid double counting. The control air quality grid was formed similarly, adding the emissions from the electric grid simulation under the 0.69 g/kWh emission standard to ambient $PM_{2.5}$ concentrations and then subtracting emissions from the 0.36 g/kWh standard.

The baseline air quality grid for Scenario 2 was developed by adding the emissions from the electric grid simulation under the 0.69 g/kWh emission standard to the ambient $PM_{2.5}$ concentrations after subtracting the emissions under the 0.36 g/kWh scenario, for the same reason as above. The control air quality grid in this case is simply the ambient $PM_{2.5}$ concentrations, which include the 2015 electricity sector emissions under the 0.36 g/kWh standard.

6.3.3.2 Air quality grids for health impacts in 2030

To assess health benefits, storage requirements and grid stability implications of high VRE penetrations and a 100% RPS electric grid, four transitions between the scenarios selected for air quality were simulated in BenMAP:

(1) Moving from the 2015 BC scenario to the 2030 HR scenario

(2) Moving from the 2015 BC scenario to the 2030 HR DY scenario

(3) Moving from the 2015 BC scenario to the 2030 HT scenario

(4) Moving from the 2015 BC scenario to the 2030 100% RPS scenario

The baseline air quality grid used to assess the expected health impacts for each transition is the ambient $PM_{2.5}$ air quality concentrations in 2015. This is because the ambient $PM_{2.5}$ concentrations include emissions from all sectors, and I

estimated changes in health outcomes based on changes total $PM_{2.5}$ concentrations and exposure. A unique ambient $PM_{2.5}$ concentrations grid was developed for Fortaleza, Recife and Salvador.

Control air quality grids were created for each transition between scenarios in each region, including Fortaleza, Recife and Salvador. As mentioned in the CALPUFF emissions and domain integration section, the number and types of thermal power plants vary from region to region, as well as their proximity to densely populated regions, making it difficult to estimate health impacts without simulating pollutant dispersion and human exposure.

Control air quality grids were developed by adding the 2015 ambient $PM_{2.5}$ concentrations with the electricity grid emissions for each 2030 scenario, and then subtracting the 2015 baseline electricity grid emissions. The 2015 baseline electricity grid emissions are represented by the 2015 electric grid simulation under the 0.36 g/kWh standard and must be subtracted because they are already included in the ambient $PM_{2.5}$ air quality concentrations. For the 2030 100% RPS scenario, all thermal generators are decommissioned and electricity sector emissions are assumed to be 0, so the control scenario is the background $PM_{2.5}$ concentrations minus the baseline electricity sector emissions.

6.3.4 Population

Population data for Brazil in 2015 were gathered from the BenMAP regional datasets (U.S. Environmental Protection Agency, 2017a). The population data were sourced from the United Nations Socioeconomic Data and Applications Center

(SEDAC). The SEDAC dataset gave 10 km x 10 km population data, totaling approximately 1024 population grid cells in each 320 km x 320 km modeling region. Its resolution is finer than the resolution of the Brazilian census data. Indeed, for the state of Ceara (where Fortaleza is located), the finest resolution I could find was on a municipality level for 184 municipalities (Instituto Brasileiro de Geografia e Estatistica, 2016).

To develop a gridded population dataset for 2030, I gathered population estimates for Brazil from the United Nations World Populations Prospects database (United Nations, 2017). The population increase from 2015 to 2030 by age group (5 year increments) was then applied to the gridded 10 km x 10 km population data.

Table 6.1. Brazilian age pyramid

Age (years)	Number of persons	Percentage of total
All	191,880,534	100.0%
0 to 4	13,877,503	7.2%
5 to 9	15,057,637	7.8%
10 to 19	34,359,033	17.9%
20 to 29	34,552,138	18.0%
30 to 39	29,807,814	15.5%
40 to 49	24,989,194	13.0%
50 to 59	18,525,211	9.7%
60 to 64	6,547,499	3.4%
65 to 69	4,869,352	2.5%
70 to 74	3,763,698	2.0%
75 to 79	2,578,562	1.3%
80 to 84	1,676,801	0.9%
85 to 89	824,315	0.4%
90 and up	451,777	0.2%

The SEDAC population dataset was not age stratified, while the C-R functions selected for this study vary by age. To age-stratify the population data, I used the age pyramid for Brazil as reported by the 2010 census. The population in each grid cell was split into 16 age groups that match the C-R function age ranges. They are in five-year increments from 0 to 20, 10-year increments from 20 to 60, and five-year increments from 60 to 90, with one final age group above 90. Table 6.1 displays the Brazilian age pyramid applied to the 2015 population dataset.

The 2030 population dataset is based on forecasted population increases in each age group listed above, and therefore the age pyramid of the 2030 population dataset varies based on the projected population changes (United Nations, 2017). Age stratification increases the accuracy of changes in disease incidence calculations because C-R functions for a given pollutant and health impact may vary based on age, sex and location. For example, young people and old people are usually the most vulnerable to increased exposure of pollutants (U.S Environmental Protection Agengy, 2013).

6.3.5 Disease incidence

I collected baseline disease incidence rates for mortality causes and hospital admissions for each health endpoint considered by the IER model: cerebrovascular disease, cardiopulmonary disease, ischemic heart disease, lower respiratory infection and lung cancer (Cohen *et al.*, 2017) . In addition, I collected baseline disease incidence data for hospital admissions and cardiovascular related hospital admissions. When available, I used all respiratory related hospital admissions and

all cardiovascular related hospital admissions C-R functions for a more complete analysis. I also collected baseline disease incidence data for asthma related and chronic lung disease related hospital admissions, because the C-R functions for those health endpoints are used for certain age groups where all respiratory related hospital admissions C-R functions are not available.

I downloaded the 2015 baseline mortality rates from the BenMAP regional datasets websites. These data were sourced from the Institute of Health Metrics and Evaluation Global Burden of Disease 2015 study (Institute of Health Metrics and Evaluation, 2015). Age-stratified baseline disease incidence rates for each premature mortality cause considered in the IER were discretized by age groups that match the age discretized population data.

The Brazilian Health Ministry online system, DATASUS, contains records of patients with public health insurance. I attempted to access the DataSUS database to find mortality and hospital admittance rates. However, access to DATASUS is private, and a license is required to download and use its data. Licenses are granted by the Brazilian Health Ministry and require a letter from a medical center. I was not able to gain access to this database, despite emailing both the Brazilian Health Ministry and my colleagues at the Federal University of Rio de Janeiro.

I obtained hospital admission rates for asthma and chronic lung disease from journal publications (Board of Representatives for the Global Initiative for Chronic Obstructive Lung Disease, 2016; Duarte *et al*. 2014). However, hospital admission rates for all respiratory disease and all cardiovascular diseases could not be found.

Based on hospital admission rates for asthma and chronic lung disease in Brazil and IHME GBD DALY data for Brazil, I found ratios for asthma hospital admissions/DALY (0.04722) and chronic lung disease hospital admissions/DALY (0.06148). A DALY is a disability adjusted life year, which can be thought of as the loss of one healthy year of life. DALYs are used more commonly in Europe than in the U.S. to measure premature mortality and morbidity (van Zelm *et al*., 2008). The average of these ratios (0.0544) was multiplied by IHME GDB DALY results for all respiratory as well as all cardiovascular diseases to get an estimate of hospital admission rates for all respiratory diseases and all cardiovascular disease in Brazil in 2015. This method was developed based on a conversation with the U.S. EPA Risk and Benefits Group, who developed and maintains BenMAP at the Office of Air Quality Planning and Standards.

6.3.6 Health impact functions

There are many factors to take into account when selecting C-R functions, including study design and location, characteristics of the study population, and how recently the study was performed (Fann *et al.,* 2012). I thoroughly searched the epidemiological literature to find the exposure-response studies that have been conducted in Brazil and Latin America, as well as the recently published studies conducted in the U.S., Europe and globally.

While I found several relative risk studies specific to Latin America and Brazil, only two of the studies considered $PM_{2.5}$ (Loomis *et al.,* 1999; Cifuentes *et al.*, 2000). The older studies focus on PM_{10}, including almost all of published Latin American

exposure-response studies, while more recent studies focus on $PM_{2.5}$ because finer particles have been shown to be more dangerous than coarser particles (PM_{10}) (Kampa & Castanas, 2008).

Previous studies have used a weighted average of C-R functions when country specific functions are not available (Bell *et al.,* 2006). Recent studies accessing health impacts related to $PM_{2.5}$ exposure globally have used the integrated-exposure response (IER) model developed by Burnett *et al.* (2014) because it uses a weighted average of relative risk functions from many different countries and spans the entire exposure $PM_{2.5}$ exposure range (Apte *et al.,* 2015; Lelieveld *et al.,* 2015) Additionally, the IER has specific mortality relative risk functions for different age ranges in adults, including 25 – 44, 45 – 64 and 65 to 99.

I selected the IER model for several reasons. First, it is the only C-R model that spans the entire global range of $PM_{2.5}$ exposure, from 1 – 300 $\mu g/m^3$, for the five PM-related causes of mortality in adults. A large range of $PM_{2.5}$ exposure is necessary to capture the effects of high PM air quality concentrations in case that moves from a high PM_{10} emissions standard (28.15 g/kWh) to a lower standard (0.69 g/kWh). Second, the IER averages relative risk functions from different regions around the globe for exposure ranges for each cause of PM related mortality, allowing for specific relative risk increases depending on the health impact and magnitude of pollutant exposure that are based on studies in developed and developing countries. And third, the IER model was tested against seven other exposure-response functions previously used in disease burden assessments and it

was found to be a superior predictor of the change in relative risk of mortality due to fine particle exposure by Burnett *et al.* (2014).

The IER model estimates premature mortality from 25 to 99 and 30 to 99, depending on the mortality cause. To capture premature mortality in children, I developed a health impact function in BenMAP using the results of Loomis *et al.* (1999) study, which estimated the relative risk of mortality in children from 0 to 1 years due to $PM_{2.5}$ exposure in Mexico City, Mexico. Mortalities between 1 and 25 years of age are not considered in the low or high estimates.

Table 6.2 displays the $PM_{2.5}$ C-R functions I selected to estimate mortality.

Table 6.2. C-R functions selected for mortality

Mortality	Health impact function authors	$PM_{2.5}$ range (µg/m3)	Locations	Age range
Mortality, Cerebrovascular Disease	Cohen *et al.* (2017)	1 - 300	Global	25-99
Mortality, Chronic Obstructive Pulmonary Disease	Cohen *et al.* (2017)	1 - 300	Global	30-99
Mortality, Ischemic Heart Disease	Cohen *et al.* (2017)	1 - 300	Global	25-99
Mortality, Lung Cancer	Cohen *et al.* (2017)	1 - 300	Global	30-99
Mortality, Lower Respiratory Infection	Cohen *et al.* (2017)	1 - 300	Global	30-99
Mortality, All Cause	Loomis *et al.* (1999)	4 - 85	Mexico City	0-1

For many health endpoints, such as cardiovascular related hospital admissions, Latin American studies are not available (Bell *et al.,* 2006). I selected

two C-R functions to estimate all cardiovascular related hospital admissions. One of them was developed based on the Moolgavkar (2000) study, and it is the only EPA Standard Health Impact Function for all cardiovascular related hospital admissions with an age range for 18-64 (Moolgavkar, 2000). To capture cardiovascular related hospital admissions in the elderly from 65 to 99, I selected the Zanobetti *et al.* EPA Standard Health Impact function (Zanobetti *et al.,* 2009). Hospital admissions related to cardiovascular disease are not considered for people less than 18 years old.

Table 6.3. C-R functions selected for hospital admissions

Hospital Admissions	Health impact function sources	$PM_{2.5}$ range (µg/m3)	Locations	Age range
Hospital Admissions, All Cardiovascular	Moolgavkar (2000)	4 - 86	Los Angeles, CA, U.S.	18-64
Hospital Admissions, All Cardiovascular	Zanobetti *et al.* (2009)	6.1 - 24	26 U.S. Communities	65-99
Hospital Admissions, Asthma	Babin *et al.* (2007)	Not reported	Washington D.C.	0-17
Hospital Admissions, Asthma	Slaughter (2003)	5 - 60	Seattle, Washington	18-64
Hospital Admissions, Chronic Lund Disease (less Asthma)	Moolgavkar (2000)	4 - 86	Los Angeles, CA, U.S.	18-64
Hospital Admissions, All Respiratory	Zanobetti *et al.* (2009)	6.1 - 24	26 U.S. Communities	65-99

Four health impact functions were selected for respiratory related hospital admissions. For children from 0 to 17, a relative risk function was derived from a

2007 study by Babin *et al.* (2007) relating $PM_{2.5}$ exposure and asthmatic hospital admissions. The Babin *et al.* function is the only EPA Standard Health Impact function that estimates changes in respiratory related hospital admissions for children. To estimate respiratory related hospital admissions in people between 18 and 64, a relative risk function based on chronic lung disease incidence due to $PM_{2.5}$ was selected (Moolgavkar, 2000) as well as a relative risk function for asthma in adults 18 to 64 (Slaughter *et al.*, 2003). For elderly respiratory related hospital admissions, a relative risk function derived by Zanobetti *et al.* (2009) that spans the age group of 65-99 was selected because it is the only EPA Standard Health Impact function that estimates all respiratory related hospital admissions for the elderly. Table 3 displays the C-R functions used to estimate hospital admissions.

Each C-R function was developed over a different range of $PM_{2.5}$ exposure. Figure 6.4 graphically displays the Lepeule *et al.* (2012) C-R function for mortality in adults and the Loomis C-R function for mortality. Figure 6.5 displays each C-R function I selected to estimate hospital admissions. There is a semi-transparent yellow highlighted layer over the unique range of $PM_{2.5}$ exposure for each epidemiology study.

As seen by the yellow highlighted portion of the line, the Lepeule *et al.* (2012) was developed based low concentrations. Although the low concentrations match ambient PM concentrations in NE Brazil, I decided not to report the Lepeule *et al*. (2012) results because the IER is a better match for this studies, due to its range of PM emissions and integration of relative risk functions from around the world.

Figure 6.4. Mortality C-R Functions

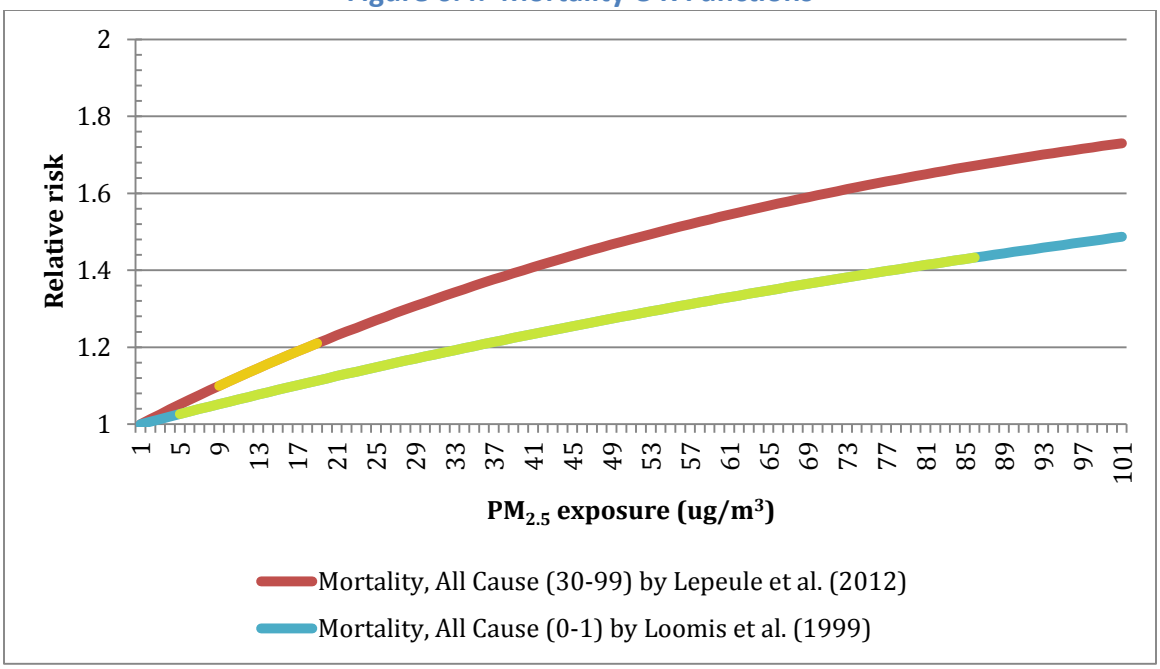

Figure 6.5. Hospital admissions relative risk functions

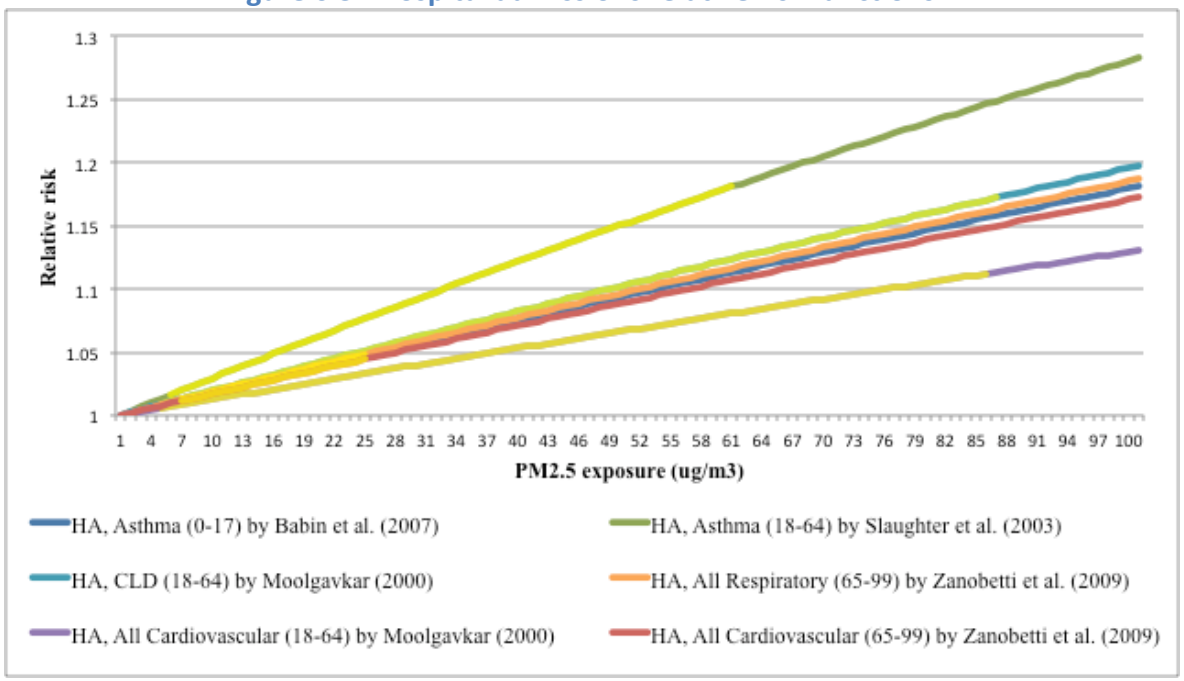

The IER was developed based on aggregating epidemiological study results for the main air pollutant related mortality causes in adults across the entire $PM_{2.5}$

exposure range. For each spline, or portion of the exposure range for which RR functions were averaged, there are 1,000 relative risk estimates that correspond to the lower bound and 1,000 relative risk estimates that correspond to the upper bound. An averaged C-R function for each spline of each cause of mortality was calculated by taking the natural log of the quotient of the upper bound RR and lower bound RR divided by the $PM_{2.5}$ range covered by the spline.

6.3.7 Valuation functions

Expected health costs can be estimated by applying monetary valuation functions to changes in expected health outcomes, such as premature mortality, hospital admissions and the work days lost associated with hospital admissions. Valuation methods vary and can generate substantially different cost estimates for the same study.

6.3.7.1 Background

BenMAP was designed to use the VSL (Value of a Statistical Life) approach to value premature mortality, and the COI (cost of illness) and WTP (willingness to pay) techniques to value morbidity. The VSL method values premature mortality at the same value regardless of the age of the person, which is in part to avoid the moral and political controversy of valuing people's lives based on age (Desaigues *et al.*, 2007). There are many implications of using this method as opposed to the DALY method, which are discussed in greater detail below.

The VSL approach assigns a standard dollar amount to the loss of a life. The U.S. EPA recommends VSL values for the U.S. for each year, considering inflation and wage growth adjustments. The recommended VSL for 2015 in 2015 dollars is 10 million (U.S. Environmental Protection Agency, 2017b).

VSL estimates vary widely across different years, countries and calculation methods. The Organization for Economic Co-operation and Development (OECD) analyzed the distribution of over 800 VSL estimates by many studies in different countries (Organisation for Economic Co-operation and Development, 2012). China and other non-OECD countries have the highest frequency of low VSL estimates, which are less than 1 million dollars (2005 USD, PPP-adjusted). The United Kingdom, U.S., Canada and Europe have the highest frequency of high VSL estimates, which are over 10 million dollars (2005 USD, PPP-adjusted). Interestingly, the U.S. has a somewhat even distribution of VSL values across the range of low and high VSL estimates.

The cost of illness (COI) approach assigns dollar amounts to the medical cost of a particular illness and the lost wages during the average hospital stay for that illness. The WTP approach estimates a population's willingness to pay to avoid a specific health impact, which is directly related to that population's disposable income or per capita GDP (Pizzol *et al.*, 2015).

The DALY approach is more commonly used in Europe, which is uses a standard metric to measure morbidity and mortality. One DALY is equivalent to the loss of one life year. To value mortality, the number of years between the age of premature death and estimated life expectancy is the number of DALYs incurred. To

value morbidity, the number of years in which the illness is incurred is calculated, and then a factor of disability between 0 and 1 is assigned, which reflects how much that person is disabled during the time they have a particular disease. Complete health has a disability factor of 0 and death has a disability factor of 1 (van Zelm *et al*., 2008).

The DALY approach differentiates between the death of a young person and the death of an old person. For example, in a country with a life expectancy of 80 years, the death of a 3-year old is equivalent to 77 DALYS, while the death of a 75 year old is equivalent to 5 DALYS. This is different than the VSL approach because the VSL approach assigns the same value to mortality regardless of the age, which gives much more weight to the death of old people than the DALY method.

One of the reasons why I selected BenMAP is to avoid the controversy of valuing people's lives depending on age. While it has been argued that there is less reason to protect people from health risks that have fewer years left to live, this approach has been criticized on the basis that senior lives are not worth less than other lives. The EPA is proposing changing the term "value of a statistical life" to "value of mortality risk reduction" (VMR) because it more precisely describes health risk changes, which are usually small reductions in mortality risk for large numbers of people (U.S. Environmental Protection Agency, 2016b).

When assessing morbidity impacts, the DALY approach looks at the duration and the severity of a disease, such as asthma, and calculates the DALYS. For example, if a child contracts asthma for the rest of his/her life, it results in a large number of DALYS. This is a different valuation than the COI method, which values

hospital admissions related to asthma based on the average cost of a hospital visit and lost wages. The DALY approach is also different from the WTP to avoid adverse health affects, which again is linked to GDP and national hospital costs.

The selection of valuation methods is controversial. The BenMAP approach tends to weight mortality more heavily than morbidity, because mortality is valued based on VSL and morbidity is valued based on COI and/or WTP. The DALY approach uses a consistent metric for valuing mortality and morbidity, so mortality does not outweigh morbidity as much.

6.3.7.2 Deriving a mortality valuation function for Brazil

I derived a VSL for Brazil to value changes in premature mortality. Using the method recommended in the EPA's BenMAP training shown in Equation 2, I calculated a VSL for Brazil for 2015 in 2015 US$, including adjustments for inflation and wage growth (United States Environmental Protection Agency, 2017).

$$BR\ VSL_{2015} = US\ VSL_{2015} * \left(\frac{Brazil\ GDPPC_{2015}}{US\ GDPPC_{2015}}\right)^{elasticity} * PPP_{Brazil,2015} \quad (2)$$

I selected the baseline Value of a Statistical Life (VSL) recommended by the EPA of $10 million for U.S. for 2015 in 2015 US$, including income growth and inflation (U.S. Environmental Protection Agency, 2016b). The 2015 Brazil Gross Domestic Product (GDP) per capita in 2015 was $15,615 in international dollars (one international dollar would buy a comparable amount of goods in the cited country

as one U.S. dollar would buy in the U.S.) adjusted Purchasing Power Parity (PPP). The 2015 U.S. GDP per capita was $56,207 expressed in 2015 international PPP-adjusted dollars and (World Bank, 2015). An elasticity of 0.8 between income and willingness to pay to avoid adverse health effects was used as recommended by the OECD (Organisation for Economic Co-operation and Development, 2012). The resulting VSL for Brazil for 2015 is $6,819,641 in 2015 US$.

I selected U.S. dollars as the currency to make it easier for readers outside Brazil to understand the magnitude of costs.

6.3.7.3 Deriving a VSL for Brazil in 2030

I tested two different approaches to derive a future 2030 VSL for Brazil and compared the results. An important consideration is that the U.S. and Brazil have different inflation and wage growth rates.

In the first approach, I took the EPA recommended VSL for the United States for 2026, which is adjusted for income growth but not inflation and is in 2015 US$, and used it as the base VSL to derive a 2030 VSL for the United States in 2015 dollars. The calculation for this step is shown in Equation 2, which is from the EPA BenMAP training material. In the next step, the 2030 U.S. VSL was converted to a 2030 Brazilian VSL in 2030 US$ by using the same EPA recommended method that was used to convert the U.S. VSL for 2015 to a VSL for Brazil in 2015. Equation 4 displays the second step calculation, which produces a 2030 VSL for Brazil, adjusted for wage growth, of $7,536,210 in 2015 US$.

$$US\ VSL_{2030} = US\ VSL_{2026} * \left(\frac{CPI\ US_{2030}}{CPI\ US_{2026}}\right) \quad (3)$$

$$BR\ VSL_{2030} = US\ VSL_{2030} * \left(\frac{Brazil\ GDP_{2015}}{US\ GDP_{2015}}\right)^{elasticity} * PPP_{Brazil,2015} \quad (4)$$

In the second approach, I linearly extrapolated the EPA recommended U.S. VSL value from 2026 to 2030 to derive a 2030 VSL in 2015 US$. Note that the EPA recommends future VSL's adjusted for wage growth but not inflation, which is why the currency year is 2015. In the next step, the 2030 U.S. VSL (in 2015$) was converted to a 2030 VSL for Brazil of $7,202,908 2015 US$, according to Equation 3.

These methods provide similar results for a few reasons. First, the same U.S. 2026 VSL is used and the PPP for the U.S. is 1. Note that the 2026 VSL is based on wage growth projections from the Congressional Budget Office. Second, the 2030 VSL is derived in 2015 dollars because inflation is not considered in the VSL projection. This is consistent with the EPA VSL projections that do not include inflation. Third, when I converted the 2030 VSL for the U.S. to a 2030 VSL for Brazil, I used the same GDP ratio and PPP conversation factor as in 2015 because inflation and other economic indexes fluctuate greatly and are hard to predict, and I did not find annual projections for Brazil's GDP or inflation.

I decided to use the first method because it relies on the method and equations recommended by the EPA in its BenMAP training materials. This value for the 2030 VSL for Brazil is $7,536,210 in 2015 US$.

6.3.7.4 Deriving Cost of Illness (COI) and wage loss functions for Brazil

The cost of illness (COI) valuation method sums the average medical costs incurred from a hospital admission related to a specific illness with the wages lost associated to the average recovery time of that illness. Similar issues exist with measuring hospital costs in Brazil as with many developing countries, including poor data quality, multiple and unstandardized cost accounting systems, and managerial failure to apply available data to operations (La Forgia & Couttolenc, 2008).

I derived valuation functions for hospital admissions by updating the COI EPA Standard Health Impact Functions with the Brazilian average hospital costs and wage losses. Data for hospital admissions costs in Brazil were sourced from a World Bank publication on hospital performance in Brazil, and then scaled to 2015 hospital costs using the Brazilian medical wage index (La Forgia & Couttolenc, 2008; World Bank, 2015). The Brazilian medical cost index is more stable than the inflation index, with per capita health expenditure ranging from $600 in 2007 to $947 in 2016.

The medical costs per hospitalization were calculated by multiplying the average hospitalization cost per disease by the medical cost index. Lost wages were calculated by dividing annual median income by 52 weeks and 5 days, and then multiplying by the average length of stay in the hospital. The EPA Standard Health Impact Functions for wage loss were adjusted for Brazil by using the Brazil average per capita GDP in 2015 in USD to represent annual median income.

To derive COI estimates for Brazil in 2030, I linearly extrapolated the 2015 Brazilian medical wage index to 2030, and multiplied the conversation factor by the

same hospital admissions costs as in the 2015 scenario (La Forgia & Couttolenc, 2008).

6.4 BenMAP sensitivity tests and results validation

There are many sensitivity tests that could be run in BenMAP to characterize uncertainty. The two sensitivity tests with the biggest potential to impact results from the BenMAP analysis are (1) varying the health impact functions used to quantify changes premature mortality and (2) varying the value of the VSL for Brazil in 2015 and 2030.

The impact of using a different health impact function could be assessed by comparing results between the IER and an alternative health impact function. However, health impact functions are designed specific to a location, pollutant concentration range, demographic data and other factors that should match the study they are being used it. For example, the Lepeule *et al.* (2012) function was developed in six Eastern U.S. cities at low $PM_{2.5}$ concentration levels, and it found higher relative risk increase per $\mu g/m^3$ of $PM_{2.5}$ exposure than the other relative risk functions for mortality in BenMAP. While I compared health outcomes from the IER function with the Lepeule *et al.*, I decided not to report results from the Lepeule *et al.* study because the study characteristics are not a good match for NE Brazil.

Varying the value of the VSL for Brazil in 2015 and 2030 could substantially change results. This is because estimates for VSL range greatly between countries and within countries, from less than 1 million to more than 20 million dollars (Organisation for Economic Co-operation and Development, 2012). EPA assigns a

base VSL of 10.0 million in the U.S. for the 2015 year, in 2015 currency and accounting for wage growth. This value is one to two orders of magnitude larger than the cost of illness values used in the monetary valuation of hospital admissions.

The change in the magnitude of expected health benefits due to varying the value of the VSL for Brazil will be directly proportional to the magnitude of change of the VSL because the VSL value is multiplied by the calculated changes in premature mortality. As discussed in the valuation section, I calculated the 2015 VSL as well as the 2030 VSL two different ways each. The variance of these calculations is indicative of the sensitivity of the results to changes in the VSL value.

There are many other sensitivity tests that could be performed. For example, the selected health endpoints could be varied. The valuation functions selected to quantify and monetarily value changes in hospital admissions could also be varied, which will impact results proportionally to the differences in relative risk estimates for the same health outcome.

The resolution of incidence data could also be increased if access high resolution disease incidence data from the Brazilian Health Ministry DATASUS database were available. If these data were available, gridded disease incidence datasets and shapefiles could be created. Based on the health impact function calculations, it is possible that this could change results if disease incidence rates in densely populated cities were much higher than the average disease incidence rates. Gathering formatting this data into a dataset inputs and developing matching shapefiles would be a substantial effort.

Additionally, the medical costs and medical cost index for Brazil could also be projected in different ways.

Along with comparing results between among the sensitivity tests, I calculated the air quality delta between scenarios and compared it with the air quality delta calculations in BenMAP. Additionally, I manually spot-checked disease incidence changes and monetary valuation calculations.

6.5 Monetary valuation of CO_2 emissions

To monetarily value the climate impacts of different electricity grid scenarios, CO_2 emissions were valued according to the High-Level Commission on Carbon Prices recommended carbon price of US$50-100 per ton of CO_2 (Stiglitz *et al*., 2017). A range of climate benefits was estimated by valuing CO_2 emissions at the lowest carbon price of US$50 per ton of CO_2 and at the highest carbon price of US$100 per ton of CO_2 in the recommended range.

During the 2016 United Nations Framework Convention on Climate Change (UNFCCC), a new High-Level Commission on Carbon Prices was formed within the Carbon Pricing Leadership Coalition (CPLC), chaired by Joseph Stiglitz and comprised of specialists in economics, climate change and energy from all over the world. This Commission was created to design carbon-pricing instruments to support the achievement of the Paris Agreement, agreed on by nearly 200 countries (Stiglitz *et al*., 2017).

There are different ways to price carbon. GHG emissions can be directly priced through a carbon tax or a cap-and-trade system. Carbon prices can also be embedded in programs and incentives, such as specific project-based credits as described by the Clean Development Mechanism in the Kyoto Protocol as well as Article 6 of the Paris Agreement (United Nations, 2015). Reducing fossil fuel subsidies is another step towards pricing carbon, because fossil fuel subsidies are similar to a negative carbon emissions price.

The High-Level Commission on Carbon Prices concludes that explicit carbon-price level consistent with achieving the Paris Agreement temperature target is at least US$40-80 per ton of CO_2 by 2020 and US$50-100 per ton of CO_2 by 2030. Part of the reason for providing a carbon price range is that the appropriate carbon-price will vary between countries, due to variations in the cost of complementary actions as well as variations in the complexity of distributional and ethical issues (Stiglitz *et al*., 2017).

The changes in NE Brazil electricity grid CO_2 emissions from the 2015 BC to the 2030 HR, 2030 HR DY, 2030 HT and 2030 100% RPS scenarios were valued at the lowest recommended price per ton of CO_2 of US$50 and the highest recommended price per ton of CO_2 of $US100. I value the changes in CO_2 emissions in terms of total emissions per scenario as well as changes in CO_2 emissions due to transitioning from the 2015 BC to each 2030 scenario. Quantifying changes in climate benefits/costs between scenarios consistent with the assessment of health impacts, in which changes in health outcomes are quantified and valued between transitioning from the 2015 BC to one of the 2030 scenarios.

7 Results

The integrated modeling methodology described in the previous sections was developed to address three questions with high spatial and temporal resolution in each simulation phase:

(1) What are the health benefits and control costs of tightening emission standards?

(2) What are the health, climate and electricity grid implications of high penetrations of VRE?

(3) Is a 100% RPS electricity grid technically feasible in NE Brazil, and what are the associated health and climate benefits?.

The results for each question are presented sequentially, starting with electricity grid simulations, then air quality modeling, and ultimately the health and climate benefits. The electricity grid simulation results are presented in detail and include generation and emissions, as well as storage requirements and grid stability considerations. The NE Brazil electric system sensitivity to dry year conditions and higher than forecasted energy demand is also presented. To assess climate impacts, the electric grid CO_2 emissions are presented for each scenario considered. To assess health impacts, PM_{10} emissions are discussed, followed by air quality modeling and the human health benefits assessment of various changes in air quality.

The health outcomes are presented in terms of changes in premature mortality and morbidity incidences, along with a monetary valuation of those changes in expected death and disease incidences. For the first question, the

emission control costs of achieving tighter emission standards are also presented, along with health benefits to control costs ratio of tightening PM standards.

7.1 Health benefits and control costs of tightening PM standards

The hourly electricity dispatch and emissions of the NE Brazil electric grid were simulated for the entire 2015 year under three different scenarios that considered transitions between four different PM_{10} emission standards for coal power plants: 28.15 g/kWh, 0.69 g/kWh, 0.36 g/kWh and 0.04 g/kWh. All properties and outputs of each simulation are the same, except for the emission standards for the Porto do Pecem coal power plants.

7.1.1 Electric grid emissions

The Plexos simulations for 2015 show an annual electricity system load of 107,246 GWh, with 10,861 GWh from pumped hydroelectric storage (water is pumped from a lower reservoir to a higher one when electricity prices are low). Electric system load is the quantity of electricity being demanded from the electric grid. The annual electricity generation was 107,207 GWh, which includes 25 GWh of dump load (energy dissipated into heat because it could not be stored). Additionally, 0.06% (65 GWh) of the load was not served, which happened in a couple of summer weeks when electricity supply was not sufficient to meet demand.

Table 7.1 displays total PM_{10} emissions from the entire Northeast Brazil electric grid for 2015 for the three major fossil fuel sources under the four different PM_{10} coal power plant emission standards. Moving from the 28.15 g/kWh PM_{10} to

0.69 g/kWh PM_{10} (Scenario 1) reduced emissions from power plants in the 320 x 320 km region surrounding Fortaleza by 96%, moving from 0.69 g/kWh PM_{10} to 0.36 g/kWh PM_{10} (Scenario 2) further reduced emissions by 30%, and moving from 0.36 g/kWh PM_{10} to 0.04 g/kWh PM_{10} (Scenario 3) cut emissions by an additional 41%.

Table 7.1. Electricity grid emissions by emission standard and fuel source

Emission source	28.15 g/kWh standard	0.69 g/kWh standard	0.36 g/kWh standard	0.04 g/kWh standard
Coal (metric ton PM_{10}/yr)	254,225	6,231	3,251	361
Oil (metric ton PM_{10}/yr)	2,914	2,914	2,914	2,914
Natural Gas (metric ton PM_{10}/yr)	953	953	953	953
Total (metric ton PM_{10}/yr)	**258,092**	**10,099**	**7,118**	**4,228**

I checked Plexos results according to the system validation process described in the Plexos methodology. The electric grid generation was 0.6% greater in my simulation than in the 2015 predicted load based on the 2013 actual load profile from the ONS (Operador Nacional do Sistema Eletrico, 2016).

Simulated hydroelectric generation was within 3.2% of actual 2015 generation, and reservoir levels were restricted based on previous year fill levels and release quantities. The levelized cost of energy for each generator was checked against actual LCOE data for Brazil and the emissions profiles were validated by multiplying the emission factor by the hourly dispatch profile.

Additional results from the NE Brazil 2015 electric grid simulations are presented in the health, climate, and grid stability implications section.

7.1.2 Air quality changes

After obtaining hourly PM_{10} emissions for year 2015 from Plexos, I converted them to $PM_{2.5}$ emissions and dispersed them using CALPUFF View. Table 7.2 summarizes the average annual mean, max annual mean, and max 24-hr mean $PM_{2.5}$ concentrations due to power plant emissions. The maximum annual mean values are 91.7 $\mu g/m^3$, 2.26 $\mu g/m^3$, 1.18 $\mu g/m^3$ and 0.35 $\mu g/m^3$ under the 28.15 g/kWh, 1.18 g/kWh, 0.36 g/kWh and 0.04 g/kWh standards respectively.

Table 7.2. Air quality concentrations after CALPUFF dispersion

PM_{10} Standard	**Max 24-hr mean of all grid cells ($PM_{2.5}$ $\mu g/m^3$)**	**Max annual mean of all grid cells ($PM_{2.5}$ $\mu g/m^3$)**	**Average annual mean of all grid cells ($PM_{2.5}$ $\mu g/m^3$)**
28.15 g/kWh	260	91.7	2.01
0.69 g/kWh	6.38	2.26	0.05
0.36 g/kWh	3.33	1.18	0.03
0.04 g/kWh	2.17	0.35	0.01

The large difference between the grid cell with the highest mean annual $PM_{2.5}$ concentration (max annual mean) and the annual mean $PM_{2.5}$ concentration averaged over all grid cells (average 8760-mean) highlights the importance of high spatial resolution, especially when mapping air quality changes to population density.

Figures 1-4 display the annual mean $PM_{2.5}$ concentrations for each grid cell under each PM_{10} standard. Note that the color scale for the 28.15 g/kWh standard plot is five times greater than the than the color scales for the 0.69 g/kWh, 0.36

g/kWh and 0.04 g/kWh standard plots because the $PM_{2.5}$ concentrations are one to two orders of magnitude higher under that standard. For example, the color red indicates concentrations above 5 μg/m^3 in the 28.15 g/kWh plot, while the color red indicates concentrations above 1 μg/m3 in the 0.69 g/kWh, 0.36 g/kWh and 0.04g/kWh standard plots.

The shape of the annual average $PM_{2.5}$ concentration plots is similar under each standard because the same meteorological conditions for the Fortaleza region in 2015 are used. The 28.15 g/kWh standard air quality concentrations extend further because there are greater quantities of emissions, which also affect air quality concentrations of the Fortaleza metropolitan area that is slightly east of the Porto do Pecem coal power plants. The area affected by $PM_{2.5}$ concentrations due to power plant emissions is smallest under the 0.04 g/kWh standard because the system emissions are substantially less due to decreases in coal power plant emissions.

The plot of the peak 24-hr PM2.5 concentration plume, shown for the 28.15 g/kWh standard in Figure 5, has a distinctly different shape than the annual average $PM_{2.5}$ concentration plot that reflect meteorological conditions of that time (November 14, 2015). It corresponds to higher system load and lower than usual VRE and hydroelectric generation, leading more thermal generators to be dispatched, which caused higher $PM_{2.5}$ concentrations over a larger exposure area. Note that the color scale of the Peak 24-hr mean plot is 10 times greater than the annual mean PM2.5 concentration plot scale.

Figure 7.1 Annual mean $PM_{2.5}$ concentration for the 28.15 g/kWh standard

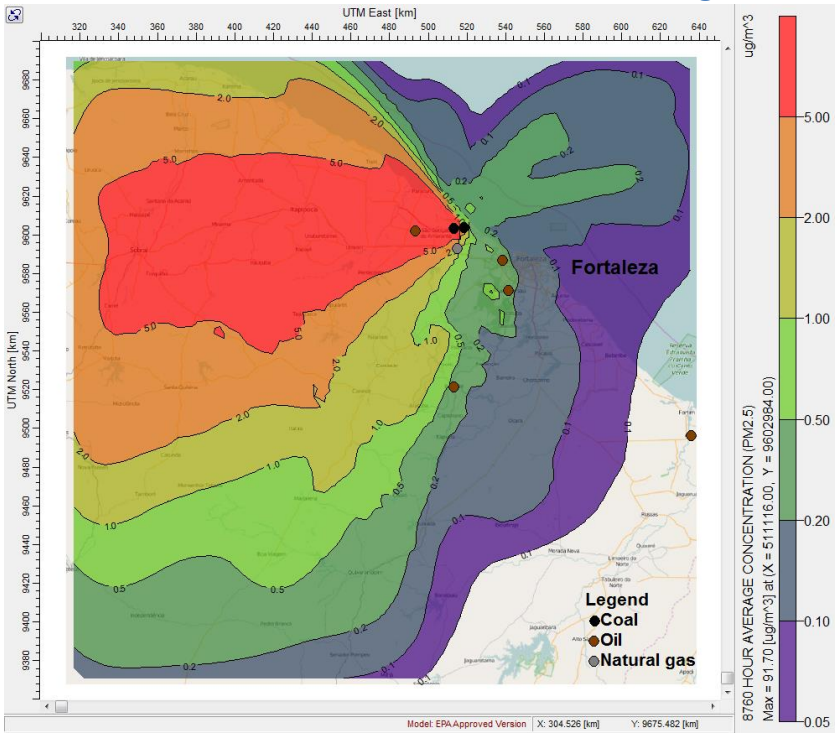

Figure 7.2. Annual mean $PM_{2.5}$ concentration for the 0.69 g/kWh standard

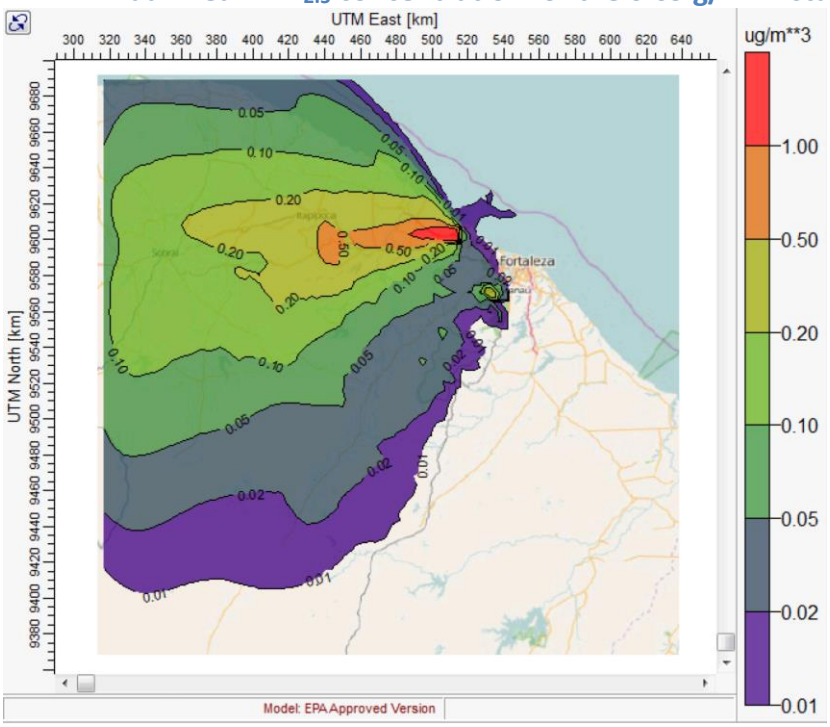

Figure 7.3. Annual mean $PM_{2.5}$ concentration for the 0.36 g/kWh standard

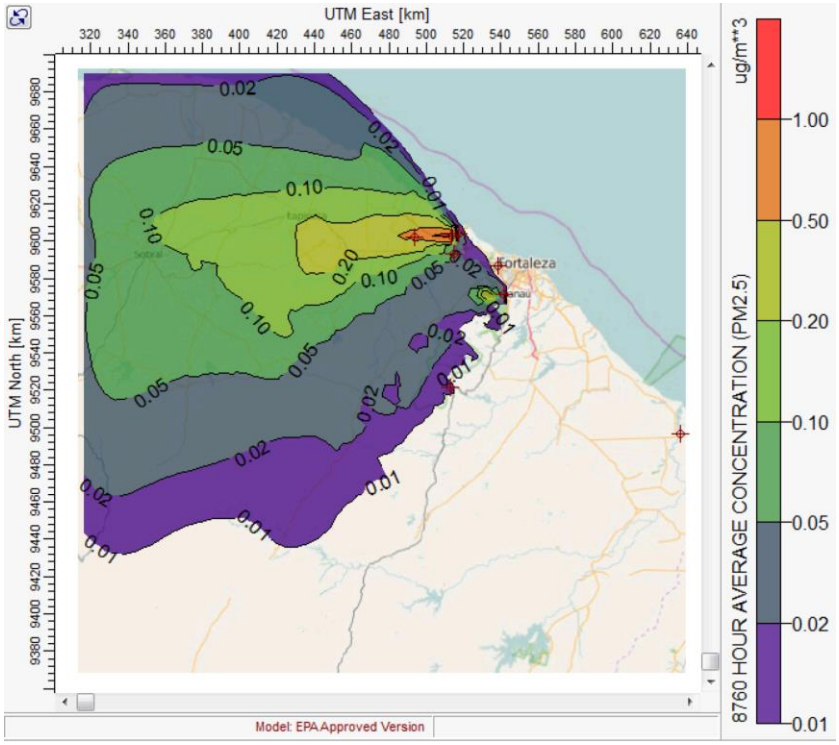

Figure 7.4. Annual mean $PM_{2.5}$ concentration for the 0.04 g/kWh standard

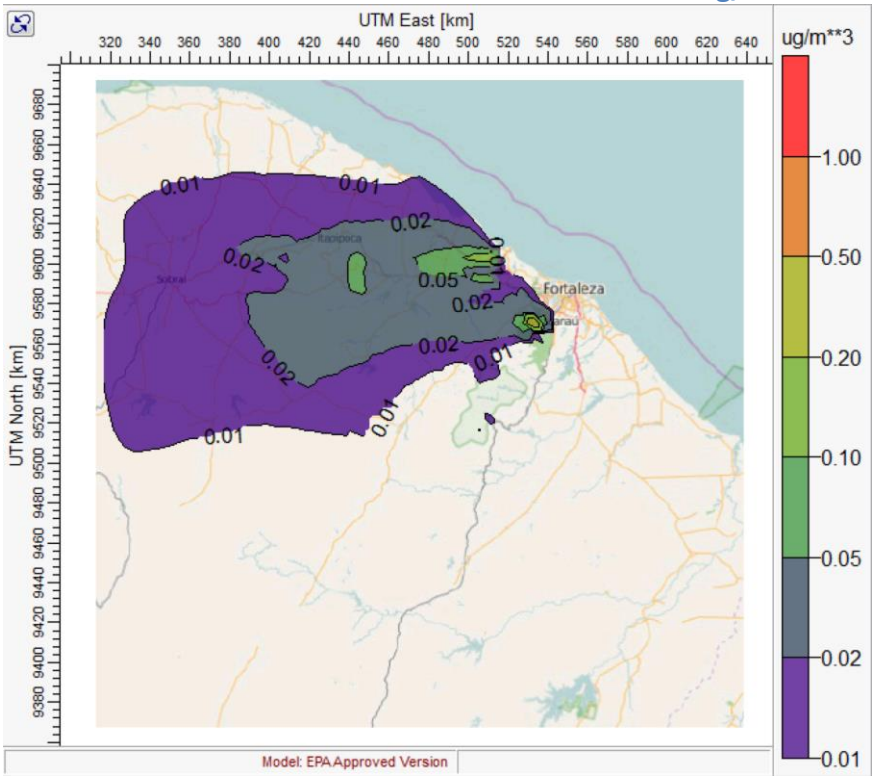

Figure 7.5. Peak 24-hr mean $PM_{2.5}$ conc. for the 28.15 g/kWh standard

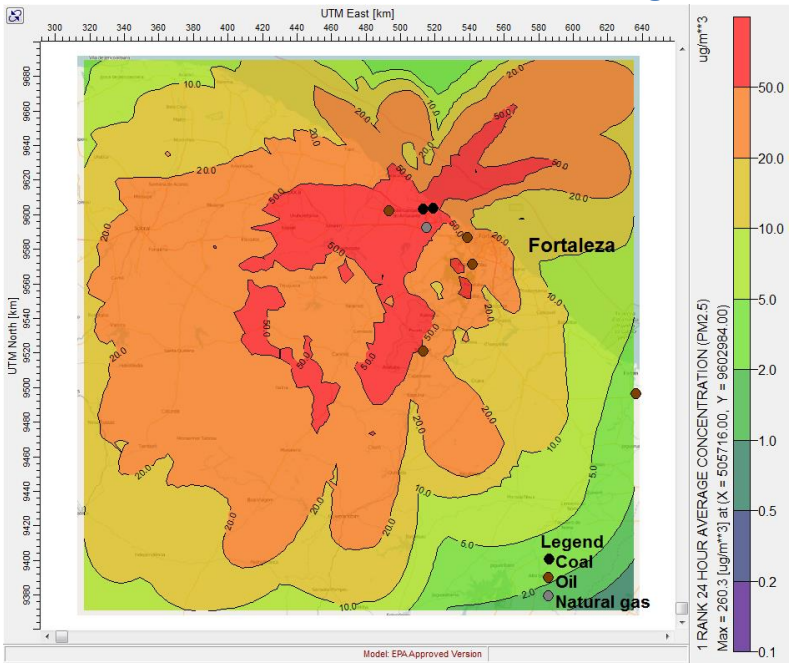

As expected, the annual mean $PM_{2.5}$ concentration plots indicate that the highest concentrations are closest to the coal power plants and disperse westerly, according to the direction of the wind rose for Fortaleza in 2015. The 2015 wind rose for Fortaleza, which displays the annual distribution of wind speeds and directions, are presented in the CALPUFF methodology.

CALPUFF results were checked as described in the air quality modeling validation section in the CALPUFF methodology. No abnormal concentrations or wind patterns were detected. A robustness test was performed by checking these results with concentrations obtained by converting PM_{10} to $PM_{2.5}$ after dispersion modeling. The mean difference in concentrations was approximately 1%, which is negligible.

Note that $PM_{2.5}$ concentration results from CALPUFF only consider power

plant emissions in the region surrounding Fortaleza; background concentrations were added in the next step to assess the impact of air quality improvements on human health outcomes.

7.1.3 Human health impacts

Using BenMAP, I estimated the expected human health benefits from tightening PM_{10} standards for the coal power plants in NE Brazil. Table 5 summarizes the expected reductions in disease incidence, monetized health benefits and control costs of changing the PM_{10} standard from the three scenarios considered.

Implementing Scenario 1 would prevent approximately 168 premature deaths per year and would reduce hospital admissions by over 16,000 cases per year, which is worth approximately 1,264 million 2015 US$ per year with our assumptions. Further tightening PM_{10} emission standards from 0.69 g/kWh to 0.36 g/kWh would prevent an additional 3.7 premature deaths along with 198 hospital admissions annually, which has a value of 26 million 2015 US$ per year with our assumptions. Further tightening PM_{10} to a stringent U.S. standards would prevent an additional 4.1 premature deaths and 194 hospital admissions, valued at 30 million 2015 US$ per year.

Table 7.3 presents the health outcomes for each scenario in terms of premature mortality in adults and infants, as well as hospital emissions. Table 7.4 presents the monetized health benefits, emission control costs and health benefits to emission control costs ratio for each scenario.

Table 7.3. Health outcomes of tightening PM standards

	Scenario 1: 28.15 ➔ 0.69 g/kWh	Scenario 2: 0.69 ➔ 0.36 g/kWh	Scenario 3: 0.36 ➔ 0.04 g/kWh
Health endpoint	**Disease incidence (reduction/yr)**	**Disease incidence (reduction/yr)**	**Disease incidence (reduction/yr)**
Mortality, All Cause (low to high estimate	162	3.6	4.1
Mortality, All Cause (infant)	6	0.1	0.1
Hospital Admissions, Cardiovascular	10,829	131	129
Hospital Admissions, Respiratory	5,428	66	65

Although premature deaths drive the value of health losses (they are 9 to 19 times larger than the value of hospital admissions), it is important to note that the number of hospital admissions is 46 to 97 times greater than the number of premature mortalities.

Based on the emission control costs estimated with the IECM model, the annualized cost of the emission control technology cost required to tighten the PM emission standard under Scenario 1 would be US $21.8 million for decreasing PM emissions by 247,993 metric tons of PM per year. Similarly, implementing Scenario 2 would cost an additional US $0.26 million annually for reducing emissions by an additional 2,980 metric tons of PM per year. Implementing the most stringent scenario (Scenario 3) would cost an additional US $0.60 million annually for reducing emissions by an additional 2,890 metric tons of PM per year.

Table 7.4. Health benefits and control costs of tightening PM standards

	Scenario 1: 28.15 ➔ 0.69 g/kWh	Scenario 2: 0.69 ➔ 0.36 g/kWh	Scenario 3: 0.36 ➔ 0.04 g/kWh
Health endpoint	**Health benefits (million U.S. 2015 $/yr)**	**Health benefits (million U.S. 2015 $/yr)**	**Health benefits (million U.S. 2015 $/yr)**
Mortality, All Cause (low to high estimate	$1,104	$24	$28
Mortality, All Cause (infant)	$39	$0.5	$0.5
Hospital Admissions, Cardiovascular	$90	$1.1	$1.1
Hospital Admissions, Respiratory	$31	$0.4	$0.4
Total (million U.S. 2015 $/yr)	**$1,264**	**$26**	**$30**
Emission Control Technology Cost	$21.8	$0.26	$0.60
Health Benefits / Emission Control Cost ratio	**58**	**101**	**50**

Although emission control costs are substantial, they are dwarfed by the expected health benefits of reducing PM pollution. Indeed, the value of expected health benefits is 58 times greater than the emissions control costs under Scenario 1, 101 times greater under Scenario 2, and 50 times greater under Scenario 3.

It is important to note that the cost of hospital admissions related to PM pollution are by themselves are 5.5 times greater than the emission control technology costs in Scenario 1, 5.6 times greater in Scenario 2, and 2.4 times greater in Scenario 3. The health benefits results were validated as described in the BenMAP Methodology chapter.

7.2 Health, climate and electricity grid impacts of high VRE penetrations

In this section, I present the health impacts, GHG emissions, storage requirements and electric grid stability implications of multiple high VRE scenarios and their sensitivity to dry year conditions and higher than forecasted electricity demand. The results are presented in the same order as for the previous question: electric grid simulations and emissions, air quality changes and human health benefits.

Table 7.5 summarizes the health benefits, climate benefits and electric system tradeoffs of moving from NE Brazil's 2015 electricity infrastructure to a 45% VRE scenario (2030 HR) and a 30% VRE scenario (2030 HT). The affects of a dry year on a 45% VRE scenario are also presented (2030 HR DY).

If NE Brazil transitions a 45% VRE (2030 HR scenario) instead of a 30% VRE (2030 HT scenario) in 2030, the required system capacity will be approximately 29% greater and the pumped storage load will be approximately 50% greater. The 45% VRE scenario also has a greater dump load requirements than the 30% VRE, which is approximately 4.6% of load, however this excess generation could be exported to provide electricity to other regions in Brazil. On the other hand, moving to a 45% VRE over a 30% VRE will provide at least US$266.9 million per year in health benefits and at least US$1,210 million per year in climate benefits. Additionally, the 45% VRE scenario is able to supply power as reliably as a 30% VRE, even during dry year conditions, as shown by all scenarios having an unserved load of approximately 0.0%.

Table 7.5. Health, climate and electricity grid tradeoffs

	2030 HR	2030 HR DY	2030 HT
System capacity (MW)	78,478	78,478	60,783
VRE (% of system capacity)	45	45	30
Pump storage load (GWh)	15,688	23,110	10,482
Unserved load (% of system load)	0.0	0.0	0.0
Dump energy (% of system load)	4.6	5.0	0.0
Health benefits low estimate (million 2015 US$/yr)	122	5	(145)
Climate benefits low estimate (million US$/yr)	(205)	(635)	(1,415)

7.2.1 Electric grid simulations

The NE Brazil electric grid operation was simulated in Plexos for two 2015 scenarios and for four future 2030 scenarios. The results include electric system generation and emissions, storage requirements and grid stability implications such as dump energy and unserved load. A summary of key metrics relating to electric grid generation and emissions, storage and stability is present in Table 7.6.

Key findings include that the pumped storage requirements are 150 % greater in the 2030 HR scenario than the 2030 HT scenario. Dry year conditions also increase pumped storage requirements by 47.3%, as shown by the pump load difference between the 2030 HR and 2030 HR DY scenarios.

Greater pump load requirements also increase total system load, but this increase is small: 2.5% more for the 2030 HR scenario than for the 2030 HT

scenario, and 3.5% more for the 2030 HR DY scenario than for the 2030 HR scenario.

Annual PM_{10} emissions are 295% greater in the 2030 HT scenario than the 2030 HR scenario. PM_{10} emissions are 151% greater in the 2030 HR DY scenario than the 2030 HR scenario, yet PM_{10} emissions are 48.8% less in the 2030 HR DY scenario than the 2030 HT scenario.

Likewise, annual CO_2 emissions are 200.0% greater in the 2030 HT scenario than the 2030 HR scenario. Although CO_2 emissions are 35.6% greater in the 2030 HR DY scenario than the 2030 HR scenario, CO_2 emissions are 47.5% less in the 2030 HR DY scenario than the 2030 HT scenario because the 2030 HR DY has approximately twice as much installed wind and solar capacity as the 2030 HT.

When considering grid stability implications, dump energy is 4.97% of system load in the 2030 HR scenario and 5.61% of system load in the 2030 HR DY scenario. This excess generation could potentially be exported to other regions, otherwise the generation needs to be curtailed or dissipated into heat, which is costly. By contrast, it is approximately under 0.01% in the 2030 HT scenarios. Unserved load increases from 0.07% of system load in the 2015 BC to 2.41% in the 2015 DY scenario, from 0.02% in the 2030 HR scenario to 0.77% in the 2030 HR DY scenario, and from 0.02% in the 2030 HT scenario to 5.54% in the 2030 HT DY 5.5% scenario. Note that unserved load is approximately the same in the 2030 HR and 2030 HT scenarios. Unserved load is an indication of electric grid instability, signaling either a partial or complete power supply disruption. Typically, the more developed a country is, the lower the threshold is for unserved load.

Table 7.6. Electricity simulations summary

Property	2015 BC	2015 DY	2030 HR	2030 HR DY	2030 HT	2030 HT DY 5.5%
System Capacity (MW)	29,570	29,570	78,478	78,478	60,783	60,783
VRE (% if system capacity)	30	30	45	45	30	30
System Load (GWh)	96,385	96,385	194,562	194,562	194,562	218,811
Pump Load (GWh)	10,861	11,064	15,688	23,110	10,482	23,104
Total System Load (GWh)	107,246	107,449	210,250	217,672	205,044	241,915
Generation (GWh)	107,207	105,158	219,896	227,094	205,017	229,800
Dump Energy (% of system load)	0.00	0.00	0.05	0.06	0.00	0.00
Unserved Load (% of system load)	0.00	0.02	0.00	0.01	0.00	0.06
PM_{10} emissions (metric ton/yr)	7,188	8,518	4,369	6,593	12,883	21,426
CO_2 emissions (metric ton/yr)	20,108,915	27,588,881	24,211,101	32,833,901	48,421,991	72,021,859

7.2.1.1 System load and generation

The system load and generation vary slightly between the 2015 BC and 2015 DY scenarios, as well as between the 2030 scenarios. When generation is less than load, there is unserved load, which is electricity demand that is not met. When electricity demand is not met, it results in partial interruptions to electricity supply to an area (brownout) or complete interruption to electricity supply to an area (blackout). When generation is greater than load, there is dump energy, which is energy that the electric system cannot use or store and must be curtailed or dissipated into heat.

Figure 7.6. Load and generation by scenario

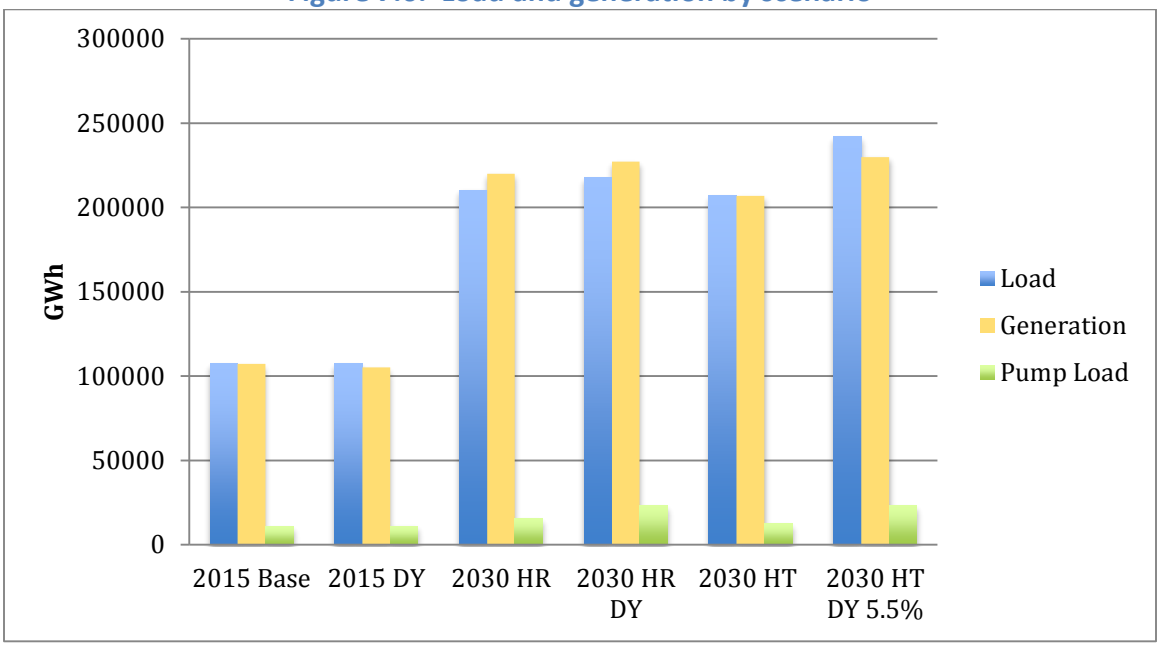

2015 BC - 2015 Base case
2015 DY – 2015 dry year. Same as 2015 BC, with dry year conditions.
2030 HR - 2030 Hydro-renewable.
2030 HR DY – 2030 Hydro-renewable dry year.
2030 HT – 2030 Hydro-thermal
2030 HT DY 5.5% – 2030 HT high demand dry year.

Figure 7.6 presents load and generation by scenario. The electric system load (including pumped storage load) varied between 107,246 GWh in the 2015 BC and 107,449 in the 2015 Dry year. In the 2030 scenarios, electric system load varied between 206,840 GWh in the 2030 HT scenario, 210,250 GWh in the 2030 Hydro-renewable scenario, 217,672 GWh in the 2030 Hydro-renewable dry year, and 241,915 GWh in the 2030 HT high energy demand dry year scenario.

Although the 2015 scenarios have the same 2015 hourly load curve (a total of 96,385 GWh), and the 2030 scenarios (except the high energy demand scenario) use the same 2030 hourly load curve (a total of 194,562 GWh), the actual system load and generation vary. The load varies between scenarios based on differences in pumped hydroelectric storage requirements because using pumped hydroelectric storage places additional load on the system. Generation varies because scenarios with high penetrations of VRE produce more intermit electricity, and at times that electricity cannot be used or storage and must be dumped.

The amount of dump energy and unserved load are presented in Figure 7.7. Generation was 2.1% less than total system load in the 2015 dry year scenario, and there was a total of 2.4% unserved load due to drought year conditions that reduced water availability for hydroelectric generation. In the 2030 high energy demand scenario, a total of 5.5% of electricity demand was not met. This is discussed in greater detail in the system sensitivity test section.

On the other hand, generation was greater than load in the 2030 HR and 2030 HR DY scenarios, resulting in 4.4% and 4.8% of total generation to be dumped in the 2030 HR and 2030 HR DY scenarios, respectively.

Figure 7.7. Dumped and unserved load by scenario

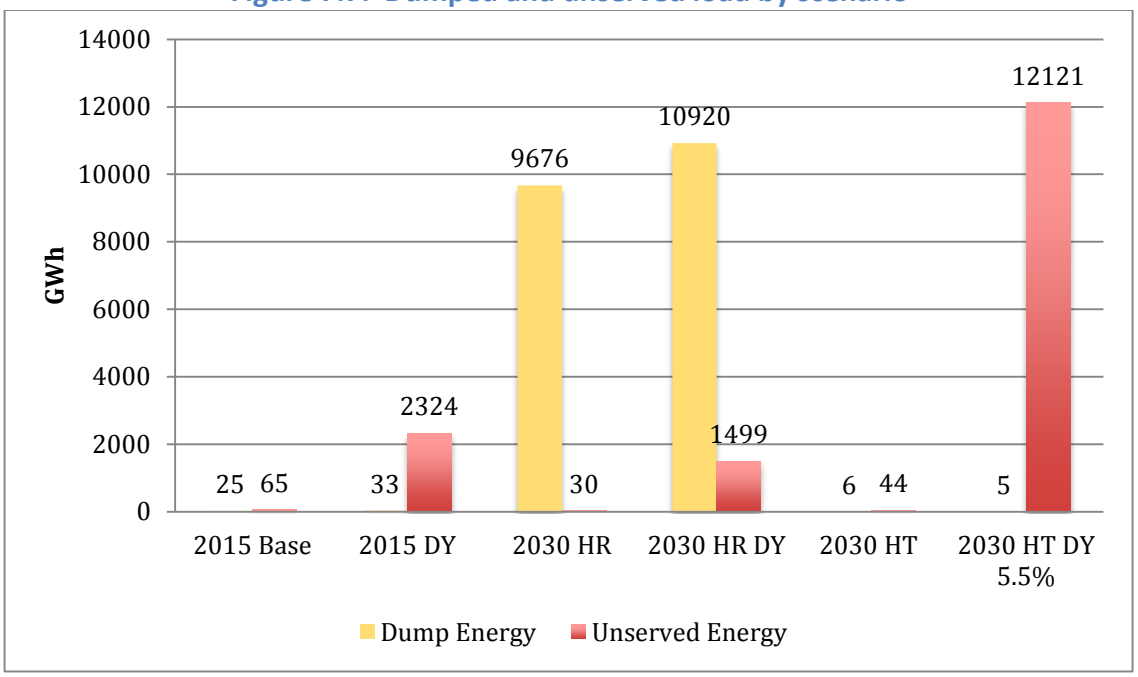

When there is dump energy, more energy storage is needed to shift load from when it is generated to when it is demanded. This mismatch is typical with high penetrations of VRE resources, which generate electricity intermittently and must be absorbed into the grid regardless of demand (Hart & Jacobson, 2011).

When there is unserved load, more flexible dispatch (load following and reserve) generators and/or energy storage resources are needed to balance load and generation. Unserved load typically happens when there are no resources available to generate additional electricity to match load and generation. In the scenarios with high penetrations of VRE and hydroelectric power plants, there are time periods with very little renewable generation that coincide with high demand, and when combined with decreased hydroelectric availability due to drought conditions, the system is occasionally unable to meet load.

In the scenarios considered, when the system capacity is comprised of 33% to 49% hydroelectric power plants, the unserved load in drought conditions highlights Brazil's dependence on hydroelectric energy and the electric grid vulnerability posed by changing precipitation patterns. It also suggests that if NE Brazil integrates higher penetrations of intermittent renewables than the current decadal electricity expansion plan, a greater system capacity of electricity generation and storage resources will be required to limit unserved demand.

7.2.1.2 PM_{10} and CO_2 Emissions

The PM_{10} and CO_2 emissions from an electric grid vary based on the amount of generation from thermal power plants, the type of power plants dispatched, and the emissions standards for each type of power plant. Figure 7.8 presents annual CO_2 emissions and Figure 7.9 presents annual PM_{10} emissions for the NE Brazil electric grid by scenario.

Figures 8 and 9 show how CO_2 emissions are lower in the 2030 HR and 2030 HR DY scenarios than in the 2030 HT and 2030 HT DY 5.5% scenarios. However, CO_2 emissions do not decrease when moving from the 2015 BC with 30% VRE to the 2030 HR scenario with 45% VRE; they actually increase by 20.4%. This highlights the difficulty of reducing GHG emissions when energy demand is increasing.

On the other hand, PM_{10} emissions decrease from the 2015 scenarios to the 2030 HR and 2030 DY scenarios. This is in part due to greater natural gas dispatch and less oil generator dispatch. As for CO_2 emissions, PM_{10} emissions increase from the 2015 scenarios to the 2030 HT and 2030 HT DY 5.5% scenarios.

Figure 7.8. CO_2 emissions by scenario

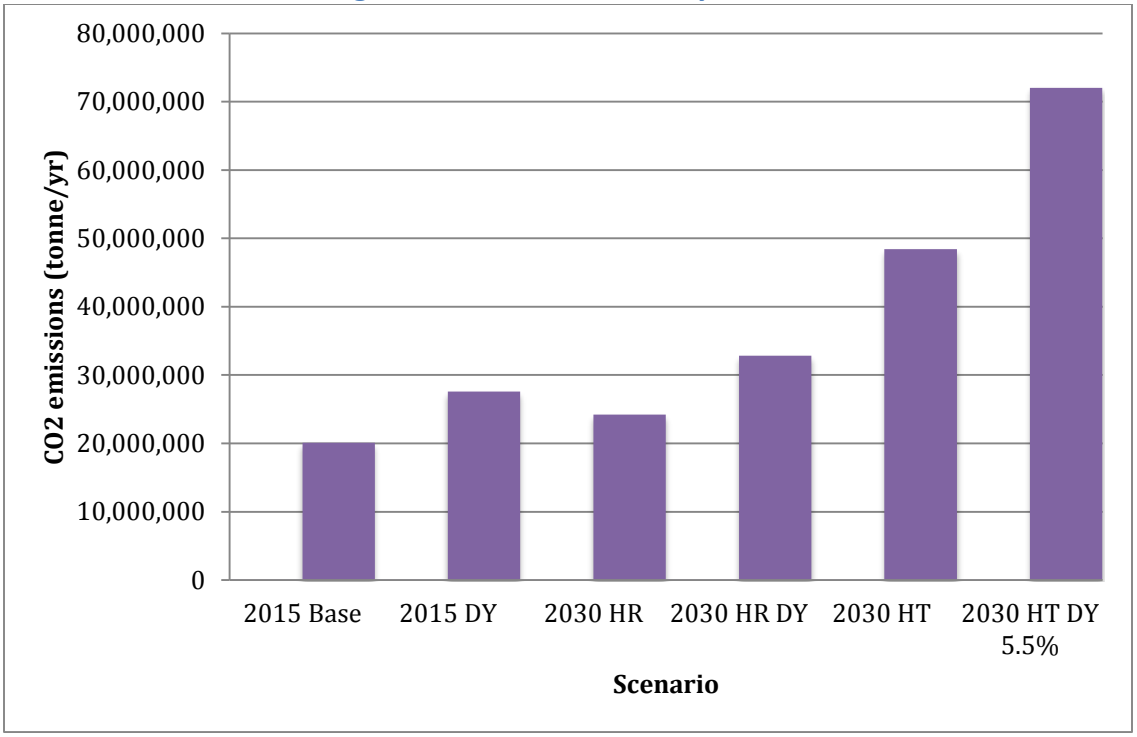

The electric grid annual emissions are 2.95 times greater in the 2030 HT scenario than the 2030 HR scenario because the 2030 HT scenario generates more electricity from coal and oil power plants than the 2030 HR scenario. Emissions from internal combustion (IC) engines and coal steam turbines (ST-Coal) are relatively much higher than combined cycle gas turbines (CCGT) and combined heat and power (CCGT-CHP).

To analyze the source contributions of emissions that produce the difference in emissions between the 2030 HR and 2030 HT scenario, Figure 7.10 presents the annual PM_{10} emissions by technology for the 2030 HR and 2030 HT Scenarios.

Figure 7.9. PM_{10} emissions by scenario

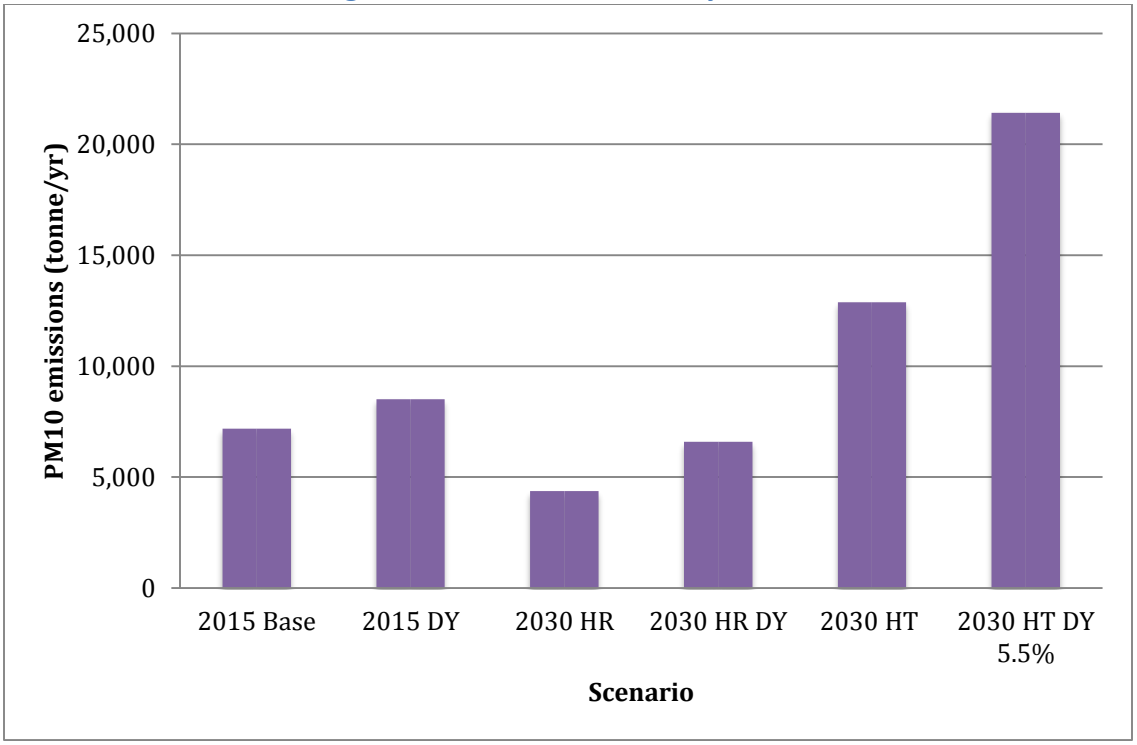

Figure 7.10. 2030 HR vs. 2030 HT emissions

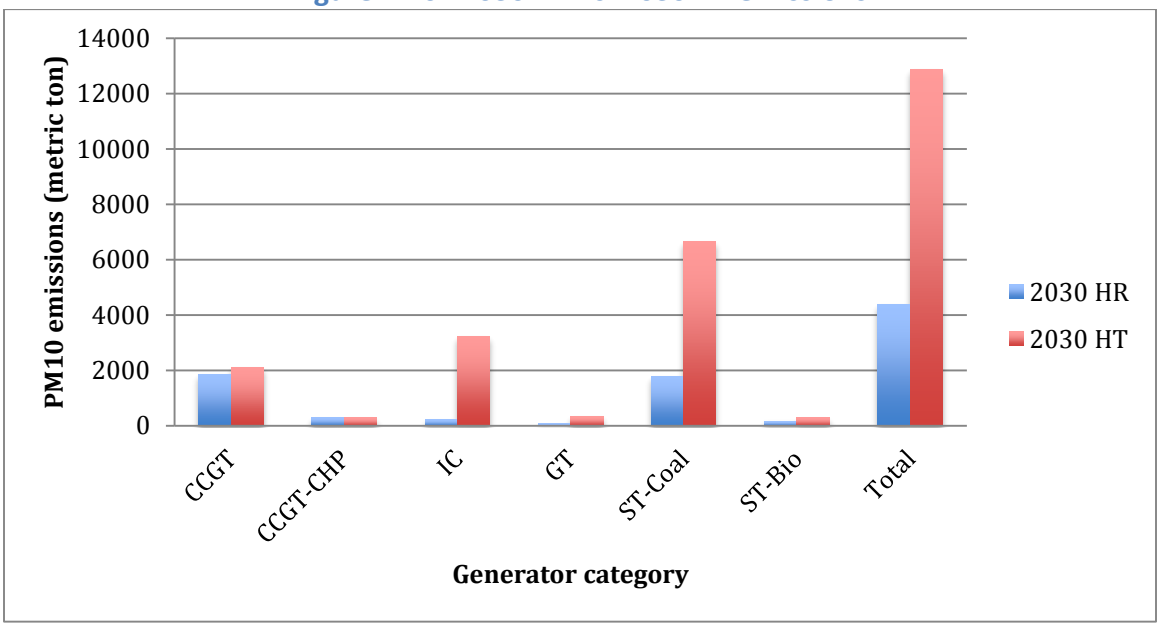

Notes: CCGT – combined cycle gas turbine; CCGT-CHP – combine cycled gas turbine with combined heat and power; IC – internal combustion engine; GT – gas turbine; ST-Coal – coal steam turbine; ST-Bio – biomass steam turbine

Emissions from coal power plants are 3.78 times greater in the 2030 HT scenario than the 2030 HR scenario because coal generation is 3.78 times greater in the 2030 HT scenario than the 2030 HR scenario. Similarly, emissions from oil power plants are 14.3 times greater in the 2030 HT scenario than the 2030 HR scenario because oil generation is 14.3 times greater in the 2030 HT scenario than the 2030 HR scenario. Figure 7.11 breaks down generation by generator category in the 2030 HR and 2030 HT scenarios.

Figure 7.11. 2030 Hydro-renewable vs. 2030 HT generation

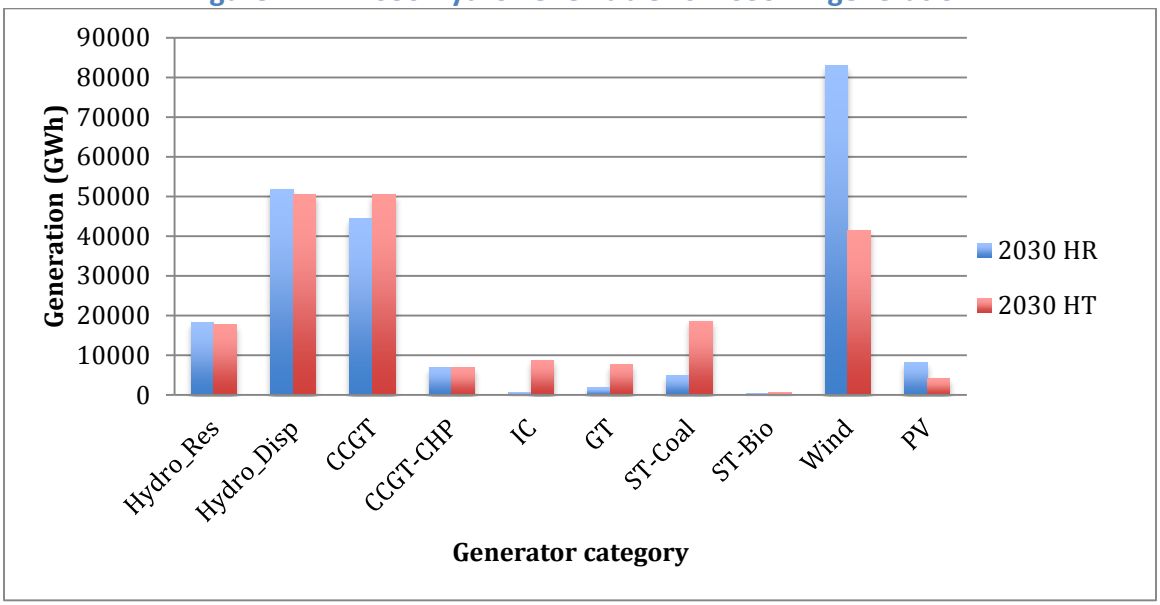

While the 2030 Hydro-renewable scenario has comparable hydroelectric and natural gas generation to the 2030 HT scenario, it has significantly more wind generation and significantly less oil and coal generation. This results in lower emissions in the 2030 HR scenario, but larger differences in load and generation

that lead to greater unserved load and dump energy when sufficient resources are not available to balance load and generation.

Tradeoffs between decreases in emissions, which lead to health and climate benefits, and increases in dump energy and unserved load, which lead to greater system generation and storage capacity requirements, are important to consider when assessing the benefits and costs of increasing VRE penetrations.

7.2.1.3 Electricity dispatch dynamics

Electric grid operators are responsible for matching electricity supply and demand on an hourly or sub-hourly basis (see the Plexos Methodology subsection on electricity supply and demand dynamics for a detailed discussion). This is essential for stabilizing the electric grid and for providing an uninterrupted power supply (i.e., for minimizing unserved load and the resulting brownouts or blackouts). Additionally, electric grid operators try to minimize dump energy because it affects their profits.

Figure 7.12 displays how coal (black) and biomass (light green) steam turbines along with hydroelectric power plants (dark and light blue) are used for baseload generation and run continuously. Wind (dark blue) and solar (green) generation are modeled as must take, leaving gas turbines and internal combustion engines to make up the difference between baseload generation plus intermittent generation and system load.

In two instances, on August 13, 2030 and August 17, 2030, electricity demand is exceptionally high and there is no available ramp up capacity to match

load and generation. In these cases, there is unserved load, shown in red. This week was selected because it is an extreme example of the weeks in the 2030 HT scenario with unserved load. In general, the 2030 HT scenario was able to continuously match supply and demand, as indicated the unserved load under 0.1% shown in Figure 7.7.

Figure 7.12. 2030 HT weekly dispatch

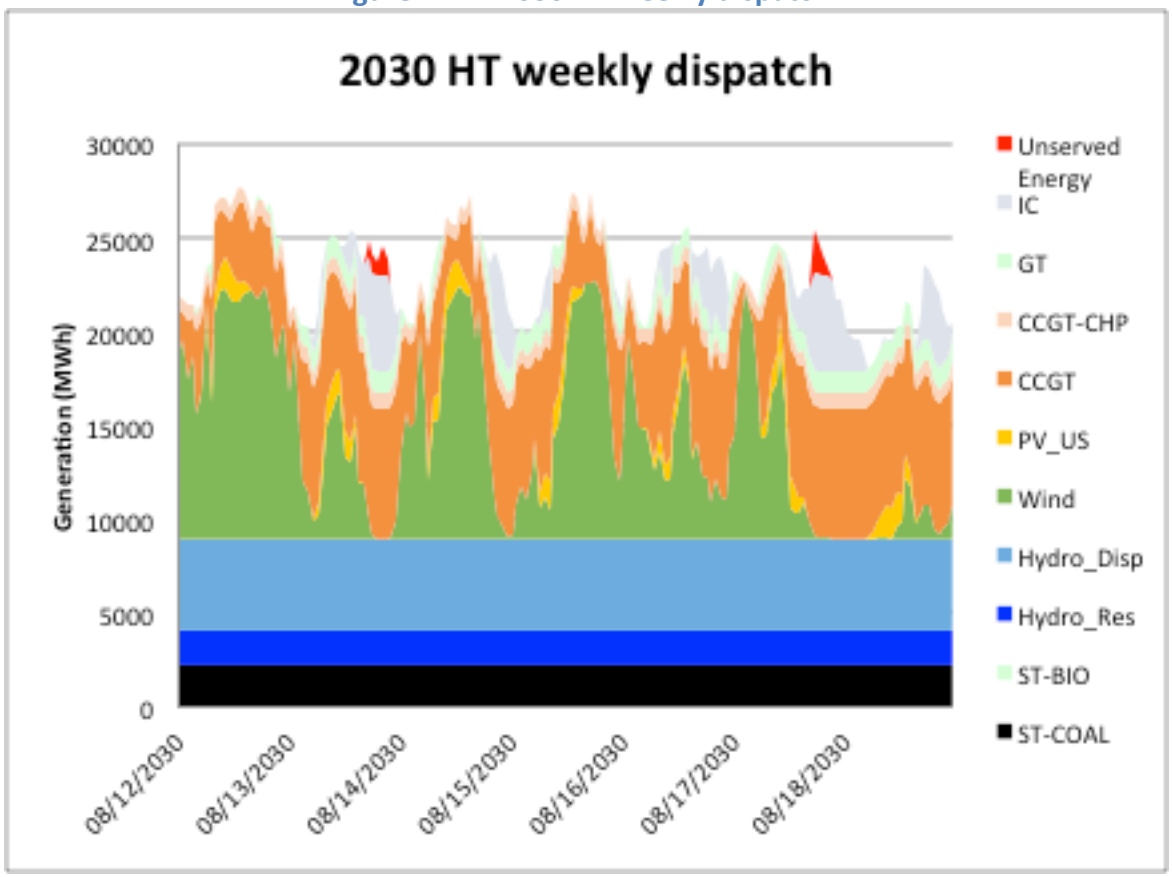

Figure 7.13 displays hourly dispatch for August 13, 2030. As wind and solar generation drop off, internal combustion engines ramp up to match load and generation. However, there is not enough capacity, which results in the unserved

load shown in red. During those hours shown in red, from 16:00 to 21:00, certain areas incurred interruptions to their power supply.

Figure 7.13. 2030 HT daily dispatch

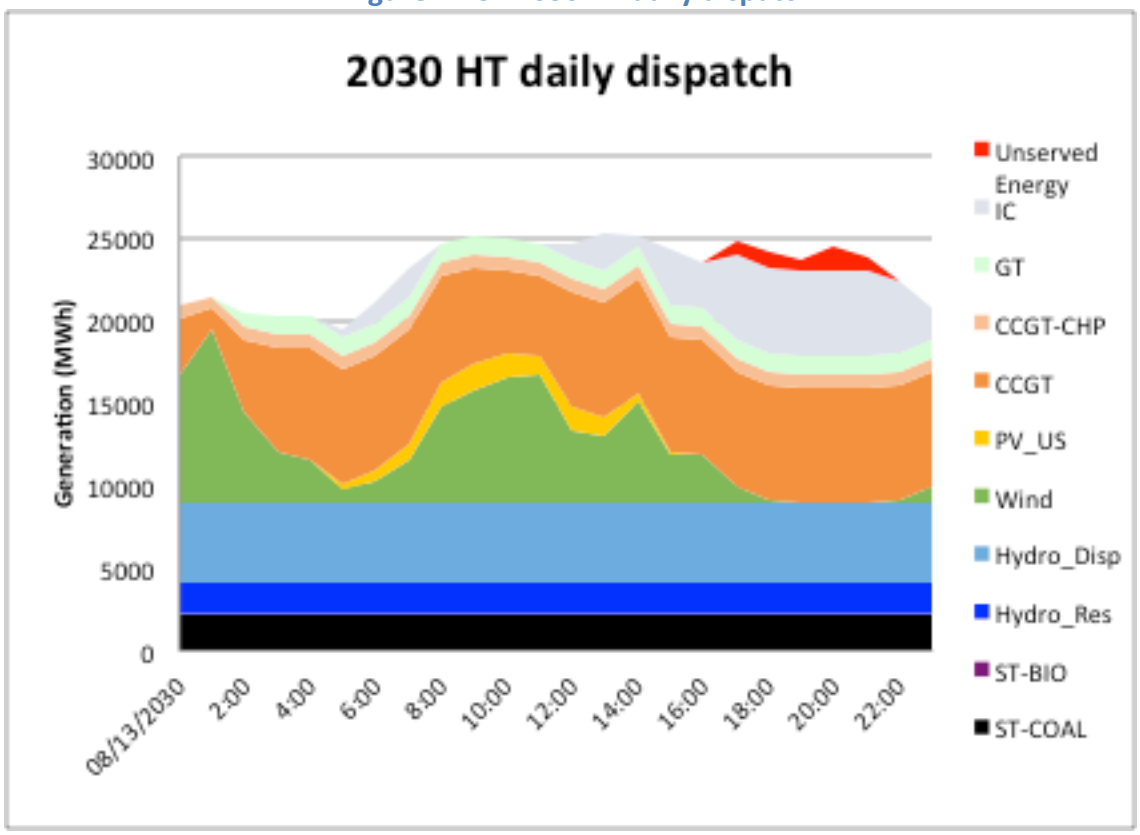

To assess potential electric grid dispatch operational challenges associated with high penetrations of intermittent renewables in NE Brazil, hourly unserved load and dump energy profiles were checked for the entire 2030 year for each scenario.

The first week of April 2030 had the highest amount of unserved load and fluctuating load for the 2030 Hydro-renewable dry year scenario, which is presented in Figure 7.14. Balancing load and generation during this week is

exceptionally difficult because large quantities of wind energy are generated at the beginning and end of the week, creating excess energy that needs to be dumped. When the wind energy drops off substantially in the middle of the week, it causes all thermal generators to be dispatched, which is still not enough to match generation and load. The unserved load is shown in red.

Figure 7.14. 2030 Hydro-renewable dry year weekly dispatch

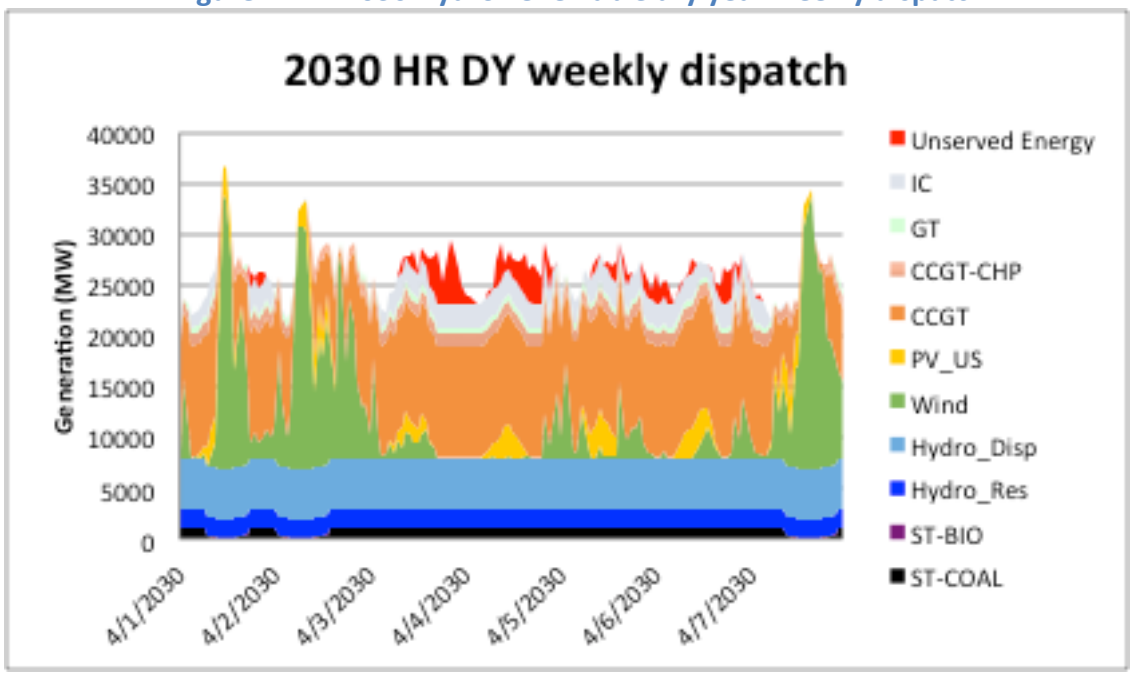

Figure 7.15 displays only the thermal generator dispatched for the same week in April 2030. Due to the very high wind generation in the beginning and end of the week, thermal generation is drastically reduced, resulting in a ramp down of all load following and baseload thermal generators. Thermal generators must be quickly ramped up the following day when there is little wind energy, and a shortage of capacity produces substantial unserved load, shown in red.

Despite days where wind and solar energy generation were low and unserved load was high, the 2030 Hydro-renewable dry year has less than 0.7% unserved load as a percentage of total load. This is because natural gas generators were added when developing the 2030 Hydro-renewable scenario to keep unserved load under 1.0% of total load.

Figure 7.15. 2030 Hydro-renewable dry year thermal generator dispatch

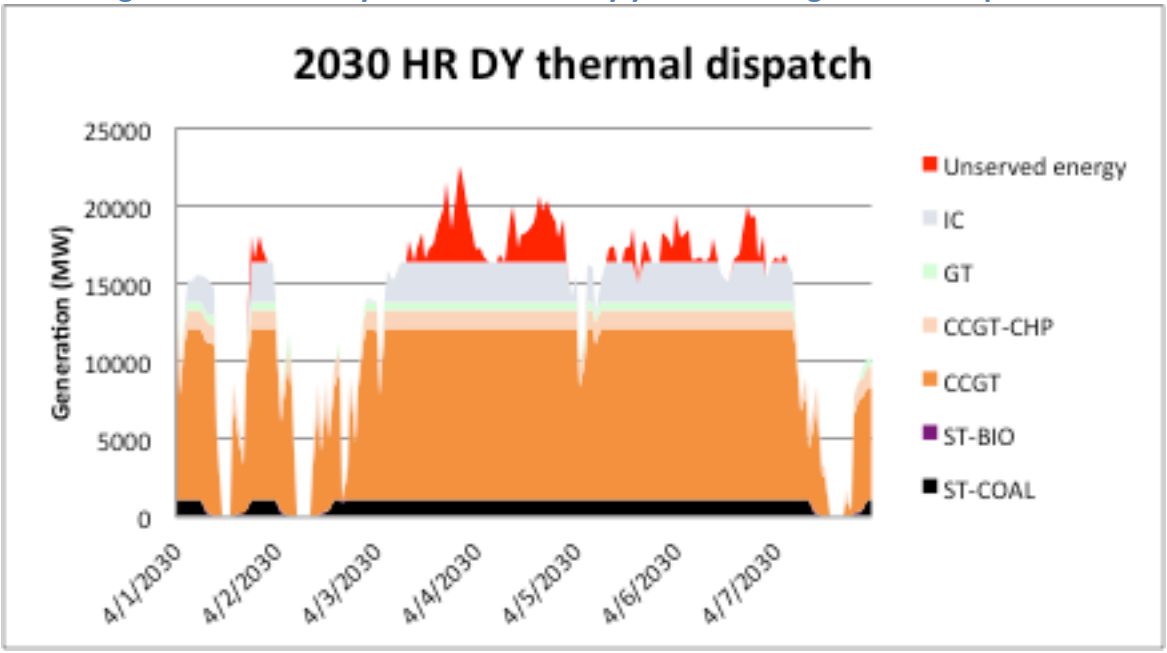

The implications of these varying electricity dispatch dynamics are summarized the set of metrics summarized in Electricity supply and demand dynamics section of the Plexos Methodology. While the 2030 HT scenario has lower pumped load requirements, and accordingly less total system load and generation and storage capacity requirements, it has greater emissions. Somewhat

surprisingly, the 2030 HR scenario is fairly resilient to extreme dry year conditions, which is discussed in the following section on system sensitivity tests.

7.2.1.4 System sensitivity tests

Sensitivity tests were run to see how electric system reacts to changes in precipitation patterns (dry year conditions) and higher than forecasted electricity demand and the consequences for health, climate and grid stability implications.

7.2.1.4.1 System sensitivity to dry year conditions

During dry year conditions, there is less hydroelectric generation due to lower water availability, which required more load following generators to be dispatched to match load and generation. Hydroelectric generation decreased by 12.8% between the 2015 BC and 2015 DY scenarios, 14.3% between the 2030 Hydro-renewable and the 2030 Hydro-renewable dry year scenarios, and 14.0% between the 2030 HT and 2030 HT high demand dry year scenarios.

When there is less hydroelectric generation, natural gas and oil power plants are dispatched more frequently to make up most of the difference between load and generation. In 2015, natural gas generation was almost identical in the baseline and dry year scenarios. However oil generator dispatch increased by 46.0% from the 2015 baseline to the 2015 dry year scenarios, leading to higher system emissions. Figure 7.16 displays PM_{10} emissions by generator category for the 2015 scenarios, which are 18.5 percent greater in the 2015 DY than the 2015 BC.

Figure 7.16. 2015 BC and 2015 DY emissions

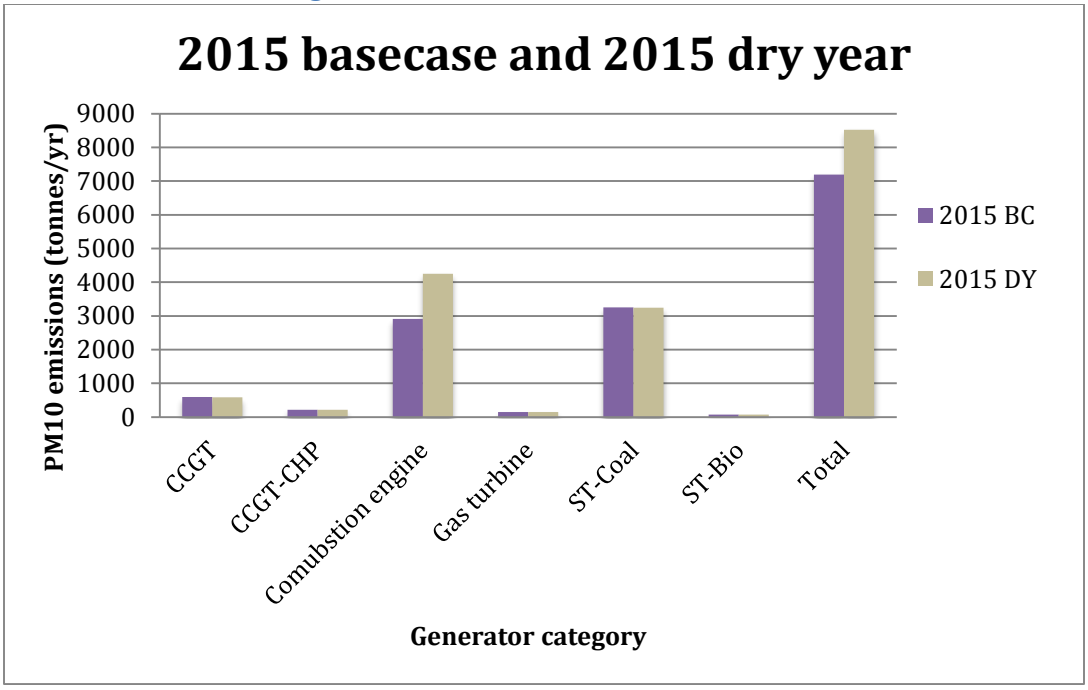

Emissions were also greater under dry year conditions in the 2030 scenarios. As for the 2015 dry year scenario, the main contribution to higher emissions is the need to dispatch natural gas and oil generators more frequently to balance load and generation because of a shortage of hydroelectric availability.

Natural gas generation increased 23.4% and oil generation increased 87.1% from the 2030 HR scenario to the 2030 HR DY scenario. The large increase in oil generation indicates that the natural gas generators were reaching their load following capacity in the dry year scenarios. This resulted in total system emissions that were 50.9% greater in the 2030 HR DY scenario than the 2030 HR scenario, as shown in Figure 7.17.

Figure 7.17. 2030 HR vs. 2030 HR dry year emissions

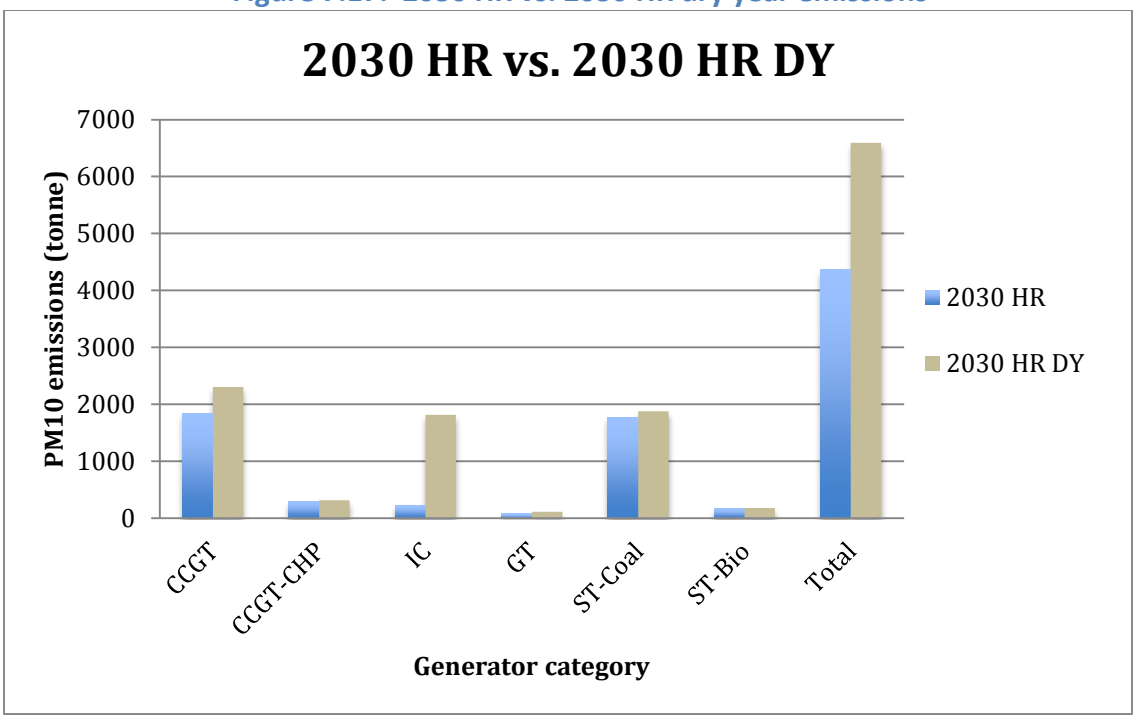

Dump energy and unserved load also increase under dry year conditions because there is less hydroelectric availability to supply additional generation when generation is less than load, and less pumped storage availability to absorb excess generation. While energy increased minimally from 0.03% of load in the 2015 BC to 0.04% in the 2015 DY scenario, the unserved load increased from 0.6% to 2.4% of load. Similarly in the 2030 scenarios, dump energy increased from 5.0% of load in the 2030 HR scenario to 5.6% in the 2030 HR DY scenario, and unserved load increases from 0.01% of load in the 2030 HR scenario to 0.8% in the 2030 HR DY scenario.

The increase in unserved load and dump energy in dry year conditions is primarily due to a shortage of hydroelectric potential, which can be quickly ramped

up or down to balance load and generation and reduce the risk of unserved load and dump energy.

Dry year conditions also increase GHG emissions. As shown in Figure 7.8, CO_2 emissions increase 37.2% when moving from the 2015 BC to the 2015 Dry year scenario, and CO_2 emissions increase 35.6% when moving from the 2030 HR to the 2030 HR DY scenario.

Although dry year conditions increase PM_{10} and CO_2 emissions, dump energy and unserved load only increase slightly, implying that the 2030 HR scenario is fairly resilient to dry year conditions.

7.2.1.4.2 System sensitivity to higher load than forecasted

As a second sensitivity test, I assessed what happens to emissions and grid stability when system load increased by 5.5% annually (2030 HT DY 5.5% scenario) from 2015 to 2030 as opposed to the 4.77% forecasted by Torrini *et al.* (2016).

Natural gas generation increased 16.0% and oil generation shot up 274.0% between the 2030 HT and the 2030 HT DY 5.5% scenarios. This indicates that while there is sufficient natural gas capacity in the 2030 HT scenario to not need to dispatch oil generators often, if energy demand is higher than expected and there are dry year conditions, there will be a heavy reliance on oil power plants.

Emissions increase substantially between the 2030 HT and the 2030 HT dry year 5.5% energy demand increase scenarios. The main cause is that if electricity demand increases annually by 5.5% as opposed to 4.77% from 2015 to 2030, the annual load in 2030 totals 218,811 GWh instead of 194,562 GWh. This 12.5%

increase in total annual load forces more diesel generators to be dispatched, which is the only option once all hydroelectric, renewable, coal and natural gas resources have been dispatched.

Figure 7.18 presents annual PM_{10} emissions by generator category for the 2030 HT and 2030 HT DY 5.5% scenarios. PM_{10} emissions are a whopping 166.3% greater in the 2030 HT DY 5.5% scenario.

Figure 7.18. 2030 HT vs. 2030 HT dry year 5.5% energy demand

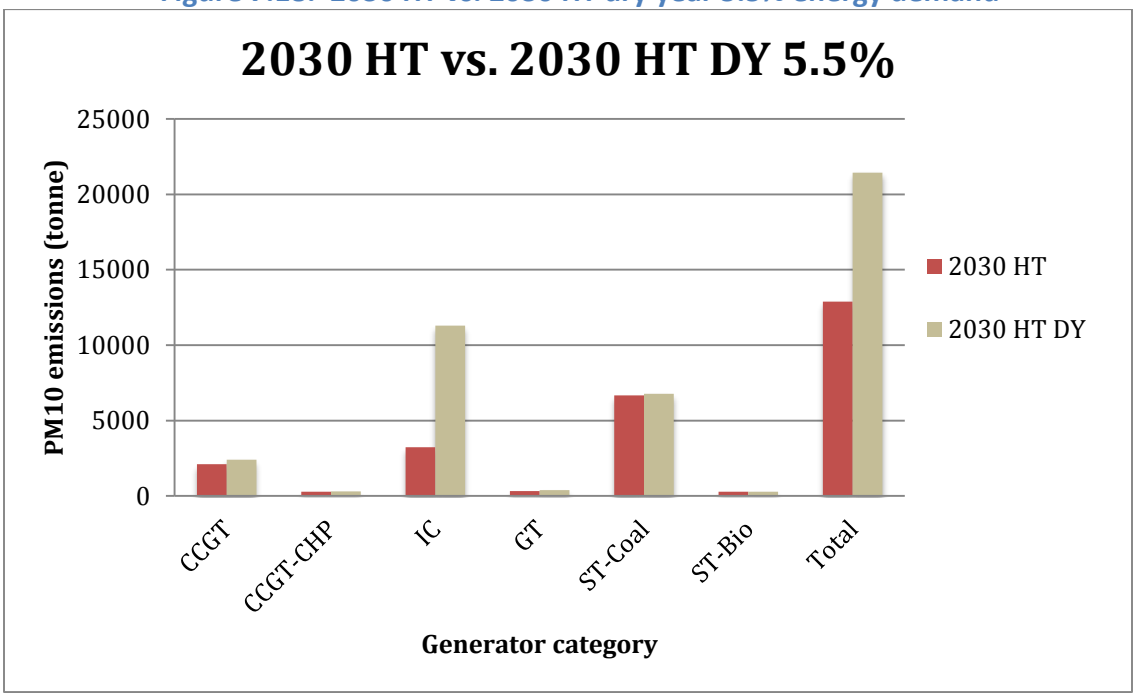

As expected, higher energy demand and dry year conditions also increase CO_2 emissions, which are 48.7% greater in the 2030 HT DY 5.5% scenario compared to the 2030 HT scenario.

Dump energy barely changes between the 2030 HT and 2030 HT DY scenarios because there is sufficient load following capacity to ramp down thermal

and hydroelectric generation when VRE generation increased. Dump energy decreases from 3E-5% in the 2030 HT scenario to 2E-5% in the 2030 HT HD DY scenario.

On the other hand, unserved load increases substantially from 0.02% of load in the 2030 HT scenario to 5.5% of load in the 2030 HT DY 5.5% scenario. This highlights the vulnerability of Brazil's electric grid to higher than expected electricity demand and to drought conditions.

The 2030 HT DY 5.5% scenario represents a worst-case emissions scenario. However, as shown in Table 7.1, if the Porto do Pecem power plants were to use the national standard for particulate matter rather than the lower standard paid for by funding form the Brazilian Development Bank, annual PM_{10} emissions of the NE Brazil electric system would be more than an order of magnitude worse.

7.2.2 Air quality changes

Table 7.7 summarizes the peak annual mean PM_{10} air quality concentration for each scenario, which represents the grid cell with the highest annual mean PM_{10} concentration due to power plant emissions alone. When averaging across a large air quality modeling domain, high concentrations are diluted by the low concentrations in areas outside the emission plume pathway. I plotted the annual mean PM_{10} concentration for each grid cell in Figure 7.19-Figure 7.21.

The 2030 HT scenario has the highest peak annual mean concentrations in each region and the 2030 HR has the lowest peak annual mean concentrations in each region. This is expected because the 2030 HT scenario has the largest amount

of thermal generation and the 2030 HR has the smallest amount of thermal generation. The peak annual mean PM_{10} concentrations are 3.07 µg/m^3, 1.20 µg/m^3, and 0.66 µg/m^3 for Fortaleza, Recife and Salvador respectively.

Table 7.7. Peak annual mean air quality concentration (µg/m^3) $PM_{2.5}$

Region	2015 (PM_{10} µg/m^3)	2030 HR (PM_{10} µg/m3)	2030 HR DY (PM_{10} µg/m^3)	2030 HT ($PM_{2.5}$ µg/m^3)
Fortaleza	0.91	0.74	0.78	3.07
Recife	0.98	0.37	0.59	1.20
Salvador	0.19	0.19	0.43	0.66

The 2030 HT scenario has a higher peak annual mean PM_{10} concentration than the 2015 BC in all grid cells, which indicates that health outcomes will likely worsen when moving from the 2015 BC to the 2030 HT scenario. On the other hand, the 2030 HR scenario has a lower peak annual average PM_{10} concentration than the 2015 BC in all grid cells, indicating that health outcomes will likely improve when moving from the 2015 BC to the 2030 HR scenario.

When considering dry year conditions, the 2030 HR DY scenario has lower peak annual mean $PM_{2.5}$ concentrations than the 2015 BC in the Fortaleza and Recife regions, but not in Salvador. Indeed, Salvador receives fewer emissions than Fortaleza and Recife, because Fortaleza has two large coal power plants running almost continuously and Recife has large load following power plants that are dispatched frequently. By contrast, Salvador has a number of oil power plants that are dispatched more frequently during dry year conditions because there is a greater need for oil generators when there is less precipitation and hydroelectric availability.

The annual hourly mean PM_{10} concentration for each grid cell, in each region and scenario are displayed in Figure 7.19-Figure 7.21. Note that the discussion above is for the peak annual mean (i.e., the grid cell that has the highest annual hourly mean for a given region and scenario.

The annual mean PM_{10} concentration results are presented by region, displaying how air pollutant concentrations change under different scenarios. The figures show that annual average hourly PM_{10} concentrations are lower in the 2030 HR scenario than in the other scenarios in each region, and that the annual average PM_{10} concentrations are greater in the 2030 HT scenario than in the other scenarios in each region.

As expected, the epicenters of higher PM_{10} concentrations typically correspond with the locations of power plants. Additionally, the higher PM_{10} concentrations in the 2030 HT scenario affect a larger area in all regions. This makes sense because even though PM_{10} concentrations diminish as they are transported, when higher quantities of emissions are released, there are higher concentrations in the emission plume pathways.

The shape of the emission plumes is fairly similar between scenarios in a given region. However, there is a small yet noticeable difference in the shape of the emissions plume in Fortaleza during the 2030 HR DY scenario (see Panel C of Figure 7.19), because I used dry year meteorological conditions for the dry year simulations. As discussed in CALPUFF Methodology chapter, the dry year meteorological conditions are from 2012, which was the driest year in NE Brazil in the available dataset from 1983 to 2015. As seen in the 2012 wind rose for

Fortaleza, which is presented in the Air quality validation section of the CALPUFF Methodology chapter, the 2012 dry year meteorological conditions have a slightly stronger southeasterly contingent than the 2015 meteorological conditions. This causes a slight northwest shift in the emission plume pathway.

To compare the peak 24-hour average PM_{10} concentration for each grid cell with the annual average, peak 24-hour PM_{10} concentration plots for the 2015 BC (Fortaleza region only) and the 2030 HT scenario (all regions) are displayed in Figure 7.22.

Note that the scale is five times greater in the peak 24-hour average plots than the annual average plots. The emission plume plots are much more irregular for the peak 24-hour average plots, which usually occur during high electricity demand and low VRE generation. In these circumstances, most of not all thermal generators are dispatched, which creates new epicenters of high PM concentrations. Additionally, the emission plumes combine to affect a larger portion of our study domain.

Figure 7.19. Annual mean PM_{10} concentrations in Fortaleza for each scenario

Panel A. 2015 BC

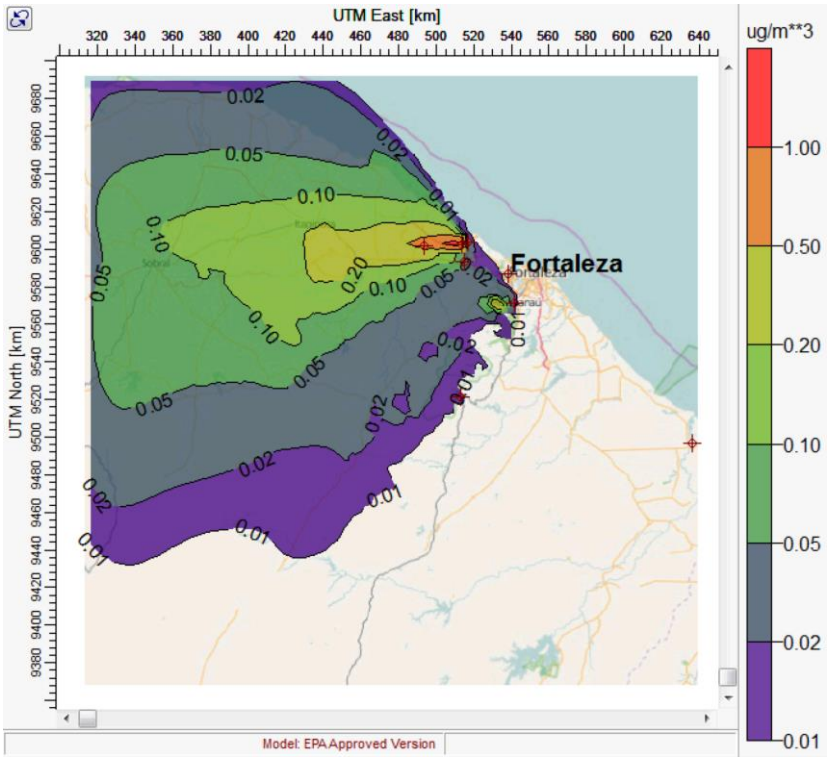

Panel B. 2030 Hydro-renewable

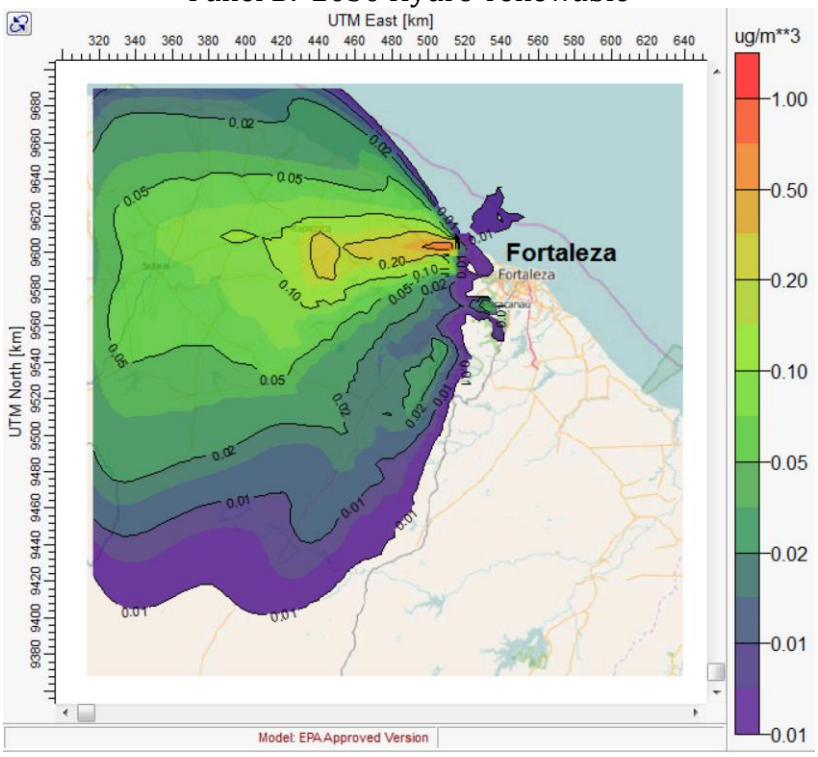

Panel C. 2030 Hydro-renewable dry year

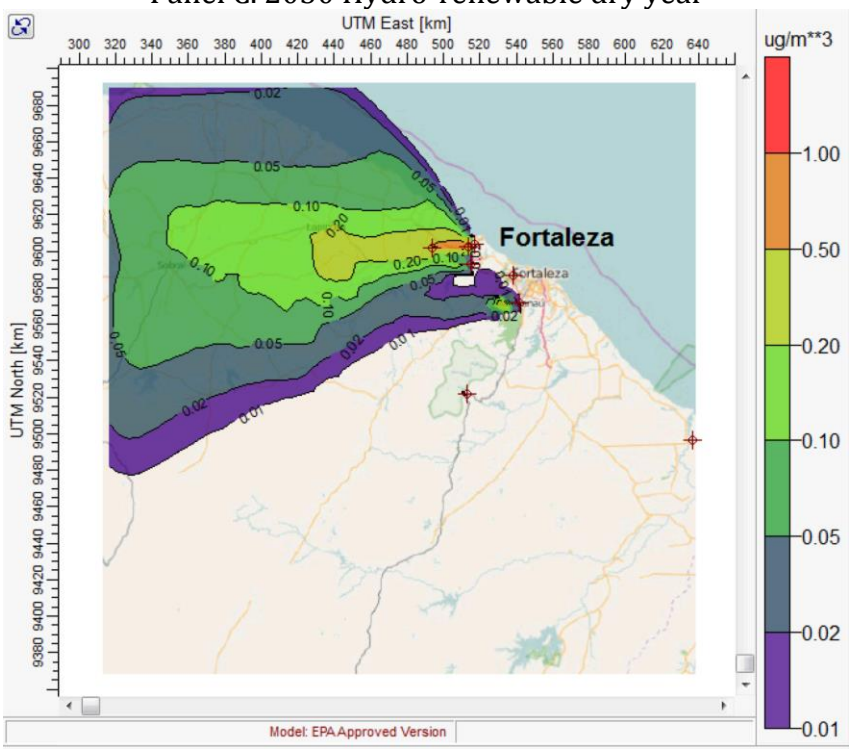

Panel D. 2030 Hydro-thermal

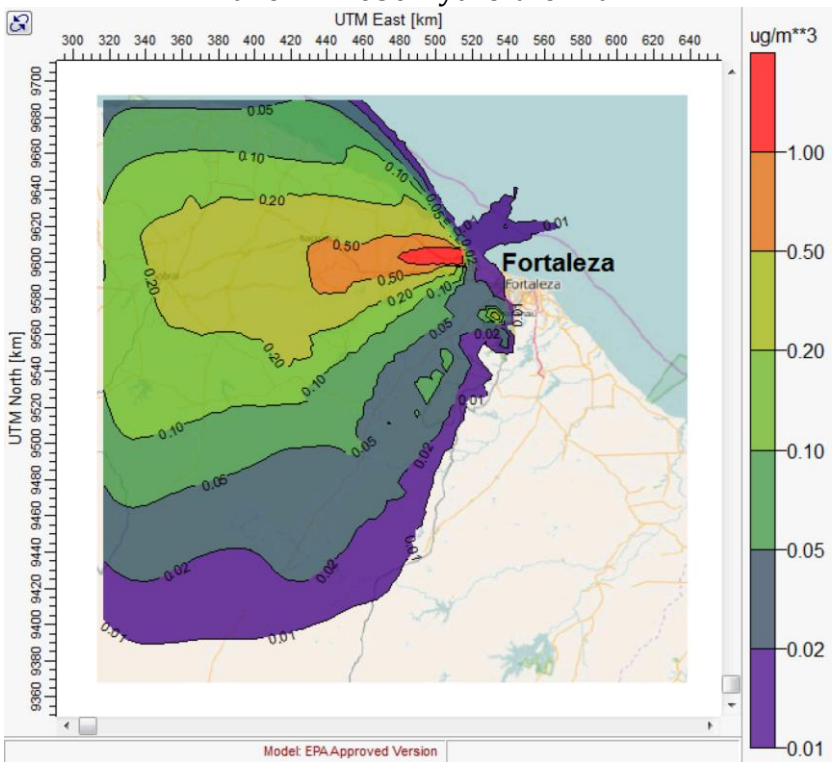

Figure 7.20. Annual mean PM_{10} concentrations in Recife for each scenario

Panel A. 2015 BC

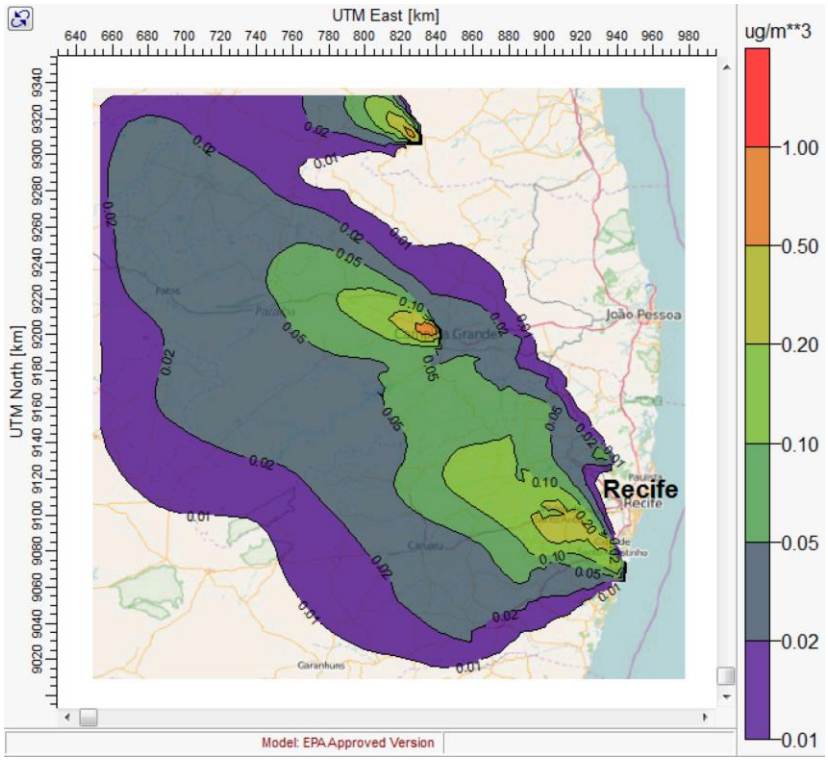

Panel B. 2030 Hydro-renewable

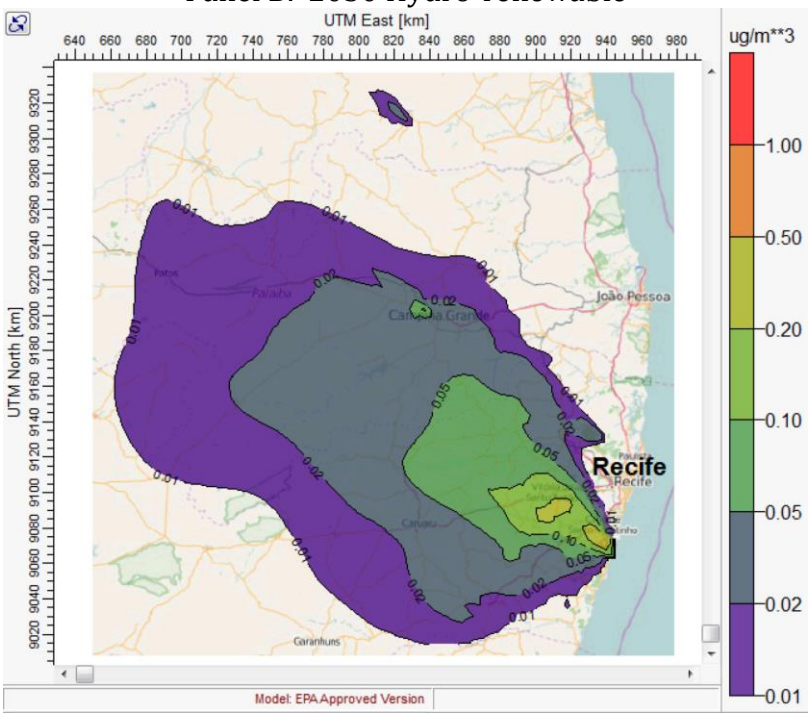

Panel C. 2030 Hydro-renewable dry year

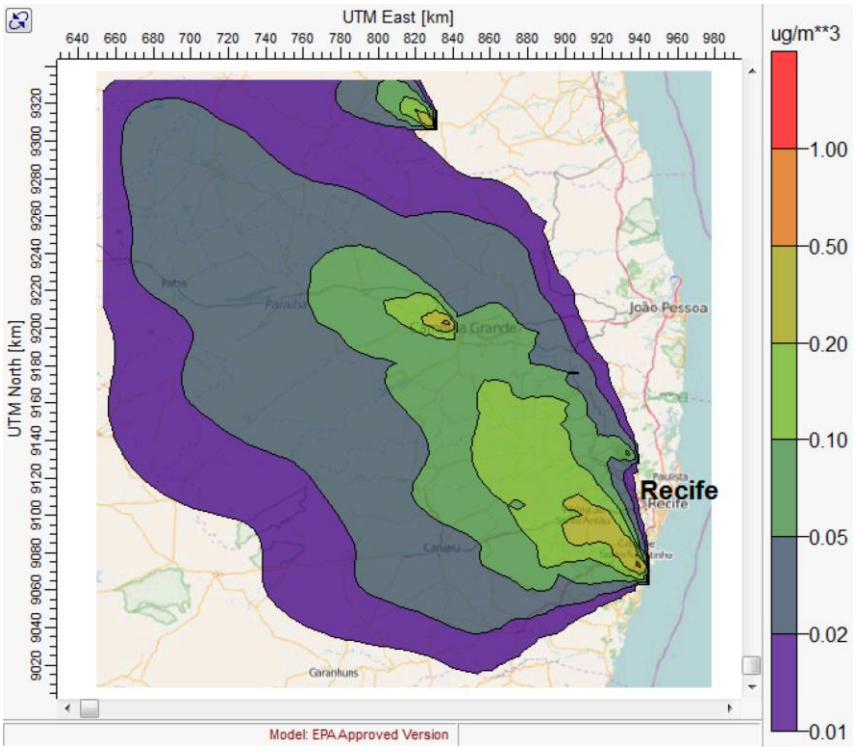

Panel D. 2030 Hydro-thermal

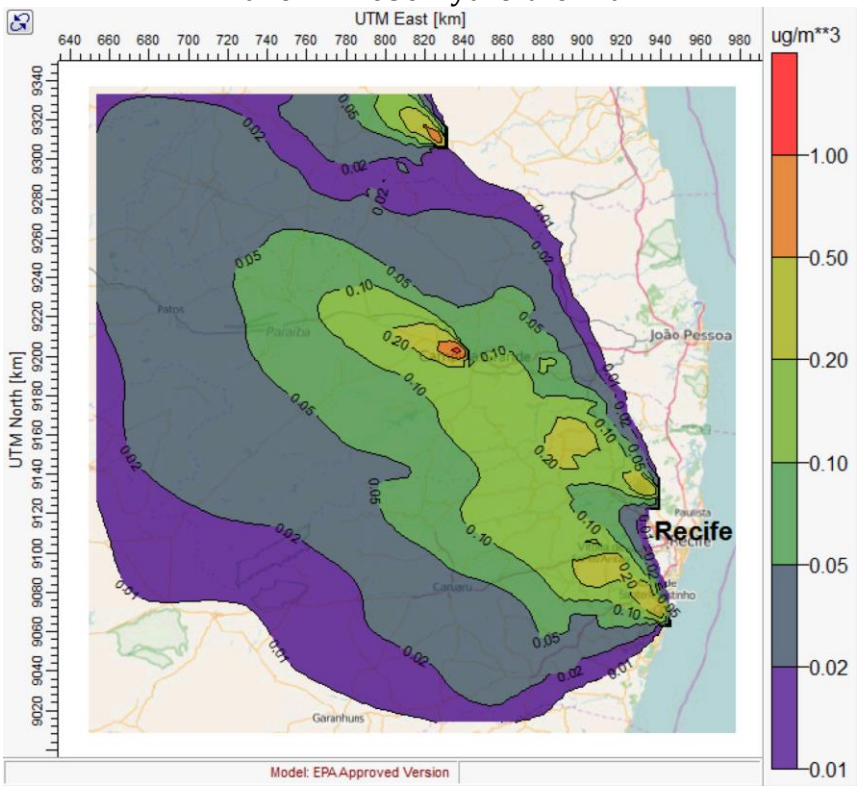

Figure 7.21. Annual mean PM_{10} concentrations in Salvador for each scenario

Panel A. 2015 BC

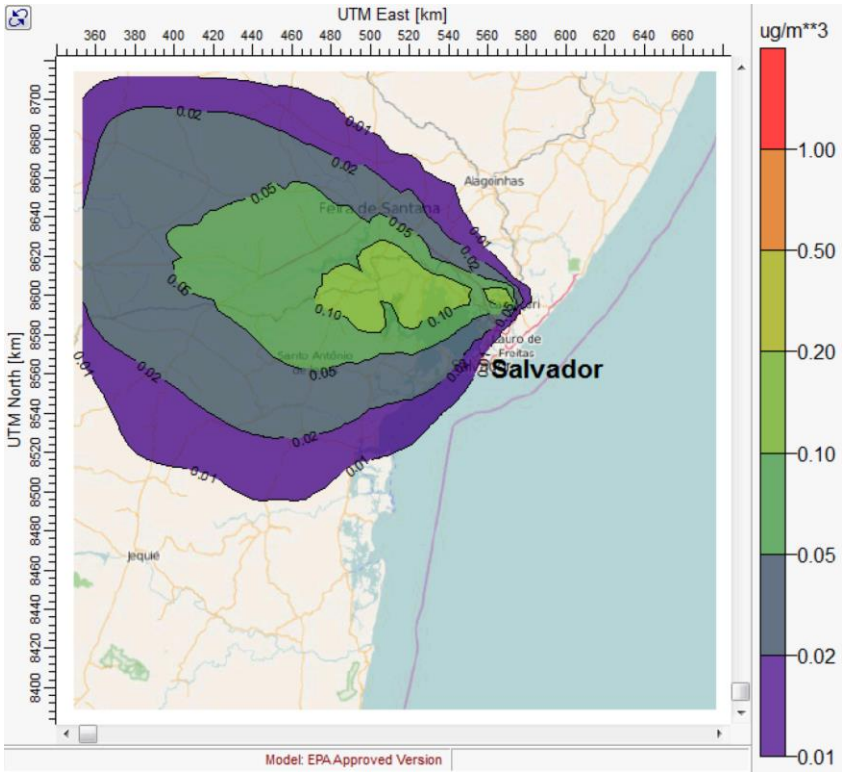

Panel B. 2030 Hydro-renewable

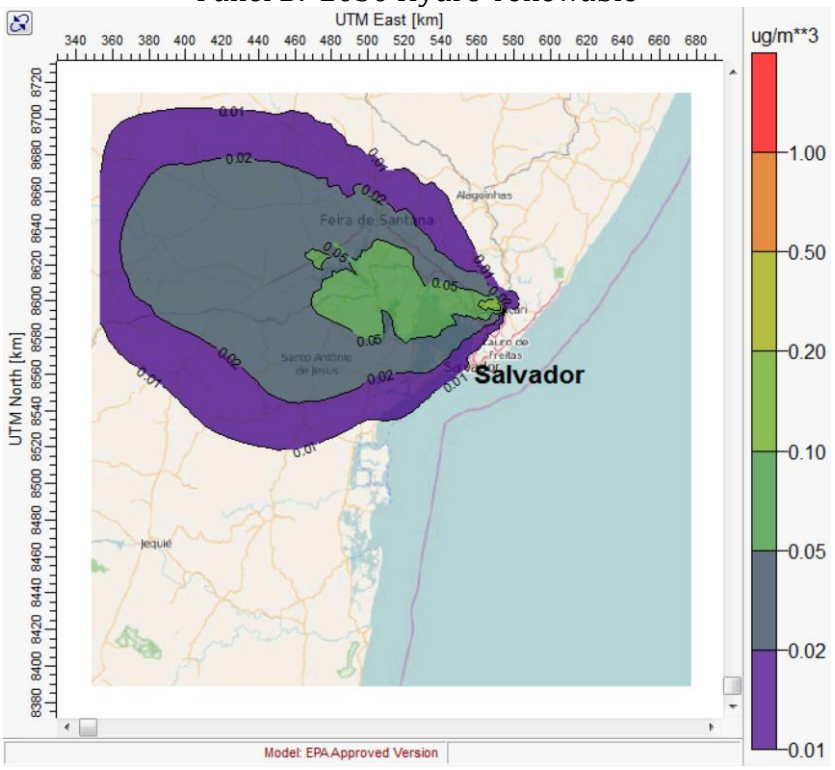

Panel C. 2030 Hydro-renewable dry year

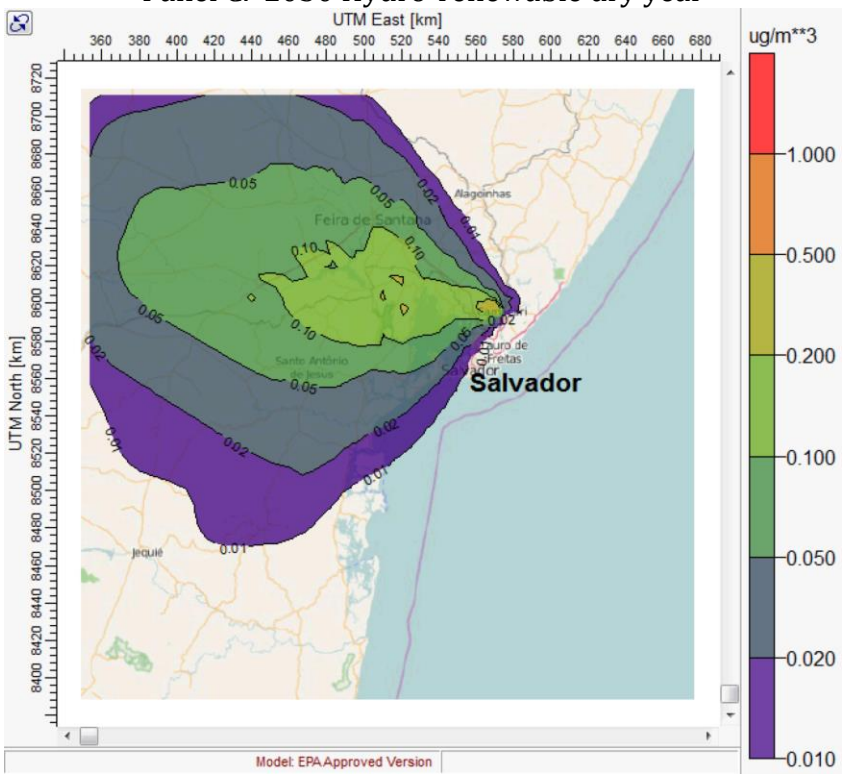

Panel D. 2030 HT

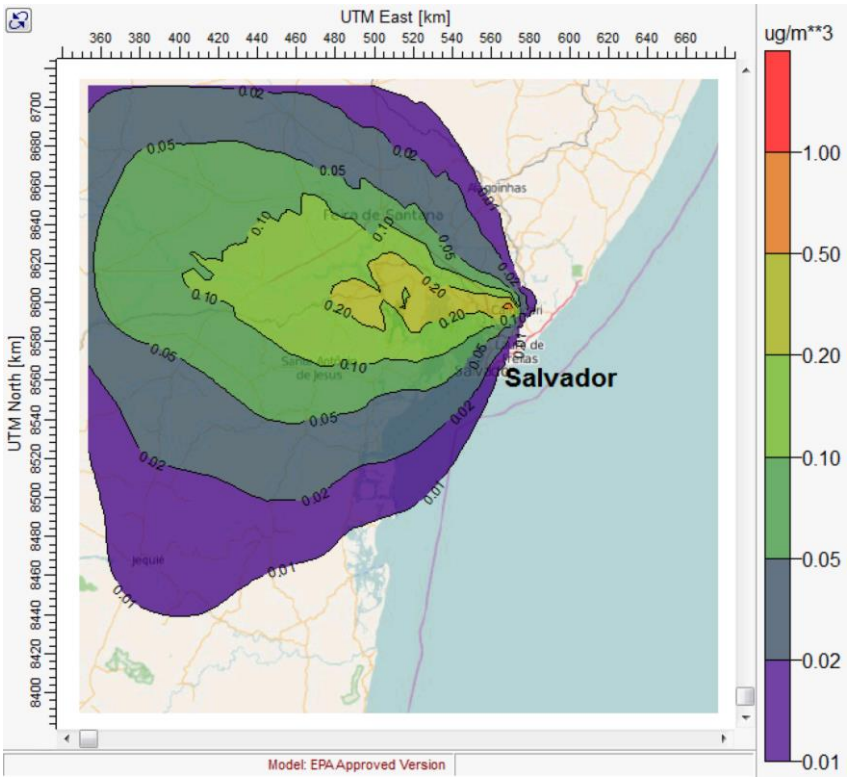

Figure 7.22 Peak 24-hour average PM_{10} concentration plots

Panel A. Fortaleza 2015 peak 24-hour average

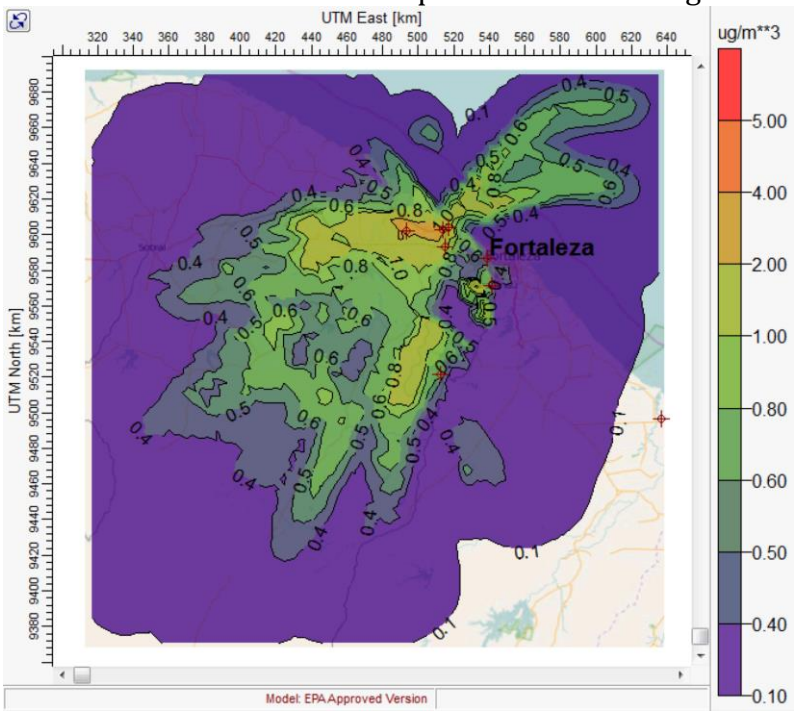

Panel B. Fortaleza 2030 HT peak 24-hour average

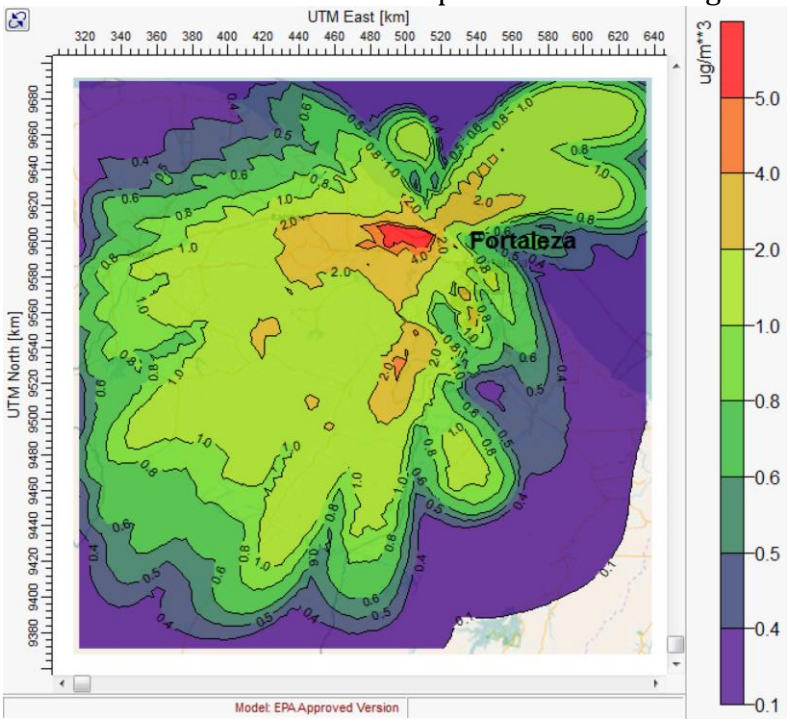

Panel C. Recife 2030 HT peak 24-hour average

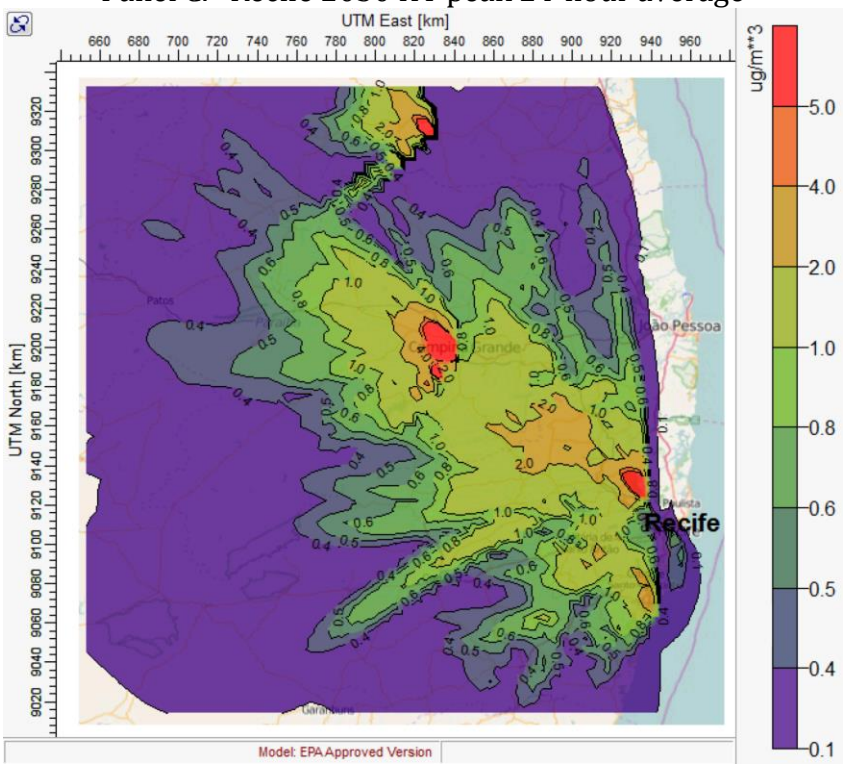

Panel D. Salvador 2030 HT peak 24-hour average

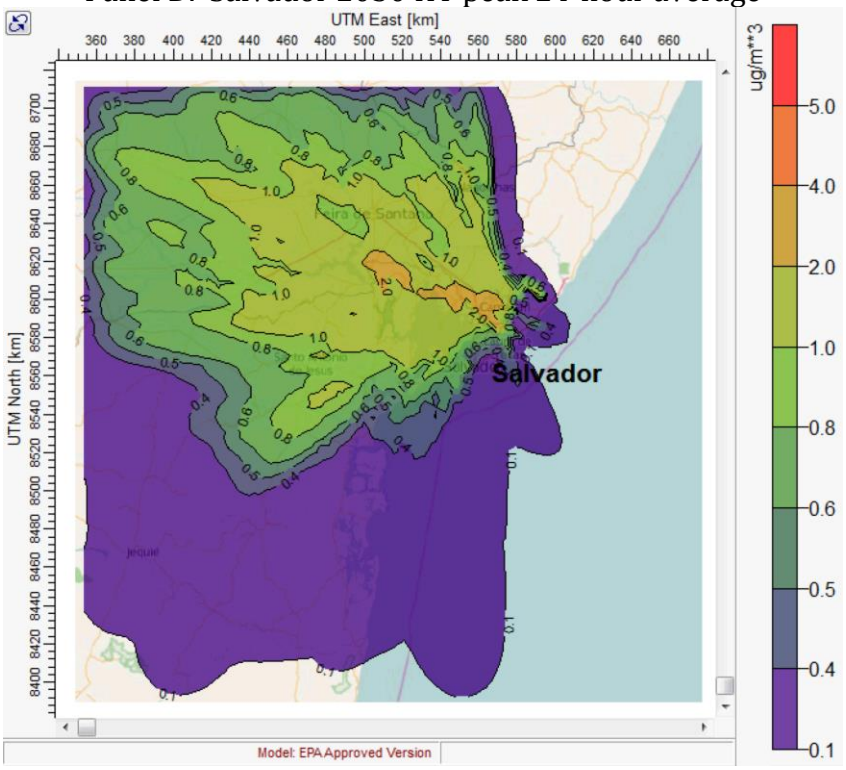

The CALPUFF results were validated according to the air quality modeling validation section in the CALPUFF Methodlogy chapter. No abnormal concentrations or wind patterns were detected.

As part of the results validation, air quality concentration plots for each region were compared with the wind rose. As expected, the highest concentrations are closest to the coal power plants and disperse westerly, according to the direction of the wind rose for each region. In general, the population west of the power plants is downwind of the emission plume pathway and exposed to higher $PM_{2.5}$ concentrations, whereas people who live east of the power plants (upwind of emissions) are mostly unaffected by these PM emissions.

To prepare air quality grid inputs for BenMAP, I converted the PM_{10} air quality concentrations to $PM_{2.5}$ air quality concentrations using the ambient ratio method described in the CALPUFF Methodology $PM_{2.5}$ and PM_{10} dispersion section. As for the first question, I performed a robustness test by converting PM_{10} to $PM_{2.5}$ before and after dispersion, and found a mean difference in the final $PM_{2.5}$ air quality concentrations of approximately 1%.

While increases in air pollutant concentrations will increase human exposure and lead to adverse health outcomes, the changes in human exposure are dependent on the air quality changes relative to population density. For example, small air pollutant concentration increases in densely populated areas typically have a greater impact than large air pollutant concentration increases in sparsely populated areas (Hubbell *et al.*, 2009). The following section discusses the health outcomes estimated based on the air quality changes for each scenario.

7.2.3 Human health and climate benefits valuation

Using BenMAP, I estimated the expected human health outcomes for each scenario based on the air quality concentration changes simulated in CALPUFF. Table 7.8 summarizes the expected health benefits for each region in each scenario. Reductions in disease incidence are considered health benefits and represented by positive numbers, increases in disease incidence are considered as health costs and represented by negative numbers.

Transitioning from the 2015 BC to the 2030 Hydro-renewable scenario will prevent an estimated 15 premature deaths per year and 402 hospital admissions per year in NE Brazil. If an extreme dry year occurs in the 2030 Hydro-renewable scenario, requiring the frequent dispatch of oil generators, then a reduction of approximately 1 premature mortality and 34 hospital admissions are estimated across all regions compared to the 2015 BC.

The 2030 HT scenario results in increases in hospital admissions and premature death across all regions, with approximately 18 more premature deaths and 536 more hospital admissions per year in NE Brazil compared to the 2015 BC scenario.

Transitioning to the 2030 HR scenario versus the 2030 HT scenario will save approximately 34 premature mortalities and 938 hospital admissions per year in NE Brazil.

The number of premature deaths and hospital admissions decreases when moving from the 2015 BC to the 2030 HR scenario, and increases when moving from the 2015 BC to the 2030 HT scenario. This is expected because $PM_{2.5}$ air quality

concentrations decrease from the 2015 to the 2030 HR scenario and increase from the 2015 to the 2030 HT scenario.

Table 7.8. Disease incidence changes by scenario (reduction of cases/yr)

Region/health endpoint	2030 HR (reduction/yr)	2030 HR DY (reduction/yr)	2030 HT (reduction/yr)
Fortaleza			
Mortality, All Causes	6.98	5.03	(6.98)
Mortality, Infant	0.04	0.03	(0.06)
Hospital Admissions, Respiratory	65.24	48.89	(83.70)
Hospital Admissions, Cardiovascular	129.54	97.07	(166.16)
Recife			
Mortality	7.45	(3.35)	(8.61)
Infant Mortality	0.04	(0.02)	(0.05)
Hospital Admissions, Respiratory	61.70	(28.72)	(73.83)
Hospital Admissions, Cardiovascular	122.52	(57.01)	(146.57)
Salvador			
Mortality	0.95	(1.05)	(2.66)
Infant Mortality	0.01	(0.01)	(0.02)
Hospital Admissions, Respiratory	7.88	(8.72)	(22.04)
Hospital Admissions, Cardiovascular	15.65	(17.31)	(43.77)
Total Mortality (reduction/yr)	**15.48**	**0.64**	**(18.37)**
Total Hospital Admissions (reduction/yr)	**402.54**	**34.21**	**(536.07)**

Interestingly, while the peak 8760-annual $PM_{2.5}$ concentration decreases in Recife from 0.76 μg/m3 in the 2015 BC to 0.46 μg/m^3 in the 2030 HR DY, the number of premature deaths increases by approximately 3 incidences, and the number of hospital admissions increases by ~86 incidences per year. The reason behind this result is that the average annual mean $PM_{2.5}$ concentration for Recife increased from 2.07 E-2 in the 2015 BC to 2.24E-2 in the 2030 HR DY scenario. Additionally, the sum of annual mean air quality concentrations for all grid cells increased from 74.4 80.7 μg/m^3 in the 2015 BC to 80.7 μg/m^3 in the 2030. Therefore, the annual mean $PM_{2.5}$ concentrations on average increase when moving from the 2015 BC to the 2030 HR DY scenario, even though the peak annual concentration (the grid cell with the highest annual mean) decreases, leading to an increase in adverse health outcomes.

In dollar terms (expressed in 2015 $), transitioning from the 2015 BC to the 2030 HR scenario will result in approximately US$121 million in health benefits (savings) per year in NE Brazil. If extreme dry year conditions occur as simulated by the 2030 HR DY scenario, the health benefits would only be US$5 million per year as compared to the 2015 BC. On the other hand, transitioning to the 2030 HT scenario would add an additional US$145 million in health costs per year in NE Brazil.

The difference between moving from the 2015 BC to the 2030 HR scenario instead of the 2030 HT scenario is the difference in health benefits between the two scenarios. Thus, moving from the 2015 BC to the 2030 HR instead of the 2030 HT scenario yields approximately US$267 million per year in health benefits.

The monetary valuation of premature deaths is 12 to 23 times larger than the value of hospital admissions, making it the predominant driver of the value of health outcomes. However, the number of hospital admissions is 26 to 53 times greater than the number of premature mortalities, meaning that most people affected by PM emissions will suffer from respiratory ailments or cardiovascular problems.

Table 7.9. Monetary valuation of health outcomes (U.S. 2015$/yr)

Region/health endpoint	2030 HR (million U.S. 2015$/yr)	2030 HR DY (million U.S. 2015$/yr)	2030 HT (million U.S. 2015$/yr)
Fortaleza	-	-	-
Mortality, All Causes	52.6	37.9	(52.6)
Mortality, Infant	0.3	0.3	(0.4)
Hospital Admissions, Respiratory	0.6	0.5	(0.8)
Hospital Admissions, Cardiovascular	1.8	1.4	(2.3)
Recife	-	-	-
Mortality	56.1	(25.2)	(64.9)
Infant Mortality	0.3	(0.1)	(0.4)
Hospital Admissions, Respiratory	0.6	(0.3)	(0.7)
Hospital Admissions, Cardiovascular	1.7	(0.8)	(2.0)
Salvador	-	-	-
Mortality	7.2	(7.9)	(20.1)
Infant Mortality	0.0	(0.0)	(0.1)
Hospital Admissions, Respiratory	0.1	(0.1)	(0.2)
Hospital Admissions, Cardiovascular	0.2	(0.2)	(0.6)
Hospital Admissions Benefits (million 2015$/yr)	**5.0**	**0.4**	**(6.7)**
Mortality Benefits (million 2015$/yr)	**116.7**	**4.9**	**(138.5)**
Total Health Benefits (million 2015$/yr)	**121.7**	**5.3**	**(145.2)**

The health benefits results in BenMAP were validated as described in the BenMAP Methodology chapter. The premature mortality estimates by the IER were somewhat similar to the premature mortality estimates by other C-R functions for premature mortality in adults. The air quality delta, disease incidence and monetary valuation calculations between scenarios in BenMAP matched the manual calculations I performed to spot check results.

To monetarily value climate benefits, a range of benefits were estimated by directly valuing CO_2 emissions at the low and high end of the carbon pricing range recommended by the High-Level Commission on Carbon Prices.

In 2016, the High-Level Commission on Carbon Prices was initiated at the 2016 Conference of the Parties of the United Nations Framework Convention on Climate Change. In 2017, the Report of the High-Level Commission on Carbon Prices was published, advising an explicit price of at least $50-100 per metric ton of CO_2 (Stiglitz *et al*., 2017).

The annual electric grid CO_2 emissions for each scenario were quantified in Plexos and valued by multiplying the number of tons of CO_2 emitted by the recommended price range per ton of CO_2. Table 7.10 presents the annual CO_2 emissions by scenario, along with annual carbon emission valuation range, estimate at a low price of $50 per metric ton CO_2, and a high price of $100 per metric ton CO_2.

The valuation of annual CO_2 emissions are $1,005 – 2,010 million in the 2015 BC, and increase to US$1,210 – 2,420 million in the 2030 HR, US$1,640 – 3,280 million in the 2030 HR DY, and US$2,420 - 4,840 million in the 2030 HT.

Table 7.10. CO_2 emissions valuation per scenario

Carbon costs	2015 BC	2030 HR	2030 HR DY	2030 HT
CO_2 emissions (million metric ton/yr)	20.1	24.2	32.8	48.4
Low estimate (million US$/yr)	1,005	1,210	1,640	2,420
High estimate (million US$/yr)	2,010	2,420	3,280	4,840

Table 7.11 displays the climate benefits for each scenario transition. The climate benefits were calculated by multiplying the changes in emissions per scenario transition by the price per metric ton of CO_2. Climate benefits are positive when CO_2 emissions decrease, representing a lower climate externality costs. Climate benefits are negative when CO_2 emissions increase, representing higher climate external costs.

Table 7.11. Climate benefits per scenario transition

Climate benefits	2015 BC ➔ 2030 HR	2015 BC ➔ 2030 HR DY	2015 BC ➔ 2030 HT
CO_2 emissions (million metric ton/yr)	4.1	12.7	28.3
Low estimate (million US$/yr)	(205)	(635)	(1,415)
High estimate (million US$/yr)	(410)	(1,270)	(2,830)

Although VRE penetration increases from 30% in the 2015 BC to 45% in the 2030 HR, CO_2 emissions also increase 21.4%, corresponding to a US$205 - 410

million increase in annual climate externality costs. This is due to an annual energy demand increase of 4.77% over the 15-year period and the expansion of natural gas generators to balance load and generation.

CO_2 emissions increase by 35.5% from the 2030 HR to the 2030 HR DY, due to lower hydroelectric potential during dry year conditions resulting in a greater reliance on natural gas and oil generators. This implies that dry year conditions in a scenario with 45% VRE in NE Brazil could increase annual climate external costs by US$635 – 1,270 million.

Annual CO_2 emissions more than double from the 2015 BC to the 2030 HT scenario. This is due to an increase in energy demand and to the expansion of fossil fuel generators. It reflects a climate external cost increase between US$1,415 – 2,830 million.

While NE Brazil will enjoy health and climate benefits if it expands its electricity infrastructure with higher VRE levels (2030 HR) compared to the lower VRE levels in the 2030 HT scenario, there will be tradeoffs including greater generation and storage capacity requirements to maintain a constant power supply. Understanding these tradeoffs provides insight to optimize the expansion of a regions electricity system.

Interestingly, these results indicate that while a transition from a 30% VRE in 2015 to a 45% VRE in 2030 will reduce PM emissions and health impacts, GHG emissions will not necessarily decrease and could even increase. The next section explores the tradeoffs of a 100% RPS scenario to gain insight into tradeoffs between

high VRE scenarios and a 100% RPS electricity grid, as well as what is required to decarbonize the NE Brazil electricity grid.

7.3 100% RPS results

While transitioning coal/oil generation to natural gas will help meet air quality goals and provide substantial health benefits, meeting climate goals requires reducing total CO_2 emissions. As seen in the health, climate and electricity grid tradeoffs of high VRE penetrations, increasing energy demand makes it difficult to reduce GHG emissions, even when increasing the share of renewables.

Table 7.12. Health, climate and electricity grid tradeoffs in a 100% RPS

	2030 HR	2030 HT	2030 100% RPS
System capacity (MW)	78,478	60,783	88,910
VRE (% of system capacity)	45	30	70
Total renewables (% of system capacity)	79	72	100
Pump storage load (GWh)	15,688	10,482	17,850
Unserved energy (% of system load)	0.0	0.0	12.6
Dump energy (% of system load)	4.6	0.0	23.0
Health Benefits low estimate (million 2015 US$/yr)	122	(145)	288
Climate Benefits low estimate (million US$/yr)	(205)	(1,415)	1,005

A 100% RPS scenario for 2030 in NE Brazil was created to explore the health, climate and electricity system tradeoffs of transitioning to a fully renewable electricity grid. Table 7.12 summarizes the health, climate, electric grid storage and

stability tradeoffs of 30% VRE, 45% VRE and 100% RPS (70% VRE) electricity systems in NE Brazil.

While a 100% RPS scenario has higher system capacity, storage and load balancing requirements, transitioning from the 2015 baseline infrastructure to a 100% RPS scenario would yield health benefits of at least US$288 million per year and climate benefits of at least $1 billion per year.

7.3.1 Electric grid stability

The annual load curve in the 2030 100% RPS scenario was the same as the other 2030 scenarios, with an electricity demand of 194,562 GWh and a total load (including pumped storage) of 212,412. However, in the 2030 100% RPS base scenario, there was 26,841 GWh of unserved load, which corresponds to 12.6% of system load. Dump energy was even greater than unserved load, totaling 55,580 GWh or 23.0% of total generation. These large amounts of unserved load and dump energy indicate that under this 100% RPS scenario, electric grid operation will not be stable and electricity demand will not be reliably met without the ability to flexibly import and export substantial amounts of electricity, otherwise additional types of load and generation balancing technology would need to be installed.

Figure 7.23 displays the hourly electricity dispatch for one of the weeks with the highest unserved load, April 8 to 15, 2030. Notice how there are spikes of VRE generation, followed by sharp decreases in VRE generation. The quick increases and decreases are mainly due to fluctuating wind patterns (eight wind hot spots were simulated with different hourly wind conditions), which cause spikes in wind

generation (shown in green) due to the large installed capacity of 53,446 MW of wind energy in the 100% RPS scenario.

Hydroelectric generation, shown in blue, ramps up to meet demand when there is sharp decrease in VRE generation. Although hydroelectric capacity was increased to it's maximum potential of 26,250 MW in the 2030 100% RPS scenario, there is not enough hydroelectric capacity to meet demand when VRE generation is very low. This leads to a substantial amount of unserved load, shown in red.

Similarly, pump load (shown by the purple line) increases when there is a sharp increases in VRE generation to utilize the excess energy for hydroelectric pumped storage. When there is not enough pumped storage capacity to absorb all the excess generation from VRE sources, the excess energy must be dumped (dump energy). In the 2030 100% RPS scenario, the dump profile is equivalent to 23.0% of generation. Therefore, there was a limited capacity to shift generation from VRE resources to a later point when they can be utilized, and thus increasing installed VRE capacity beyond the level in the 2030 100% RPS scenario would not necessarily help meet demand.

Figure 7.23. 100% RPS extreme week dispatch

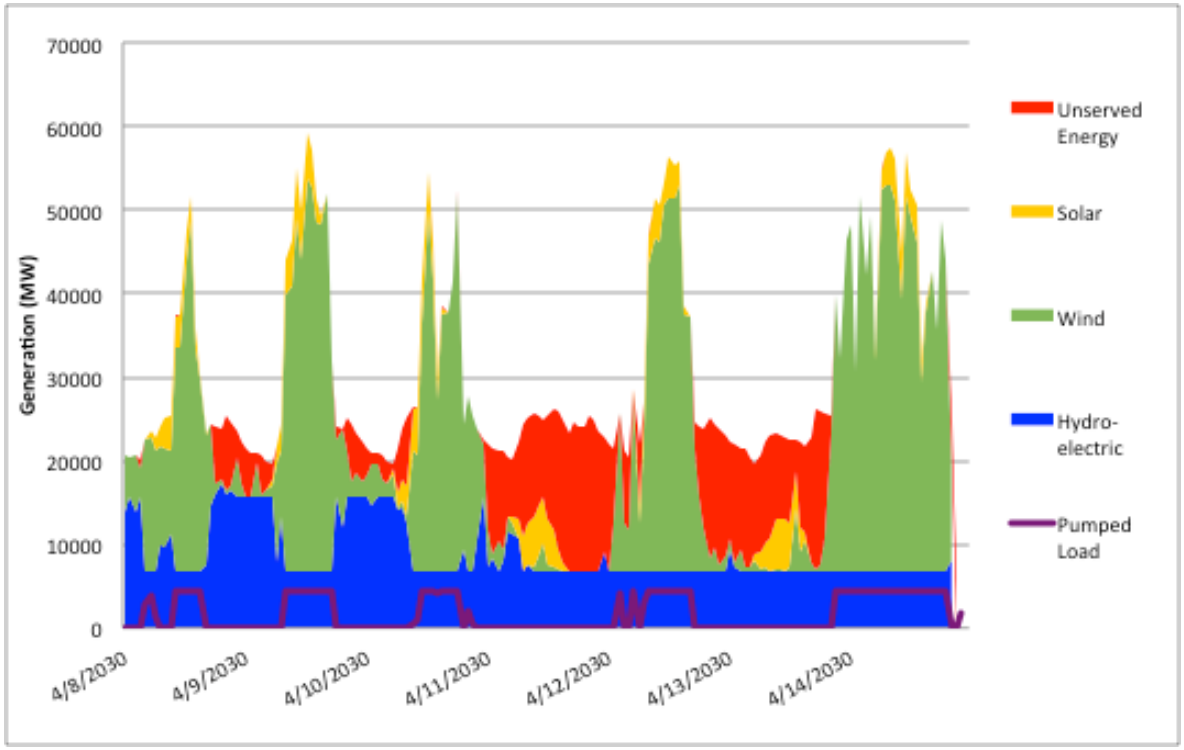

Due to limited hydroelectric generation and pumped storage potential also limiting the usefulness of further VRE installed capacity, the 2030 100% RPS scenario has approximately 13.2% higher capacity and 13.8% higher pump storage load requirements. If there was greater hydroelectric capacity available, then the NE Brazil electric system could accommodate more hydroelectric as well as more VRE resources.

The unserved load is quite substantial and demonstrates that a 100% RPS scenario in NE Brazil based on the potential wind, solar and hydro resources in NE Brazil is not feasible without the ability to import and export or store large amounts of electricity. Two previous studies have assessed the potential of 100% renewable energy systems for all of Brazil (Barbosa *et al.*, 2016; Gils *et al.*, 2017) and found that

a 100% renewable energy system for Brazil is possible if Brazil's electricity grids are interconnected and a portfolio of generation and storage technologies are deployed. Both of these studies found that interconnecting the electricity grids in Brazil with high voltage direct current lines to provide flexible imports and exports of electricity is a critical step of balancing load and generation if Brazil transitions to a 100% renewable energy system.

Brazil's electricity system is already interconnected, yet the only high voltage direct current transmission lines (600 kV) are in the Southeast electricity system. The interconnection of electric grids has allowed for flexible imports and exports of electricity between grids in Brazil. During the month of April, NE Brazil has had the highest average imports of electricity than any other month in 2013 and 2014 (Operador Nacional do Sistema Eletrico, 2015). Results from the 100% RPS scenario indicate that an unserved load of 3,565 GWh, equivalent to 20.1% of NE Brazil electric load in April, would need to be imported into the NE Brazil electric system to meet demand. Electricity is available to export to NE Brazil from the North Brazil electric grid primarily from January to June because that is the wet season, and North Brazil has substantial hydroelectric generation that increases during the wet months (Operador Nacional do Sistema Eletrico, 2015).

Although NE Brazil has not historically been an exporter of electricity to other Brazilian regions, moving to a 100% RPS scenario would allow NE Brazil to become both an electricity exporter and an importer. For example, 66.2% of the excess energy produced in NE Brazil is during the hotter and dryer months of July through December. This excess generation could be exported to other regions

during the dry months where there is less hydroelectric generation, and simultaneously reduce the dump energy requirements in NE Brazil.

The results from the NE Brazil 100% RPS simulation highlight the importance of the flexibility to import and export electricity between regions. In the 100% RPS scenario, NE Brazil would need to flexibly import an average of 12.6% of NE Brazil's projected electric system load for 2030, in a way where the imports are synchronous with hourly generation shortages, in order to eliminate unserved load. Similarly, with the ability to flexibly export 23.0% of electricity generation from the NE Brazil under the 100% RPS scenario, NE Brazil could provide electricity to other regions in Brazil while minimizing dump energy requirements and costs.

Similarly to the two previous studies that found 100% RPS scenarios feasible in Brazil, several multi-country level super grid modeling efforts have also found 100% RPS scenarios to be feasible. These studies found that 100% RPS scenarios are feasible in Central and South America (Barbosa *et al.* 2017), Eurasia (Bogdanov & Breyer, 2016), North-East Asia (Bogdanov & Breyer, 2016) and Sub-Saharan Africa (Barasa *et al*., 2016) if these four key strategies are implemented: (1) high voltage direct current transmission lines interconnecting electric grids over a large region to flexibly exchange electricity; (2) a portfolio of variable and dispatchable generation resources, including solar PV, solar CSP, wind, hydropower, biomass, waste-to-energy and geothermal; (3) a portfolio of energy storage resources, including batteries, pumped hydro storage, compressed air storage and power to gas; and (4) coupling electricity with other energy sectors, such as transportation, heat and desalination.

It is important to note that my 100% RPS simulation in NE Brazil considers only the wind, solar and hydroelectric resources available in NE Brazil. My results indicate that if an average of 12.6% of load can be flexibly imported, and an average of 23.0% of generation can be flexibly exported, that load and generation can be systemically balanced in a 100% scenario in NE Brazil without considering the additional generation, storage and energy sector coupling strategies that were considered by the previous 100% renewable energy studies for Brazil and multi-country super grids.

It is also important to note that this study does not simulate the sub-hourly distribution level and local scale system dynamics, such as harmonic distortion and flicker, which are significantly affected by VRE (Ackermann, 2005). However, the simulation modeling does consider the acceptable ranges of voltages, frequencies and power flows at the transmission level.

The 100% RPS scenarios were validated using the same process as described in the system validation subsection of the Plexos methodology, including verifying that generators were dispatched according to its constraints. In addition, the hydroelectric reservoir initial fill levels, inflow, release and final fill levels were checked in detail to make sure the system operated within defined constraints. Dump and unserved energy were also checked to ensure that generation plus unserved load minus dump energy equals total load, and that total load equals system load (electricity demand) plus pumped hydroelectric storage load.

7.3.2 Health and climate impacts valuation

While a 100% RPS electricity grid has greater capacity, storage and load balancing requirements than a 30% VRE penetration (2030 HT) and a 45% VRE penetration (2030 HR), there are substantial health and climate benefits. The following section compares the health and climate benefits of transitioning from the 2015 BC to the 2030 HR, 2030 HT and 2030 100% RPS scenarios.

Table 7.13 displays the changes in premature mortality and hospital admissions for each region in each scenario. Moving to a 100% RPS scenario from the 2015 BC decreases premature mortality by approximately 37 deaths and 951 hospital admissions per year. The 100% RPS scenario cuts approximately 21 deaths and 548 hospital admissions more than the 2030 HR scenario per year. Similarly, the 100% RPS scenario cuts approximately 55 deaths and 1,487 hospital admissions more than the 2030 HT scenario per year.

A key takeaway from modeling the three most densely populated regions in NE Brazil is that health impacts can vary widely between regions for a given scenario. For example, moving to a 100% RPS scenario in 2030 will cut approximately 3 premature deaths in the Salvador region and 20 in the Recife region. This is primarily due to fossil fuel generators in different regions being dispatched at different frequencies, as well as the proximity of emissions to dense populations and the meteorological conditions that influence the transportation of emissions between regions. Also, notice how the health benefits are positive for each region in the 2030 HR and 2030 100% RPS scenarios, and negative for each region in the 2030 HT scenario.

Table 7.13. Disease incidence changes by scenario (reduction of cases/yr)

Region/health endpoint	2030 HR (reduction/yr)	2030 HT (reduction/yr)	2030 100% RPS (reduction/yr)
Fortaleza			
Mortality, All Causes	6.98	(6.98)	13.42
Mortality, Infant	0.04	(0.06)	0.09
Hospital Admissions, Respiratory	65.24	(83.70)	127.51
Hospital Admissions, Cardiovascular	129.54	(166.16)	253.19
Recife			
Mortality	7.45	(8.61)	20.27
Infant Mortality	0.04	(0.05)	0.12
Hospital Admissions, Respiratory	61.70	(73.83)	168.16
Hospital Admissions, Cardiovascular	122.52	(146.57)	333.90
Salvador			
Mortality	0.95	(2.66)	2.76
Infant Mortality	0.01	(0.02)	0.02
Hospital Admissions, Respiratory	7.88	(22.04)	22.85
Hospital Admissions, Cardiovascular	15.65	(43.77)	45.37
Total Mortality (reduction/yr)	15.48	(18.37)	36.68
Total Hospital Admissions (reduction/yr)	402.54	(536.07)	950.97

Table 7.14 presents the monetary valuation of health outcomes for each region in each scenario. Similar to changes in disease incidence, the health benefits are positive when moving from the 2015 BC to the 2030 HR and 2030 100% scenarios, and negative when moving to the 2030 HT scenario.

Table 7.14. Monetary valuation of health outcomes

Region/health endpoint	2030 HR (million U.S. 2015$/yr)	2030 HT (U.S. million 2015$/yr)	2030 100% RPS (million U.S. 2015$/yr)
Fortaleza	-	-	-
Mortality, All Causes	52.6	(52.6)	101.2
Mortality, Infant	0.3	(0.4)	0.7
Hospital Admissions, Respiratory	0.6	(0.8)	1.2
Hospital Admissions, Cardiovascular	1.8	(2.3)	3.5
Recife	-	-	-
Mortality	56.1	(64.9)	152.8
Infant Mortality	0.3	(0.4)	0.9
Hospital Admissions, Respiratory	0.6	(0.7)	1.6
Hospital Admissions, Cardiovascular	1.7	(2.0)	4.6
Salvador	-	-	-
Mortality	7.2	(20.1)	20.8
Infant Mortality	0.04	(0.1)	0.1
Hospital Admissions, Respiratory	0.1	(0.2)	0.2
Hospital Admissions, Cardiovascular	0.2	(0.6)	0.6
Total Hospital Admissions (2015$/yr)	**5.0**	**(6.7)**	**11.8**
Total Mortality (2015$/yr)	**116.7**	**(138.5)**	**276.4**
Total Health Benefits (2015$/yr)	**121.7**	**(145.2)**	**288.2**

When the three most densely populated regions of NE Brazil are considered, moving to a 100% RPS scenario yields approximately US$166.5 million per year in

health benefits more than the 2030 HR scenario, and approximately US$433.4 million per year in health benefits than the 2030 HT scenario. To highlight the regional variation of health benefits in the 2030 100% RPS scenario, the health benefits are approximately 4.9 times greater in Fortaleza than Salvador, and 7.4 times greater in Recife than Salvador.

Health externalities are caused by local and regional pollutants, and as shown in this dissertation, their impact depends on the on the time and place they are emitted. On the other hand, climate impacts are caused by global pollutants, whose impact do not depend on where they are emitted. The CO_2 emissions are therefore presented as annual electric grid emissions.

Table 7.15. CO_2 emissions valuation per scenario

Carbon costs	2015 BC	2030 HR	2030 HT	2030 100% RPS
CO_2 emissions (million metric ton/yr)	20.1	24.2	48.4	0
Low estimate (million US$/yr)	1,005	1,210	2,420	0
High estimate (million US$/yr)	2,010	2,420	4,840	0

The annual electric grid CO_2 emissions were simulated for each scenario in Plexos. The CO_2 emissions were then valued by multiplying the number of tons of CO_2 emitted annually by US$50 per metric ton of CO_2, which is the lowest value in carbon price range of US$50-100 per metric ton of CO_2, as recommended by the

High-Level Commission on Carbon Prices (Stiglitz *et al.*, 2017). Table 7.15 displays the annual CO_2 emissions and monetary valuation of climate benefits per scenario.

While CO_2 emissions increase from the 2015 BC to the 2030 HR and 2030 HT scenarios, there are no CO_2 emissions in the 2030 100% RPS scenario. This indicates that moving from the 2015 BC with 30% VRE to the 2030 HR with 45% VRE will not reduce CO_2 emissions, due to a 4.77% average annual energy demand increase and an expansion of natural gas generators to help balance load and generation. This implies that in order to reduce CO_2 emissions, no new thermal generators can be added to the energy mix unless they are replacing less efficient generators, and existing generators must be decommissioned or at least dispatched less frequently.

Table 7.16. Climate benefits per scenario transition

Climate benefits	2015 BC ➔ 2030 HR	2015 BC ➔ 2030 HT	2015 BC ➔ 2030 100% RPS
CO_2 emissions (million metric ton/yr)	4.1	28.3	(20.1)
Low estimate (million US$/yr)	(205)	(1,415)	1,005
High estimate (million US$/yr)	(410)	(2,830)	2,010

Table 7.16 presents the climate benefits of moving from the 2015 BC to the 2030 HR, 2030 HT and 2030 100% RPS scenarios. While moving to the 2030 HR and 2030 HT scenarios increase CO_2 emissions, which cause negative climate

benefits, moving to the 2030 100% RPS scenario reduces CO_2 emissions and yields climate benefits between $US1,005 – 2,010 million per year.

The total value of moving to the 2030 100% RPS scenario over the 2030 HR and 2030 HT scenarios is the difference between their climate benefits. Therefore, moving to the 2030 100% RPS scenario instead of the 2030 HR scenario (45% VRE) would yield between US$1.21 - 2.42 billion per year in climate benefits. Similarly, moving to the 2030 100% RPS scenario instead of the 2030 HT scenario (30% VRE) yields between $2.42 and $4.84 billion per year in climate benefits.

8 Conclusions

8.1 The health benefits and control costs of tightening PM standards

To my knowledge, this study is the first to model hourly electricity grid dispatch for an entire year to better estimate emissions and health impacts from power plants. Compared to existing studies, I also went a step further by comparing the value of expected health benefits from tightening PM emission standards with the control costs required to achieve those benefits.

My new methodology improves on previous studies by using more advanced models, considering power dispatching to the grid, employing higher temporal and spatial resolution over a relatively wide area during a whole year, and using a new integrated exposure-response model with updated valuation methods. Although the key driver of our results compared to older studies (e.g., see Krupnick and Portney 1991; Lopez *et al.*, 2005; Palmer *et al.,* 1995; Pervin *et al.,* 2008) is the higher value of a statistical life (VSL), decreasing the VSL would not change the conclusions: the mere benefit of avoiding PM-related illnesses leading to hospital admissions would exceed emission control costs by a factor of at least 5 in Scenario 1 and Scenario 2.

The benefit-cost ratio is 101 when moving from a moderate to a relatively low emission standard (Scenario 2), which is even greater than the benefit-cost ratio of 58 that results when moving from a high to a low standard (Scenario 1), because the relative risk of disease incidence per increase in $\mu g/m^3$ $PM_{2.5}$ is greater at low exposure than high exposure (Burnett *et al.*, 2014). Moving from a relatively low to

a very low standard (Scenario 3) also has a high benefit-cost ratio of 50, despite the higher emission control costs per ton.

These results are noteworthy because the ambient PM concentrations in NE Brazil are below the WHO guidelines. They suggest that a strong case can be made to clean up the PM emissions of coal power plants not only in heavily polluted areas but also in relatively clean environments, including in developing countries.

Furthermore, it is important to note that the range of expected health benefits we report is conservative for at least two reasons. First, I did not account for secondary PM, although its impact is likely quite substantial (Behera and Sharma, 2010), because modeling secondary PM is currently much more involved. Second, I was not able to consider mortality induced by PM exposure in people aged 1 to 25 years because of data limitations. These expansions are left for future work.

Tightening standards alone is not sufficient; the standards must also to be enforced. This is especially challenging when open emission monitoring data are rarely available at the plant level, which is the case in many developing countries (Guttikunda and Jawahar, 2014). In Brazil, regulatory agencies in different states have different levels of resources, monitoring policies and enforcement strategies; however, it seems that Brazilian firms are responsive to regulatory pressures, despite different starting points, paces of change and relationships with regulators (Barton *et al.,* 2000). It is likely that NE Brazil will gain the health benefits of low PM emission standards for coal power plants because BNDES provided funding to build the coal power plants in NE Brazil under the contingency that they adhere to a PM emission standard of 0.36 g/kWh, as modeled in Scenario 2.

In future work, it would be of interest to apply this methodology to other areas with different PM standards, ambient $PM_{2.5}$ concentrations, population densities, terrain, meteorological conditions and mixes of power plants; as well as to model secondary PM. In addition, other pollutants could be modeled jointly with PM to analyze the benefits and costs of joint standards.

Coal power plants will likely play an important role until the emergence of more cost-effective storage systems that can provide reliable base loads from renewable energy plants. However, the substantial difference between health benefits and control costs presented in this study make strong arguments for tightening the emission standards of coal power plants worldwide to improve local and regional air quality.

8.2 Health, climate and electricity grid tradeoffs of high VRE penetrations

Electricity demand is increasing in most countries, and understanding the tradeoffs between different energy infrastructure expansion paths will provide national energy planning organizations with insights to design and deploy more beneficial energy expansion plans. This study establishes a methodology to assess three key tradeoffs: health, climate and electric grid storage and stability.

If NE Brazil transitions a 45% VRE (2030 HR scenario) instead of a 30% VRE (2030 HT scenario) in 2030, the required system capacity will be approximately 29% greater and the pumped storage load will be approximately 50% greater. The 45% VRE scenario also has a greater dump energy requirement than the 30% VRE, which is approximately 4.6% of load. However, there are compelling health benefits

of at least US$267 million/yr and climate benefits of at least US$1.2 billion/yr incentivizing a 45% VRE (2030 HR) instead of a 30% VRE (2030 HT).

The range of expected health and climate benefits in this study is conservative for at least three reasons. First, I did not account for secondary PM in estimating health impacts, although its impact is likely quite substantial (Behera & Sharma, 2010; López *et al*., 2005), because modeling secondary PM is currently much more involved. Second, I did not consider health impacts outside of the Fortaleza, Recife and Salvador regions, nor the mortality induced by PM exposure in people aged 1 to 25 years, because of data limitations. Third, the climate benefits are estimated at the lowest value (US$50/ton CO_2) of the recommended carbon price range of US$50 – 100 per metric ton of CO_2 (Stiglitz *et al*., 2017).

Interestingly, the monetary value of climate benefits is 4.5 times greater than the health benefits when looking at the difference between the 2030 HR and 2030 HT scenarios. This is in part due to the valuation techniques that were chosen. For example, if the climate benefits were valued at $10/ton CO_2 instead of $50/ton CO_2, the climate and health benefits would have a similar value.

Although PM_{10} emissions decrease by 39.2% when moving from the 2015 BC with 30% VRE to the 2030 HR scenario with 45% VRE, CO_2 emissions increase by 20.4%. The reduction in PM_{10} emissions is achieved by replacing oil generator dispatch with natural gas, however adding new natural gas power plants to meet higher load balancing and electricity demand requirements increased overall fossil fuel generation and CO_2 emissions. This suggests that constructing new natural gas power plants cannot be relied on to meet additional load balancing and higher

energy demand requirements, unless they are replacing less efficient fossil fuel generators, if progress is to be made towards meeting climate goals.

The inability to rely on new natural gas power plants to balance load and generation incentivizes investment in dispatchable renewable energy and energy storage resources, as well as interconnecting electricity grids and coupling electricity with other energy sectors to balance load and generation (Barbosa *et al*., 2016). When considering investing in additional renewable energy, storage and interconnection resources, the question that inevitably arises is, is it worth it? This study shows that there health and climate benefits that total at least US$1.5 billion/yr when moving to a 45% VRE over a 30% VRE. If the health and climate benefits outweigh the additional generation and storage costs, then investing in higher renewable energy penetrations to address air quality and climate externalities is worthwhile from a social perspective.

If investing in higher renewable energy penetrations to address air quality and climate externalities is worth it, then it is possible a 100% renewable electricity grid is an optimal solution. Another key reason to explore the tradeoffs of different shares of renewables leading up to a 100% RPS electricity grid is that global energy demand is projected to increase by 60% from 2010 to 2040 (Leahy *et al.*, 2013), while at the same time most countries are committing to substantial GHG reductions (United Nations, 2015).

Key future work includes comparing an economic cost analysis of the greater electric system capacity, storage and load balancing requirements with the health and climate benefits to determine the benefit-cost ratio of addressing air quality and

climate goals through higher VRE penetrations. To assess the feasibility of high VRE penetrations, sub-hourly electricity distribution modeling should be done at the local level to determine the distribution system upgrades required to control local issues such as voltage and frequency control, and harmonic distortion and flicker (Krauter, 2005; Borba *et al.*, 2012).

Developing a replicable methodology that could be used to determine the optimal VRE and total renewable penetration for any country, accounting for electricity system, health and climate costs and benefits would be one way to maximize the benefit-cost ratio of addressing air quality and climate goals. This insight will empower national energy planning organizations to design policy and electricity infrastructure expansion plans that provide the highest benefit to society.

8.3 The tradeoffs of high VRE and a 100% RPS electricity grid in NE Brazil

A 100% RPS electricity grid in NE Brazil in 2030 would yield at least US$433 million/yr in health benefits and at least US$2.5 billion/yr in climate benefits as compared to a 30% VRE (2030 HT scenario) infrastructure. However, relying only on wind, solar PV and hydroelectric resources would require the ability to flexibly import and export substantial portions of demand and generation; otherwise additional types of renewable generation, storage and load balancing technology would need to be deployed.

While 12.6% of load was not met and 23.0% of generation could not be used (due to hourly mismatches between VRE generation and system load) in the 2030 100% RPS scenario, it is important to highlight that scenario considers only the

wind, solar and hydroelectric technology options that were operational in NE Brazil in 2015, along with the ability to increase the installed capacity of each technology to its full potential. Additionally, the NE Brazil electric system was simulated as an individual electricity grid, although it is part of Brazil's S2 electricity subsystem, which comprises the North and Northeast electricity grids.

The extent to which NE Brazil could import and export electricity based on hourly demands is the extent to which load and generation would be balanced in the NE Brazil in the 2030 100% RPS scenario. NE Brazil's net imports were on average 2,389 MW in 2013, which was the year with the highest average imports from 2001 to 2014. This is approximately 10.8% of the average load of 22,210 MW in the 2030 load profile (Operador Nacional do Sistema Eletrico, 2015).

These results suggest that when there is not enough hydroelectric capacity to balance load and generation in a 100% RPS scenario, additional technologies and strategies are required. These technologies and strategies include: (1) high voltage direct current transmission lines for interconnecting electricity grids to flexibly import and export electricity; (2) dispatchable renewable energy, including solar CSP with thermal storage, biomass and biogas, and hydrogen fuel cells; (3) energy storage options, including batteries, compressed air storage, thermal storage and power-to-gas, and (4) coupling the electricity sector with other energy sectors like transportation, industrial heat and desalination (Barbosa *et al*. 2017; Bogdanov & Breyer, 2016a; Bogdanov & Breyer, 2016b; Gulagi *et al*. 2017). Two previous studies found that by deploying these four strategies, a 100% renewable electricity grid in Brazil is technically feasible (Barbosa *et al.*, 2016; Gils *et al.*, 2017).

Results from this dissertation support the importance of implementing these strategies to make a 100% RPS electricity grid feasible. For example, if NE Brazil could import electricity in a manner that matches to the hourly unserved load profile, which averages 12.6% electricity demand, as well as export electricity in a manner equivalent to the hourly dump energy profile, which averages 23.0% of generation, then load and generation would be balanced at a system level in the 100% RPS scenario. This makes a compelling case for developing high voltage direct current transmission lines connecting electricity grids in Brazil, because currently there is just one alternating current 500kV transmission line connecting the North/Northeast and South/Southeast electricity subsystems (see Figure 2.2).

This dissertation suggests that if the health and climate benefits from transitioning to a 100% RPS scenario are greater than the additional system capacity, storage and load balancing costs, then a 100% RPS scenario could be preferable for Brazil. It is important to note that the estimated health and climate benefits are conservative for a few reasons. First, secondary PM formation was not modeled, which can be substantial (Behera and Sharma, 2010). Additionally, the health impacts outside of the Fortaleza, Recife and Salvador regions, as well as the deaths of persons 1 to 25 years old were not included due to data limitations. The climate benefits were conservatively priced at the lowest value of the recommended carbon price range of at least US$50-100 per ton of CO_2 (Stiglitz *et al*., 2017).

Valuable future work includes understanding the extent to which interconnecting electricity grids and coupling energy sectors can support flexible importing and exporting of electricity based on hourly demand to balance load and

generation at the system level. The role that distribution scale modeling, such as controlling frequency and voltage as well as harmonic distortion and flicker, in 100% RPS scenarios must also be explored before designing national and regional transitions to fully integrated renewable energy systems.

This dissertation illustrates the importance of coupling the economic analysis of electricity system costs with an analysis of health and climate benefits in regional, national and multi-national energy planning. Indeed, the sum of health and climate benefits of moving to a 100% RPS scenario is on the order of US$2-3 billion per year. The sheer magnitude of health and climate benefits, even in a region like NE Brazil where ambient PM concentrations below WHO guidelines (U.S. Environmental Protection Agency, 2017a; World Health Organization, 2017), strongly suggests that both an economic analysis and a health and climate benefits analysis are necessary to determine an optimal energy infrastructure expansion plan for all countries. A process to implement the health and climate benefits analysis presented in this dissertation into existing national energy planning is needed to optimize the evolution of energy infrastructures and their impact on public health and the Earth's climate.

References

Ackermann, T. (2005). *Wind power in power systems*. John Wiley & Sons.

Agencia Nacional De Energia Electrica. (2000). *Atlas de Energia Electrica do Brazil*. Titulares dos direitos da ANEEL e OMM. CDU: 912:621.31(81).

Agencia Nacional de Energia Eletrica. (2016). Generation information bank. Retrieved from http://www.aneel.gov.br/.

Akkala, A., Devabhaktuni, V., & Kumar, A. (2010). Interpolation techniques and associated software for environmental data. *Environmental progress & sustainable energy*, *29*(2), 134-141.

Alves, L. A., & Uturbey, W. (2010). Environmental degradation costs in electricity generation: The case of the Brazilian electrical matrix. *Energy Policy*, *38*(10), 6204-6214.

Anaya-Lara, O., Jenkins, N., Ekanayake, J. B., Cartwright, P., & Hughes, M. (2011). *Wind energy generation: modelling and control*. John Wiley & Sons.

André, P. A. D., Veras, M. M., Miraglia, S. G. E. K., & Saldiva, P. H. N. (2012). Lean diesel technology and human health: a case study in six Brazilian metropolitan regions. *Clinics*, *67*(6), 639-646.

ANEEL. (2017). Geographic information system for the electric sector. Retrieved October 3, 2017, from http://sigel.aneel.gov.br/portal/home/.

Anenberg, S. C., Belova, A., Brandt, J., Fann, N., Greco, S., Guttikunda, S., … Van Dingenen, R. (2016). Survey of Ambient Air Pollution Health Risk Assessment Tools. *Risk Analysis : An Official Publication of the Society for Risk Analysis*. http://doi.org/10.1111/risa.12540.

Apte, J. S., Marshall, J. D., Cohen, A. J., & Brauer, M. (2015). Addressing global mortality from ambient PM2. 5. *Environmental science & technology*, *49*(13), 8057-8066.

Atkinson, R. W., Kang, S., Anderson, H. R., Mills, I. C., & Walton, H. A. (2014). Epidemiological time series studies of PM2. 5 and daily mortality and hospital admissions: a systematic review and meta-analysis. *Thorax*, thoraxjnl-2013.

FT Avelino, A., Hewings, G., & Guilhoto, J. (2012). EPSIM-A Social-Environmental Regional Sequential Interindustry Economic Model for Energy Planning: Evaluating the Impacts of New Power Plants in Brazil.

Babin, S. M., Burkom, H. S., Holtry, R. S., Tabernero, N. R., Stokes, L. D., Davies-Cole, J. O., ... & Lee, D. H. (2007). Pediatric patient asthma-related emergency department visits and admissions in Washington, DC, from 2001–2004, and associations with air quality, socio-economic status and age group. *Environmental Health*, *6*(1), 9.

Barasa, M., Bogdanov, D., Oyewo, A. S., & Breyer, C. (2016, June). A cost optimal resolution for sub-Saharan Africa powered by 100% renewables for year 2030 assumptions. In *32nd European Photovoltaic Solar Energy Conference and Exhibition* (pp. 20-24).

Barbosa, L. D. S. N. S., Orozco, J. F., Bogdanov, D., Vainikka, P., & Breyer, C. (2016). Hydropower and power-to-gas storage options: the Brazilian energy system case. *Energy Procedia*, *99*, 89-107.

Barbosa, L. D. S. N. S., Bogdanov, D., Vainikka, P., & Breyer, C. (2017). Hydro, wind and solar power as a base for a 100% renewable energy supply for South and

Central America. *PloS one*, *12*(3), e0173820.

Barton, J; Brown, F; Chudnovsky, D; Dalcomuni, S; Dominguez-Villalobos, L; Freylejer, V. (2000). *Industry and Environment in Latin America*. (R. Jenkins, Ed.). Routledge.

Behera, S. N., & Sharma, M. (2010). Reconstructing primary and secondary components of PM2. 5 composition for an urban atmosphere. *Aerosol Science and Technology*, *44*(11), 983-992.

Bell, M. L., Davis, D. L., Gouveia, N., Borja-Aburto, V. H., & Cifuentes, L. a. (2006). The avoidable health effects of air pollution in three Latin American cities: Santiago, São Paulo, and Mexico City. *Environmental Research*, *100*(3), 431–440.

Bell, M. L., Ebisu, K., Peng, R. D., Walker, J., Samet, J. M., Zeger, S. L., & Dominici, F. (2008). Seasonal and regional short-term effects of fine particles on hospital admissions in 202 US counties, 1999-2005. *American Journal of Epidemiology*, *168*(11), 1301–1310.

Blair, N., Dobos, A. P., Freeman, J., Neises, T., Wagner, M., Ferguson, T., ... & Janzou, S. (2014). *System advisor model, sam 2014.1. 14: General description* (No. NREL/TP-6A20-61019). National Renewable Energy Laboratory (NREL), Golden, Colorado.

Bogdanov, D., & Breyer, C. (2016). Eurasian Super Grid for 100% Renewable Energy Power Supply: Generation and Storage Technologies in the Cost Optimal Mix. *Proceedings of the ISES Solar World Congress 2015*, November, 1–15.

Bogdanov, D., & Breyer, C. (2016). North-East Asian Super Grid for 100% renewable energy supply: Optimal mix of energy technologies for electricity, gas and heat

supply options. *Energy Conversion and Management*, *112*, 176–190.

Boldo, E; Lumbreras, J; Borge, R; Garcia-Perez, J; Fernandez-Navarro, P; Perez-Gomez, B; Aragones, N; Pollan, M, Ramis, R; Moreno, T; Lopez-Abente, G. (2010). *Associated Health Benefits on Mortality of Reducing Particulate Matter (PM2.5) in Spain*.

Boldo, E., Medina, S., LeTertre, A., Hurley, F., M??cke, H. G., Ballester, F., … Eilstein, D. (2006). Apheis: Health impact assessment of long-term exposure to PM2.5 in 23 European cities. *European Journal of Epidemiology*, *21*(6), 449–458.

Borenstein, S. (2012). The Private and Public Economics of Renewable Electricity Generation. *Journal of Economic Perspectives*, *26*(1), 67–92.

Borba, B. S. M. C., Szklo, A., & Schaeffer, R. (2012). Plug-in hybrid electric vehicles as a way to maximize the integration of variable renewable energy in power systems: The case of wind generation in northeastern Brazil. *Energy*, *37*(1), 469–481.

Braga, A., Saldiva, P., Saldiva, P. H. N., Pereira, L. a. a., Menezes, J. J. C., Conceicao, G. M. S., … Dockery, D. W. (2001). Health effects of air pollution exposure on children and adolescents in São Paulo, Brazil. *Pediatric Pulmonology*, *31*, 106–113.

Brauer, M., Freedman, G., Frostad, J., Van Donkelaar, A., Martin, R. V., Dentener, F., ... & Balakrishnan, K. (2015). Ambient air pollution exposure estimation for the global burden of disease 2013. *Environmental science & technology*, *50*(1), 79-88.

Brouwer, A. S., van den Broek, M., Seebregts, A., & Faaij, A. (2014). Impacts of large-scale Intermittent Renewable Energy Sources on electricity systems, and how

these can be modeled. *Renewable and Sustainable Energy Reviews*, *33*, 443–466.

Burnett, R. T., Arden Pope, C., Ezzati, M., Olives, C., Lim, S. S., Mehta, S., … Cohen, A. (2014). An integrated risk function for estimating the global burden of disease attributable to ambient fine particulate matter exposure. *Environmental Health Perspectives*, *122*(4), 397–403.

Bussar, C., Moos, M., Alvarez, R., Wolf, P., Thien, T., Chen, H., … Moser, A. (2014). Optimal allocation and capacity of energy storage systems in a future European power system with 100% renewable energy generation. *Energy Procedia*, *46*, 40–47.

Callaway, D. S. (2009). Tapping the energy storage potential in electric loads to deliver load following and regulation, with application to wind energy. *Energy Conversion and Management*, *50*(5), 1389–1400.

Carnegie Mellon University. (2017). Integrated Environmental Control Model. Retrieved July 16, 2017, from https://www.cmu.edu/epp/iecm/

Center for Hydrometeorology and Remote Sensing. (2016). Retrieved January 6, 2016, from http://rainsphere.eng.uci.edu/.

Chae, Y., & Park, J. (2011). Quantifying costs and benefits of integrated environmental strategies of air quality management and greenhouse gas reduction in the Seoul Metropolitan Area. *Energy Policy*, *39*, 5296–5308.

Chang, M. K., Eichman, J. D., Mueller, F., & Samuelsen, S. (2013). Buffering intermittent renewable power with hydroelectric generation: A case study in California. *Applied Energy*, *112*, 1–11.

Chen, L., Shi, M., Gao, S., Li, S., Mao, J., Zhang, H., … Wang, Z. (2017). Assessment of

population exposure to PM2.5 for mortality in China and its public health benefit based on BenMAP. *Environmental Pollution*, *221*, 311–317.

Cifuentes, L., Vega, J., Köpfer, K., & Lave, L. B. (2000). Effect of the Fine Fraction of Particulate Matter versus the Coarse Mass and Other Pollutants on Daily Mortality in Santiago, Chile. *Journal of the Air & Waste Management Association*, *50*(8), 1287–1298.

Cohen, A. J., Anderson, H. R., Ostro, B., Pandey, K. D., Krzyzanowski, M., Kunzli, N., … Smith, K. (2005). The Global Burden of Disease Due to Outdoor Air Pollution. *Journal of Toxicology and Environmental Health, Part A: Current Issues*, *68*(13–14), 1301–1307.

Cohen, A. J., Brauer, M., Burnett, R., Anderson, H. R., Frostad, J., Estep, K., … Forouzanfar, M. H. (2017). Estimates and 25-year trends of the global burden of disease attributable to ambient air pollution: an analysis of data from the Global Burden of Diseases Study 2015. *The Lancet*, *389*(10082), 1907–1918.

Cohen, A. J., Brauer, M., Burnett, R., Anderson, H. R., Frostad, J., Estep, K., … Forouzanfar, M. H. (2017). Estimates and 25-year trends of the global burden of disease attributable to ambient air pollution: An analysis of data from the Global burden of Diseases Study 2015: Supplementary Appendix. *The Lancet*, *In-press*(17), 1363.

Conceição, G. M., Miraglia, S. G., Kishi, H. S., Saldiva, P. H., & Singer, J. M. (2001). Air pollution and child mortality: a time-series study in São Paulo, Brazil. *Environmental Health Perspectives*, *109 Suppl*(July 2000), 347–50.

Connolly, D., Lund, H., & Mathiesen, B. V. (2016). Smart Energy Europe: The

technical and economic impact of one potential 100% renewable energy scenario for the European Union. *Renewable and Sustainable Energy Reviews*, *60*, 1634–1653.

Ćosić, B., Krajačić, G., & Duić, N. (2012). A 100% renewable energy system in the year 2050: The case of Macedonia. *Energy*, *48*(1), 80–87.

Crampes, C., & Moreaux, M. (2010). Pumped storage and cost saving. *Energy Economics*, *32*(2), 325–333.

Cromar, K. R., Gladson, L. A., Perlmutt, L. D., Ghazipura, M., & Ewart, G. W. (2016). American thoracic society and marron institute report estimated excess morbidity and mortality caused by air pollution above American thoracic society-recommended standards, 2011-2013. *Annals of the American Thoracic Society*, *13*(8), 1195–1201.

Currie, J., Neidell, M., & Schmieder, J. F. (2009). Air pollution and infant health: What Can We Learn From California's Recent Experience? *Journal of Health Economics*, *28*(3), 688–703.

Da Motta, R. S., Huber, R. M., & Jack, R. H. (1999). Policy Options Market based instruments for environmental policymaking in Latin America and the Caribbean : lessons from eleven countries. *Environment and Development Economics*, *4*, 177–201.

Davidson, E. A. (2009). The contribution of manure and fertilizer nitrogen to atmospheric nitrous oxide since 1860. *Nature Geoscience*, *2*(9), 659–662.

Davidson, K., Hallberg, A., McCubbin, D., & Hubbell, B. (2007). Analysis of PM2.5 using the Environmental Benefits Mapping and Analysis Program (BenMAP).

Journal of Toxicology and Environmental Health. Part A, *70*(3–4), 332–346.

de Fatima Andrade, M., de Miranda, R. M., Fornaro, A., Kerr, A., Oyama, B., de Andre, P. A., & Saldiva, P. (2012). Vehicle emissions and PM 2.5 mass concentrations in six Brazilian cities. *Air Quality, Atmosphere and Health*, *5*(1), 79–88.

de Jong, P., Kiperstok, A., Sánchez, A. S., Dargaville, R., & Torres, E. A. (2016). Integrating large scale wind power into the electricity grid in the Northeast of Brazil. *Energy*, *100*, 401–415.

de Leon, K., & Leno, M. SB-350 Clean Energy and Pollution Reduction Act of 2015 (2015). Retrieved February 4, 2016, http://leginfo.legislature.ca.gov/faces/billNavClient.xhtml?bill_id=201520160SB350.

Barbosa, L. D. S. N. S., Orozco, J. F., Bogdanov, D., Vainikka, P., & Breyer, C. (2016). Hydropower and Power-to-gas Storage Options: The Brazilian Energy System Case. *Energy Procedia*, *99*(March), 89–107.

Deligiorgi, D., & Philippopoulos, K. (2011). Spatial interpolation methodologies in urban air pollution modeling: application for the greater area of metropolitan Athens, Greece. In *Advanced Air Pollution*. InTech.

Desaigues, B., Ami, D., Hutchison, M., Rabl, A., Chilton, S., Metcalf, H., ... & Szántó, R. (2007). Final Report on the monetary valuation of mortality and morbidity risks from air pollution. *Deliverable D6*, *7*.

Doolla, S., & Bhatti, T. S. (2006). Load frequency control of an isolated small-hydro power plant with reduced dump load. *IEEE Transactions on Power Systems*, *21*(4), 1912–1919.

Edenhofer, O., Pichs-Madruga, R., Sokona, Y., Minx, J., & Farahani, E. (2014). Climate Change 2014: Mitigation of Climate Change Technical Summary. *Intergovernmental Panel on Climate Change*.

Eichman, J. D., Mueller, F., Tarroja, B., Schell, L. S., & Samuelsen, S. (2013). Exploration of the integration of renewable resources into California's electric system using the Holistic Grid Resource Integration and Deployment (HiGRID) tool. *Energy*, *50*, 353–363.

Emerson, R. (2010). Updates in International Standards: Harmonics and Flicker. Retrieved August 8, 2017, from https://ieee.li/pdf/viewgraphs/international_standards_harmonics_flicker.pdf

Energy Exemplar. (2014). http://wiki.energyexemplar.com/. Retrieved January 9, 2016, from http://wiki.energyexemplar.com/

Environmental Systems Research Institute. (1998). *ESRI Shapefile Technical Description*. *Computational Statistics* (Vol. 16).

Environmental Systems Research Institute Inc. (2016). How Kriging Works. Retrieved October 1, 2017, from http://desktop.arcgis.com/en/arcmap/10.3/tools/3d-analyst-toolbox/how-kriging-works.htm

Empresa de Pesquisa Energética (2007). Plano Nacional de Energia 2030-Geração Termelétrica-Biomassa.

Fann, N., Baker, K. R., & Fulcher, C. M. (2012). Characterizing the PM2.5-related health benefits of emission reductions for 17 industrial, area and mobile emission sectors across the U.S. *Environment International*, *49*, 141–151.

Fann, N., Lamson, A. D., Anenberg, S. C., Wesson, K., Risley, D., & Hubbell, B. J. (2012). Estimating the National Public Health Burden Associated with Exposure to Ambient PM2.5 and Ozone. *Risk Analysis*, *32*(1), 81–95.

Fant, C., Schlosser, C. A., & Strzepek, K. (2015). The impact of climate change on wind and solar resources in southern Africa. *Applied Energy*, *161*, 556–564.

Ferreira, F. S. M. M., Lora, E. E. S., Andrade, R. V. (2015). PADRÕES DE QUALIDADE DO AR E LIMITES DE EMISSÕES PARA AS CENTRAIS TÉRMICAS: ANÁLISE DA LEGISLAÇÃO APLICADA AO SETOR ENERGÉTICO NO BRASIL.

Fichter, T., Soria, R., Szklo, A., Schaeffer, R., & Lucena, A. F. P. (2017). Assessing the potential role of concentrated solar power (CSP) for the northeast power system of Brazil using a detailed power system model. *Energy*, *121*, 695–715.

Francisco, C. M. (2012). Connecting Renewable Power Plant To the Brazilian Transmission Power System, 37.

Gils, H. C., Simon, S., & Soria, R. (2017). 100% Renewable energy supply for Brazil-The role of sector coupling and regional development. *Energies*, *10*(11).

Gouveia, N.; Bremner, S. A.; Novaes, H. M. D. (2004). Association between ambient air pollution and birth weight. *Epidemiol Community Health*, *58*(2), 11–17.

Governo do Estado do Ceará, ; Instituto Centro de Ensino Technologico. (n.d.). COMPLEXO INDUSTRIAL DO PECÉM – CIP ESTUDO DE DISPERSÃO ATMOSFÉRICA.

Gray, W. B., & Shimshack, J. P. (2011). The effectiveness of environmental monitoring and enforcement: A review of the empirical evidence. *Review of Environmental Economics and Policy*, *5*(1), 3–24.

Gulagi, A., Bogdanov, D., & Breyer, C. (2016). Solar photovoltaics - a driving force towards 100 renewable energy for India and SAARC. *32nd European Photovoltaic Solar Energy Conference and Exhibition*, (June).

Gulagi, A., Bogdanov, D., & Breyer, C. (2017). A cost optimized fully sustainable power system for Southeast Asia and the Pacific Rim. *Energies*, *10*(5).

Guttikunda, S. K., & Jawahar, P. (2014). Atmospheric emissions and pollution from the coal-fired thermal power plants in India. *Atmospheric Environment*, *92*, 449–460.

Ha, J., & Moon, N. (2013). Uncertainty and estimation of health burden from particulate matter in Seoul metropolitan region. *Journal of Korean Society for Atmospheric Environment*, *29*(3), 275-286.

Hansen, J., Nazarenko, L., Ruedy, R., Sato, M., Willis, J., Genio, A. Del, … Tausnev, N. (2005). Earth's Energy Imbalance: Confirmation and Implications. *Science*, *308*(June), 1431–1435.

Hao, J., Wang, L., Shen, M., Li, L., & Hu, J. (2007). Air quality impacts of power plant emissions in Beijing. *Environmental Pollution*, *147*(2), 401–408.

Hart, E. K., & Jacobson, M. Z. (2011). A Monte Carlo approach to generator portfolio planning and carbon emissions assessments of systems with large penetrations of variable renewables. *Renewable Energy*, *36*(8), 2278–2286.

He, K., Lei, Y., Pan, X., Zhang, Y., Zhang, Q., & Chen, D. (2010). Co-benefits from energy policies in China. *Energy*, *35*(11), 4265–4272.

Herreras, S., Koberle, A., Rochedo, P., Schaeffer, R., Lucena, A., Szklo, A., … Vuuren, D. P. Van. (2015). Technological Forecasting & Social Change Possible energy

futures for Brazil and Latin America in conservative and stringent mitigation pathways up to 2050, *98*, 186–210.

Hoek, G., Boogaard, H., Knol, A., de Hartog, J., Slottje, P., Ayres, J. G., … Van Der Sluijs, J. P. (2009). Concentration Response Functions for Ultrafine Particles and All-Cause Mortality and Hospital Admissions: Results of a European Expert Panel Elicitation. *Environmental Science & Technology*, *44*(1), 476–482.

Holmes, N. S., & Morawska, L. (2006). A review of dispersion modelling and its application to the dispersion of particles: An overview of different dispersion models available. *Atmospheric Environment*, *40*(30), 5902–5928.

Hubbell, B. J., Fann, N., & Levy, J. I. (2009). Methodological considerations in developing local-scale health impact assessments: Balancing national, regional, and local data. *Air Quality, Atmosphere and Health*, *2*(2), 99–110.

Institute of Health Metrics and Evaluation. (2015). Global Health Data Exchange. Retrieved July 27, 2017, from http://ghdx.healthdata.org/gbd-results-tool

Instituto Brasileiro de Geografia e Estatistica. (2016). http://www.ibge.gov.br/.

IPCC WGII AR5. (2014). FINAL DRAFT IPCC WGII AR5 Chapter 14, (October 2013), 1–51.

Jacobson, M. Z., Delucchi, M. A., Bazouin, G., Bauer, Z. A. F., Heavey, C. C., Fisher, E., … Yeskoo, T. W. (2015). 100% clean and renewable wind, water, and sunlight (WWS) all-sector energy roadmaps for the 50 United States. *Energy Environ. Sci.*, *8*(7), 2093–2117.

Jacobson, M. Z., Delucchi, M. a., Ingraffea, A. R., Howarth, R. W., Bazouin, G., Bridgeland, B., … Yeskoo, T. (2014). A roadmap for repowering California for all

purposes with wind, water, and sunlight. *Energy*, *73*, 875–889.

Jerrett, M., Burnett, R. T., Ma, R., Pope, C. A., Krewski, D., Newbold, K. B., … Thun, M. J. (2005). Spatial analysis of air pollution and mortality in Los Angeles. *Epidemiology (Cambridge, Mass.)*, *16*(6), 727–736.

Kampa, M., & Castanas, E. (2008). Human health effects of air pollution. *Environmental Pollution*, *151*(2), 362–367.

Keohane, N. O., Mansur, E. T., & Voynov, A. (2009). Averting regulatory enforcement: Evidence from new source review. *Journal of Economics and Management Strategy*, *18*(1), 75–104.

Klein, D. H., Andren, A. W., Carter, J. A., Emery, J. F., Feldman, C., Fulkerson, W., … Bolton, N. (1975). Pathways of Thirty-seven Trace Elements Through Coal-Fired Power Plant. *Environmental Science and Technology*, *9*(10), 973–979.

Krauter, S. (2005). Wind Power in Brazil. *International Journal of Distributed Energy Resources*, *1*(3), 213–225.

Krewski, D., Jerrett, M., Burnett, R. T., Ma, R., Hughes, E., Shi, Y., … Tempalski, B. (2009). Extended follow-up and spatial analysis of the American Cancer Society study linking particulate air pollution and mortality. *Res Rep Health Eff Inst*, (140), 5–36.

Krupnick, A. J., & Portney, P. R. (1991). Controlling Urban Air Pollution: A Benefit Cost Assesment. *Science*, *252*, 522–527.

Kutlar Joss, M., Eeftens, M., Gintowt, E., Kappeler, R., & Künzli, N. (2017). Time to harmonize national ambient air quality standards. *International Journal of Public Health*, *62*(4), 453–462.

La Forgia, G. M., & Couttolenc, B. F. (2008). *Hospital Performance in Brazil*. Retrieved August 23, 2016, from http://doi.org/10.1596/978-0-8213-7358-3

Laden, F., Schwartz, J., Speizer, F. E., & Dockery, D. W. (2006). Reduction in fine particulate air pollution and mortality: Extended follow-up of the Harvard Six Cities Study. *American Journal of Respiratory and Critical Care Medicine*, *173*(6), 667–672.

Leahy, M., Barden, J. L., Murphy, B. T., Slater-thompson, N., & Peterson, D. (2013). International Energy Outlook 2013. *United States Energy Information Administration*.

Lehmann, J. (2007). A handful of carbon. *Nature*, *447*(7141), 143–144.

Lelieveld, J., Evans, J. S., Fnais, M., Giannadaki, D., & Pozzer, A. (2015). The contribution of outdoor air pollution sources to premature mortality on a global scale. *Nature*, *525*(7569), 367–71.

Lepeule, J., Laden, F., Dockery, D., & Schwartz, J. (2012). Chronic exposure to fine particles and mortality: An extended follow-up of the Harvard six cities study from 1974 to 2009. *Environmental Health Perspectives*, *120*(7), 965–970.

Levy, J. I., Hammitt, J. K., Yanagisawa, Y., & Spengler, J. D. (1999). Development of a New Damage Function Model for Power Plants: Methodology and Applications. *Environmental Science & Technology*, *33*(24), 4364–4372.

Levy, J. I., Spengler, J. D., Hlinka, D., Sullivan, D., & Moon, D. (2002). Using CALPUFF to evaluate the impacts of power plant emissions in Illinois: Model sensitivity and implications. *Atmospheric Environment*, *36*(6), 1063–1075.

Lima, F., Portugal-Pereira, J., Lucena, A. F. P., Rochedo, P., Cunha, J., Lopes Nunes, M.,

& Szklo, A. S. (2015). Analysis of energy security and sustainability in future low carbon scenarios for Brazil. *Natural Resources Forum*, *39*(3–4), 175–190.

Liu, Z., Lin, M., Wierman, A., Low, S. H., & Andrew, L. L. H. (2011). Geographical load balancing with renewables. *ACM SIGMETRICS Performance Evaluation Review*, *39*, 62. http://doi.org/10.1145/2160803.2160862

Loomis, D., Castillejos, M., Gold, D. R., Mcdonnell, W., & Borja-Aburto, V. H. (1999). Air pollution and infant mortality in Mexico City. *Epidemiology*, *10*(2), 118–123.

López, M. T., Zuk, M., Garibay, V., Tzintzun, G., Iniestra, R., & Fernández, A. (2005). Health impacts from power plant emissions in Mexico. *Atmospheric Environment*, *39*(7), 1199–1209.

Lu, G. Y., & Wong, D. W. (2008). An adaptive inverse-distance weighting spatial interpolation technique. *Computers and Geosciences*, *34*(9), 1044–1055.

Lucena, A. F. P., Clarke, L., Schaeffer, R., Szklo, A., Rochedo, P. R. R., Nogueira, L. P. P., … Kober, T. (2016). Climate policy scenarios in Brazil : A multi-model comparison for energy, *56*, 564–574.

Lund, H., & Mathiesen, B. V. (2009). Energy system analysis of 100% renewable energy systems-The case of Denmark in years 2030 and 2050. *Energy*, *34*(5), 524–531.

Machol, B., & Rizk, S. (2013). Economic value of U.S. fossil fuel electricity health impacts. *Environment International*, *52*, 75–80.

Makarov, Y. V., Loutan, C., Ma, J., & De Mello, P. (2009). Operational impacts of wind generation on California power systems. *IEEE Transactions on Power Systems*, *24*(2), 1039-1050.

Markandya, A., & Wilkinson, P. (2007). Electricity generation and health. *Lancet*, *370*(9591), 979–990.

Martins, M. C. H., Fatigati, F. L., Véspoli, T. C., Martins, L. C., Pereira, L. a a, Martins, M. a, … Braga, a L. F. (2004). Influence of socioeconomic conditions on air pollution adverse health effects in elderly people: an analysis of six regions in São Paulo, Brazil. *Journal of Epidemiology and Community Health*, *58*(1), 41–46.

Mehta, S., Shin, H., Burnett, R., North, T., & Cohen, A. J. (2011). Ambient particulate air pollution and acute lower respiratory infections: a systematic review and implications for estimating the global burden of disease. *Air Quality, Atmosphere & Health*, 69–83.

Ministerio das Minas e Energia, (MME), & Empresa de Pesquisa Energetica, (EPE). (n.d.). *Plano Nacional de Energia 2030: Geração Termelétrica – Petróleo e Derivados*.

Ministério de Minas e Energia. (2007). Plano Nacional de Energia 2030: Geração termelétrica - Carvão mineral, 146. Retrieved October 16, 2017, from http://doi.org/10.1371/journal.pone.0004742.

Ministério de Minas e Energia Secretaria de Planejamento e Desenvolvimento Energético; (2014). Plano Decenal de Expansao de Energia 2023.

Miraglia, S. G. E. K., Saldiva, P. H. N., & Böhm, G. M. (2005). An evaluation of air pollution health impacts and costs in São Paulo, Brazil. *Environmental Management*, *35*(5), 667–676.

Miranda, R., Soria, R., Schaeffer, R., Szklo, A., & Saporta, L. (2017). Contributions to the analysis of “Integrating large scale wind power into the electricity grid in

the Northeast of Brazil" [Energy 100 (2016) 401–415]. *Energy*, *118*, 1198–1210.

Moolgavkar, S. H. (2000). Air Pollution and Hospital Admissions for Diseases of the Circulatory System in Three U.S. Metropolitan Areas. *Journal of the Air & Waste Management Association*, *50*(7), 1199–1206.

Nazareno, A. G., & Laurance, W. (2015). Brazil's drought: deforestation beware. *Science*, *347*(July), 1427–1428.

Nordin, N., Majid, M. R., Siong, H. C., & Kurata, G. (2016). Co-benefit modeling and optimization of air pollution control in Iskandar Malaysia: A methodology using BenMap. *Planning Malaysia*, *4*(Special Issue 4), 285–294.

Olmo, N. R. S., do Nascimento Saldiva, P. H., Braga, A. L. F., Lin, C. A., de Paula Santos, U., & Pereira, L. A. A. (2011). A review of low-level air pollution and adverse effects on human health: implications for epidemiological studies and public policy, *66*(4), 681–690.

Operador Nacional do Sistema Eletrico. (2015). Operation History. Retrieved March 12, 2015, from http://ons.org.br/pt/paginas/resultados-da-operacao/historico-da-operacao

Operador Nacional do Sistema Eletrico. (2016a). http://www.ons.org.br/. Retrieved January 1, 2015, from http://www.ons.org.br/

Operador Nacional do Sistema Eletrico. (2016b). Resultados Operacao. Retrieved December 8, 2016, from http://www.ons.org.br/resultados_operacao/boletim_diario/index.htm

Organisation for Economic Co-operation and Development. (2012). Mortality risk

valuation in environment, health and transport policies, *1*, 13–23.

Ostro, B. D. (1998). *Air pollution and health effects: a study of respiratory illness among children in Santiago, Chile* (Vol. 1932). World Bank Publications.

Ostro, B., Feng, W. Y., Broadwin, R., Green, S., & Lipsett, M. (2007). The effects of components of fine particulate air pollution on mortality in California: Results from CALFINE. *Environmental Health Perspectives*, *115*(1), 13–19.

Ostro, B., Lipsett, M., Reynolds, P., Goldberg, D., Hertz, A., Garcia, C., … Bernstein, L. (2010). Long-term exposure to constituents of fine particulate air pollution and mortality: Results from the California Teachers Study. *Environmental Health Perspectives*, *118*(3), 363–369.

Palmer, K., Oates, W. E., Portney, P. R., The, S., Perspectives, E., Autumn, N., … Portney, P. R. (1995). Tightening Environmental Standards : The Benefit-Cost or the No-Cost Paradigm ? *Journal of Economic Perspectives*, *9*(4), 119–132.

Pereira, M. G., Camacho, C. F., Freitas, M. A. V., & Silva, N. F. Da. (2012). The renewable energy market in Brazil: Current status and potential. *Renewable and Sustainable Energy Reviews*, *16*(6), 3786–3802.

Pervin, T., Gerdtham, U.-G., & Lyttkens, C. H. (2008). Societal costs of air pollution-related health hazards: A review of methods and results. *Cost Effectiveness and Resource Allocation*, *6*, 19.

Pizzol, M., Weidema, B., Brandão, M., & Osset, P. (2015). Monetary valuation in Life Cycle Assessment: a review. *Journal of Cleaner Production*, *86*, 170–179.

Pleßmann, G., Erdmann, M., Hlusiak, M., & Breyer, C. (2014). Global energy storage demand for a 100% renewable electricity supply. *Energy Procedia*, *46*, 22–31.

Pope, A. C., Burnett, R. T., Krewski, D., Jerrett, M., Shi, Y., Calle, E. E., & Thun, M. J. (2009). Cardiovascular mortality and exposure to airborne fine particulate matter and cigarette smoke shape of the exposure-response relationship. *Circulation*, *120*(11), 941–948.

Pope, C. A., Ezzati, M., & Dockery, D. W. (2009). Fine-particulate air pollution and life expectancy in the United States. *The New England Journal of Medicine*, *360*(4), 376–386.

Pope III, C. A., Burnett, R. T., Thun, M. J., Calle, E. E., Krewski, D., & Thurston, G. D. (2002). Lung Cancer, Cardiopulmonary Mortality, and Long-term Exposure to Fine Particulate Air Pollution. *The Journal of the American Medical Association*, *287*(9), 1132–1141.

Portugal-Pereira, J., Köberle, A. C., Soria, R., Lucena, A. F., Szklo, A., & Schaeffer, R. (2016). Overlooked impacts of electricity expansion optimisation modelling: The life cycle side of the story. *Energy*, *115*, 1424-1435.

Premalatha, M., Tabassum-Abbasi, Abbasi, T., & Abbasi, S. a. (2014). A critical view on the eco-friendliness of small hydroelectric installations. *The Science of the Total Environment*, *481*, 638–43.

Pupo, L., Oliveira, N. De, Rua, P., Rochedo, R., Portugal-pereira, J., Milani, R., … Schaeffer, R. (2016). Critical technologies for sustainable energy development in Brazil : technological foresight based on scenario modelling, *130*, 12–24.

Ray, M. R., & Sarma, A. K. (2011). Minimizing diurnal variation of downstream flow in hydroelectric projects to reduce environmental impact. *Journal of Hydro-Environment Research*, *5*(3), 177–185.

REN21. (2017). *Renewables 2017: global status report*. *Renewable and Sustainable Energy Reviews* (Vol. 72).

Richter, M. (2012). Utilities' business models for renewable energy: A review. *Renewable and Sustainable Energy Reviews*, *16*(5), 2483–2493.

Roy, R. (2016). The cost of air pollution in Africa. Retrieved May 4, 2017, from http://www.oecd-ilibrary.org/development/the-cost-of-air-pollution-in-africa_5jlqzq77x6f8-en

Saldiva, P. H. N., Pope III, C. A., Schwartz, J., Dockery, D. W., Lichtenfels, A. J., Salge, J. M., … Bohm, G. M. (1995). Air pollution and mortality in elderly people: A time-series study in Sao Paulo, Brazil. *Archives of Environmental Health*, *50*(2), 159–163.

Samoli, E., Analitis, A., Touloumi, G., Schwartz, J., Anderson, H. R., Sunyer, J., … Katsouyanni, K. (2005). Estimating the exposure-response relationships between particulate matter and mortality within the APHEA multicity project. *Environmental Health Perspectives*, *113*(1), 88–95.

Sangkapichai, M., Saphores, J.-D. M., Ogunseitan, O., Ritchie, S. G., You, S. I., & Lee, G. (2010). An Analysis of the health impacts from PM and NOx emissions resulting from train operations in the Alameda Corridor, CA. *University of California Transportation Center*, 1–21.

Schleicher-Tappeser, R. (2012). How renewables will change electricity markets in the next five years. *Energy Policy*, *48*, 64–75.

Shindell, D., Faluvegi, G., Walsh, M., Anenberg, S. C., Van Dingenen, R., Muller, N. Z., … Milly, G. (2011). Climate, health, agricultural and economic impacts of tighter

vehicle-emission standards. *Nature Climate Change*, *1*(1), 59–66.

Sigma Research Corporation. (2011). CALPUFF Modeling System - Version 6 User Instructions, (April), 873.

Silva, L. F. O., Oliveira, M. L. S., Boit, K. M., & Finkelman, R. B. (2009). Characterization of Santa Catarina (Brazil) coal with respect to human health and environmental concerns. *Environmental Geochemistry and Health*, *31*(4), 475–485.

Silva, R. C. D., De Marchi Neto, I., & Silva Seifert, S. (2016). Electricity supply security and the future role of renewable energy sources in Brazil. *Renewable and Sustainable Energy Reviews*, *59*, 328–341.

Sioshansi, F. P., & Pfaffenberger, W. (2006). *Electricity Market Reform: An International Perspective*. ELSEVIER Inc.

Slaughter, J. C., Lumley, T., Sheppard, L., Koenig, J. Q., & Shapiro, G. G. (2003). Effects of ambient air pollution on symptom severity and medication use in children with asthma. *Annals of Allergy, Asthma & Immunology*, *91*(4), 346–353.

Smith, K. R., Frumkin, H., Balakrishnan, K., Butler, C. D., Chafe, Z. a, Fairlie, I., … Schneider, M. (2013). Energy and human health. *Annual Review of Public Health*, *34*, 159–88.

Song, Q., Christiani, D. C., XiaorongWang, & Ren, J. (2014). The global contribution of outdoor air pollution to the incidence, prevalence, mortality and hospital admission for chronic obstructive pulmonary disease: a systematic review and meta-analysis. *International Journal of Environmental Research and Public Health*, *11*(11), 11822–11832.

Soria, R., Lucena, A. F. P., Tomaschek, J., Fichter, T., Haasz, T., Szklo, A., … Hoffmann,

S. (2016). The role of CSP in Brazil: A multi-model analysis. *AIP Conference Proceedings*, *1734*.

South Coast Air Quality Management District. (2016). *2016 Air Quality Management Plan, Appendix II*. Retrieved October 28, 2016, from http://www.aqmd.gov/docs/default-source/clean-air-plans/air-quality-management-plans/2016-air-quality-management-plan/final-2016-aqmp/appendix-ii.pdf.

Stiglitz, J. E., Stern, N., Duan, M., Edenhofer, O., Giraud, G., Heal, G., ... & Shukla, P. R. (2017). Report of the high-level commission on carbon prices. *Carbon Pricing Leadership Coalition*, *29*.

Tarroja, B., AghaKouchak, A., Sobhani, R., Feldman, D., Jiang, S., & Samuelsen, S. (2014). Evaluating options for balancing the water-electricity nexus in california: Part 1–securing water availability. *Science of the total environment*, *497*, 697-710.

Torrini, F. C., Souza, R. C., Cyrino Oliveira, F. L., & Moreira Pessanha, J. F. (2016). Long term electricity consumption forecast in Brazil: A fuzzy logic approach. *Socio-Economic Planning Sciences*, *54*, 18–27.

U.S. Energy Information Administration. (2017a). Carbon Dioxide Emissions Coefficients. Retrieved August 5, 2017, from https://www.eia.gov/environment/emissions/co2_vol_mass.php.

U.S. Energy Information Administration. (2017b). Carbon Dioxide Emissions Coefficients. Retrieved July 26, 2017, from https://www.eia.gov/environment/emissions/co2_vol_mass.php.

U.S. Environmental Protection Agency. (2017a). BenMAP-CE Regional Datasets. Retrieved January 1, 2017, from https://www.epa.gov/benmap/benmap-ce-regional-datasets.

U.S. Environmental Protection Agency. (2017b). National Ambient Air Quality Standards. Retrieved February 6, 2017, from https://www.epa.gov/criteria-air-pollutants/naaqs-table.

U.S. Environmental Protection Agency. (2017c). National Emissions Inventory. Retrieved April 4, 2017, from https://www.epa.gov/air-emissions-inventories/2014-national-emissions-inventory-nei-data.

U.S. Environmental Protection Agency. (2017d). BenMAP-CE Training Materials. Retrieved October 1, 2017, from https://www.epa.gov/benmap/benmap-ce-training-materials

U.S. Environmental Protection Agency. (2016a). BenMAP-CE Applications: Articles and Presentations. Retrieved August 4, 2016, from https://www.epa.gov/benmap/benmap-ce-applications-articles-and-presentations.

U.S. Environmental Protection Agency. (2016b). Mortality Risk Valuation. Retrieved Feburary 15, 2017, from https://www.epa.gov/environmental-economics/mortality-risk-valuation.

U.S. Environmental Protection Agency. (2015). Environmental Benefits Mapping and Analysis Program (BenMAP). *User Manual*.

U.S. Environmental Protection Agency. Subpart Da—Standards of Performance for Electric Utility Steam Generating Units, 7Federal Register 159–194 (2015).

U.S. Environmental Protection Agengy. (2013). Regulatory Impact Analysis for the Final Revisions to the National Ambient Air Quality Standards for Particulate Matter. Retrieved on May 7, 2014, from https://www3.epa.gov/ttnecas1/regdata/RIAs/finalria.pdf.

U.S. Environmental Protection Agency. (1999). The Benefits and Costs of the Clean Air Act 1990 to 2010 EPA Report to Congress. *United States Environmental Protection Agency*, (November 1999), 654.

United Nations. (2017). World Populations Prospects 2017. Retrieved April 24, 2017, from https://esa.un.org/unpd/wpp/.

United Nations. (2015). Adoption of the Paris Agreement, *21930*(December), 32.

van Zelm, R., Huijbregts, M. a J., den Hollander, H. a., van Jaarsveld, H. a., Sauter, F. J., Struijs, J., … van de Meent, D. (2008). European characterization factors for human health damage of PM10 and ozone in life cycle impact assessment. *Atmospheric Environment*, *42*, 441–453.

Vasconcelos, M. (2014). Brazil Market Overview: Coal. Retrieved November 6, 2017, https://build.export.gov/build/idcplg?IdcService=DOWNLOAD_PUBLIC_FILE&RevisionSelectionMethod=Latest&dDocName=eg_br_088985

Voorhees, A. S., Wang, J., Wang, C., Zhao, B., Wang, S., & Kan, H. (2014). Public health benefits of reducing air pollution in Shanghai: A proof-of-concept methodology with application to BenMAP. *Science of the Total Environment*, *485–486*(1), 396–405.

Vormittag, E. M. P. A. A., Costa, R. R., Braga, A. A., MIRANDA, M. D., Nascimento, N. C.,

& SALDIVA, P. (2014). Monitoramento da qualidade do ar no Brasil. *Instituto Saúde e Sustentabilidade*.

Wei, M., Nelson, J. H., Greenblatt, J. B., Mileva, A., Johnston, J., Ting, M., … Kammen, D. M. (2013). Deep carbon reductions in California require electrification and integration across economic sectors. *Environmental Research Letters*, *8*(1), 14038.

Wesson, K., Fann, N., Morris, M., Fox, T., & Hubbell, B. (2010). A Multi-pollutant, risk-based approach to air quality management: Case study for Detroit. *Atmospheric Pollution Research*, *1*, 296–304.

Western Electricity Coordinating Council. (2016). Transmission Expansion Policy Planning Committee. Retrieved February 19, 2017, from https://www.wecc.biz/TEPPC/Pages/Default.aspx

World Bank. (2015). http://data.worldbank.org/.

World Health Organization. (2015). Global Burden of Disease Estimates. Retreived May 14, 2015, from http://www.who.int/healthinfo/global_burden_disease/estimates/en/index1.html.

World Health Organization. (2017). Ambient air quality and health. Retrieved March 19, 2017, from http://www.who.int/mediacentre/factsheets/fs313/en/

Wu, J., Ren, C., Delfino, R. J., Chung, J., Wilhelm, M., & Ritz, B. (2009). Association between local traffic-generated air pollution and preeclampsia and preterm delivery in the South Coast Air Basin of california. *Environmental Health Perspectives*, *117*(11), 1773–1779.

Yang, C., Yeh, S., Zakerinia, S., Ramea, K., & McCollum, D. (2014). Achieving California's 80% greenhouse gas reduction target in 2050: Technology, policy and scenario analysis using CA-TIMES energy economic systems model. *Energy Policy*, *77*, 118–130.

Yoshida, K. (2015). *Ambient air quality standards*. Retrieved December 6, 2015, from https://www.epa.gov/criteria-air-pollutants/naaqs-table

Zanobetti, A., Franklin, M., Koutrakis, P., & Schwartz, J. (2009). Fine particulate air pollution and its components in association with cause-specific emergency admissions. *Environmental Health*, *8*(1), 58.

Zhou, Y., Levy, J. I., Hammitt, J. K., & Evans, J. S. (2003). Estimating population exposure to power plant emissions using CALPUFF: A case study in Beijing, China. *Atmospheric Environment*, *37*(6), 815–826.